Elastic Properties of Molecular Glass Thin Films

by

Jessica Torres

A Dissertation Presented in Partial Fulfillment
of the Requirements for the Degree
Doctor of Philosophy

Approved July 2011 by the
Graduate Supervisory Committee:

Bryan Vogt, Chair
Christopher Stafford
Lenore Dai
Ranko Richert
Kaushal Rege

ARIZONA STATE UNIVERSITY

August 2011

ABSTRACT

This dissertation provides a fundamental understanding of the impact of bulk polymer properties on the nanometer length scale modulus. The elastic modulus of amorphous organic thin films is examined using a surface wrinkling technique. Potential correlations between thin film behavior and intrinsic properties such as flexibility and chain length are explored. Thermal properties, glass transition temperature (T_g) and the coefficient of thermal expansion, are examined along with the moduli of these thin films. It is found that the nanometer length scale behavior of flexible polymers correlates to its bulk T_g and not the polymers intrinsic size. It is also found that decreases in the modulus of ultrathin flexible films is not correlated with the observed T_g decrease in films of the same thickness. Techniques to circumvent reductions from bulk modulus were also demonstrated.

However, as chain flexibility is reduced the modulus becomes thickness independent down to 10 nm. Similarly for this series minor reductions in T_g were obtained.

To further understand the impact of the intrinsic size and processing conditions; this wrinkling instability was also utilized to determine the modulus of small organic electronic materials at various deposition conditions.

Lastly, this wrinkling instability is exploited for development of poly furfuryl alcohol wrinkles. A two-step wrinkling process is developed via an acid catalyzed polymerization of a drop cast solution of furfuryl alcohol and photo acid generator. The ability to control the surface topology and tune the wrinkle

wavelength with processing parameters such as substrate temperature and photo acid generator concentration is also demonstrated. Well-ordered linear, circular, and curvilinear patterns are also obtained by selective ultraviolet exposure and polymerization of the furfuryl alcohol film. As a carbon precursor a thorough understanding of this wrinkling instability can have applications in a wide variety of technologies.

DEDICATION

To my parents,

Juan and Constance Torres,

who emphasized the importance of an education and instilled in me the inspiration

to set high goals and the confidence to achieve them

ACKNOWLEDGEMENTS

I would like to thank everyone who helped and inspired me during my doctoral study. First, I am thankful to my advisor Prof. Bryan D. Vogt for his support throughout my PhD study. His insight and advice made this research thesis possible. To Dr. Christopher M. Stafford for his active role in the development of my project, through his ideas as well as his strong support from the very beginning of this project. I would also like to thank the rest of my dissertation committee: Prof. Leonore Dai, Prof. Ranko Richert, and Prof. Kashual Rege for their questions and advice during my dissertation and comprehensive exams.

My fellow labmates: Mingzhi Dai, Todd Prichard, and Alpha Labiano for their stimulating discussions and insights. To Dr. Lingyan Song, Dr. Xinxin Li, and Dr. Parul Dhagat for their friendship, advice, and encouragement throughout these years. I would also like to thank researchers at the Flexible Display Center Prof. Jian Li, Nathan Bakken, and Barry O'Brien for allowing me to work on collaborative projects and the opportunity to learn in new fields.

Lastly, I would like to thank my entire family for their unfaltering love and support throughout my life; this dissertation is simply impossible without them. I thank my sisters, Christina and Vanessa, and brother in laws for their love. I thank my parents for their guidance throughout my life; their faith in my abilities encouraged me to take advantage of all my educational opportunities. My husband, Charlie, this accomplishment was only possible with his support.

TABLE OF CONTENTS

Page

CHAPTER Page

CHAPTER Page

LIST OF TABLES

LIST OF FIGURES

Figure Page

Figure Page

Figure Page

Figure Page

CHAPTER 1

INTRODUCTION

1.1 Overview

The nanometer length scale behavior of glassy materials are of valuable fundamental interest for the development of advanced materials in microelectronics,[1] coatings,[2] and adhesives.[3] As technology demands the use of materials at the nanometer length scale thermal and mechanical properties become a critical parameter for accessing their stability and performance. Understanding properties such as modulus and glass transition temperature of organic glasses at sub 100 nm length scales will provide guidance needed for implementation of organic glasses in thin films and nanostructures. More specifically the goal of the research presented here is to determine whether bulk material properties and correlations such as time temperature superposition hold at the nanoscale, a length scale that approaches their characteristic length. Lastly, surface wrinkling will also be exploited to obtain substrates with controlled topology.

Mechanical properties of organic thin films are challenging to measure using traditional techniques for inorganic films. Common techniques such as indentation are limited when attempting to characterize ultrathin films as the data commonly exhibits artifacts as a result of the stiffer underlying substrate.[4] These artifacts are further complicated in polymer thin films due to their relative softness. Here, a wrinkling based metrology is used to overcome these experimental difficulties and to determine the elastic moduli of ultrathin organic glass films. Understanding fundamental behavior of organic glasses will

contribute to the use of these thin films in a variety of applications including photonics,[5] nanostructures in microelectronics,[6] non-linear optics,[7] and biosensors.[7]

In this introduction, a brief summary of each chapter is provided, along with a discussion on the properties of ultrathin films, mechanical measurements of thin films, the wrinkling based metrology, as well as the buckling mechanics used to calculate the elastic moduli of thin films.

In Chapter 2, the elastic moduli as a function of quench depth in the glass, the difference between the bulk glass transition temperature ($T_{g,bulk}$) and the experimental temperature (T), ($T_{g,bulk}$-T), are examined in order to determine correlations between $T_{g,bulk}$ and modulus. Although it has been widely shown that the glass transition temperature (T_g) in thin polymer films can deviate from bulk values as the film thickness is decreases to the materials characteristic length scale.[8-21] Some results suggest that these deviations are preparation artifacts and given proper sample treatment no deviation from bulk values can be obtained.[22] On the other hand a decrease in bulk values at sub 100 nm length scales is also reported in the absence of strong favorable interactions between the polymer and substrate and an increase from bulk values is reported given strong interactions.[8-12] These results therefore suggest that parameters such as polymer affinity for the substrate and sample preparation are critical for sub-100 nm T_g. However, there is little known about the modulus of sub-100 nm polymer films. Thus, one might use this depressed T_g as a surrogate to estimate how the modulus of nanoconfined polymeric materials deviates from the bulk.[23] Therefore a better understanding

on the relationship between bulk T_g and modulus is needed. The first series of polymers studied is poly (alkyl methacrylate)s. This series of polymers was chosen due to a large impact on $T_{g,bulk}$ ($27°C<T_{g,bulk}<105°C$) as the alkyl chain length is increased.[24] This large range in $T_{g,bulk}$ allows for a systematic study of quench depth while still performing experiments at ambient with no increased experimental setup.

The second set of polymers studied is a series of polystyrene (PS) with a wide range of molecular mass (1.2 kg/mol up to 990 kg/mol). This PS series allows for an understanding on the effect of the materials intrinsic size on the modulus of ultra thin films, while still maintaining a systematic variation in quench depth, as T_g becomes molecular weight dependent below the entanglement molecular weight.[25] All of the polymers in these two series showed a decrease in the modulus in ultrathin films with the onset of confinement effects shifting to larger film thicknesses as the quench depth decreases. However, this deviation length scale does not scale with molecular weight. The results also show that the decrease in modulus of ultrathin films is not directly correlated with the observed T_g decrease in films of the same thickness.

In Chapter 3 the addition of small diluent molecule (Dioctyl phthalate) to PS and poly (methyl methacrylate) (PMMA) as well as ultraviolet-ozone (UVO) surface treatment to the same polymers is examined. This is done in an effort to maintain the polymers robustness at sub 40 nm length scales as small molecules can reduce the length scale for collective motion. Although small molecule diluents tend to plasticize and hence reduce the bulk modulus, previous work on

the T_g of PS thin films show promising results, an increase in T_g at sub 50 nm length scales.[26] PS films thicker than 40 nm exhibit a reduction in modulus when compared to neat PS. However, for sub 40 nm films the diluent molecule effect is reversed, and the modulus of the PS is increased when compared to the neat polymer at identical thickness. The small molecule diluent can eliminate the substantial reduction in modulus for ultrathin films.

UVO surface treatment oxidizes and crosslinks the near surface of PS.[27] UVO treatment is successful for maintaining the mechanical roboustness for the high molecular weight PS as it completely crosslinks the ≈4 nm free surface layer responsible for the decrease in sub 40 nm modulus. For the lower molecular weight PS, results from Chapter 2 reveal an increased free surface layer, ≈50 nm, UVO is unsuccessful as research shows it only crosslinks the top 5 nm.[27] On the other hand, Poly(methyl methacrylate) undergoes a chain scission reaction when exposed to UVO leading to an unchanged modulus at short exposure times.

In Chapter 4, the modulus and T_g for a series of polymers with varying backbone flexibility and architecture are studied as a function of film thickness. Aryl-phosphonate copolymers poly (aryl phosphonate)s and poly [5-(2-phenylethylnorbornene)] (PENb) with differing extents of hydrogenation are studied. Addition polymerized PENb (AddPENb) contains an unsaturated backbone with a pendent phenyl ring, which leads to a relatively rigid polymer with a high bulk T_g (186.3 ± 2.3˚C). Both T_g and modulus are statistically thickness independent; selective hydrogenation of the pendent phenyl ring leads to a small increase in T_g and decrease in modulus for the bulk, but these properties

remain thickness independent. PENb polymers formed by ring opening metathesis polymerization (hROMP PENb) yield saturated backbones, while the pendant phenyl ring can be subsequently hydrogenated to provide analogous polymers to the addition polymers. However, both hROMP PENb exhibit a thickness dependent modulus and T_g. This difference between the ROMP and addition polymers is attributed to the preservation of the bridged ring in the polymer backbone in the addition polymer that decreases its flexibility. To further investigate the role of backbone flexibility, a series of poly(arylate-phosponate) copolymers were investigated with varied aryl:phosphate ratios; a decrease in this ratio leads to a decrease in bulk T_g and an increase in bulk modulus. For the thin films, high aryl content leads to near thickness independent moduli and T_g, while as the phosphate ratio increases properties become thickness dependent at 20 nm and 40 nm for 50:50 and 0:100 ratios.

Furthermore, the impact of polymer architecture is also examined as PS branching is systematically increased from trifunction (comb), to tetrafunctional (centipede), to hexafunctional (star). The bulk T_g for these PS films is independent of branching and all exhibit a bulk T_g of approximately 103.5 ± 1 °C, statistically invariant from their linear counter parts. However, films thinner than 40 nm show significant reductions in T_g for linear and centipede PS, 25 K and 40 K, respectively. Interestingly, the modulus of the thick films is dependent upon the chain architecture with the star and comb polymers being the most compliant (~ 2 GPa) while the centipede PS is most rigid (~ 5 GPa). However at 10 nm, the modulus of the centipede polymer is less than that of the star or comb PS. The

comb PS exhibits no thickness dependence in moduli, while all other PS architectures examined show a decrease in modulus as the film thickness is decreased below approximately 40 nm. These results suggest that thickness dependent properties for polymer films are related to chain flexibility and this provides a route to systematically explore the origins for size dependent behavior in polymeric glasses.

In Chapter 5, the modulus of widely utilized small molecule organic electronic materials, 4,4'-N,N'-dicarbazole-biphenyl (CBP), N,N-diphenyl-N,N-bis(3-methylphenyl)-1,1-biphenyl-4,4-diamine (TPD), N,N'-Di-[(1-Naphthyl)-(N,N'-diphenyl]-1,1'-biphenyl)-4-4'-diamine (NPD), and tri(8-hydroxyquinolinato)aluminum (Alq_3) is studied. Similar to most organic glasses,[28] the Young's modulus of these materials is on the order of 1-2 GPa. The moduli are statistically invariant for thicknesses > 20 nm. However, a dramatic decrease or increase in modulus is observed for films less than 20 nm thick. This behavior is found to be dependent upon the bulk glass transition (T_g) temperature of the material. For both CBP and TPD, which have similar T_g's (60 ºC and 62 ºC, respectively), the modulus at room temperature decreases ≈50% when the thickness is decreased to 10 nm. Conversely, the modulus of NPD, with a bulk T_g of 95 ºC, increases by nearly a factor of two when the thickness is decreased below 20 nm, as does the aluminoquinone glass with a T_g of 175 ºC. This behavior could have significant implications for engineering of organic electronics, as our results indicate that sub-20 nm vapor deposited glasses may behave electronically significantly different from thicker films due to variations in

packing density. This result illustrates that the thickness of active layers in OLEDs impacts not only the device performance as previously determined,[29] but also their elastic properties; these properties are important for use in flexible devices.[30]

In Chapter 6, polyfurfuryl alcohol films with controlled surface morphologies are obtained from a photo polymerization process. A wrinkling or creasing morphology is obtained by drop casting a photo acid generator and furfuryl alcohol solution onto a heated substrate followed by ultraviolet ozone exposure. The wavelength, amplitude, and surface morphology can be tuned by varying the concentration of photo acid generator and substrate temperature. By controlling the rate of polymerization wavelengths in the range of 80-150 μm were obtained. Both surface wrinkling and creasing regimes can also be controlled with these parameters. Furthermore selective polymerization of the drop cast film obtained by limiting UV exposure through masks allows for ordering of the wrinkling morphologies.

In Chapter 7, a brief description of future work is given, including work aimed at a continued understanding of confinement on the modulus of ultra thin films. It is proposed to study the impact of aging on the modulus of polymeric thin films critical for end use applications. The impact of nanofiller in polymer matrixes at the nanoscale is also of interest given the increase in interface interactions as well as its applicability to organic electronics.[31] For example, the impact of C_{60} nanoparticles on polymer matrixes (PS and PMMA) will be studied. Effects of C_{60} nanoparticles can then be related back to the small molecule diluent

effect on PS and PMMA leading to a better understanding of nanoconfinement. Continued work on organic electronics from Chapter 5 and use of wrinkled polyfurfuryl alcohol substrates from Chapter 6 is also discussed.

1.2 Properties of organic glass thin films

1.2.1 Glass transition temperature

Although mechanical properties of organic glasses at the nanometer length scale have not been examined in detail, the glass transition temperature has been studied extensively.[12, 14, 18, 32-35] The relative ease of these measurements coupled with the strong correlation of T_g on other properties of polymeric materials such as Young's modulus and loss modulus[36] has provided a wealth of information regarding the properties of thin polymer films. Correlations such as time-temperature superposition principles rely on the fact that viscoelastic properties of polymers show a strong temperature dependence near T_g. For example, the elastic modulus exhibits a transition profile, where at low temperatures a plateau in modulus is observed and as the temperature is increased to above T_g the modulus will undergo a transition where the modulus decreases several orders of magnitude to the "rubbery plateau". Overall time temperature superposition allows the response time function of the modulus at a given temperature to be shifted following the empirical equation given by Williams-Landel-Ferry (WLF). The WLF equation allows for the development of isotherms of polymer properties over large time scales. For example, data taken at a given temperature on a rapid time scale can be used to determine the data at a lower temperature and slower time scale once the shift factor and empirical constants are determined. This

technique is limited to noncrystalline polymers, stable polymers in the temperature range studied, and pure polymers with no composites.

Given the sensitivity of other properties on T_g significant work on T_g of organic glasses confined to the nanometer length scale has been performed. Studies involving glass-forming liquids confined to small glass pores pioneered research of nanometer length scale effects on T_g.[15, 37] Confinement arises as the materials film thickness is reduced to length scales approaching its characteristic dimensions. The first comprehensive study on the T_g of materials in confined geometries were done by Jackson and McKenna using differential scanning calorimetry.[15] They observed an 18 K depression in bulk T_g for o-terphenyl confined to 4 nm pores. Work by Zhang et al. confirmed the reduction in T_g for a series of small molecules confined to sol-gel silica nanopores.[38] These observations lead to significant interest in understanding the properties of confined materials. The transition from glass pores to thin films was influenced by the many advantages of thin film geometries. Most notably the fact that the confining dimension, film thickness, can be easily controlled over a wide range of length scales approaching the materials characteristic length scale. Additionally thin films allow for more facile exploration of interfacial effects and surface treatments when compared to nanopores.

Similar to the confining pore geometry for small molecule glasses, Keddie et al. found a 20K decrease in T_g for PS as the film thickness is reduced to 10 nm.[18] The glass transition temperature of ultrathin films has been determined with a wide range of techniques such as: ellipsometry,[18, 39] Brillouin light

scattering,[40] X-ray reflectivity,[41, 42] acoustic wave spectroscopy,[43] shear modulation force microscopy,[44] positron annihilation lifetime spectroscopy,[9, 45] dielectric spectroscopy,[46] and probe diffusion.[12] The T_g of nanoconfined polymer films have shown inconsistent results; where the T_g increases, decreases, or remains unchanged as the film thickness is reduced. [14, 18, 42, 47-51] Attempts to understand confinement effects have then progressed in two distinct directions: first, the importance of interfaces and interfacial interactions[12, 52]; and second, a fundamental examination of the controlling length scales such as molecular weight[14, 33, 35] and cooperative rearrangement length, ξ(CRR), of the polymer segments.[33] Polymer-substrate interfacial interactions are critical to the observed confinememnt effects on the T_g of thin films. Ellipsometric measurements have shown and increase in the T_g of PMMA while supported on a native oxide silicon wafer and decrease while supported on a gold coated silicon surface.[19]

Using the same technique, Grohens showed the T_g of isotatic PMMA to increase and the T_g of syndiotatic PMMA to decrease as the film thickness decreased below 100 nm suggesting molecular architecture has an effect on the T_g of thin flims.[53, 54] While utilizing a variety of techniques such as spectroscopy, reflectivity, and differential scanning calorimetry Kremer and coworkers report only a ± 3 K change in T_g for PMMA and PS at 5 nm. [55] Furthermore, Kremer and coworkers also report no confinement effects for atactic PMMA on hydrophobic nor hydrophilic substrates when studied via ellipsometry and dielectric spectroscopy.[22] In these experiments deviations from bulk values is attributed to variations in sample preparation. Reductions in T_g due to the characteristic length

of the molecules have been studied via variations in molecular weight. Results reveal that supported polymer films have shown no significant reduction in T_g with varying molecular weight,[10, 18] but free standing films are strongly molecular weight dependent on T_g.[10, 20, 56] Forest et al. used Brillouin light scattering to measure T_g of thin free standing PS films, their results show an onset of confinement, a deviation from bulk values, at 70 nm and a 70K depression of T_g at ~30 nm unlike support PS films where a 30K depression is observed beginning at 40 nm.[13, 57] Unlike supported films, free standing PS and PMMA films with similar molecular weight show different magnitudes of T_g depression, also suggesting a polymer-free surface interface effect.[20] DeGennes proposed that this increased reduction in T_g for freely standing films is due to collective motion taking place only on chain loops as chain ends segregate to the free surface region increasing the free volume and consequently increasing polymer chain mobility.[8] On the other hand, Kremer and coworkers attributed the lack of reduction in T_g to preparation techniques allowing residual solvent in the film.[55] These results suggest that the chemistry and surface energy of the substrate as well as sample preparation can play an important role on the behavior of ultra thin films.[19, 47, 48, 58-60]

One key advance in understanding the T_g of thin films was made by Ellison and Torkelson who demonstrated that a gradient in T_g exist as a gradient from both the substrate and free interface.[12] This was done by using a fluorescent probe method in a multilayer film, where dye labeled layers were systematically placed at various known depths from the free surface. In particular, a region of

enhanced mobility (lower T_g) at the free surface was found to penetrate several tens of nanometers into the polymer film, with the reduction for thicker films greater than very thin films.[12, 61] Recently, a study by Tsui and coworkers have measured the viscosity of unentangled polystyrene films and determined that the transition temperature for the viscosity decreased with decreasing film thickness also due to the presence of a mobile surface liquid layer, consistent with previous reports of a decrease in T_g at sub 40 nm's.[62] Furthermore, recent work by Tsui and coworkers revealed no correlation between T_g and film dewetting at the nanoscale and therefore the fluidity of polymer thin films is not completely predicted by T_g.[63] This lack of correlation at the nanoscale was attributed to confinement and interface effects such as enhanced dynamics at the free surface.[63] Fakhraai and Forest examined this liquid like layer at the surface by annealing a system of gold spheres on top of PS films and measuring the recovery of the film. Fakhraai and Forrest observed a layer of increased mobility at the surface both at annealing temperature above and below T_g.[64] The existence of a layer of increased mobility at temperatures below T_g could lead to a significant impact on ultrathin film properties even for molecules deep in the glass as the surface to volume ratio is increased and the free surface becomes more significant.

1.2.2 Thin film polymer dynamics

This enhancement of surface mobility has been studied by direct measurements of dynamics at the polymer-free surface interface. Using slow-positron-annihilation spectroscopy of PS thin films, Jean and coworkers show variations in T_g with implantation distance from the free surface down to ~40 nm,

with the top 5 nm showing a 57 K T_g depression.[16] Molecules within 15 nm of the polymer-air interface have higher mobility than those in the bulk via optical birefringence measurements of ~10μm thick films and dewetting studies of ultrathin PS films on float glass.[65, 66] Furthermore a significant amount of work has been done on polymer mobility utilizing incoherent neutron scattering (INS). INS studies of polycarbonate (PC) thin films have shown a significant reduction in mean-square atomic displacement, a direct measure of polymer mobility, at sub 30 nm length scales.[67] More detailed studies on PMMA, poly(vinyl chloride) (PVC), and PC show a complex mobility behavior. For example a general reduction in mobility is found with decreasing film thickness at temperatures above T_g.[68, 69] However, at temperatures below T_g the magnitude in the reduction becomes polymer dependent. With decreased mobility in ultrathin films, a decrease in diffusion at these length scales would be expected. In agreement, Frank et al. found a slight decrease in lateral diffusion for films less than ~150 nm when supported on an attractive substrate.[70] Similarly, measurements on chain self diffusion near an attractive solid surface show a two order of magnitude decrease in diffusion coefficient near the polymer-substrate interface for both PS and PMMA on silicon oxide from a few R_g's up to $10R_g$ respectivly.[71-73] Translational diffusion of small molecules in PS films supported on fused quartz showed a reduction in diffusion at thicknesses below 150nm, with no change in diffusion for in poly (isobutyl methacrylate) nor poly (2-vinylpyridine) films.[74] These results suggest that not only is polymer affinity for the substrate important at the nanoscale but suggests that polymer flexibility and architecture can also

play an important role. In contrast, Tseng and coworkers use fluorescence recovery of a tracer in PS to show an increase in the diffusion coefficient with a decrease in film thickness. [75] The discrepancy on the direction and magnitude of variation in diffusion coefficient is attributed to a complex combination of surface and substrate effects. These interactions are believed to play a major role in observed T_g behavior at the nanometer length scale.[9]

1.2.3 Rheological properties

Viscoelastic properties of polymer thin films have been measured via dewetting, nanobubble inflation,[76] and thermal wrinkling[77]. Utilizing nanobubble inflation, McKenna and coworkers have reported creep compliance down to 13nm measured by using an atomic force microscope to image nanobubbles as a function of time, temperature, and film thickness.[78] Most recently, they have reported a dramatic reduction in rubbery compliance, an increase in modulus, for sub 40nm thick PS and poly (vinyl acetate) films.[79] Bodiguel and coworkers report a reduced viscosity beginning at a film thickness of 200 nm and a surface layer in which chain motion is enhanced on the range of R_g.[80] In order to address viscoelastic properties at a polymer surface, surface rheological experiments have been conducted via the decay of imprinted surface corrugation gratings. Johannsmann et al. found a chain length dependence on the near-surface moduli of PS films >1μm.[81] The surface modulus for PS above entanglement molecular weight exhibited bulk like values; however, a 10 fold increase in apparent stiffness was found for PS below entanglement molecular weight.[81] While utilizing broadband dielectric spectroscopy, Kremer and coworkers report no

broadening in the dynamic glass transition temperature at the surface of polymer thin films.[82] Furthermore, the dielectric spectroscopy of annealed PS films capped by aluminum layers revealed an increase in T_g at the interfaces which the authors attributed to reduced chain mobility due improved packing with annealing.[83] These results are inconsistent with an increase in surface mobility and deviation length scales observed for T_g in the sub 100 nm range. This inconsistency can be attributed to a wide range of materials studied as well variations in experimental techniques.

1.2.4 Phase behavior and physical properties

Surface and substrate effects also have an impact on phase behavior, crystallization, chain conformation, gas permeability, thermal, and mechanical properties of thin films. Using a PS/poly(vinyl methyl ether) blend, Tanaka and coworkers noticed phase separation of the two components in films below 25 nm.[84] These results indicate a decrease in the spinodal temperature for the blend at sub 25 nm length scales. The surface composition and structures of PS/PMMA blends are dependent on film thickness, where at sub 10nm length scales a phase-separated structure with uniform domain sizes was obtained.[85] Using UV absorption spectroscopy, Frank et al. found a reduction in the rate of crystallization and in the crystallinity of poly (di-n-hexylsilane) for film thicknesses below 50 nm, due to a transition between bulk nucleation and one-dimensional nucleation.[86] Polysulfone thin films have shown an increase in selectivity and a slight decrease in permeability compared to bulk. [87, 88] If the films are subsequently aged, a further and significant decrease in permeability is

observed.[87, 88] Results on aging of nanoconfined films performed by Priestley and coworkers show a dependence on a variety of factors including molecular structure and interface interactions, whereby controlling these factors can enhance or eliminate aging effects.[89] For example, a significant reduction in aging is found in a 20nm PMMA film on an attractive substrate compared to the 500 nm counterpart due to the attractive substrate interaction significantly increasing T_g.[90] While bulk like aging is observed in a 500 nm PS film on a silicon wafer, aging is suppressed for the 10 nm films. This observation is attributed to a 30K T_g depression in the 10nm film, as physical aging is only possible below T_g. With properties of thin films exhibiting a complex behavior, understanding the confinement effect on the mechanical properties of glassy materials becomes critical as a significant decrease in mechanical robustness is detrimental to device performance.

1.2.5 Elastic modulus

Traditional techniques such as nano-indentation,[91] atomic force microscopy (AFM),[4] Brillouin light scattering (BLS),[92] scanning probe miscroscopy (SPM),[44, 93] and surface acoustic wave spectroscopy (SAWS),[94] have been used to measure the elastic modulus of thin films, but are hindered when attempting to characterize ultrathin polymer films. Indentation studies apply either a constant loading rate or a constant displacement rate, with the resulting loading and unloading curves dependent on the precise characterization of the indenter's geometry.[95, 96] The modulus is determined from a the load displacement curves and known information about the indenter tip. However

nanoindentation is optimized for hard surfaces. Polymeric materials are complex due to their soft characteristic challenging sub-micrometer length scale lateral and depth penetration.[4] Nanoindentation requires an indentation depth less than 10% of the film leading to instrumental limitations such as load resolution, large error in determining initial contact loads, and calibration requirements limit the accuracy for thin polymeric films.[4] Reported measurements using nano-indentation show an indentation size effect, or decreasing elastic modulus with increasing penetration depth.[97, 98] The AFM traditionally used for adhesion and surface topology can also be used to probe surface forces and indentation, most recently the interfacial force miscroscope (IFM).[99] In AFM/IFM indentation techniques, the force on the tip is measured as a function of the vertical movement of the scanner. Although promising, difficulties with these measurements lie in accurate knowledge about the tip geometry, therefore requiring idealized assumptions, as well as the use of the Hertz contact mechanics model that do not account for polymers viscoelastic behavior.[100] Non contact techniques such as SAWS and BLS have been successful in the determination of the glass transition temperature of thin films. [92] However only limited data for the out-of-plane elastic properties of polymers has been determine due to difficulties in film handling and substrate interaction for both techniques.[101]

An alternative technique to measure thin film modulus was reported by Stafford et al.[102] This technique termed strain-induced elastic buckling instability for mechanical measurements (SIEBIMM) uses a wrinkling instability that occurs as a response to compression of a polymeric film on a thick elastic substrate.[28, 102]

Details describing the mechanism as well as the mechanics used to determine the elastic modulus will be described in Section 1.3.

1.3 Wrinkling

The wrinkling used to determine the elastic modulus of thin film is observed throughout nature. For example, a dehydrating fruit and human skin, where dehydration of the fruit or epidermins places a compressive force on the skin inducing wrinkling.[103, 104] In human skin, a stiff epidermis layer lies below a much softer elastic dermis layer. With time, the elasticity of the dermis layer is reduced placing the system under strain, which is relieved as the skin wrinkles. Similarly, reversible wrinkles appear due to the force applied as muscles contract; when the force is removed, they disappear. For fruits, the soft outer skin is placed under a compressive force as the fruit begins to dehydrate; the outer skin wrinkles in response to this force. This wrinkling phenomena commonly found in nature has potential in a variety of fields including material assembly,[103] adhesion,[105] antifouling surfaces,[2] and flexible devices[106].

For example, the success of flexible devices depends on the ability of stretchable interconnects and electrodes to remain conductive under operational induced strain. Wrinkling has been used to develop successful flexible features by depositing gold and chromium strips onto flexible substrates such as PDMS.[107-109] These electrodes and interconnects have been strained, which wrinkles the metal, while maintaining conductivity to approximately 22% strain, with negligible loss in conductivity as the sample is cycled between the strain and unstrained states.[107-110] Recently, researchers have utilized wrinkling to wrap

silicon-based electronic circuits onto curvilinear surfaces for use as flexible electronics in medical sensors.[111] Furthermore, by wrinkling plasma or ultraviolet treated PDMS slabs, groups have shown the ability to control the amplitude of the wrinkles allowing them to tune the intensity of the diffraction and therefore use wrinkled surfaces as an optical grating.[112, 113] The plasma or ultraviolet exposure crosslinks the surface creating a silica thin film on the elastic PDMS; under compression this system wrinkles, the wavelength is controlled by plasma or ultraviolet exposure while the amplitude is controlled with strain.[112] Crosby and coworkers have demonstrated the use wrinkling patterns to develop smart adhesives, where the adhesion of the material is tailored by geometric patterns.[3] A wrinkled surface has 7-fold increase in strength when compared to a smooth film as well as an increase in the reversibility of the adhesion. For example, Lin and coworkers utilized crosslinked PDMS to develop tunable dry adhesives, that demonstrate real-time adhesive tunability by adhering and releasing a glass bead by controlling the strain on the PDMS substrate.[114] Efimenko et al. have shown wrinkled surfaces to be promising in the fight against marine fouling; their research showed a decrease in fouling on wrinkled surface as compared to smooth surfaces.[2] Wrinkled hierarchical and functionalized surfaces have also been used for contact guidance of cells,[115] microfluidic sieves for ordering of spheres,[116] and as a tool for separation.[116] Here we use this wrinkling instability as a technique to measure the elastic modulus of ultrathin films. The naturally occurring wrinkling instability is harnessed by utilizing a homogenous in plane compressive force of a stiff film on an elastic substrate yielding a uniform wrinkled film. The

mechanism, shown schematically in Figure 1.1, begins with an unstrained slab of PDMS mounted onto a custom-built strain stage, discussed in Section 1.9. The PDMS is pre-strained followed by the transferring of a thin film. By releasing the pre-strain applied to the PDMS, the film is compressed and wrinkling is induced in order to minimize the total strain energy in the system.

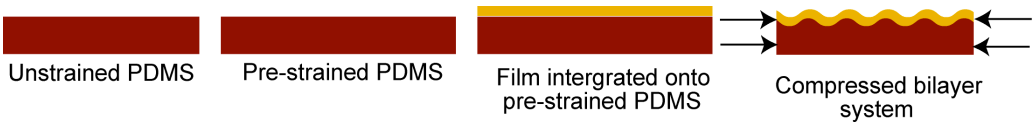

Figure 1.1 Schematic of mechanical induced wrinkling.

When compressed, the film can undergo two different deformations. As shown in Figure 1.2 the film can buckle and delaminate from the substrate, or remain bonded to the substrate and deform concurrently wrinkling.[117, 118] With the deformation mechanism determined by the substrate (compliant substrates, $E_s << E_f$, will buckle, while stiff substrates, $E_s >> E_f$, delaminate).[117, 118] Where E_s and E_f are the modulus of the substrate and film respectively.

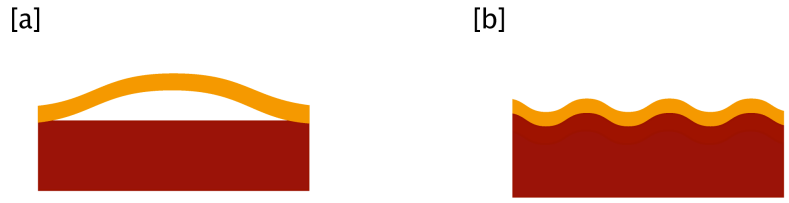

Figure 1.2 Two different deformation mechanisms [a] delamination [b] wrinkled.

The mechanics behind wrinkling begins with the following expression for bending of an elastic layer on an elastic foundation while neglecting shear stresses between the two layers:[119, 120]

$$\frac{E_f}{1-\upsilon_f^2} I \frac{d^4 y}{dx^4} + F \frac{d^2 y}{dx^2} + ky = 0 \qquad (1)$$

Where, as shown in Figure 1.3, y is the displacement orthogonal to the plane of the film, x is the distance along the direction of wrinkling, F is the compressive force, ν_f and E_f are poisson's coefficient and film modulus of the film, I is the second moment of area of the film about the axis of bending, and k is Wrinkler's modulus of half-space.

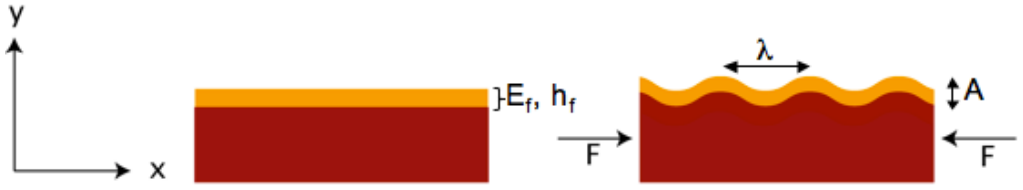

Figure 1.3 Schematic of an elastic film on an elastic substrate with the coordinate system showing the y-axis perpendicular to the film and x-axis along the wrinkling direction. Followed by the same system under a compressive force, F.

The second moment of bending is dependent on the width of the film, w, film thickness, h_f, and amplitude A:

$$I = \frac{w h_f^3}{12} \qquad (2)$$

Wrinkler's modulus of half-space represents the modulus resistance to displacement from the film into the substrate and is given by:[121]

$$k = \frac{E_s w}{1-\nu_f^2} \frac{\pi}{\lambda} \qquad (3)$$

Where λ represents the wrinkle wavelength, w the film width, and E_s and ν_s are the substrate modulus and poisson's ratio. The above Wrinkler's modulus is only valid for a sinusoidal deflection of the coating, $y = A\sin\frac{2\pi}{\lambda}$ where small

perturbations are assumed. Combining this deflection and Wrinkler's modulus into Equation 1 the compressive force in the film, F is:[120]

$$F = E_f I\left(\frac{4\pi^2}{(1-\nu_f^2)\lambda^2} + \frac{E_s w}{4\pi(1-\nu_s^2)E_s I}\lambda\right) \tag{4}$$

The minimal value of the compressive force per unit area represents the critical compressive strain, ε_c, beyond which point wrinkling is induced. The compressive strain is dependent on the ratio of the plane strain moduli of the substrate to the plane strain moduli of the film, $\frac{\overline{E}_s}{\overline{E}_f}$, as shown in Equation 5.

$$\varepsilon_c = -\frac{1}{4}\left(\frac{3\overline{E}_s}{\overline{E}_f}\right)^{2/3} \tag{5}$$

Where $\overline{E}_s = E/(1-\nu^2)$ is the plane strain modulus, E is Young's modulus, ν is poisson's ratio, and the subscripts f and s denote film and substrate respectively. The negative sign in Equation 5 denotes compression. When the prestrain (ε) is greater than the critical strain ($\varepsilon > \varepsilon_c$), a bifurcation occurs that results in the stable equilibrium state of the film being wrinkled into a series of patterns dependent on the anisotropy of the compressive stress, with a uniform compression resulting in a sinusoidal wrinkling.[122, 123] Below this critical strain, the film is stable and no wrinkling will be observed.

Equation 4 can be rewritten in a dimensionless form with as shown in Equation 6.

$$\Sigma = \frac{\pi^2}{3}\Lambda^{-2} + \frac{1}{4\pi}\Lambda \tag{6}$$

Where:

$$\Sigma = \frac{\sigma}{\sqrt[3]{\overline{E}_f \overline{E}_s^2}} \tag{6a}$$

$$\Lambda = \sqrt[3]{\frac{\overline{E}_s}{\overline{E}_f h_f^3}}\lambda \tag{6b}$$

Differentiation of Equation 6 determines the wavelength where the compressive stress is minimized and found to be $\Lambda = \frac{2\pi}{3^{1/3}}$. By inserting this value in Equation 6b the wavelength of the films is given by Equation 7.

$$\lambda = 2\pi h_f \left(\frac{\overline{E}_f}{3\overline{E}_s}\right)^{1/3} \tag{7}$$

Thus, as long as the film behaves elastically, the substrate is much thicker than the film (semi infinite), and $\overline{E}_f >> \overline{E}_s$, the wrinkling wavelength is invariant to the applied stress/strain. This strain invariance of the equilibrium wavelength results in a simple route to back calculate the thin film modulus if the modulus of the substrate, $\overline{E}_s$ and the film thickness, h_f, are known.

$$\overline{E}_f = 3\overline{E}_s \left(\frac{\lambda}{2\pi h_f}\right)^3 \tag{8}$$

Additional strain in the system acts to increase the equilibrium amplitude of the wrinkles while determined from the sinusoidal deflection and shown in Equation 9,

$$A_{eq} = h_f \left(\frac{\varepsilon}{\varepsilon_c} - 1\right)^{1/2} \tag{9}$$

This wrinkling instability is a consequence of the competition between elastic strain energy in the film and that in the substrate. The effects of surface energy are neglected in this derivation, as the role of surface energy is generally negligible. [117, 124, 125] Outside of the linear elastic regime the wavelength becomes dependent on the applied strain and a decrease in wavelength and amplitude with increasing strain is observed as shown in Equation 10 and 11.[126] The wavelength and amplitude become strain dependent due to finite deformations at large strains.

$$\lambda = \frac{\lambda_0}{\left(1+\varepsilon_{pre}\right)\left(1+\xi\right)^{1/3}} \tag{10}$$

$$A = \left(\frac{A_0}{\sqrt{\left(1+\varepsilon_{pre}\right)}\left(1+\xi\right)^{1/3}} \right)^3 \tag{11}$$

Where, $\lambda_0 = 2\pi h\left(\frac{E_f}{3E_s}\right)^{1/3}$ and $A_0 = h\sqrt{\frac{\varepsilon_{pre}}{\varepsilon_c}-1}$ (or Equations 7 and 8), and $\xi = 5\varepsilon_{pre}(1+\varepsilon_{pre})/32$, therefore at low strains, $\varepsilon \rightarrow 0$, Equation 7 and 8 are recovered.

1.4 Two-plate buckling

The wrinkling instability presented earlier is limited to cases where the films of interest can be deposited directly onto the substrate. In cases where the material is not amenable to deposition directly on the PDMS substrate, a material is chosen as an intermediate in the deposition chain. The material can be chosen such that it will act as a barrier film or allow for increased adhesion between the PDMS and the film of interest. The resulting system is a two-plate composite, or

two layers on a substrate, that exhibits a wrinkling instability when subjected to the same compressive forces as its homogenous (single film) counterpart. By using composite bean theory and deconvoluting the mechanical contributions of each layer from the behavior of the two-plate composite film, Nolte et al have obtained an expression for the Young's modulus for the film of interest.[127]

Figure 1.4 Schematic of mechanical induced two-plate wrinkling. The PDMS is pre-strained 2-5% followed by the integration of two thin films. Wrinkling is induced by compressing the pre-strained system.

The schematic for the system is shown in Figure 1.4, where E_1 and E_2 represent the modulus of the film of interest and the modulus of the barrier film respectively. The modulus of the top layer is given by the following expression,

$$\overline{E}_2 = \frac{\frac{\overline{E}_{eff}}{4} - \overline{E}_1\left[\left(\phi_1 - \frac{\kappa}{2}\right)^3 + \left(\frac{\kappa}{2}\right)^3\right]}{\left(1 - \frac{\kappa}{2}\right)^3 - \left(\phi_1 - \frac{\kappa}{2}\right)^3} \qquad (12)$$

Where $\overline{E}_{eff}$ is the effective modulus, or the modulus of the two-plate composite as if it were a homogenous system as shown below in Equation 13. Equation 12 is similar to the expression shown for modulus of the homogenous system with the exception of d_t which is the total thickness of the film, h_1+h_2.

$$\overline{E}_{eff} = 3\overline{E}_s\left(\frac{\lambda}{2\pi d_t}\right)^3 \quad (13)$$

The deviation factor for the neutral axis of bending is represented by κ. If the apparent modulus of both layers is identical κ=1, meaning the neutral axis of bending is located at the center of the two films. This deviation factor is represented by Equation 14 as a function of ϕ_1, or the height fraction of layer 1 (i.e. $h_1/(h_1+h_2)$), and the ratio of the apparent modulus of layer 1 to layer 2, $\frac{\overline{E}_1}{\overline{E}_2}$.

$$\kappa = \frac{1+\phi_1^2\left(\frac{\overline{E}_1}{\overline{E}_2}-1\right)}{1+\phi_1\left(\frac{\overline{E}_1}{\overline{E}_2}-1\right)} \quad (14)$$

This system of equations is solved iteratively for $\overline{E}_2$ until the value converged with no variations to at least the third decimal point.

1.5 Wrinkling and the modulus of ultrathin films

Stafford and co-workers used this wrinkling instability and buckling mechanics to determine the modulus of ultrathin PS and PMMA films: the reduced modulus, $\overline{E}_f / \overline{E}_{bulk}$, for both polymers collapses onto a simple curve and a decrease from bulk values is observed.[28] This decrease in the modulus is attributed to a surface anomaly similar to those observed in T_g and rheological measurements. The modulus as a function of film thickness for PMMA down to 5 nm is shown in figure 1.5.[28] The bulk modulus of PMMA is approximately 3GPa and remains statistically invariant from 150 nm+ down to 40 nm. Below 40 nm

the modulus begins to decrease significantly and at 5 nm the modulus is one third of the bulk modulus. The T_g of PMMA on a gold surface is simultaneously plotted as open triangles in Figure 1.5.

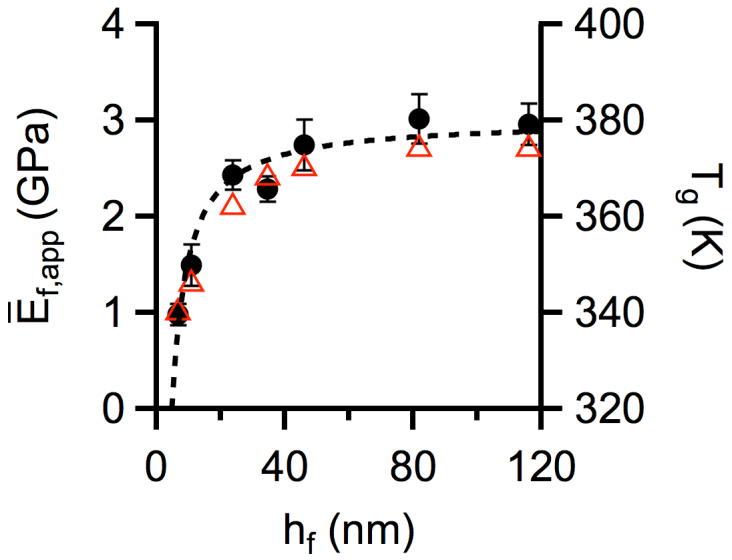

Figure 1.5 Apparent modulus as a function of film thickness for PMMA (●)[28] and T_g as a function of film thickness for PMMA (△),[19] the dashed line represents a fit to the bilayer modulus discussed below.

The ultrathin film T_g behavior is similar to the modulus were a significant decrease from bulk values is observed at ~40 nm. These results are in agreement with those reported from research groups for both PS and PMMA, where the T_g and modulus begins to decrease at 40 nm.[17-19, 28, 128] This is also in agreement with simulations that suggest modulus deviations of materials deep in the glass, with high T_g's, occur near 40 nm.[129] However, simulations also suggest a dependence of mechanical properties on bulk T_g's.[129, 130] This prediction raises questions as to the relationship between T_g and modulus in polymer thin films and their correlations at the nanometer length scale.

This surface wrinkling instability has also been utilized to determine the modulus of polyelectrolyte multilayer (PEM) systems.[127, 131, 132] By simply introducing a polymer film whose surface can be modified and used in a layer by layer assembly process, Nolte and coworkers determined the modulus of polyelectrolytes a function of deposited layers.[127] Furthermore, Nolte and coworkers have been able to determine the modulus of PEM, PS, and PMMA as a function of relative humidity by *in situ* measurements of surface wrinkling.[132] This surface wrinkling technique also allowed for the study of the mechanical robustness of PEM systems under a variety of biologically relevant conditions.[131]

1.6 Surface effects

In order to account for the deviation in modulus and T_g shown in Figure 1.5 bilayer models accounting for surface effects have been developed. It is well understood that at the surface, materials exhibit properties that differ from the bulk.[12, 16, 94, 118, 133, 134] For example, stress is increased at the surface as compared to the bulk due to the nature in chemical bonding at the interface. In the interior of a film molecules are constrained due to their bonding to underlying molecules, while molecules at the surface remain unconstrained. This difference in bonding causes the constrained inner atoms to exert stress on the surface atoms. [135] In polymer thin films it is well known that end groups segregate to the free surface in which can lead to free surface effects.[136] When determining bulk properties these variations in surface properties are considered negligible; however at the nanometer length scale, the surface to volume ratio is increased leading to a

significant contribution of surface effects on the material properties measured. As previously mentioned in Section 1.2, experimental work has also shown a region on enhanced mobility at the free surface.

Models accounting for this free surface and fitted to the experimental values have been developed for both the modulus and thermal properties at the nanometer length scale. For example, the coefficient of thermal expansion (β_R) above T_g for H-passivated PS shows a significant decrease at sub-50 nm length scale.[9] The following two-layer model was able to accurately represent the data: [9]

$$\beta_R(h) = \beta_R(h)\left(1 - \frac{\delta}{h}\right)$$

Where δ represents the layer of reduced T_g. Similarly, T_g of PS has been modeled with a simple model as follows:[137]

$$T_d(h) = T_g^{\infty}\left(1 - \frac{\delta}{h}\right)$$

Where T_g^{∞} is the bulk Tg and δ represents the layer of reduced T_g. In an effort to quantify these surface effects on the modulus of thin films, a simple two-layer model has been derived utilizing the rules of mixtures. The model consists of a film of total thickness, h_f, divided into two regions with distinct modulus. The free surface layer is characterized by a finite thickness, δ, and modulus, $\overline{E}^*$, with the remainder of the film, (h_f-δ), exhibiting bulk-like modulus, $\overline{E}_{bulk}$. In this derivation it is assumed that the surface stress is uniformly distributed throughout

the thickness of the surface layer. The effective modulus of bending for the bilayer system is given by Equation 14.

$$\overline{E}_{bending} = \overline{E}_{bulk}\left(1-\frac{\delta}{h_f}\right)^3 + \overline{E}^*\left(\frac{\delta}{h_f}\right)^3 + 3\overline{E}_{bulk}\left(1-\frac{\delta}{h_f}\right)\left(1-\xi-\frac{\delta}{h_f}\right)^2 + 3\overline{E}^*\left(\frac{\delta}{h_f}\right)\left(2-\xi-\frac{\delta}{h_f}\right)^2 \quad (14)$$

From wrinkling mechanics, the expression for the wavelength then takes the form shown in Equation 16. [118]

$$\lambda = 2\pi h_f\left(\frac{\overline{E}_{bulk}\left(1-\frac{\delta}{h_f}\right)^3 + \overline{E}^*\left(\frac{\delta}{h_f}\right)^3 + 3\overline{E}_{bulk}\left(1-\frac{\delta}{h_f}\right)\left(1-\xi-\frac{\delta}{h_f}\right)^2 + 3\overline{E}^*\left(\frac{\delta}{h_f}\right)\left(2-\xi-\frac{\delta}{h_f}\right)^2}{3E_s}\right)^{2/3} \quad (16)$$

Where:

$$\xi = \frac{E_{bulk}\left(1-\frac{\delta}{h_f}\right) + E^*\left(\frac{\delta}{h_f}\right)\left(2-\frac{\delta}{h_f}\right)}{E_{bulk}\left(1-\frac{\delta}{h_f}\right) + E^*\left(\frac{\delta}{h_f}\right)} \quad (17)$$

With no free surface layer, δ=0, the modulus is homogenous throughout the thickness of the film, $\overline{E}_{bulk} = \overline{E}^*$, and the modulus becomes thickness independent. When h>>δ, the surface layer does not significantly contribute to the overall modulus of the bilayer system. As h→δ, the surface modulus becomes significant and the bulk properties of the film begin to deviate. A hard free surface, $\overline{E}^* > \overline{E}_{bulk}$, leads to an increase in the average modulus of the thin film, while a soft free surface, $\overline{E}^* < \overline{E}_{bulk}$, leads to a decrease in the overall modulus of the thin film. This model is likely an extreme simplification of a potential gradient

in modulus that extends from the free surface, similar to proposed gradients in T_g.[12] However, without a clear idea of the shape of the gradient, the two-layer model approach provides a model with a minimal number of fitting parameters. As shown in Figure 1.5 this bilayer model is a good fit for the experimental data previously published by Stafford and coworkers, where $\overline{E}_{bulk}$=3.2GPa, $\overline{E}^{*}$=0.1GPa, and δ=2 nm.[28]

1.7 Additional applications for wrinkling

Although wrinkling has been a successful tool for studying the modulus of ultrathin organic glasses, there has been a significant amount of research into other techniques to utilize wrinkling. Wrinkling of polymer films is a result of a critical compressive stress, which can be induced in a variety of ways.[138-144] Previously discussed wrinkled surfaces have been developed via a unidirectional compressive force resulting in sinusoidal wrinkles. Other wrinkling mechanisms such as thermal contraction and constrained swelling relieve stresses isotropically leading to wrinkles coexisting in all directions.

Constrained swelling was first observed by Southern and Thomas, while studying crosslinked rubber vulcanizates with various swelling agents.[145] Recently, surface wrinkling is induced by creating regions with local differences in the elastic moduli of laterially confined materials materials via surface treatments such as Ultraviolet-Ozone (UVO) exposure[146, 147] or by using photocurable swelling agents[3]. Once the surface is treated the system is exposed to swelling agents, which due to preferential swelling of the lower moduli

material generates the compressive force required for the surface instability. Other techniques utilizing focused ion beams and hydrogel swelling have also been reported with the underlying mechanism being a geometric constraint following by swelling or crosslinking of the surface layer.[147-149]

In order to induce a surface instability utilizing swelling agents a surface treatment is required such as UVO. However, polymers exposed to UVO can undergo both cross-linking and chain scission simultaneously.[150] The dominance of each process is dependent on the polymer structure,[151] in order to create a local difference in the elastic moduli, cross-linking of only the near surface of the polymer is required. The portion of the polymer not crosslinked retains its capability to swell, a reversible deformation, attributed to the large network of covalent crosslinks absorbing the solvent.[152, 153] While the UVO exposed area have a reduced capability to swell. Therefore, exposure to a swelling agent creates an osmotic pressure difference as the uncrosslinked area is preferentially swollen when compared to the UVO exposed area. This resistance of the stiffer oxide surface creates a compressive stress in the uncrosslinked area, once this stress reaches the material-defined critical stress wrinkling is observed. The schematic for swelling induced wrinkling is shown in Figure 1.6 below. Using this process Chung and coworkers have shown wrinkling instabilities with morphologies ranging from spokes, targets, labyrinths, and dotted patterns coupled to the degree of UV crosslinking.[147] It is speculated that these patterns are generated as imperfection or impurities on the surface of the film initiate swelling followed by a decrease in diffusion in the radial direction. Imperfections

at serve as an initiation site for solvent uptake and therefore initiate the instability. The patterns also varied with UVO exposure time due to a decrease in solvent diffusion with increased exposure time. The authors suggest these results could allow for understanding the diffusion kinetics of solvents into the films as long as proper monitoring of the temporal growth is possible.[147] Perhaps a stepping stone for the development of a new technique for monitoring diffusion of solvent into polymer films. Understanding the kinetics of solvent diffusion is important for the continued growth of this instability driven self-assembly.

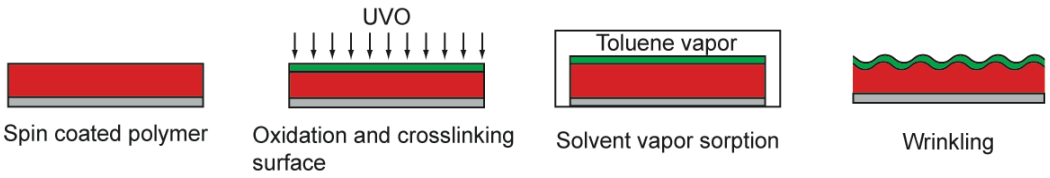

Figure 1.6 Schematic of swelling induced wrinkling. The top 5 nm of the film is oxidized and crosslinked via UVO exposure. The crosslinked film is placed in a chamber with toluene. Where an osmotic pressure differential induces wrinkling.[147]

A second method to induced wrinkling in laterally confined system consists of a photocurable elastomer being used as the film and swelling agent. The photocurable elastomer is deposited onto a substrate and cured with Ultraviolet (UV) exposure. A second doze of photocurable elastomer is deposited onto the film and allowed to swell the system. The same osmotic stress and geometric constraints similar to the previous mechanism develops surface wrinkling. UV light is then used to photopolymerize the system and hence stabilize the wrinkles. The schematic for this process is shown in Figure 1.7. A series of complex wrinkling instabilities can be created via constrained swelling by varying UV exposure time,[3, 147] crosslinker concentration,[154] and defect

locations.[147] For example, work by Whitesides and coworkers reveals that the patterns etched into the PDMS substrates act as stress relief structures.[139] Therefore when the PDMS/oxidized surface system is placed under compressive force the surface wrinkles begin and end at defect locations. Guvendiren et al. use poly(hydroxylethyl methacrylate) hydrogel films confined on a substrate to create ordered hexagonal, lamellar, and worm-like structures, where the surface morphology is determined from crosslinker concentrations.[154] That is at compressive stress greater than ≈0.33% creasing, or folding of the surface, is observed while at moderate and low strains wrinkling or no surface microstructure is observed respectively.[155] Hayward and coworkers have studied the stability and wrinkling patterns of poly(acrylamide) hydrogels as a function of monomer and cross-linker concentration, their results show a decrease in compressive stress (i.e. no creasing) with high cross-linker concentration while at low cross linker concentration creasing increases linearly.[155] This stress variation with cross-linker concentration seems to be the controlling factor in surface morphologies described above.

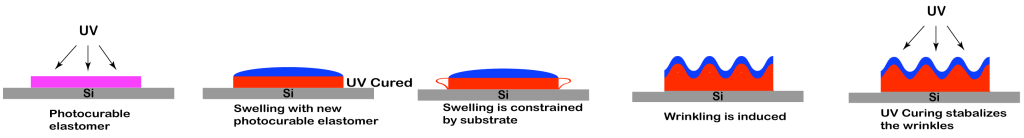

Figure 1.7 Schematic of photocurable elastomer swelling. The first film of elastomer is cured with UV then swelled with fresh photocurable elastomer. The constrained swelling induces wrinkles which are stabilized with a second dose of UV.[3]

Lastly, wrinkling phenomena will also occur through differential thermal expansion between the film and the substrate. For example, if a film is deposited onto a thermally expanded polymer, or the film and substrate are allowed to thermally expand, upon cooling a mismatch between the coefficient of thermal expansion of the film and substrate place a compressive stress onto the film. Once the stress is greater than the critical value surface wrinkling is observed.[112, 139] The compressive force due to thermal contraction is equi-biaxial therefore there is neither preferred orientation nor ordering of the wrinkles. Further cooling leads to an increase in the compressive force on the system increasing the amplitude of the wrinkles following by folding or creasing.

On the other hand, researchers have been able to eliminate wrinkling due to thermal expansions in poly electrolytic/PDMS systems by incorporating silica nanoparticles.[156] Hendricks and coworkers were able to use layer by layer assembly to incorporate nanoparticles throughout the film and attribute the dissipation of compressive stress to the isotropically dispersed nanoparticles.

1.8 Tools and characterization techniques

Well ordered sinusoidal wrinkling is obtained via a homogenous in-plane compressive force. A custom built strain stage shown in Figure 1.8 is used to exert the in-plane compressive force onto the bilayer system.[157] The stage allows for generation of periodic wrinkles oriented perpendicular to the strain direction. The design followed a previously documented strain stage used by Stafford et al as a tool for a high throughput modulus measurement technique for thin films.[157]

The strain stage has a fixed grip as well as an adjustable grip that is controlled with an actuator. A 7.5 cm by 2.5 cm slab of PDMS is clamped between the grips and the adjustable grip is displaced via the actuator so that the PDMS is strained. The strain stage has locking groves, allowing for the strain to be maintained while also having the ability to separate the strain stage from the actuator.

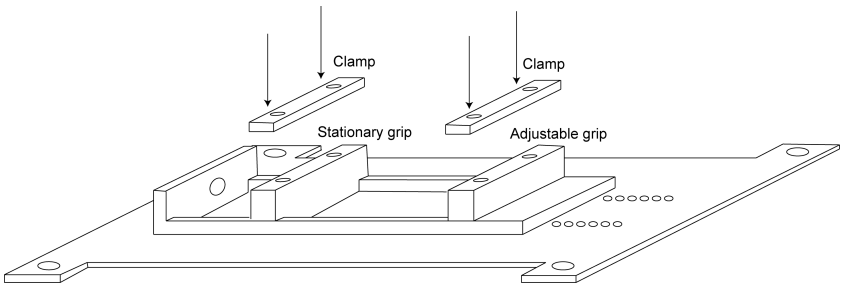

Figure 1.8 Strain stage design. The PDMS is placed between the clamps and the strain rate/quantity is controlled with a motorized actuator. The dimensions of the stage were designed such that it would be compatible with a motorized actuator.

A film of known thickness is then integrated onto the PDMS. For most of the work presented here, vacuum deposition or a preferential adhesion method is used. First a film is spun cast onto a silicon wafer, the supported film is then placed into direct contact with the PDMS substrate and allowed to softly bond to the PDMS prior to immersion in water. Then through preferential adhesion the film transfersfrom the wafer onto the PDMS due to preferential segregation of water to the polymer-wafer interface.[157] Once the transfer is complete and the thickness of the thin film is determined the strain stage is placed onto the actuator for release of the pre-strain. The actuator allows for accurate and precise control of the rate and magnitude of the compressive force required for wrinkling, control of the release rate allows for minimization of structural defects.[116]

As previously shown in Equation 7, in order to determine the modulus of the wrinkled film, the substrate modulus, film thickness, and the wrinkling wavelength need to be determined. The modulus of the elastic substrate is determined using a texture analyzer (TA.XT Plus, Texture Technologies). A pure slab of PDMS is clamped into the analyzer and the stress strain behavior is obtained as shown in Figure 1.9.

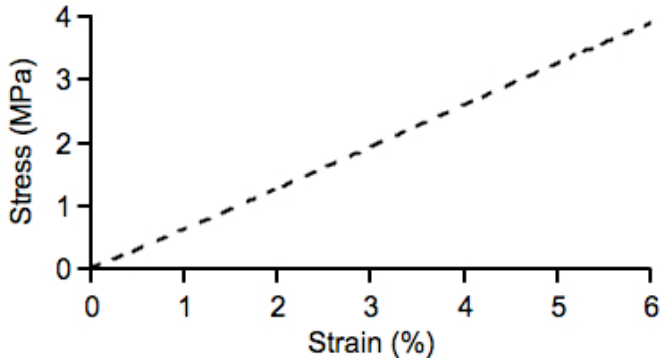

Figure 1.9 Stress-strain behavior for a PDMS slab obtained from the texture analyzer. The slope of the line, 0.6MPa, represents the modulus of the substrate.

The thickness of the thin films can be determined from various techniques such as ellipsometry,[158] interferometry,[159] profilometry,[160] and x-ray reflectivity[161]. For this work, ellipsometry (J.A. Woollam M-2000) is used. Ellipsometry is a non-destructive optical technique used in determining the optical properties and thickness of thin. Ellipsometry does not directly measure the thickness or optical constants of a film; instead it measures changes in polarization of light. Model based analysis is used to convert the measured values into film thickness. A schematic setup of an ellipsometer is shown in Figure 1.10.

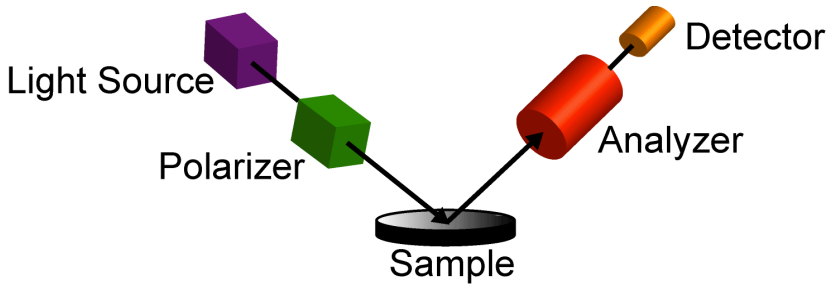

Figure 1.10 Schematic of a spectroscopic ellipsometer used to determine film thickness.

Light emitted from the light sources first goes through a polarizer where it becomes linearly polarized. The light interacts with the sample and is then reflected back to the analyzer. The light reflected from the sample is elliptically polarized, this change in polarization is measured through the ellipsometric angles, Ψ and Δ, describing the amplitude ratio and the phase difference. The detector converts the change in polarization of light to an electronic signal. Measurements are taken over a wavelength range from 250 nm to 1700 nm using three incident angles, 50°, 60°, 70°, and 80° in order to cover the Brewster angle of PDMS (~50°). The ellipsometric angles used to describe the change in polarization for the PDMS as a function of wavelength are saved and fit to a Cauchy layer, shown in Equation 18.

$$n(\lambda) = A + \frac{B}{\lambda^2} + \frac{C}{\lambda^4} \qquad (18)$$

Where A, B, and C are constants and λ represents the wavelength of light.

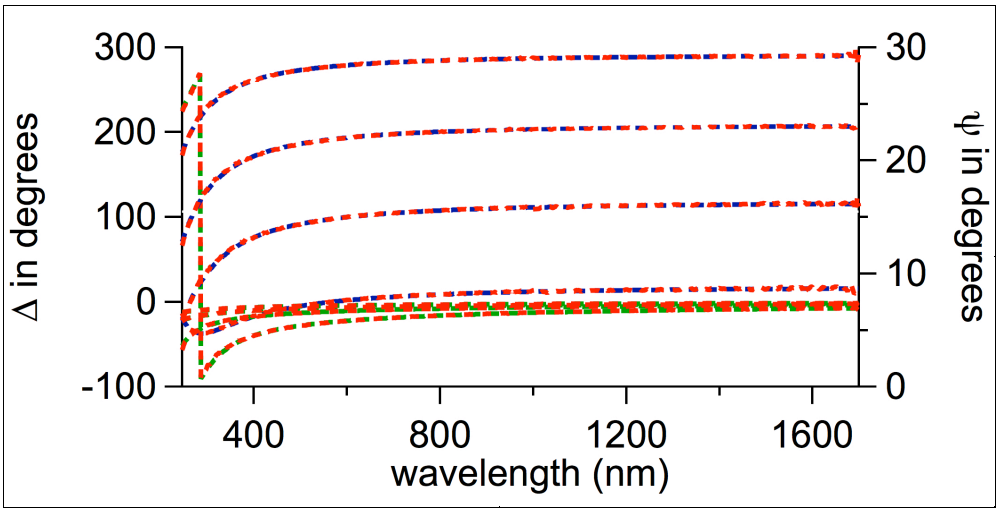

Figure 1.11 Ellipsometric angles, Δ (green) and Ψ (blue), for PDMS with a Cauchy fit (red).

This model is used to fit the predicted response from Fresnel's equations to experimental data as shown in Figure 1.11 and then the optical constants for PDMS are determined. The PDMS fit is saved as a material model and used as a substrate for the polymer film. Once the thin film is transferred onto the PDMS spectroscopic ellipsometric the used to calculate the film thickness. Another Cauchy layer is used to describe the thin film and the ellipsometric data obtained from the thin film is fit to this model in order to determine the film thickness and optical constants. The Cauchy model used in the above analysis is limited to transparent nonabsorbent layers over the entire measuring wavelength. The phase information obtained from an ellipsometer is sensitive for films down to a thickness of approximately 2 nm and an upper limit of tens of microns, making it suitable to determine thickness for ultra thin films.[162]

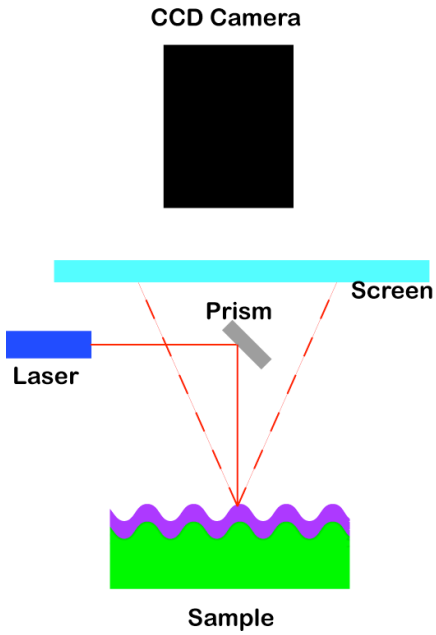

Figure 1.12 Small Angle Light Scattering schematic, showing the laser transmitting through the sample and a detector measuring the intensity and angular distribution of the scattered light.

In order to determine the wavelength of the wrinkled films techniques such as optical micrscopy (OM), small angle light scattering (SALS), and atomic force microscopy (AFM) can be used. AFM and SALS are valid techniques for the investigation of wavelengths and amplitudes at sub micrometer length scales, while OM is only valid for wavelengths greater than 5 μm.

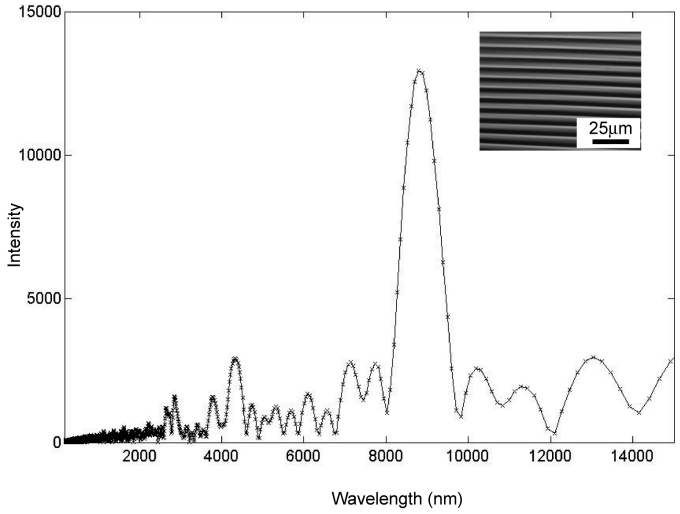

Figure 1.13 Fast Fourier transform of a 100nm Polystyrene film showing a characteristic wavelength of 8.7μm. The insert represents the optical micrograph of the film.

In SALS, coherent light from a laser is passed normal to the sample surface. The magnitude in the phase shift of the light as it passes through the wrinkled surface is proportional to the wrinkling amplitude while the diffraction pattern is related to the wrinkling wavelength. Therefore, angular distribution of the scattered light is analyzed to determine the wavelength of the wrinkled film. A laser incident normal to the surface is scattered by the wrinkled surface. The value of the scattering vector is given by the following relationship:

$$q \approx \frac{2\pi}{d} \tag{19}$$

Where λ_l is the wavelength of the laser used, d is the wrinkle wavelength, and θ represents the scattering angle. A schematic of the SALS setup is shown in Figure 1.12.

In order to increase accuracy analysis time, the images obtained using OM are converted to Fourrier space using custom code written in Matlab. The characteristic wavelength is determined per image then used to calculate the modulus. A sample FFT is shown below in figure 1.13. AFMs can be used to provide information on the hardness of a sample,[163] the adhesion between the tip and the sample,[164] and interactions between molecules[165]. It can also provide a 3D profile of a surface. This is used for characterization of sub 50 μm wavelengths. Because of potential damage to the soft wrinkled surface, the AFM is operated in intermittent contact mode. In this mode, the cantilever is oscillated at its resonant frequency with a piezoelectric crystal. Due to the proximity of the tip and the surface, between 0.5 and 2 nm, during scanning the tip interacts with the Van der Waal forces from the surface. In order to maintain a constant oscillation amplitude the feedback loop adjusts the tip-sample separation. To acquire an image, the vertical and lateral deflections of the cantilever are measured by variations in frequency of the tip. The reflected laser is sent to a photodiode detector where the signal is converted to an image.

AFM images for this work are all acquired at ambient temperature (T=21± 2°C) in tapping mode. AFM images are analyzed using the AFM software, which include a 1D FFT to obtain the characteristic wavelength of the wrinkles, a sample image is shown below in Figure 1.14. The AFM image is of a wrinkled 38 nm PS film, where the amplitude is ~200 nm and the characteristic wavelength is 1.8 μm.

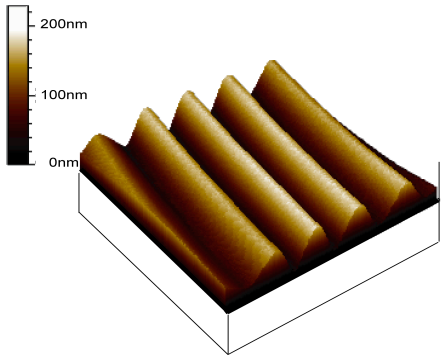

Figure 1.14 AFM micrograph of a 38 nm polystyrene film. The scan size of 7.5μm by 7.5μm and the height scale for this image is 250nm.

1.9 Summary

The modulus as a function of film thickness will be studied utilizing surface wrinkling. Techniques such as AFM and OM combined with buckling mechanics will allow for the characterization of the surface microstructure and the modulus determination. In this study relationships between the materials flexibility, architecture, bulk T_g, intrinsic material size (R_g) and moduli will be obtained. Proper understanding of the moduli behavior at the nanometer length scale is critical for the use of organic materials in of next generation technologies. Furthermore, this surface microstructure will be explored for the development of substrates with controlled topography.

1.10 References

1. Winey, K. I.; Vaia, R. A., Polymer nanocomposites. *MRS Bulletin* **2007,** *32*, 314-322.

2. Efimenko, K.; Finlay, J.; Callow, M. E.; Callow, J. A.; Genzer, J., Development and Testing of Hierarchically Wrinkled Coatings for Marine Antifouling. *Acs Applied Materials & Interfaces* **2009,** *1* (5), 1031-1040.

3. Chan, E. P.; Smith, E. J.; Hayward, R. C.; Crosby, A. J., Surface wrinkles for smart adhesion. *Advanced Materials* **2008,** *20* (4), 711-+.

4. VanLandingham, M. R., Villarrubia, J.S., Guthrie, W.F., Meyers, G.F., Nanoindentation of polymers: An overview. *Macromolecules Symposium* **2001,** *167*, 15-43.

5. Ozin, G. A.; Yang, S. M., The race for the photonic chip: Colloidal crystal assembly in silicon wafers. *Advanced Functional Materials* **2001,** *11* (2), 95-104.

6. Hartschuh, R.; Ding, Y.; Roh, J. H.; Kisliuk, A.; Sokolov, A. P.; Soles, C. L.; Jones, R. L.; Hu, T. J.; Wu, W. L.; Mahorowala, A. P., Brillouin scattering studies of polymeric nanostructures. *Journal of Polymer Science Part B-Polymer Physics* **2004,** *42* (6), 1106-1113.

7. Lei, J.; Fan, J.; Yu, C. Z.; Zhang, L. Y.; Jiang, S. Y.; Tu, B.; Zhao, D. Y., Immobilization of enzymes in mesoporous materials: controlling the entrance to nanospace. *Microporous and Mesoporous Materials* **2004,** *73* (3), 121-128.

8. de Gennes, P. G., Glass transitions in thin polymer films. *European Physical Journal E* **2000,** *2* (3), 201-203.

9. DeMaggio, G. B.; Frieze, W. E.; Gidley, D. W.; Zhu, M.; Hristov, H. A.; Yee, A. F., Interface and surface effects on the glass transition in thin polystyrene films. *Physical Review Letters* **1997,** *78* (8), 1524-1527.

10. Dutcher, J. R.; Forrest, J. A.; Dalnoki-Veress, K., Interface and chain confinement effects on the glass transition temperature of thin polymer films. *Abstracts of Papers of the American Chemical Society* **1998,** *215*, 276-COLL.

11. Ellison, C. J.; Kim, S. D.; Hall, D. B.; Torkelson, J. M., Confinement and processing effects on glass transition temperature and physical aging in ultrathin polymer films: Novel fluorescence measurements. *European Physical Journal E* **2002,** *8* (2), 155-166.

12. Ellison, C. J.; Torkelson, J. M., The distribution of glass-transition temperatures in nanoscopically confined glass formers. *Nature Materials* **2003,** *2* (10), 695-700.

13. Forrest, J. A.; DalnokiVeress, K.; Stevens, J. R.; Dutcher, J. R., Effect of free surfaces on the glass transition temperature of thin polymer films (vol 77, pg 2002, 1996). *Physical Review Letters* **1996,** *77* (19), 4108-4108.

14. Forrest, J. A.; Mattsson, J., Reductions of the glass transition temperature in thin polymer films: Probing the length scale of cooperative dynamics. *Physical Review E* **2000,** *61* (1), R53-R56.

15. Jackson, C. L.; McKenna, G. B., The glass-transition of organic liquids confined to small pores. *Journal of Non-Crystalline Solids* **1991,** *131*, 221-224.

16. Jean, Y. C.; Zhang, R. W.; Cao, H.; Yuan, J. P.; Huang, C. M.; Nielsen, B.; AsokaKumar, P., Glass transition of polystyrene near the surface studied by slow-positron-annihilation spectroscopy. *Physical Review B* **1997,** *56* (14), R8459-R8462.

17. Keddie, J. L.; Jones, R. A. L., Glass-transition behavior in ultra-thin polystyrene films. *Israel Journal of Chemistry* **1995,** *35* (1), 21-26.

18. Keddie, J. L.; Jones, R. A. L.; Cory, R. A., Size-dependent depression of the glass-transition temperature in polymer-films. *Europhysics Letters* **1994,** *27* (1), 59-64.

19. Keddie, J. L.; Jones, R. A. L.; Cory, R. A., Interface and surface effects on the glass-transition temperature in thin polymer films. *Faraday Discussions* **1994,** *98*, 219-230.

20. Roth, C. B.; Dutcher, J. R., Glass transition temperature of freely-standing films of atactic poly(methyl methacrylate). *European Physical Journal E* **2003,** *12*, S103-S107.

21. Roth, C. B.; Dutcher, J. R., Glass transition and chain mobility in thin polymer films. *Journal of Electroanalytical Chemistry* **2005,** *584* (1), 13-22.

22. Erber, M.; Tress, M.; Mapesa, E. U.; Serghei, A.; Eichhorn, K.-J.; Voit, B.; Kremer, F., Glassy Dynamics and Glass Transition in Thin Polymer Layers of PMMA Deposited on Different Substrates. *Macromolecules* **2010,** *43* (18), 7729-7733.

23. Williams, M. L.; Landel, R. F.; Ferry, J. D., Mechanical properties of substances of high molecular weight .19. The temperature dependence of relaxation mechanisms in amorphous polymers and other glass-forming liquids. *Journal of the American Chemical Society* **1955,** *77* (14), 3701-3707.

24. Rogers, S. S.; Mandelkern, L., Glass formation in polymers 1. The glass transitions of the Poly-(-Alkyl Methacrylates). *Journal of Physical Chemistry* **1957,** *61* (7), 985-990.

25. Hintermeyer, J.; Herrmann, A.; Kahlau, R.; Goiceanu, C.; RoÃàssler, E. A., Molecular Weight Dependence of Glassy Dynamics in Linear Polymers Revisited. *Macromolecules* **2008,** *41* (23), 9335-9344.

26. Ellison, C. J.; Ruszkowski, R. L.; Fredin, N. J.; Torkelson, J. M., Dramatic Reduction of the Effect of Nanoconfinement on the Glass Transition of Polymer Films via Addition of Small-Molecule Diluent. *Physical Review Letters* **2004,** *92* (9), 095702.

27. Efimenko, K.; Wallace, W. E.; Genzer, J., Surface Modification of Sylgard-184 Poly(dimethyl siloxane) Networks by Ultraviolet and Ultraviolet/Ozone Treatment. *Journal of Colloid and Interface Science* **2002,** *254* (2), 306-315.

28. Stafford, C. M.; Vogt, B. D.; Harrison, C.; Julthongpiput, D.; Huang, R., Elastic moduli of ultrathin amorphous polymer films. *Macromolecules* **2006,** *39* (15), 5095-5099.

29. Benor, A.; Takizawa, S.-y.; PÈrez-BolÌvar, C.; Anzenbacher Jr, P., Efficiency improvement of fluorescent OLEDs by tuning the working function of PEDOT:PSS using UV-ozone exposure. *Organic Electronics* **2010,** *11* (5), 938-945.

30. Wong, W. S.; Sallea, A., *Flexible electronics: materials and applications*. Springer: New York, 2009.

31. Kang, H.-S.; Park, K.-N.; Cho, Y.-R.; Park, D.-W.; Choe, Y., Enhanced performance of organic electroluminescence diodes with a 2-TNATA:C60 hole injection layer. *Journal of Industrial and Engineering Chemistry* **2009,** *15* (5), 752-757.

32. Campbell, C. G.; Vogt, B. D., Examination of the influence of cooperative segmental dynamics on the glass transition and coefficient of thermal expansion in thin films probed using poly(n-alkyl methacrylate)s. *Polymer* **2007,** *48* (24), 7169-7175.

33. Ellison, C. J.; Mundra, M. K.; Torkelson, J. M., Impacts of polystyrene molecular weight and modification to the repeat unit structure on the glass transition-nanoconfinement effect and the cooperativity length scale. *Macromolecules* **2005,** *38* (5), 1767-1778.

34. Kim, J. H.; Jang, J.; Zin, W. C., Estimation of the thickness dependence of the glass transition temperature in various thin polymer films. *Langmuir* **2000,** *16* (9), 4064-4067.

35. Singh, L.; Ludovice, P. J.; Henderson, C. L., Influence of molecular weight and film thickness on the glass transition temperature and coefficient of thermal expansion of supported ultrathin polymer films. *Thin Solid Films* **2004,** *449* (1-2), 231-241.

36. Ngai, K. L.; Plazek, D. J., Identification of different modes of molecular-motion in polymers that cause themorheological complexity. *Rubber Chemistry and Technology* **1995,** *68* (3), 376-434.

37. Arndt, M.; Stannarius, R.; Groothues, H.; Hempel, E.; Kremer, F., Length scale of cooperativity in the dynamic glass transition. *Physical Review Letters* **1997,** *79* (11), 2077-2080.

38. Zhang, J.; Liu, G.; Jonas, J., Effects of confinement on the glass-transition temperature of molecular liquids. *Journal of Physical Chemistry* **1992,** *96* (8), 3478-3480.

39. Beaucage, G.; Composto, R.; Stein, R. S., Ellipsometric study of the glass-transition and thermal-expansion coefficients of thin polymer-films. *Journal of Polymer Science Part B-Polymer Physics* **1993,** *31* (3), 319-326.

40. Dalnoki-Veress, K.; Forrest, J. A.; Murray, C.; Gigault, C.; Dutcher, J. R., Molecular weight dependence of reductions in the glass transition temperature of thin, freely standing polymer films. *Physical Review E* **2001,** *63* (3).

41. Orts, W. J.; Vanzanten, J. H.; Wu, W. L.; Satija, S. K., Observation of temperature-dependent thicknesses in ultrathin polystyrene films on silicon. *Physical Review Letters* **1993,** *71* (6), 867-870.

42. Wallace, W. E.; Vanzanten, J. H.; Wu, W. L., Influence of an impenetrable interface on a polymer glass-transition temperature. *Physical Review E* **1995,** *52* (4), R3329-R3332.

43. Alig, I.; Lellinger, D.; Sulimma, J.; Tadjbakhsch, S., Ultrasonic shear wave reflection method for measurements of the viscoelastic properties of polymer films. *Review of Scientific Instruments* **1997,** *68* (3), 1536-1542.

44. Ge, S.; Pu, Y.; Zhang, W.; Rafailovich, M.; Sokolov, J.; Buenviaje, C.; Buckmaster, R.; Overney, R. M., Shear modulation force microscopy study of near surface glass transition temperatures. *Physical Review Letters* **2000,** *85* (11), 2340-2343.

45. Xie, L.; Demaggio, G. B.; Frieze, W. E.; Devries, J.; Gidley, D. W.; Hristov, H. A.; Yee, A. F., Positronium formation as a probe of polymer surfaces and thin-films. *Physical Review Letters* **1995,** *74* (24), 4947-4950.

46. Fukao, K., Dynamics in thin polymer films by dielectric spectroscopy. *European Physical Journal E* **2003,** *12* (1), 119-125.

47. Kawana, S.; Jones, R. A. L., Character of the glass transition in thin supported polymer films. *Physical Review E* **2001,** *63* (2).

48. Kawana, S.; Jones, R. A. L., Effect of physical ageing in thin glassy polymer films. *European Physical Journal E* **2003,** *10* (3), 223-230.

49. Torres, J. A.; Nealey, P. F.; de Pablo, J. J., Molecular simulation of ultrathin polymeric films near the glass transition. *Physical Review Letters* **2000,** *85* (15), 3221-3224.

50. VanZanten, J. H.; Wallace, W. E.; Wu, W. L., Effect of strongly favorable substrate interactions on the thermal properties of ultrathin polymer films. *Physical Review E* **1996,** *53* (3), R2053-R2056.

51. Alcoutlabi, M.; McKenna, G. B., Effects of confinement on material behaviour at the nanometre size scale. *Journal of Physics-Condensed Matter* **2005,** *17* (15), R461-R524.

52. Lin, E. K.; Kolb, R.; Satija, S. K.; Wu, W. L., Reduced polymer mobility near the polymer solid interface as measured by neutron reflectivity. *Macromolecules* **1999,** *32* (11), 3753-3757.

53. Grohens, Y., Hamon, L., Carriere, P., Holl, Y., Schultz, J., Tacticity and surface chemistry effects on the glass transition temperature of thin supported PMMA films. *Materials Research Society Symposium* **2001,** (629), FF171-77.

54. Grohens, Y.; Hamon, L.; Reiter, G.; Soldera, A.; Holl, Y., Some relevant parameters affecting the glass transition of supported ultra-thin polymer films. *European Physical Journal E* **2002,** *8* (2), 217-224.

55. Tress, M.; Erber, M.; Mapesa, E. U.; Huth, H.; Muller, J.; Serghei, A.; Schick, C.; Eichhorn, K.-J.; Voit, B.; Kremer, F., Glassy Dynamics and Glass Transition in Nanometric Thin Layers of Polystyrene. *Macromolecules* **2010,** *43* (23), 9937-9944.

56. Mattsson, J.; Forrest, J. A.; Borjesson, L., Quantifying glass transition behavior in ultrathin free-standing polymer films. *Physical Review E* **2000,** *62* (4), 5187-5200.

57. Forrest, J. A.; DalnokiVeress, K.; Dutcher, J. R., Interface and chain confinement effects on the glass transition temperature of thin polymer films. *Physical Review E* **1997,** *56* (5), 5705-5716.

58. Prucker, O.; Christian, S.; Bock, H.; Ruhe, J.; Frank, C. W.; Knoll, W., On the glass transition in ultrathin polymer films of different molecular architecture. *Macromolecular Chemistry and Physics* **1998,** *199* (7), 1435-1444.

59. Tate, R. S.; Fryer, D. S.; Pasqualini, S.; Montague, M. F.; de Pablo, J. J.; Nealey, P. F., Extraordinary elevation of the glass transition temperature of

thin polymer films grafted to silicon oxide substrates. *Journal of Chemical Physics* **2001,** *115* (21), 9982-9990.

60. Fryer, D. S.; Nealey, P. F.; de Pablo, J. J., Thermal probe measurements of the glass transition temperature for ultrathin polymer films as a function of thickness. *Macromolecules* **2000,** *33* (17), 6439-6447.

61. Jones, R. A. L., The dynamics of thin polymer films. *Current Opinion in Colloid & Interface Science* **1999,** *4* (2), 153-158.

62. Yang, Z.; Fujii, Y.; Lee, F. K.; Lam, C.-H.; Tsui, O. K. C., Glass Transition Dynamics and Surface Layer Mobility in Unentangled Polystyrene Films. *Science* **2010,** *328* (5986), 1676-1679.

63. Clough, A.; Peng, D.; Yang, Z.; Tsui, O. K. C., Glass Transition Temperature of Polymer Films That Slip. *Macromolecules* **2011,** *44* (6), 1649-1653.

64. Fakhraai, Z.; Forrest, J. A., Measuring the Surface Dynamics of Glassy Polymers. *Science* **2008,** *319* (5863), 600-604.

65. Schwab, A. D.; Agra, D. M. G.; Kim, J. H.; Kumar, S.; Dhinojwala, A., Surface dynamics in rubbed polymer thin films probed with optical birefringence measurements. *Macromolecules* **2000,** *33* (13), 4903-4909.

66. Reiter, G., Mobility of polymers in films thinner than their unperturbed size. *Europhysics Letters* **1993,** *23* (8), 579-584.

67. Soles, C. L.; Douglas, J. F.; Wu, W. l.; Dimeo, R. M., Incoherent Neutron Scattering and the Dynamics of Confined Polycarbonate Films. *Physical Review Letters* **2002,** *88* (3), 037401.

68. Soles, C. L.; Douglas, J. F.; Wu, W.-l.; Dimeo, R. M., Incoherent Neutron Scattering as a Probe of the Dynamics in Molecularly Thin Polymer Films. *Macromolecules* **2003,** *36* (2), 373-379.

69. Soles, C. L.; Douglas, J. F.; Lin, E. K.; Lenhart, J. L.; Jones, R. L.; Wu, W.-L.; Goldfarb, D. L.; Angelopoulos, M., Incoherent neutron scattering and the dynamics of thin film photoresist polymers. *Journal of Applied Physics* **2003,** *93* (4), 1978-1986.

70. Frank, B.; Gast, A. P.; Russell, T. P.; Brown, H. R.; Hawker, C. J., Polymer mobility in thin films. *Macromolecules* **1996,** *29* (20), 6531-6534.

71. Lin, E. K.; Wu, W. I.; Satija, S. K., Polymer interdiffusion near an attractive solid substrate. *Macromolecules* **1997,** *30* (23), 7224-7231.

72. Zheng, X.; Rafailovich, M. H.; Sokolov, J.; Strzhemechny, Y.; Schwarz, S. A.; Sauer, B. B.; Rubinstein, M., Long-range effects on polymer diffusion induced by a bounding interface. *Physical Review Letters* **1997,** *79* (2), 241-244.

73. Zheng, X.; Sauer, B. B.; Vanalsten, J. G.; Schwarz, S. A.; Rafailovich, M. H.; Sokolov, J.; Rubinstein, M., Reptation dynamics of polymer melt near an attractive solid surface. *Physical Review Letters* **1995,** *74* (3), 407-410.

74. Hall, D. B.; Torkelson, J. M., Small Molecule Probe Diffusion in Thin and Ultrathin Supported Polymer Films. *Macromolecules* **1998,** *31* (25), 8817-8825.

75. Tseng, K. C.; Turro, N. J.; Durning, C. J., Tracer diffusion in thin polystyrene films. *Polymer* **2000,** *41* (12), 4751-4755.

76. O'Connell, P. A.; McKenna, G. B., Novel nanobubble inflation method for determining the viscoelastic properties of ultrathin polymer films. *Review of Scientific Instruments* **2007,** *78* (1), 013901-12.

77. Chan, E. P.; Kundu, S.; Lin, Q.; Stafford, C. M., Quantifying the Stress Relaxation Modulus of Polymer Thin Films via Thermal Wrinkling. *ACS Applied Materials & Interfaces* **2010,** *3* (2), 331-338.

78. O'Connell, P. A.; McKenna, G. B., Rheological Measurements of the Thermoviscoelastic Response of Ultrathin Polymer Films. *Science* **2005,** *307* (5716), 1760-1763.

79. O'Connell, P.; McKenna, G., Dramatic stiffening of ultrathin polymer films in the rubbery regime. *The European Physical Journal E: Soft Matter and Biological Physics* **2006,** *20* (2), 143-150.

80. Bodiguel, H.; Fretigny, C., Reduced Viscosity in Thin Polymer Films. *Physical Review Letters* **2006,** *97* (26), 266105.

81. Hamdorf, M.; Johannsmann, D., Surface-rheological measurements on glass forming polymers based on the surface tension driven decay of imprinted corrugation gratings. *Journal of Chemical Physics* **2000,** *112* (9).

82. Serghei, A.; Huth, H.; Schick, C.; Kremer, F., Glassy Dynamics in Thin Polymer Layers Having a Free Upper Interface. *Macromolecules* **2008,** *41* (10), 3636-3639.

83. Rotella, C.; Napolitano, S.; De Cremer, L.; Koeckelberghs, G.; Wubbenhorst, M., Distribution of Segmental Mobility in Ultrathin Polymer Films. *Macromolecules* **2010,** *43* (20), 8686-8691.

84. Tanaka, K.; Yoon, J.-S.; Takahara, A.; Kajiyama, T., Ultrathinning-Induced Surface Phase Separation of Polystyrene/Poly(vinyl methyl ether) Blend Film. *Macromolecules* **1995,** *28* (4), 934-938.

85. Tanaka, K.; Takahara, A.; Kajiyama, T., Film Thickness Dependence of the Surface Structure of Immiscible Polystyrene/Poly(methyl methacrylate) Blends. *Macromolecules* **1996,** *29* (9), 3232-3239.

86. Despotopoulou, M. M.; Frank, C. W.; Miller, R. D.; Rabolt, J. F., Kinetics of Chain Organization in Ultrathin Poly(di-n-hexylsilane) Films,Ä†. *Macromolecules* **1996,** *29* (18), 5797-5804.

87. Pfromm, P. H.; Koros, W. J., Accelerated physical ageing of thin glassy polymer films: evidence from gas transport measurements. *Polymer* **1995,** *36* (12), 2379-2387.

88. Huang, Y.; Paul, D. R., Effect of Film Thickness on the Gas-Permeation Characteristics of Glassy Polymer Membranes. *Industrial & Engineering Chemistry Research* **2007,** *46* (8), 2342-2347.

89. Priestley, R. D., Physical aging of confined glasses. *Soft Matter* **2009,** *5* (5), 919-926.

90. Priestley, R. D.; Broadbelt, L. J.; Torkelson, J. M., Physical Aging of Ultrathin Polymer Films above and below the Bulk Glass Transition Temperature: Effects of Attractive vs Neutral Polymer,àíSubstrate Interactions Measured by Fluorescence. *Macromolecules* **2005,** *38* (3), 654-657.

91. Burnham, N. A.; Colton, R. J., Measuring the nanomechanical properties and surface forces of materials using an atomic force microscope. *Journal of Vacuum Science & Technology a-Vacuum Surfaces and Films* **1989,** *7* (4), 2906-2913.

92. Forrest, J. A.; Dalnoki-Veress, K.; Dutcher, J. R., Brillouin light scattering studies of the mechanical properties of thin freely standing polystyrene films. *Physical Review E* **1998,** *58* (5), 6109-6114.

93. Kajiyama, T.; Tanaka, K.; Satomi, N.; Takahara, A., Surface Relaxation Process of Monodisperse Polystyrene Film Based on Lateral Force Microscopic Measurements. *Macromolecules* **1998,** *31* (15), 5150-5151.

94. Every, A. G., Measurement of the near-surface elastic properties of solids and thin supported films. *Measurement Science & Technology* **2002,** *13* (5), R21-R39.

95. Corcoran, S. G.; Colton, R. J.; Lilleodden, E. T.; Gerberich, W. W., Anomalous plastic deformation at surfaces: Nanoindentation of gold single crystals. *Physical Review B* **1997,** *55* (24), 16057-16060.

96. Oliver, W. C.; Pharr, G. M., An improved technique for determining hardnress and elastic-modulus using load and dispalcement sensing indentation experiments. *Journal of Materials Research* **1992,** *7* (6), 1564-1583.

97. Briscoe, B. J.; Sebastian, K. S.; Sinha, S. K., Application of the compliance method to microhardness measurements of organic polymers. *Philosophical Magazine a-Physics of Condensed Matter Structure Defects and Mechanical Properties* **1996,** *74* (5), 1159-1169.

98. Burnham, N. A.; Colton, R. J., Measuring the nanomechanical properties and surface forces of materials using an atomic force miscroscope. *Journal of Vacuum Science & Technology a-Vacuum Surfaces and Films* **1989,** *7* (4), 2906-2913.

99. Joyce, S. A.; Houston, J. E., A new force sensor incorporating force-feedback control for interfacial force microscopy. *Review of Scientific Instruments* **1991,** *62* (3), 710-715.

100. Dimitriadis, E. K.; Horkay, F.; Maresca, J.; Kachar, B.; Chadwick, R. S., Determination of elastic moduli of thin layers of soft material using the atomic force microscope. *Biophysical Journal* **2002,** *82* (5), 2798-2810.

101. Gomopoulos, N.; Cheng, W.; Efremov, M.; Nealey, P. F.; Fytas, G., Out-of-Plane Longitudinal Elastic Modulus of Supported Polymer Thin Films. *Macromolecules* **2009,** *42* (18), 7164-7167.

102. Stafford, C. M.; Harrison, C.; Beers, K. L.; Karim, A.; Amis, E. J.; Vanlandingham, M. R.; Kim, H. C.; Volksen, W.; Miller, R. D.; Simonyi, E. E., A buckling-based metrology for measuring the elastic moduli of polymeric thin films. *Nature Materials* **2004,** *3* (8), 545-550.

103. Genzer, J.; Groenewold, J., Soft matter with hard skin: From skin wrinkles to templating and material characterization. *Soft Matter* **2006,** *2* (4), 310-323.

104. Huck, W. T. S., Artificial skins: Hierarchical wrinkling. *Nat Mater* **2005,** *4* (4), 271-272.

105. Jeong, H. E.; Kwak, M. K.; Suh, K. Y., Stretchable, Adhesion-Tunable Dry Adhesive by Surface Wrinkling. *Langmuir 26* (4), 2223-2226.

106. Graz, I. M.; Cotton, D. P. J.; Lacour, S. P., Extended cyclic uniaxial loading of stretchable gold thin-films on elastomeric substrates. *Applied Physics Letters* **2009,** *94* (7), 071902-3.

107. Lacour, S. P., Huang, Z., Suo, Z., Wagner, S., Deformable interconnects for conformal integrated circuits. *Materials Research Society Symposium* **2002,** *736* (D4.8), 1-6.

108. Lacour, S. P.; Wagner, S.; Huang, Z. Y.; Suo, Z., Stretchable gold conductors on elastomeric substrates. *Applied Physics Letters* **2003,** *82* (15), 2404-2406.

109. Wagner, S.; Lacour, S. P.; Jones, J.; Hsu, P. H. I.; Sturm, J. C.; Li, T.; Suo, Z. G., Electronic skin: architecture and components. *Physica E-Low-Dimensional Systems & Nanostructures* **2004,** *25* (2-3), 326-334.

110. Jones, J., Lacour, S.P., Suo, Z., Wagner, S., A method for making elastic metal interconnects. *Materials Research Society Symposium* **2003,** *736* (H6), 1-6.

111. Wang, S.; Xiao, J.; Song, J.; Ko, H. C.; Hwang, K.-C.; Huang, Y.; Rogers, J. A., Mechanics of curvilinear electronics. *Soft Matter* **2010,** *6* (22), 5757-5763.

112. Bowden, N.; Huck, W. T. S.; Paul, K. E.; Whitesides, G. M., The controlled formation of ordered, sinusoidal structures by plasma oxidation of an elastomeric polymer. *Applied Physics Letters* **1999,** *75* (17), 2557-2559.

113. Harrison, C.; Stafford, C. M.; Zhang, W. H.; Karim, A., Sinusoidal phase grating created by a tunably buckled surface. *Applied Physics Letters* **2004,** *85* (18), 4016-4018.

114. Lin, P.-C.; Vajpayee, S.; Jagota, A.; Hui, C.-Y.; Yang, S., Mechanically tunable dry adhesive from wrinkled elastomers. *Soft Matter* **2008,** *4* (9), 1830-1835.

115. Jiang, X. Y.; Takayama, S.; Qian, X. P.; Ostuni, E.; Wu, H. K.; Bowden, N.; LeDuc, P.; Ingber, D. E.; Whitesides, G. M., Controlling mammalian cell spreading and cytoskeletal arrangement with conveniently fabricated continuous wavy features on poly(dimethylsiloxane). *Langmuir* **2002,** *18* (8), 3273-3280.

116. Efimenko, K.; Rackaitis, M.; Manias, E.; Vaziri, A.; Mahadevan, L.; Genzer, J., Nested self-similar wrinkling patterns in skins. *Nature Materials* **2005,** *4* (4), 293-297.

117. Huang, R., Kinetic wrinkling of an elastic film on a viscoelastic substrate. *Journal of the Mechanics and Physics of Solids* **2005,** *53* (1), 63-89.

118. Huang, R.; Stafford, C. M.; Vogt, B. D., Effect of surface properties on wrinkling of ultrathin films. *Journal of Aerospace Engineering* **2007,** *20* (1), 38-44.

119. Mei, H. X.; Huang, R.; Chung, J. Y.; Stafford, C. M.; Yu, H. H., Buckling modes of elastic thin films on elastic substrates. *Applied Physics Letters* **2007,** *90* (15).

120. Volynskii, A. L.; Bazhenov, S.; Lebedeva, O. V.; Bakeev, N. F., Mechanical buckling instability of thin coatings deposited on soft polymer substrates. *Journal of Materials Science* **2000,** *35* (3), 547-554.

121. Biot, M. A., Bending of an infinite beam on an elastic foundation. *Journal of Applied Mechanics* **1937,** *203* (A1).

122. Huang, Z. Y.; Hong, W.; Suo, Z., Evolution of wrinkles in hard films on soft substrates. *Physical Review E* **2004,** *70* (3).

123. Lin, P. C.; Yang, S., Spontaneous formation of one-dimensional ripples in transit to highly ordered two-dimensional herringbone structures through sequential and unequal biaxial mechanical stretching. *Applied Physics Letters* **2007,** *90* (24).

124. Huang, Z. Y.; Hong, W.; Suo, Z., Nonlinear analyses of wrinkles in a film bonded to a compliant substrate. *Journal of the Mechanics and Physics of Solids* **2005,** *53* (9), 2101-2118.

125. Wilder, E. A.; Guo, S.; Lin-Gibson, S.; Fasolka, M. J.; Stafford, C. M., Measuring the modulus of soft polymer networks via a buckling-based metrology (vol 39, pg 4138, 2006). *Macromolecules* **2006,** *39* (17), 5956-5956.

126. Balmforth, N. J.; Craster, R. V.; Slim, A. C., On the buckling of elastic plates. *Q J Mechanics Appl Math* **2008,** *61* (2), 267-289.

127. Nolte, A. J.; Cohen, R. E.; Rubner, M. F., A two-plate buckling technique for thin film modulus measurements: Applications to polyelectrolyte multilayers. *Macromolecules* **2006,** *39* (14), 4841-4847.

128. Tsui, O. K. C.; Russell, T. P.; Hawker, C. J., Effect of interfacial interactions on the glass transition of polymer thin films. *Macromolecules* **2001,** *34* (16), 5535-5539.

129. Bohme, T. R.; de Pablo, J. J., Evidence for size-dependent mechanical properties from simulations of nanoscopic polymeric structures. *Journal of Chemical Physics* **2002,** *116* (22), 9939-9951.

130. Liu, Y.; Russell, T. P.; Samant, M. G.; Stohr, J.; Brown, H. R.; Cossy-Favre, A.; Diaz, J., Surface Relaxations in Polymers. *Macromolecules* **1997,** *30* (25), 7768-7771.

131. Nolte, A. J.; Takane, N.; Hindman, E.; Gaynor, W.; Rubner, M. F.; Cohen, R. E., Thin Film Thickness Gradients and Spatial Patterning via Salt Etching of Polyelectrolyte Multilayers. *Macromolecules* **2007,** *40* (15), 5479-5486.

132. Nolte, A. J.; Treat, N. D.; Cohen, R. E.; Rubner, M. F., Effect of Relative Humidity on the Young's Modulus of Polyelectrolyte Multilayer Films and Related Nonionic Polymers. *Macromolecules* **2008,** *41* (15), 5793-5798.

133. Mansfield, M.; Needs, R. J., Surface energy and stress of lead (111) and (110) surfaces. *Physical Review B* **1991,** *43* (11), 8829.

134. Marlo, M.; Milman, V., Density-functional study of bulk and surface properties of titanium nitride using different exchange-correlation functionals. *Physical Review B* **2000,** *62* (4), 2899.

135. Cammarata, R. C.; Sieradzki, K., Effects of surface stress on the elastic moduli of thin films and superlattices. *Physical Review Letters* **1989,** *62* (17), 2005.

136. Li, L.; Ng, K.-M.; Chan, C.-M.; Feng, J.-Y.; Zeng, X.-M.; Weng, L.-T., Surface Studies of the Rearrangement of End Groups of a Polymer by ToF‚àíSIMS and AFM. *Macromolecules* **2000,** *33* (15), 5588-5592.

137. Fukao, K.; Miyamoto, Y., Glass transition temperature and dynamics of Œ±-process in thin polymer films. *EPL (Europhysics Letters)* **1999,** *46* (5), 649.

138. Boudaoud, A.; Chaieb, S., Mechanical phase diagram of shrinking cylindrical gels. *Physical Review E* **2003,** *68* (2).

139. Bowden, N.; Brittain, S.; Evans, A. G.; Hutchinson, J. W.; Whitesides, G. M., Spontaneous formation of ordered structures in thin films of metals supported on an elastomeric polymer. *Nature* **1998,** *393* (6681), 146-149.

140. Chua, D. B. H.; Ng, H. T.; Li, S. F. Y., Spontaneous formation of complex and ordered structures on oxygen-plasma-treated elastomeric polydimethylsiloxane. *Applied Physics Letters* **2000,** *76* (6), 721-723.

141. Hayward, R. C.; Chmelka, B. F.; Kramer, E. J., Template cross-linking effects on morphologies of swellable block copolymer and mesostructured silica thin films. *Macromolecules* **2005,** *38* (18), 7768-7783.

142. Kwon, S. J.; Park, J. H.; Park, J. G., Wrinkling of a sol-gel-derived thin film. *Physical Review E* **2005,** *71* (1).

143. Mora, T.; Boudaoud, A., Buckling of swelling gels. *European Physical Journal E* **2006,** *20* (2), 119-124.

144. Tanaka, H.; Tomita, H.; Takasu, A.; Hayashi, T.; Nishi, T., Morphological and kinetic evolution of surface patterns in gels during the swelling process- evidence of dynamic pattern ordering. *Physical Review Letters* **1992,** *68* (18), 2794-2797.

145. Southern, E.; Thomas, A. G., Effect of constraints on equilibrium swelling of rubber vulcanizates. *Journal of Polymer Science Part a-General Papers* **1965,** *3* (2PA), 641-&.

146. Chan, E. P.; Crosby, A. J., Spontaneous formation of stable aligned wrinkling patterns. *Soft Matter* **2006,** *2* (4), 324-328.

147. Chung, J. Y.; Nolte, A. J.; Stafford, C. M., Diffusion-Controlled, Self-Organized Growth of Symmetric Wrinkling Patterns. *Advanced Materials* **2009,** *21* (13), 1358-1362.

148. Myoung-Woon, M.; Sang Hoon, L.; Jeong-Yun, S.; Kyu Hwan, O.; Ashkan, V.; John, W. H., Controlled formation of nanoscale wrinkling patterns on polymers using focused ion beam. **2007,** *57* (8), 747-750.

149. Matsuo, E. S.; Tanaka, T., Patterns in shrinking gels. *Nature* **1992,** *358* (6386), 482-485.

150. Klein, R. J.; Fischer, D. A.; Lenhart, J. L., Systematic oxidation of polystyrene by ultraviolet-ozone, characterized by near-edge X-ray absorption fine structure and contact angle. *Langmuir* **2008,** *24* (15), 8187-8197.

151. Nie, H. Y.; Walzak, M. J.; Berno, B.; McIntyre, N. S., Atomic force microscopy study of polypropylene surfaces treated by UV and ozone exposure: modification of morphology and adhesion force. *Applied Surface Science* **1999,** *144-145*, 627-632.

152. Hong, W.; Liu, Z.; Suo, Z., Inhomogeneous swelling of a gel in equilibrium with a solvent and mechanical load. *International Journal of Solids and Structures* **2009,** *46* (17), 3282-3289.

153. Flory, P. J.; Rehner, J. J., Statistical Mechanics of Cross-Linked Polymer Networks II. Swelling. *The Journal of Chemical Physics* **1943,** *11* (11), 521-526.

154. Guvendiren, M. Y., S.; Burdick, J.A., Swelling-induced surface patterns in hydrogels with gradient crosslinking density. *Advanced Functional Materials* **2009,** *19*, 3038-3045.

155. Trujillo, V.; Kim, J.; Hayward, R. C., Creasing instability of surface-attached hydrogels. *Soft Matter* **2008,** *4* (3), 564-569.

156. Hendricks, T. R.; Lee, I., Wrinkle-Free Nanomechanical Film: Control and Prevention of Polymer Film Buckling. *Nano Letters* **2006,** *7* (2), 372-379.

157. Stafford, C. M.; Guo, S.; Harrison, C.; Chiang, M. Y. M., Combinatorial and high-throughput measurements of the modulus of thin polymer films. *Review of Scientific Instruments* **2005,** *76* (6).

158. JELLISON; #160; E., G., *Data analysis for spectroscopic ellipsometry*. Elsevier: Lausanne, SUISSE, 1993.

159. Conroy, M., Advances in thick and thin film analysis using interferometry. *Wear* **2009,** *266* (5-6), 502-506.

160. Kim, D.; Kim, S.; Kong, H. J.; Lee, Y., Measurement of the thickness profile of a transparent thin film deposited upon a pattern structure with an acousto-optic tunablefilter. *Opt. Lett.* **2002,** *27* (21), 1893-1895.

161. Mukherjee, M.; Singh, A.; Daillant, J.; Menelle, A.; Cousin, F., Effect of Solvent,àíPolymer Interaction in Swelling Dynamics of Ultrathin Polyacrylamide Films:,Äâ A Neutron and X-ray Reflectivity Study. *Macromolecules* **2007,** *40* (4), 1073-1080.

162. Herzinger, C. M.; Johs, B.; McGahan, W. A.; Woollam, J. A.; Paulson, W., Ellipsometric determination of optical constants for silicon and thermally grown silicon dioxide via a multi-sample, multi-wavelength, multi-angle investigation. *Journal of Applied Physics* **1998,** *83* (6), 3323-3336.

163. Goken, M.; Kempf, M.; Nix, W. D., Hardness and modulus of the lamellar microstructure in PST-TiAl studied by nanoindentations and AFM. *Acta Materialia* **2001,** *49* (5), 903-911.

164. Bowen, W. R.; Lovitt, R. W.; Wright, C. J., Atomic Force Microscopy Study of the Adhesion of Saccharomyces cerevisiae. *Journal of Colloid and Interface Science* **2001,** *237* (1), 54-61.

165. Boland, T.; Ratner, B. D., Direct measurement of hydrogen bonding in DNA nucleotide bases by atomic force microscopy. *Proceedings of the National Academy of Sciences of the United States of America* **1995,** *92* (12), 5297-5301.

CHAPTER 2

DEPENDENCE OF THE ELASTIC MODULUS ON THE GLASS TRANSITION TEMPERATUE AND MOLECULAR MASS

2.1 Introduction

One of the fundamental principles used in understanding the viscoelastic properties of polymers is time-temperature superposition, which enables the collapse of temperature and rate dependencies of the complex modulus to a single master curve.[1, 2] This correlation enables prediction of long-term mechanical properties of polymers. Williams, Landel and Ferry (WLF) illustrated the use of a single empirical shift factor and a reference temperature to correlate the rheological data for several macromolecules.[2] The glass transition temperature (T_g) is commonly employed as the reference condition due to the viscoelastic behavior of the polymer being extremely sensitive to temperature near T_g.[3] For example the Young's modulus can decrease orders of magnitude as the temperature is decreased from just above T_g to just below T_g. Additionally, universal empirical parameters have been found when setting the reference temperature near T_g.[4] This dependence of modulus of T_g in the bulk has been proposed to also apply to polymers at the nanoscale.[5, 6] Understanding the modulus and its dependence on T_g at the nanoscale is essential since the long-term mechanical stability of polymer nanostructures is critical for numerous developed and emerging applications including photonics,[7] microelectronics,[8] non-linear optics, and biosensors[9]. For example, the future for semiconductor manufacturing aims at the production of polymeric nanostructures in the sub 32 nm range. Nanometer sized features are fabricated by a lithographic process.[10] The

traditional photolithography process involves the deposition of a resist layer. This resist layer is patterned, etched, and then removed by a developer. It is during the development step where the surface tension of the rinse liquid causes the nanoscale pattern to collapse.[11] The future of nanoscale features has lead to the development of an alternative nanolithographic techniques including nanoimprint and block copolymer lithography. A key advantage with these lithographic techniques is the ability to pattern sub 25 nm structures over a large area with high throughput and relatively low cost.[12] For block copolymer lithography, the molecular scale self-assembly of diblock copolymers is harnessed to create the nanoscale features. The feature size is control via domain length with successful features including pillars and cylinders being reported.[13] Selective removal of domain structures provides the template for pattern transfer. Nanoimprint lithography is a two-step process where a mold with etched nanostructures is pressed onto a thin resist film. This step creates a thickness contrasts pattern that is transferred throughout the resist film via reactive ion etching or ultraviolet exposure. Therefore, decreases in the mechanical properties at small length scales would be detrimental to patterning for next generation lithography.[14] In nanoimprint lithography[15] for example, the flow resistance of polymer melts in confined geometries has recently been reported to decrease when the slit width is comparable to the molecular dimensions of the polymer.[16] More importantly, the induced flow of the polymer into the mold creates a large amount of shear stress, therefore the molded structure then has tremendous residual stress,[17] thus understanding the elastic modulus in confined geometries is also critical to the

stability of structures formed via nanoimprint lithography. Lastly, block copolymer lithography utilizes polystyrene below its entanglement molecular mass to create nanostructures; [18, 19] therefore mechanical properties as a function of molecular mass are important to the ultimate stability of these nanostructures. Thus for predicting mechanical stability of polymeric nanostructures, direct measurements of the mechanical properties such as Young's modulus is desired for polymers when confined to nanometer dimensions. As the ability to correlate deviations at bulk T_g with modulus behavior at the nanometer length scale is unknown.

The T_g of ultrathin polymer films has exhibited deviations from bulk values at the nanometer length scale. However, the origins of the deviations in properties of thin polymer films are still being debated.[3, 20-27] In particular, polystyrene (PS) and poly (methyl methacrylate) have become model systems for thin film measurements,[3, 27, 28] but even for these systems, there are inconsistent results regarding the direction of deviations[23, 29] in T_g and the influence of molecular mass.[30, 31] For example the T_g of PS has shown no molecular mass effect when confined to a substrate, however free standing PS films exhibit significant reductions in T_g with increasing molecular mass.[32] Two potential origins for the observed deviations have been discussed based upon (1) the confinement of the polymer chains[25, 33] and (2) increased contributions from interfacial effects as the film thickness is decreased (increased surface area to volume ratio)[3]. Typically the characteristic size used is the radius of gyration, R_g, which is the average distance from the center of gravity to the chain end. As the

radius of gyration gives a quantitative way to measure the effective size of the polymer under given conditions. At film thicknesses of several R_g, deviations in the physical properties of the polymer relative to the bulk are generally observed for a host of different properties such as polymer interdiffusion, mobility, and thermal expansion.[34-36] The radius of gyration has been found to be proportional to the square root of the number of polymer units or molecular mass.[37] Thus, due to the dependence of R_g on molecular mass it is expected that changing the molecular mass would significantly influence the behavior of thin films.[25] That is as the intrinsic size of the polymer is decreased, the deviation from bulk values due to confinement effects would be reduced. However based upon recent reports, there exists growing evidence that T_g is independent of molecular mass in thin films.[30, 38] Understanding if there is any dependence of the modulus on M_n for thin films is important from both a fundamental and practical prospective. It is fundamentally interesting to understand the impact of intrinsic size on the nanometer length scale modulus while practically polymers with different molecular weights are employed in a variety of applications at the nanometer length scale.

Although limited experimental data exists on the modulus of polymeric thin films, a series of discontinuous molecular dynamic simulations have been conducted.[39, 40] These simulations have suggested that deviations in the modulus of a polymer deep in the glass, when bulk T_g is significantly higher than the experimental temperature, occur near 40 nm as observed from extracted apparent Young's Moduli.[39] For example, in previous wrinkling studies, the reduced

modulus, (E_f / E_{bulk}), for PS and PMMA thin films is found to exhibit statistically identical behavior with deviations from the bulk modulus at approximately 40 nm at ambient temperature,[41] in agreement with the above simulations as both PS (T_g~100°C) and PMMA (T_g~105°C) are deep in the glass. However, 40 nm is also close to the length scale where changes in the thin film T_g for PMMA and PS are typically observed.[42, 43] Interestingly, simulations by Bohme and de Pablo suggest the existence of significant stress relaxation occurring at the air-polymer interface even at temperatures deep in the glass where a deviation in mechanical properties would not be expected.[39]

These experimental and simulation results[39] call into question some of the common assumptions regarding the relationship between thin film T_g and mechanical properties.[5, 44] For example, if a significant decrease in modulus would be observed as bulk T_g is approached or a correlation between thin film T_g and modulus behavior. However, McKenna and coworkers have demonstrated that the creep compliance of thin polymer films experience stiffening in the rubbery regime in comparison to the bulk even in the absence of any change in the T_g of thin films.[45] This results suggest that changes in polymer T_g due to confinement are not correlated with the moduli of polymer thin films. To develop a more clear understanding of the relationship between T_g and elastic modulus of ultrathin polymer films, experiments need to be conducted over a wide range of bulk T_g's. By varying the bulk T_g of the materials studied at room temperature a wide range in quench depth ($T_{g,bulk}$-T) is examined. It is in the region, T→T_g, that the mechanical properties of bulk polymeric materials exhibit increased

cooperativity and molecular motions that lead to a depression in modulus.[46] By understanding the modulus behavior for ultrathin films near their bulk glass transition temperature as well as the nanometer length scale T_g behavior, we will be able to establish whether fundamental concepts such as the WLF equation, considered basic tenets of polymer science, indeed hold true at the nanoscale.

In this Chapter, the impact of quench depth and intrinsic polymer size will be studied. First, a series of methacrylate polymers are examined to determine how the quench depth into the glass for the bulk polymer impacts the moduli of thin films. The use of methacrylate polymers allows for the quench depth to be readily varied without requiring in-situ heating or cooling during the experiments, as T_g is significantly impacted by unbranched alkyl chain length.[47] Moreover, the chemistry difference is less for these methacrylate polymers than between PMMA and PS examined previously where these two glassy polymers exhibited statistically identical fractional changes in modulus as the film thickness is decreased below approximately 40 nm.[48] Thus, we hypothesize that the chemistry effects from changes in the alkyl chain length from methyl to n-propyl on the thin film modulus behavior will be minor in comparison to the large changes in quench depth (75°C), if simulations capture the physics of thin film mechanics.[39, 40] Additionally, a wide range of PS molecular mass from 1.2 kg/mol to 990 kg/mol is examined to determine how molecular mass impacts the elastic modulus of thin polymer films. Decreasing the molecular mass from 990kg/mol to 1.2 kg/mol leads to an order of magnitude change in R_g, 20 nm to 0.6 nm respectively, allowing for the mechanical behavior of thin films to be related back

to the characteristic size. However, a decrease in molecular mass also impacts the glass transition temperature below the entanglement molecular mass.[37] Therefore, studying both the PS and poly (alkyl methacrylate)s leads to an improved understanding of the modulus with respect to quench depth and characteristic size.

2.2 Experimental

Poly(methyl methacrylate) (PMMA) was purchased from Polymer Source (M_w=91 kg/mol, T_g=105°C). Four other methacrylate polymers, poly(ethyl methacrylate) (PEMA) (M_w=250 kg/mol, T_g=65°C), poly(n-propyl methacrylate) (PnPMA) (M_w=70 kg/mol, T_g=36.1°C), poly(benzyl methacrylate) (PBzMA) (M_w=70 kg/mol, T_g=54°C), and poly(isobutyl methacrylate) (PiBMA) (M_w=200 kg/mol, T_g=47 °C) were obtained from Scientific Polymer Products. M_w is the mass average relative molecular mass. The T_g of each methacrylate polymer was determined from the discontinuity in the CTE of thick (> 100 nm) films using ellipsometry as reported previously.[24]

Table 2.1 Physical characteristics of PS utilized in this study.

M_n (kg/mol)	M_w/M_n	$T_{g, bulk}$(°C)
990	1.05	106.3 ± 2.0
492	1.03	106.1 ± 2.5
9.4	1.06	94.1 ± 2.3
3.2	1.05	76.1 ± 2.2
2.3	1.05	62.3 ± 1.5
1.3	1.13	29.9 ± 3.1
1.2	1.13	21.3 ± 3.2

PS with varying molecular mass were purchased from Polymer Laboratories. The PS used in this study was synthesized with butyllithium initiator and are methyl terminated. The molecular mass of the PS samples were independently measured by gel permeation chromatography (GPC) using a Waters Breeze 2 equipped with a Waters 1515 high-performance liquid chromatography pump and a Waters 2414 refractive index detector. Two size exclusion chromatography columns (Waters HT2 and HT6E) with tetrahydrofuran as the mobile phase were used at a flow rate of 1 mL/min to separate, identify, and quantify samples. Samples were prepared at 2 mg/mL. Data processing was conducted using the GPC Isocratic Technique in the Breeze software. A 3rd order calibration was conducted using Polymer Labs Easical PS2B as the calibrant. The glass transition temperature of each PS was measured using differential scanning calorimetry (DSC), which was performed on a TA Instruments Q1000 heat flux DSC under a dry nitrogen purge (50.0 mL/min). All runs were performed at heating and cooling rates of 10 °C/min in T4P mode, and temperature calibration for heating runs was achieved using an indium standard at the same heating rate. The physical characteristics of these polymers are listed in Table 2.1.

Silicon wafers (450 mm thick) were used as substrates for PS films after being cut into 2.5 cm × 1 cm pieces and cleaned with ultraviolet/ozone (model 342, Jelight, Inc.). Mica substrates were used for the poly (alkyl methacrylate) series due to the increase in bonding between the methacrylate and the silanol. Dilute polymer solutions were spin-cast from toluene onto the substrates to create thin films of uniform thickness.

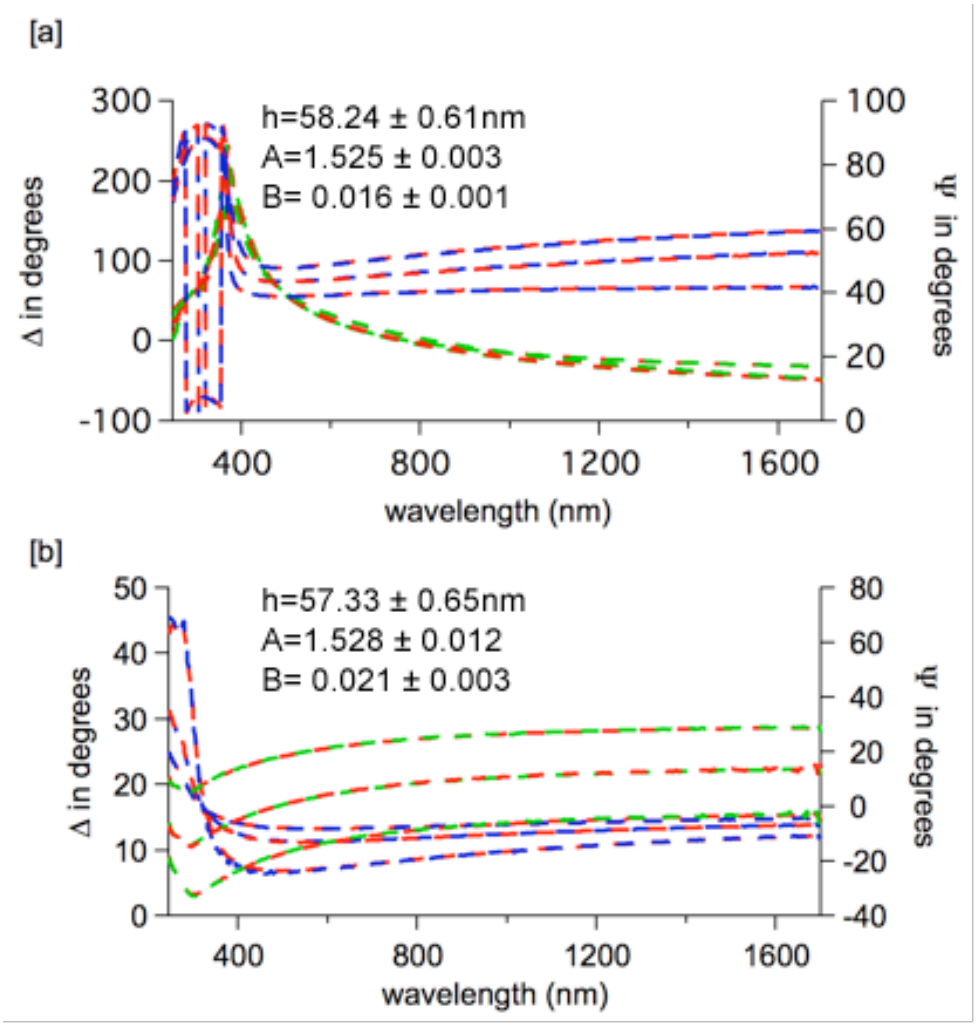

Figure 2.1 Ellipsometric angles, Δ (green) and Ψ (blue), for PS on [a] Si wafer [b] PDMS with a Cauchy fit (red).

Film thickness was controlled by polymer concentration (0.2 % to 2 % by mass polymer) and spin speed (150 rad/s to 265 rad/s). The thickness of the polymer film was determined using a Variable Angle Spectroscopic Ellipsometer (VASE, J.A. Woollam Co., Inc.) over a wavelength range from 250 nm to 1700 nm at three incident angles, 67°, 70°, and 73° in order to account for the Brewster angle of the substrate which allows for increased light transmission and decreased reflection. The data were fit using a Cauchy layer to represent optical constants of the polymer. Figure 2.1 shows the Cauchy fit of 990kg/mol PS on

both the Si wafer and once transferred onto the PDMS substrate. The fits to the Cauchy model, A and B, as well as the film thickness are shown as inserts in each figure. From the fits, the film thickness for both remains statistically invariant. For a detailed discussion on the Cauchy fit refer to Chapter 1. Polydimethylsiloxane (PDMS) (Sylgard 184, Dow Corning) was prepared at a ratio of 20:1 by mass of base to curing agent and cast on float glass to a thickness of approximately 1.5 mm. The PDMS was allowed to gel at room temperature for 3 h before curing at 100 °C for 2 h. After cooling, the PDMS sheet was cut into 2.5 cm × 7.5 cm × 1.5 mm slabs. The modulus of the bulk PDMS sheets was determined using a tensile test (Instron) at a cross head speed of 0.01 mm/s along the long dimension. The PDMS was pre-strained to 3 % on a custom stage.[41] The supported polymer film was placed in contact with the strained PDMS, and allowed to soft bond prior to being immersed in water. Due to the hydrophobic nature of the polymers, water preferentially segregates to the wafer surface. The film is therefore transfered from the wafer onto the PDMS. The sample was allowed to dry under vacuum at 10 °C below its bulk T_g to prevent thermal wrinkling. Heating above T_g would induce the required compressive force required for wrinkling due to the difference in the coefficient of thermal expansion of the polymer and PDMS. The film thickness of some samples was then re-measured with VASE, no statistical difference in film thickness was observed after transfer as discussed with Figure 2.1. The pre-strain on the PDMS was released at a rate of 0.1 mm/s in order to minimize defects and cracks. All samples were released at ambient temperature (T = 21 °C ± 2 °C).

The wrinkled surfaces were characterized using AFM and optical microscopy. AFM micrographs were acquired at ambient temperature on an Agilent Technologies 5500 system in tapping mode using Pico Plus 1.0 software at constant scan size of 7.5 μm × 7.5 μm and scan speed of 1 Hz. Optical micrographs were acquired on a Mititoyo Ultraplan FS-110 with an image resolution of 768 pixels × 1024 pixels. The wrinkling wavelength was determined using 1-D fast Fourier transforms (FFT) of the micrographs.

2.3 Results

The modulus of ultrathin films is examined using the wrinkling based metrology discussed in Chapter 1. The relationship between the film modulus and the wrinkling wavelength is given by[41]

$$\lambda = 2\pi h_f \left(\frac{\overline{E}_f}{3\overline{E}_s} \right)^{1/3} \xrightarrow{\text{rearranging}} \overline{E}_f = 3\overline{E}_s \left(\frac{\lambda}{2\pi h_f} \right)^3$$

(1)

Accurate metrologies for determining both the film thickness and the modulus of the substrate are well established, thereby allowing for the determination of the film modulus by measuring the wavelength, λ.

Figure 2.2 illustrates the sinusoidal structure resulting from the wrinkling of PMMA and PS films. These micrographs illustrate the increase in wavelength associated with an increase in film thickness as expected from Equation 1, where the substrate modulus, E_s, was maintained nominally constant at ≈ 1MPa. As the

film thickness is decreased from 200 nm to 47 nm for PMMA, the equilibrium wavelength decreases from 14.7 μm ± 0.9 μm to 4.3 μm ± 0.3 μm, respectively.

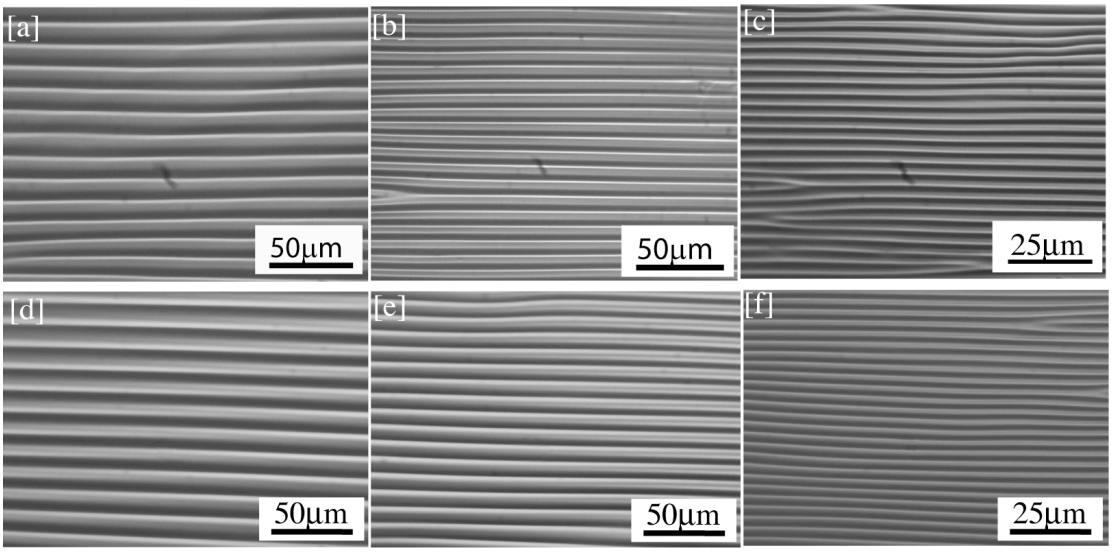

Figure 2.2 Optical micrographs of wrinkled 91kg/mol PMMA films that are (a) 200 nm, (b) 100 nm, (c) 47 nm thick, and 990 kg/mol PS films that are (d) 211 nm, (e) 121 nm, and (f) 48 nm thick. The wavelength of the wrinkles decreases as the film thickness is decreased.

Similarly, for the PS films the wavelength decreases from 14.3μm ± 0.41 μm to 3.7μm ± 0.22μm as the film thickness is decreased from 211 nm to 48 nm. Given the similar wavelengths as well as the linear relationship of wavelength to thickness the calculated modulus for these films is approximately 4 GPa and 3.8 GPa for PMMA and PS respectively. This is statistically invariant down to the 47 and 48 nm films. For thinner films, the wrinkles cannot be well-resolved with optical microscopy and instead AFM is utilized. As shown in Figure 2.3, the wrinkling wavelength for a 33 nm film of PMMA and a 25 nm film of 990kg/mol PS decreases to 2.5 μm ± 0.2 μm and 1.3 μm ± 0.3 μm respectively. However, this reduction in wavelength is greater than expected: suggesting a decrease in the modulus of the film. By examining the thickness dependence of the wavelength, a

more comprehensive picture of how the moduli of thin films vary with thickness can be constructed.

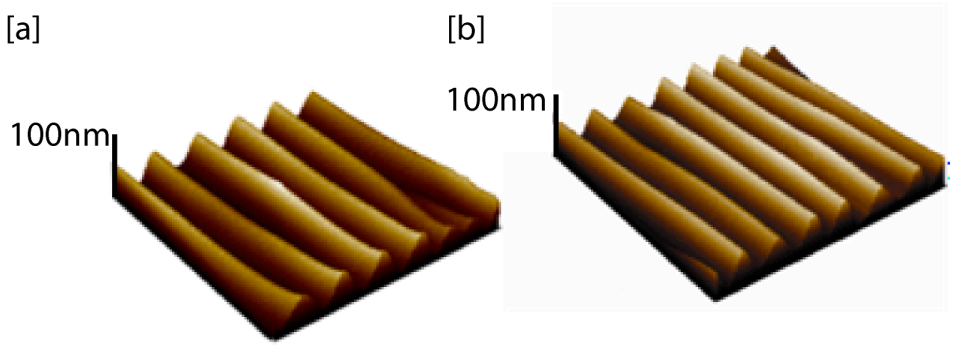

Figure 2.3 AFM images of wrinkled films of [a] 33 nm thick PMMA film and [b] 25 nm 990kg/mol PS film. Scan size is 7.5 mm × 7.5 mm and the height scale of the micrograph is 70 nm as shown.

According to simulations,[39] the quench depth into the bulk glassy state is an important factor in determining the length scale at which deviations in elastic modulus occur in thin films. By extraction of the apparent Young's moduli simulations suggest that as quench depth is decreased the deviation length scale is increased.[39] A schematic of critical length scales is shown in Figure 2.4, where for polymers deep in the glass (red), large quench depth, a deviation length scale of ≈40 nm is expected and those with $T_{g,bulk}$ closer to the experimental temperature show an increase in deviation length scales.

Although temperature-dependent measurements of the modulus would be preferred, the *in-situ* heating of a polymer-PDMS bilayer through all processing steps and characterization is impractical. Instead, a constant temperature (T=21 °C ± 2 °C) is utilized in these studies. The influence of quench depth is probed by variation in polymer chemistry to examine materials with widely varying T_g's; the series of poly(n-alkyl methacrylate)s represents an ideal series, as PMMA has been widely studied with regards to T_g and modulus. Furthermore, the bulk T_g of

these poly(n-alkyl methacrylate)s can be varied from well above ambient to below ambient temperature, simply by increasing the length of the alkyl chain from methyl to n-butyl.

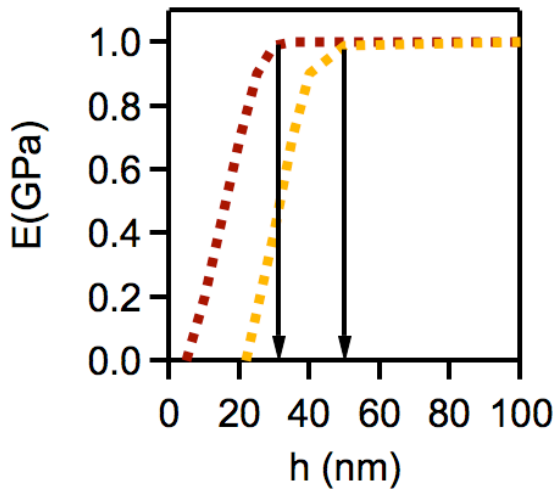

Figure 2.4 Schematic of the definition for deviation length scale from bulk modulus as discussed in the text. The deviation length scale is defined as the point at which deviation from bulk properties is observed denoted by the black arrow.

Figure 2.5 shows optical micrographs for approximately 100 nm thick films of PMMA, poly(ethyl methacrylate) (PEMA), and poly (n-propyl methacrylate) (PnPMA) that are wrinkled on a PDMS substrate. One salient feature to note is that the wavelength of the wrinkles also decreases as the alkyl chain length increases; this corresponds to a lower modulus in the longer alkyl polymers, as expected. The wavelength, λ, as a function of film thickness, h_f, for PMMA, PEMA, and PnPMA is shown in Figure 2.6 with nominally constant $\overline{E}_s$~0.7 MPa. The slope of the linear fits to the wavelength data decreases as the alkyl chain length is increased, 75 μm/nm (PMMA), 68 μm/nm (PEMA), 57 μm/nm and (PnPMA), which is consistent with a progressively smaller modulus

for PMMA to PEMA to PnPMA as increasing the alkyl chain has shown to lead to interal plasticization.[49] Additionally, the extrapolated wavelength does not extend through the origin as expcted due to the linear dependence of wavelength on film thickness. Instead, there appears to be a finite thickness (h_f^*) where the film might be intrinsically stable (zero wavelength), where no wrinkling is observed, if the linear thickness dependence on λ continues.

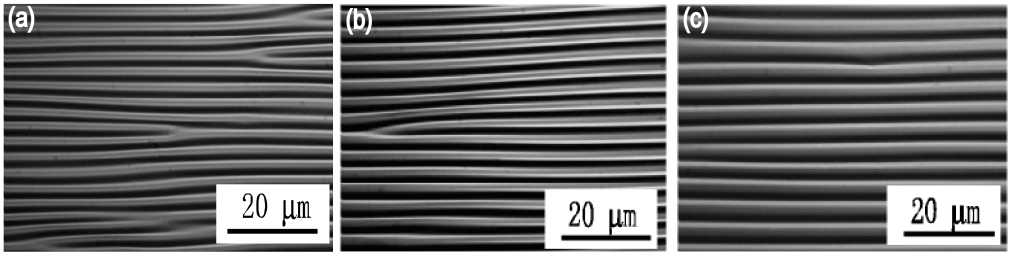

Figure 2.5 Optical micrographs of wrinkled ≈ 100 nm thick films of (a) PnPMA, (b) PEMA, and (c) PMMA. Note that the wavelength of the wrinkles decreases from PMMA to PEMA to PnPMA corresponding to a decreasing modulus.

However, this behavior has been previously reported for PS thin films and is attributed to free surface effects.[41] This free surface effect has been attributed both a reduction in steric constraints as well as an increase in free volume. In the case of the poly(n-alkyl methacrylate)s examined here, extrapolated thicknesses for null wavelength wrinkles are observed, up to nearly 15 nm for PnPMA as shown in Figure 2.6. As explained in the introduction in order to observed this wrinkling instability a pre-strain greater than the critical strain must be applied. As shown below the critical strain (ε_c) is proportional to the ratio of the plain-straine moduli of the substrate to the film ($\frac{\overline{E}_s}{\overline{E}_f}$).

$$\varepsilon_c = -\frac{1}{4}\left(\frac{3\bar{E}_s}{\bar{E}_f}\right)^{2/3}$$

(1)

Therefore a null wavelength would exists only when the critical strain could not be exceeded, or the film becomes liquid like.

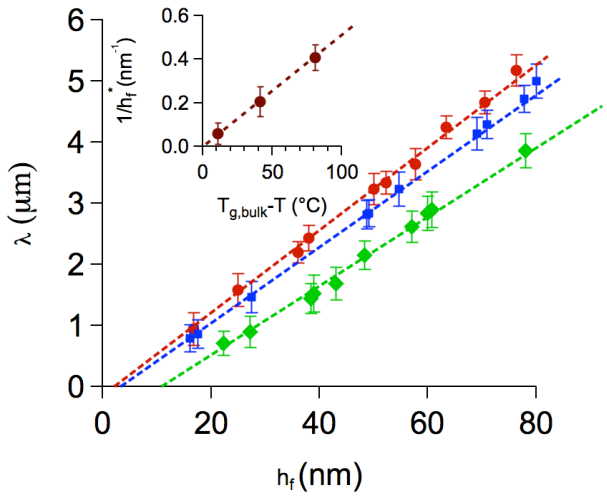

Figure 2.6 Wrinkling wavelength as a function of film thickness for PMMA (●), PEMA (■), and PnPMA (♦). The extrapolated wavelength-thickness correlation deviates from the origin, consistent with thickness dependent moduli.

The inset in Figure 2.6 shows that as the quench depth into the bulk glass is decreased, the extrapolated thickness for the zero wavelength shifts to larger values. Interestingly, this thickness appears inversely proportional to the quench depth (T_g-T). As T→T_g, h_f* increases (as $1/h_f^*$ decreases). Moreover, extrapolation to T = T_g results in the bulk polymer being apparently intrinsically stable from wrinkling ($h_f^* \approx \infty$). This result is expected, as a rubbery material (T ≈ T_g) would not exhibit stable wrinkles due to rapid relaxation. Moreover the critical strain in the material significantly exceeds the applied strain, $\varepsilon_c >> \varepsilon$. This

correlation between h_f* and (T_g-T) is consistent with simulations from de Pablo and coworkers where an increase in free surface mobility is expected as bulk T_g is approached.[44] The wavelength versus thickness should transverse the origin in the case of constant film and substrate moduli as discussed in Chapter 1 and shown in Equation 2. However since the wavelength becomes non-linear, it can be determined from Figure 2.6 that the moduli of these films are thickness dependent.

$$\lambda = 2\pi h_f \left(\frac{\bar{E}_f}{3\bar{E}_s} \right)^{1/3} \qquad (2)$$

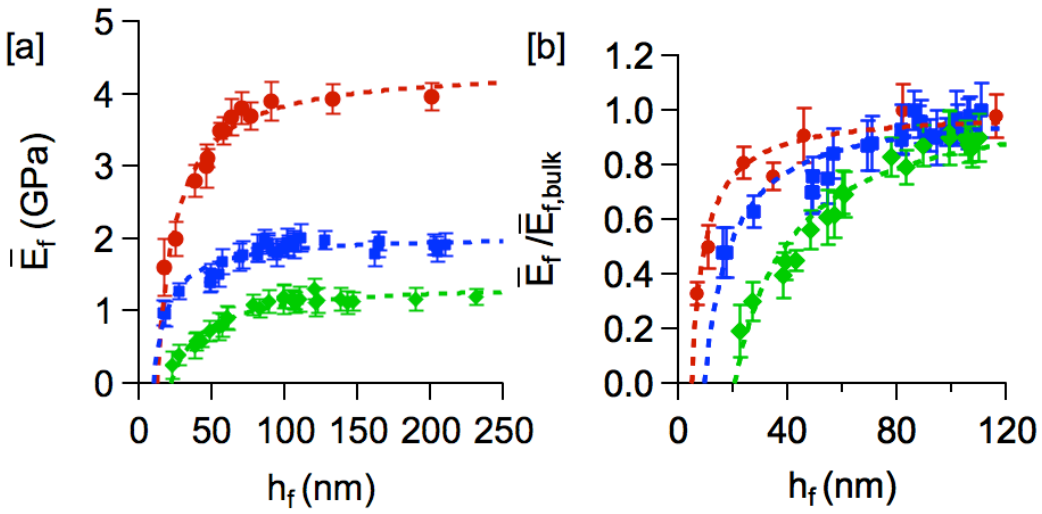

Figure 2.7 Elastic moduli of PMMA (●), PEMA (■), and PnPMA (♦) thin films as a function of film thickness. The dashed lines are a fit to the bilayer model.

Figure 2.7a illustrates the apparent moduli, $\bar{E}_f$, as a function of film thickness for PMMA, PEMA, and PnPMA as determined from film wrinkling. The modulus for thick films (> 100 nm) examined here was found to be independent of film thickness. By assuming a Poisson's ratio of 0.33[50], the Young's modulus of these >100 nm thick polymer films is estimated to be 3.48

GPa, 1.72 GPa, and 1.01 GPa for PMMA, PEMA, and PnPMA, respectively. These moduli correspond well with the corresponding bulk modulus reported in the literature of 3.2 GPa for PMMA, 1.8 GPa for PEMA, and 0.98 GPa for PnPMA.[41, 51, 52] The modulus of PMMA decreases as the thickness of the film is decreased below ≈ 50 nm and reaches a value that is 45% of the bulk value (1.65 GPa) at ≈ 20 nm, in agreement with previous reports for moduli of PMMA thin films.[41] The modulus of PEMA appears to deviate at slightly larger thicknesses (≈ 57 nm) and reaches 50% of its bulk value (0.86 GPa) at approximately 20 nm. However, due to statistical variation in the data, there is no significant difference in the deviation length scale from bulk modulus for PMMA and PEMA as shown in Figure 2.7b where the normalized data is plotted for PMMA, PEMA, and PnPMA. For PMMA and PEMA, both polymers are well into the glassy regime with bulk T_g's of 105 °C and 65 °C for PMMA and PEMA, respectively, in comparison to the measurement temperature, 21° C ± 2 °C. Additionally, h_f* are comparable between these two polymers, 5 nm (PMMA) vs. 7 nm (PEMA), so a large difference in the thickness dependence on the modulus might not be expected. The moduli of PnPMA, having a lower quench depth ($T_{g,bulk}$ = 36.1 °C), begins to deviate from bulk at a significantly larger length scale ≈ 80 nm, decreasing to 0.31 GPa at ≈ 20 nm, or 31% of its bulk modulus. This correspondence between bulk quench into the glass ($T_{g,bulk}$ − T) and deviation thickness is consistent with predictions from simulations.[40] Additionally, to better assess the surface layer or the intrinsically stable layer, as discussed in Chapter 1, a bilayer model is used.[53] In this model, the polymer film consists of two distinct

layers: a surface layer of thickness δ with elastic modulus $\overline{E}_f^*$, and the remainder of the film of thickness h_f - δ with bulk elastic modulus $\overline{E}_f$. Additionally, δ is assumed to be a material property and independent of h_f. The film elastic modulus is then a function of both the bulk $\overline{E}_f$ and the surface elastic modulus ($\overline{E}_f^*$). The dashed lines in Figure 2.7 represent the fit to this bilayer model. The fits to the bilayer model reveal an increasing free surface layer, δ, from 4.6 nm, 7.1 nm, to 22 nm with increasing alkyl chain length. Similarly, h_f^*,or the linear fit of λ with respect to film thickness, increases from 5 to 7 to 15 nm from PMMA to PEMA to PnPMA respectively. Lastly, the bilayer model shows a systematic decrease in $\overline{E}_f^*$ with increasing alkyl chain length from 0.2 ± 0.04 GPa, 0.06 ± 0.02 GPa, to 0.02 ± 0.01 GPa where a systematic reduction in $\overline{E}_f$ is also observed. This reduced modulus for the free surface layer is one to two orders of magnitude less than their bulk counterparts.

One issue with the series of poly(n-alkyl methacrylate)s is that both modulus and T_g decrease with alkyl chain length; thus it is not clear if the correlation in length scale for thin film moduli deviations from the bulk is due to the changes in bulk T_g or modulus. To delineate these effects, two methacrylate polymers with similar T_g but different moduli, poly(isobutyl methacrylate) (PiBMA, E_{bulk} =2.23 GPa, $T_{g,bulk}$ = 47 °C) and poly(benzyl methacrylate) (PBzMA, E_{bulk} =3.02 GPa, $T_{g,bulk}$ = 54 °C), are interrogated for the impact of film thickness on their elastic moduli. Figure 2.8a shows the apparent moduli,

$\overline{E}_{f,app} = \frac{E}{(1-\upsilon^2)}$, of both polymers as a function of film thickness. The film thickness dependence exhibits similar features to the poly(n-alkyl methacrylate)s series: a plateau of their bulk moduli at large thicknesses (h>40 nm) followed by significant decrease in moduli as the film thickness is decreased. Comparison of the moduli of the two polymers in thin films appears to show a common length scale (≈ 70 nm) where a deviation from the bulk-like moduli occurs.

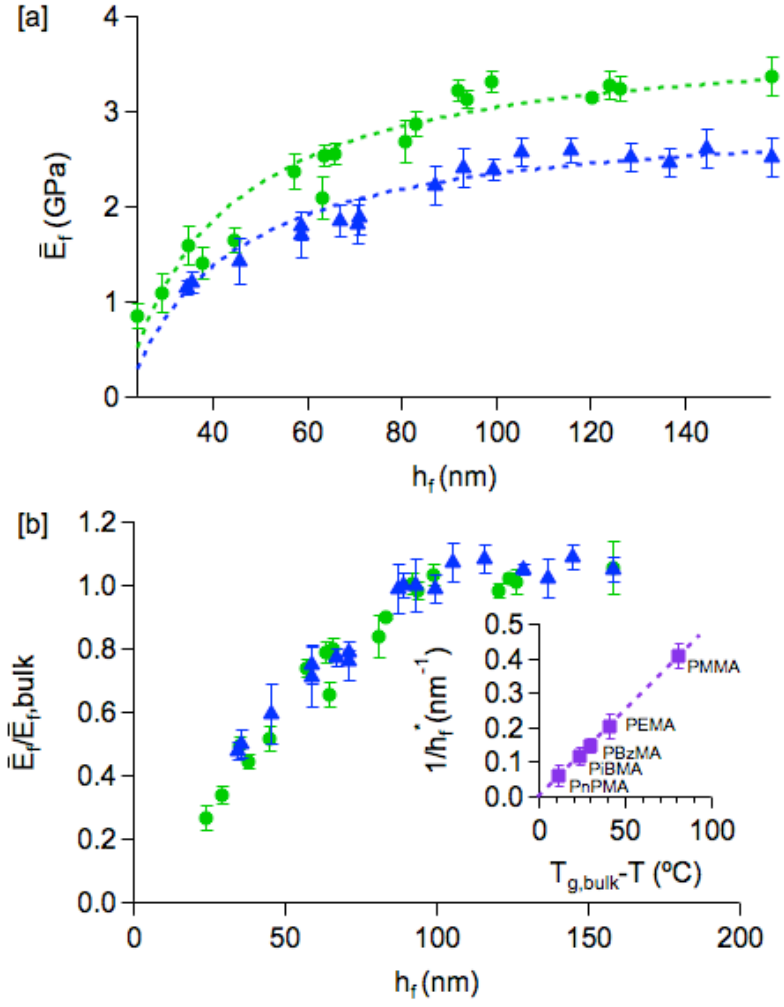

Figure 2.8 [a] Moduli of PiBMA(▲) and PBzMA(●) [b] Normalized moduli of PiBMA(▲) and PBzMA(●). The data shows differing bulk moduli for both films with similar deviations observed at ≈ 85 nm.

This is consistent with a correlation between modulus and quench depth into the glass for thin polymer films,[39] as the modulus of the bulk PiBMA is only approximately 70 % of that of PBzMA. Again the moduli of these films can be fit with the simple bilayer model[53] with an order of magnitude decrease in the modulus at the near surface of the films. The bilayer fit reveals a statistically invariant free surface layer of 10 and 12 nm for PiBMA and PBzMA respectively.

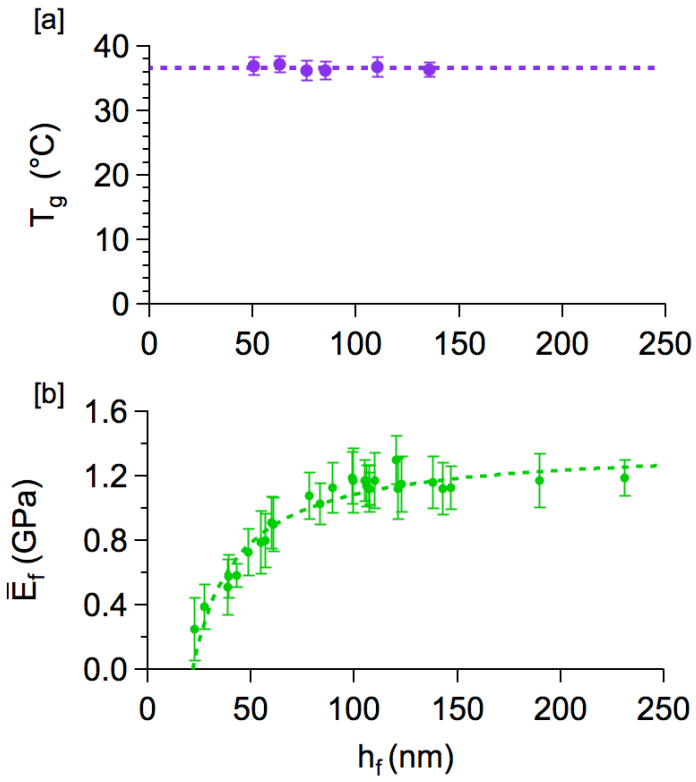

Figure 2.9 Comparison of the [a]T_g and [b]moduli of PnPMA in thin films on PDMS. The solid line is a fit of the data to a bilayer model.

To better illustrate the similarity in the thin film behavior between PiBMA and PBzMA, Figure 2.8b shows the reduced modulus ($\overline{E}_f / \overline{E}_{bulk}$) where the data collapses onto a single master curve. Additionally as shown in the inset in Figure

2.8b, the extrapolated film thickness at zero wavelength (h_f^*) for these two additional polymers falls on the same line as for the poly(n-alkyl methacrylates). This suggests that the modulus of thin glassy polymer films is predominately influenced by the quench depth into the glass (T_g-T).

This longer length scale for observed changes in the modulus of polymer films is consistent with simulations while approaching $T_{g,bulk}$.[41] This begs the question as to whether the T_g of PnPMA films is also impacted on this size scale? It is known that the glass transition temperature of supported thin polymer films is strongly dependent upon the interactions with the substrate. Thus to compare the changes in thin film modulus and T_g, identical substrate interactions should be considered. Fortuitously, PnPMA films thicker than approximately 50 nm are stable on a PDMS surface in the rubbery state (no dewetting), thus enabling the T_g of the films to be measured from the discontinuity in the coefficient of thermal expansion between the glass and rubbery state. Also to avoid aging artifacts, the measurements are performed by cooling from the rubbery state into the glass. Interestingly, the T_g of PnPMA films on PDMS does not statistically vary as the thickness is decreased down to nearly 50 nm, as shown in Figure 2.9. This result suggests that typical deviations in the apparent T_g of thin films, as measured by x-ray reflectivity[54, 55], ellipsometry[42, 56], and Brillouin light scattering[8, 43, 57] do not always correlate with the size scales where changes in the mechanical properties of polymers occur.

The results shown in Figure 2.9 are similar to novel bubble rheology experiments from McKenna and coworkers that showed changes in rheological

properties of thin films where no change in T_g was observed.[45] Even when considering gradients in the polymer properties permeating from the interfaces, there are differences in length scales involved in the changes in T_g (α-relaxations) and physical aging (β-relaxations).[58] The results show that α and β relaxations are influenced differently by the surfaces and interfaces. Where perturbations to the β-relaxations extend over 100 nm from the interfaces while no impact on α-relaxations is observed at these lengths scales. There exists a clear need to determine the local distribution of moduli in these films in order to gain further insight into nature of the surface effect. However, there are limited reports for the gradient in polymer thin film T_g's[59] and no reports to date on the distribution of mechanical properties in thin films. Simulations have suggested that the free surface mobility/relaxations are responsible for the decrease in the modulus of polymer thin films.[39, 40] Thus, these thin film moduli as reported in Figure 2.9b are only the average properties of the film in the case that gradients in mechanical properties may exist. Simulations appear to provide one method to address a distribution of mechanical properties in thin films of polymers. Regardless, the lack of correlation between the length scale for thickness-dependent modulus and T_g raises questions as to the relevant parameters that control the mechanical stability of polymeric nanostructures.

To continue to address this issue, a wide range of PS molecular mass from 1.2 kg/mol to 990 kg/mol is examined to determine how molecular mass impacts the elastic modulus of thin polymer films. Furthermore a range of T_g will be concurrently studied as T_g ranges from 32°C at 1.2 kg/mol to 98°C at

M_n>10kg/mol. [37] Figure 2.10 illustrates how the wrinkle wavelength, λ, depends upon the film thickness, h_f, for the series of different molecular mass PS films.

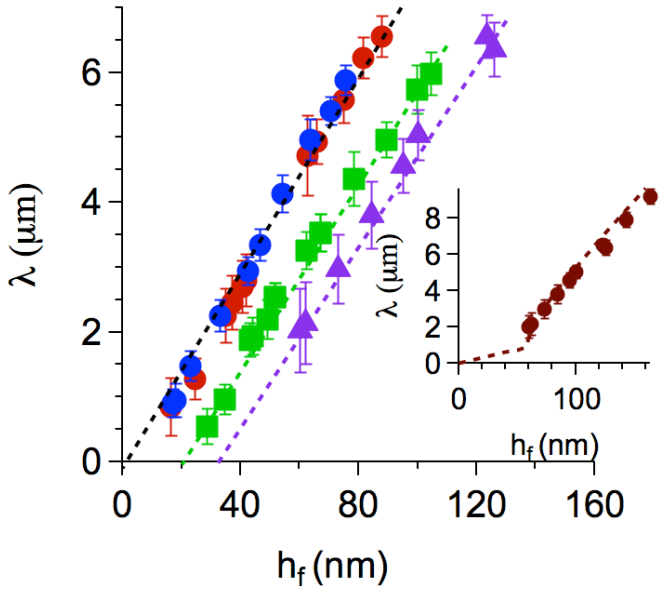

Figure 2.10 Wrinkle wavelength dependence on film thickness for (●) 990 kg/mol, 492 kg/mol, 9.4 kg/mol, 3.2 kg/mol (■) 1.3 kg/mol, (▲) 1.2 kg/mol PS, and extrapolated fit through origin for 1.2kg/mol PS (inset). The extrapolated wavelengths intersect at increasing thicknesses.

The wavelength shows a linear dependence upon the film thickness for all molecular masses examined, but the slope of the data begins to decrease slightly when the molecular mass is decreased below 3.2 kg/mol. The slope changes from 77.6 μm/nm for Mn > 3.2 kg/mol PS to 70 μm/nm for 1.3 kg/mol PS to 65 μm/nm for 1.2 kg/mol PS. This decrease in slope is a result of a decrease in the bulk modulus of the films. Note that bulk T_g of PS also decreases precipitously in this molecular mass region (Table 1). It should be noted that the modulus of PS might be expected to decrease at much higher molecular mass that is the entanglement M_n based upon bulk rheological properties of PS melts. However in this case, the

elastic moduli of the PS glass are probed with small strain deformations. Only short length scales are probed with this wrinkling measurement; for entanglements to become important larger deformations are necessary in glassy films. The length scales probed and underlying polymer physics involved in determining the elastic modulus of these glassy PS films using wrinkling differs substantially from measurements of PS film viscoelasticity[60] determined by dewetting kinetics. In this later experiment, large-scale chain motion is required and thus the measurement is sensitive to entanglements as well as the stress state in the film. Furthremore, it is found that the reduction in viscosity is controlled by the coil size while T_g involves shorter length scales and therefore different deviation length scales are observed. Concluding that sensitivity to confinement is dependent on different regions of the time spectrum.

A second feature in Figure 2.10 is the shift to larger thickness for the extrapolated wavelength as M_n is decreased below 3.2 kg/mol. From the linear fit of the data, the thickness of this apparent free surface layer, h_f^*, increases with decreasing molecular mass, from approximately 5 nm for 990 kg/mol PS to nearly 35 nm for the 1.2 kg/mol PS films as listed in Table 2.2 (h_f^* is obtained from extrapolation of the data to zero λ and δ as a fit parameter of $\overline{E}_f$ as a function of film thickness in the bilayer model). The thickness of the free surface layer at sub 3.2kg/mol is significantly larger than has been reported in previous modulus studies. [41, 61] However, by studying surface recovery Fahkarai and Forrest observed enhanced surface mobility to extend several nanometers (≈10 nm).[62]

This increase in the thickness of the free surface layer is expected to significantly impact the overall modulus in the ultrathin film regime.

Table 2.2 Bilayer model fit for different molecular mass PS films with comparison of the thickness of surface layer from the bilayer model (model) and the linear extrapolation (linear) to zero wavelength.

M_n (kg/mol)	$\overline{E}_f$ (GPa)	$\overline{E}_f^*$ (GPa)	δ (nm) (model)	h_f^* (nm) (linear)
990	3.81 ± 0.22	0.171 ± 0.037	5.4 ± 1	5.5 ± 0.5
492	3.92 ± 0.27	0.139 ± 0.045	5.6 ± 1.2	5.7 ± 0.5
9.4	3.90 ± 0.21	0.095 ± 0.079	5.9 ± 1.6	5.9 ± 0.3
3.2	3.44 ± 0.21	0.086 ± 0.046	7.0 ± 1.9	6.0 ± 0.7
2.3	3.37 ± 0.26	0.052 ± 0.014	10.3 ± 1.9	10.1 ± 0.1
1.3	1.76 ± 0.10	0.046 ± 0.010	27.5 ± 1.6	18.2 ± 0.1
1.2	1.30 ± 0. 17	0.026 ± 0.003	59.1 ± 2.5	37.3 ± 0.2

Table 2.2 lists the thickness of the free surface layer as well as the apparent modulus of both the free surface layer and the bulk layer as a function of molecular mass that is obtained from the fits. The free surface layer maintains a near statistically invariant thickness of approximately 5.7 nm and plane-strain modulus of ≈ 0.1 GPa for > 3.2 kg/mol PS. As the molecular mass decreases below 3 kg/mol, the free surface layer thickness (h_f^*) increases significantly. For high molecular masses, the h_f^* from the bilayer fits corresponds well with the h_f^* (intercept) obtained from linear fits of the wavelength data, as shown in Table 2.2. However, the dependence of h_f^* on wavelength is non-linear.[53] While the curvature is small, this leads to underestimation of the thickness of the soft surface layer. As the thickness of the layer increases, the disagreement with the extrapolated estimate increases. For example, there is disagreement in h_f^* for M_n

= 1.2 kg/mol between the two methods, with h^* from the fit and the extrapolation differing by a factor of 2 with a smaller value from the extrapolation. The linear extrapolation is only an approximation, but it provides an accurate estimate at h_f^* < 15 nm as shown previously.[61, 63] As the bulk T_g of the polymer is decreased (due to the decrease in M_n), the surface layer thickness increases for a fixed measurement temperature, in this case 21 °C ± 2 °C. The increase in the length scale at which a deviation in modulus occurs with decreasing quench depth, from 5 nm to 59 nm, agrees with predictions from de Pablo and coworkers.[39, 40] The deviation length scale from bulk modulus actually increases as R_g is decreased; this result strongly suggests that the change in mechanical properties of thin polymer films is not a result of an intrinsic effect from confinement on the polymer chains. Instead there appears to be a correlation between bulk T_g and the free surface layer. This suggests that the change in mechanical properties of thin polymer films is due to increased interfacial area of the free surface layer with decreasing film thickness. For PS films with M_n > 3.2 kg/mol, the reduced modulus ($E_f / E_{f,bulk}$) as a function of film thickness collapses onto a single curve, as shown in the inset in Figure 2.11a. The thickness at which this observed deviation in elastic modulus, the critical thickness, occurs is ≈50 nm, which is consistent with prior reports for high molecular mass PS.[41] Again, simulations suggest a length scale of ≈40 nm for deviations in mechanical properties when the polymer is quenched deep into the glass.[39] For M_n of 3.2 kg/mol and 2.3 kg/mol, the thick film ("bulk") modulus is reduced relative to the higher M_n PS films by approximately 10%. The thickness at which the deviation from bulk behavior is

observed is not greatly effected and still occurs at ≈50 nm. However, a further decrease in M_n to 1.3 kg/mol results in a significant decrease in the bulk modulus to 1.2 GPa as well as a shift in the critical thickness to nearly 70 nm. In this case, the quench depth into the bulk glass is less than 10 ºC. Simulations have suggested that near bulk T_g the mechanical properties of polymer thin films will begin to deviate from the bulk at approximately 80 nm.[39, 40]

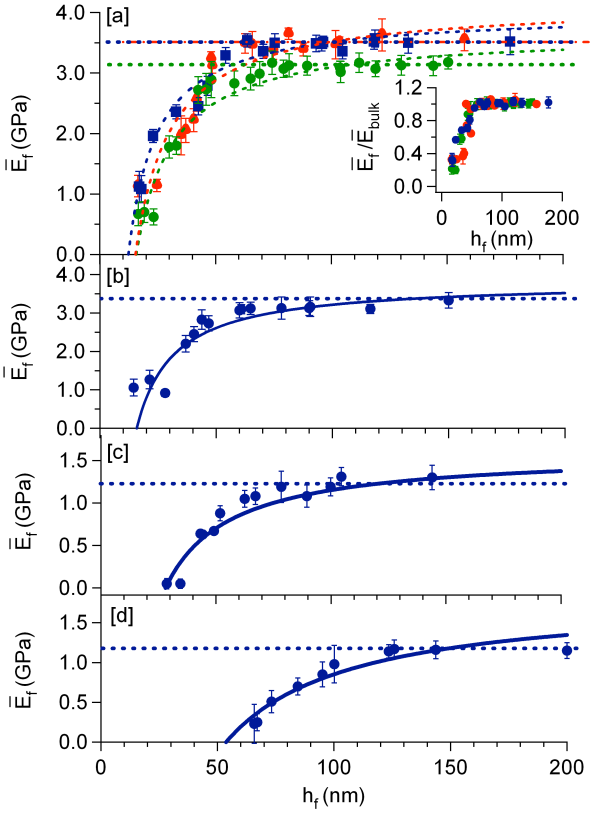

Figure 2.11 Film thickness dependence of the modulus of PS thin films for molecular masses of (a) 990 kg/mol (●, red), 9.4 kg/mol (●, blue), 3.2 kg/mol (●, green), and reduced modulus collapsing onto a single curve (inset) (b) 2.3 kg/mol, (c) 1.3 kg/mol, and (d) 1.2 kg/mol.

The experimental results reported here are in good agreement with those simulations. Interestingly, when the quench depth into the glass is ≈1 ºC (i.e., 1.2.

kg/ mol PS) the polymer films begin to exhibit deviations from bulk modulus values at approximately 100 nm. This length scale is extremely long for observing nanoconfinement effects, although even longer length scales for T_g deviations have been reported.[30] For example Ellison and coworkers report the critical length scale for the T_g of poly(4-tert-butylstyrene) between 300-400 nm.[30] However, it is compelling that the deviation observed here occurs for such a small M_n PS. On the other hand, the T_g of PS begins to decrease at the entanglement molecular (~18 kg/mol) weight sub 10kg/mol approximately where the modulus begins to decrease (below ~9.4 kg/mol). Thus, it appears that the quench depth into the bulk glass ($T_{g,bulk}$ - T) is the a parameter for determining the elastic moduli behavior of thin glassy films.

The increase in critical thickness with decreasing M_n for the low molecular mass PS suggest the quench depth, ($T-T_{g,bulk}$), rather than finite chain confinement based upon molecular size, is a key parameter in determining the mechanical behavior of polymer thin films. Figure 2.12 illustrates the dependency of quench depth on the length scales where deviations in the elastic modulus of thin PS films occurs, as revealed by δ determined from the bilayer fit. At large quench depths, $T-T_g>50°C$,the surface layer thickness is essentially constant at approximately 5 nm. This result suggests that there is a nearly constant thickness soft surface for high M_n PS films. This thickness is consistent with prior reports in the literature regarding a soft surface layer that is approximately 5 nm thick.[22, 56, 64] For example, Fischer and coworkers studied the T_g of PS spheres in an aqueous suspension utilizing a dynamic scanning

calorimeter. There results show a heat capacity jump that is consistent with a mobile layer ~4 nm thick near the outer shell of the spheres.[22] While Keddie and coworkers utilize AFM equipped with a thermal probe to study the surface of bulk polystyrene, their results also suggest a thin surface layer ~3-5 nm thick.[65]

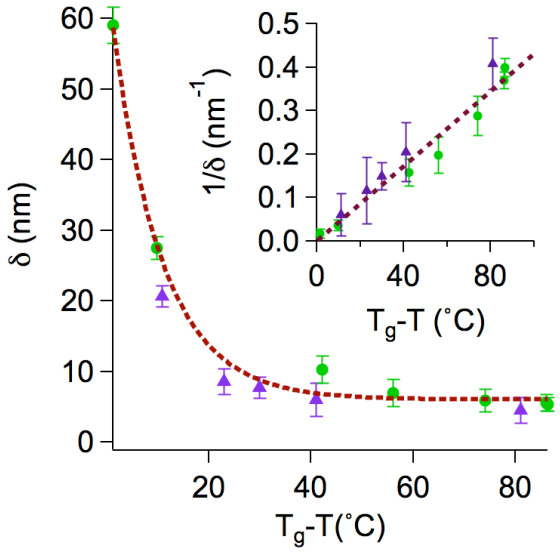

Figure 2.12 Free surface layer thickness as determined from the bilayer model is strongly correlated with quench depth into the glass, PS(●), poly (alkyl methacrylate)s (▲).

As M_n and $T_{g,bulk}$ decrease, the thickness of the surface layer increases dramatically. As T approaches T_g, δ appears to diverge. Due to the dependence of bulk modulus on temperature; at $T=T_g$, it would be expected that the entire film irrespective of thickness would have a lower modulus, which would be similar to the bulk modulus of the rubber. The dependency of the surface layer thickness, as determined from our modulus measurements and shown in Table 2.2 and Figure 2.12, on the proximity of the bulk T_g may lend insight into glass formation in polymers where the near surface remains more mobile (lower modulus) than the bulk. The expansion of the rubbery-like surface layer as the bulk T_g is approached

is reminiscent of the growth of the liquid phase from the free interface into glassy tris-naphthylbenzene.[66] The surface layer dependence on quench depth can be fit equally well by an exponential and inverse (inset) relationship as shown in Figure 2.12. The linear characteristic scaling universal for all the M_n PS films as well as the poly(alkyl methacrylate) series has implications for the development of polymeric composites, where baring any variations in chain flexibility or intrachain/interchain interactions by controlling the quench depth the mechanical properties can be controlled.

Simulations have suggested that fast segmental motions[67-69] near the free surface initiate cooperative motion of many segments and results in an enhanced polymer mobility[70] that leads to a decrease in modulus.[39, 40] However, additional theoretical work on the relationship between quench depth and the modulus of nanoconfined polymers is required to understand exactly how the soft surface thickness scales. Nonetheless, the surface layer thickness appears to be well correlated with the quench depth into the bulk glass for all molecular masses of poly (alkyl methacrylate)s and PS examined here. Other factors influencing the surface layer still need to be examined, for example chain end segregation and polymer rigidity. By controlling end groups functionality segregation of chain ends and surface energetics can be controlled thus impacting the free surface layer composition and impacting nanometer length scale T_g.[71] Furthermore increasing polymer backbone rigidity limits end group segregation also impacting the free surface layer composition, that is due to steric hindrance the polymer is more sensitive to conformational changes with confinement.[72] More importantly

techniques for controlling the surface layer thickness and maintaining mechanical robustness (eliminating increased surface mobility) still need to be researched.

2.4 Conclusion

In summary, the thin film modulus for a series of poly (alkyl methacrylate)s and PS was determined using an approach based on Euler type wrinkling of a stiff polymeric film on an elastic substrate. For the poly (alkyl methacrylate) series, there is a clear decrease in moduli compared to bulk values as film thickness was decreased. The length scale at which deviations from bulk moduli occurred was proportional to the bulk glass transition temperature of the polymer. As the quench depth into the bulk glass decreases, the critical thickness at which the polymer film exhibits deviations from bulk-like values progressively increases to larger thicknesses. Additionally, changes in the modulus of PnPMA thin films do not correlate with the thin film T_g behavior of identical films.

For the PS series, the bulk modulus decreased as M_n decreases below a threshold (≈3.2 kg/mol). However, for all the M_n PS films examined deviations from bulk values were observed. For high M_n (> 3.2 kg/mol), the deviation in modulus is independent of molecular mass and begins when the film thickness is less than ≈50 nm. However at M_n = 1.2 kg/mol, the modulus decreases at much larger thickness (≈100 nm). The deviation in the modulus of thin films appears to scale directly with the quench depth into the bulk glass and not with molecular size effects. The deviation is attributed to the free surface effect at the polymer/air interface and the variation in length scales is directly related to the thickness of the surface layer with lower modulus.

The thickness of the soft surface layer determined from the bilayer model varies from ≈5 nm deep in the glass to greater than 50 nm when the measurement occurs within ≈1 ºC of $T_{g,bulk}$. This result is in agreement with discontinuous molecular dynamics simulations which suggest that as T_g is approached the effect of a mobile surface layer increases, leading to decreases in the modulus at longer length scales.[15,24] It was also found that the inverse of the free surface layer scaled linearly with the quench depth. These results have direct implications in the robustness of polymeric nanostructures critical for future microelectronics, coatings, and adhesives.

2.5 References

1. Ferry, J. D., *Viscoelastic properties of polymers*. John Wiley and Sons: New York, 1980.

2. Williams, M. L.; Landel, R. F.; Ferry, J. D., Mechanical Properties of Substances of High Molecular Weight .19. the Temperature Dependence of Relaxation Mechanisms in Amorphous Polymers and Other Glass-Forming Liquids. *Journal of the American Chemical Society* **1955,** *77* (14), 3701-3707.

3. DeMaggio, G. B.; Frieze, W. E.; Gidley, D. W.; Zhu, M.; Hristov, H. A.; Yee, A. F., Interface and surface effects on the glass transition in thin polystyrene films. *Physical Review Letters* **1997,** *78* (8), 1524-1527.

4. Ohno, H.; Kobayashi, N.; Takeoka, S.; Ishizaka, H.; Tsuchida, E., Larger cations can move faster in solid polymer electrolytes. *Solid State Ionics* **1990,** *40-41* (Part 2), 655-658.

5. Cappella, B.; Kaliappan, S. K.; Sturm, H., Using AFM force-distance curves to study the glass-to-rubber transition of amorphous polymers and their elastic-plastic properties as a function of temperature. *Macromolecules* **2005,** *38* (5), 1874-1881.

6. Mackay, M. E.; Dao, T. T.; Tuteja, A.; Ho, D. L.; Van Horn, B.; Kim, H.; Hawker, C. J., Nanoscale effects leading to non-Einstein-like decrease in viscosity. *Nature Materials* **2003,** *2* (11), 762-766.

7. Ozin, G. A.; Yang, S. M., The race for the photonic chip: Colloidal crystal assembly in silicon wafers. *Advanced Functional Materials* **2001,** *11* (2), 95-104.

8. Hartschuh, R.; Ding, Y.; Roh, J. H.; Kisliuk, A.; Sokolov, A. P.; Soles, C. L.; Jones, R. L.; Hu, T. J.; Wu, W. L.; Mahorowala, A. P., Brillouin scattering studies of polymeric nanostructures. *Journal of Polymer Science Part B-Polymer Physics* **2004,** *42* (6), 1106-1113.

9. Lei, J.; Fan, J.; Yu, C. Z.; Zhang, L. Y.; Jiang, S. Y.; Tu, B.; Zhao, D. Y., Immobilization of enzymes in mesoporous materials: controlling the entrance to nanospace. *Microporous and Mesoporous Materials* **2004,** *73* (3), 121-128.

10. Chou, S. Y.; Krauss, P. R.; Zhang, W.; Guo, L.; Zhuang, L. In *Sub-10 nm imprint lithography and applications*, Papers from the 41st international conference on electron, ion, and photon beam technology and nanofabrication, Dana Point, California (USA), AVS: Dana Point, California (USA), 1997; pp 2897-2904.

11. Tanaka, T.; Morigami, M.; Atoda, N., MECHANISM OF RESIST PATTERN COLLAPSE DURING DEVELOPMENT PROCESS. *Japanese Journal of Applied Physics Part 1-Regular Papers Short Notes & Review Papers* **1993,** *32* (12B), 6059-6064.

12. Stoykovich, M. P.; Nealey, P. F., Block copolymers and conventional lithography. *Materials Today* **2006,** *9* (9), 20-29.

13. Ramanathan, M.; Darling, S. B.; Sumant, A. V.; Auciello, O. In *Nanopatterning of ultrananocrystalline diamond thin films via block copolymer lithography*, AVS: 2010; pp 979-983.

14. Solak, H. H.; David, C.; Gobrecht, J.; Golovkina, V.; Cerrina, F.; Kim, S. O.; Nealey, P. F., Sub-50nm Period Patterns with EUV Interference Litrhography. *Microelectronic Engineering* **2003,** *67*, 56-62.

15. Chou, S. Y.; Krauss, P. R.; Renstrom, P. J., Imprint Lithography with 25-Nanometer Resolution. *Science* **1996,** *272* (5258), 85-87.

16. Rowland, H. D.; King, W. P.; Pethica, J. B.; Cross, G. L. W., Molecular Confinement Accelerates Deformation of Entangled Polymers During Squeeze Flow. *Science* **2008,** *322* (5902), 720-722.

17. Ding, Y.; Ro, H.; Douglas, J. F.; Jones, R. L.; Karim, A.; Soles, C. L., Polymer viscoelasticity and residual stress effects on nanoimprint lithography. *Advanced Materials* **2007,** *19*, 1377-1382.

18. Park, M.; Harrison, C.; Chaikin, P. M.; Register, R. A.; Adamson, D. H., Block copolymer lithography: Periodic arrays of similar to 10(11) holes in 1 square centimeter. *Science* **1997,** *276* (5317), 1401-1404.

19. Thurn-Albrecht, T.; Schotter, J.; Kastle, C. A.; Emley, N.; Shibauchi, T.; Krusin-Elbaum, L.; Guarini, K.; Black, C. T.; Tuominen, M. T.; Russell, T. P., Ultrahigh-density nanowire arrays grown in self-assembled diblock copolymer templates. *Science* **2000,** *290* (5499), 2126-2129.

20. Ellison, C. J.; Torkelson, J. M., Sensing the glass transition in thin and ultrathin polymer films via fluorescence probes and labels. *Journal of Polymer Science Part B-Polymer Physics* **2002,** *40* (24), 2745-2758.

21. Ellison, C. J.; Torkelson, J. M., The distribution of glass-transition temperatures in nanoscopically confined glass formers. *Nature Materials* **2003,** *2* (10), 695-700.

22. Fischer, H., Thermal probe surface treatment of a bulk polymer: Does a surface layer with a lower glass transition than the bulk exist? *Macromolecules* **2002,** *35* (9), 3592-3595.

23. Forrest, J. A.; DalnokiVeress, K.; Dutcher, J. R., Interface and chain confinement effects on the glass transition temperature of thin polymer films. *Physical Review E* **1997,** *56* (5), 5705-5716.

24. Forrest, J. A.; DalnokiVeress, K.; Stevens, J. R.; Dutcher, J. R., Effect of free surfaces on the glass transition temperature of thin polymer films. *Physical Review Letters* **1996,** *77* (10), 2002-2005.

25. Forrest, J. A.; Mattsson, J., Reductions of the glass transition temperature in thin polymer films: Probing the length scale of cooperative dynamics. *Physical Review E* **2000,** *61* (1), R53-R56.

26. Fryer, D. S.; Peters, R. D.; Kim, E. J.; Tomaszewski, J. E.; de Pablo, J. J.; Nealey, P. F.; White, C. C.; Wu, W.-l., Dependence of the Glass Transition Temperature of Polymer Films on Interfacial Energy and Thickness. *Macromolecules* **2001,** *34* (16), 5627-5634.

27. Fukao, K.; Miyamoto, Y., Glass transitions and dynamics in thin polymer films: Dielectric relaxation of thin films of polystyrene. *Physical Review E* **2000,** *61* (2), 1743-1754.

28. Kanaya, T.; Miyazaki, T.; Watanabe, H.; Nishida, K.; Yamana, H.; Tasaki, S.; Bucknall, D. B., Annealing effects on thickness of polystyrene thin films as studied by neutron reflectivity. *Polymer* **2003,** *44* (14), 3769-3773.

29. Huth, H.; Minakov, A. A.; Serghei, A.; Kremer, F.; Schick, C., Differential AC-chip calorimeter for glass transition measurements in ultra thin polymeric films. *European Physical Journal-Special Topics* **2007,** *141*, 153-160.

30. Ellison, C. J.; Mundra, M. K.; Torkelson, J. M., Impacts of polystyrene molecular weight and modification to the repeat unit structure on the glass transition-nanoconfinement effect and the cooperativity length scale. *Macromolecules* **2005,** *38* (5), 1767-1778.

31. Singh, L.; Ludovice, P. J.; Henderson, C. L., Influence of molecular weight and film thickness on the glass transition temperature and coefficient of thermal expansion of supported ultrathin polymer films. *Thin Solid Films* **2004,** *449* (1-2), 231-241.

32. Dalnoki-Veress, K.; Forrest, J. A.; Murray, C.; Gigault, C.; Dutcher, J. R., Molecular weight dependence of reductions in the glass transition temperature of thin, freely standing polymer films. *Physical Review E* **2001,** *63* (3).

33. Forrest, J. A.; Dalnoki-Veress, K., The glass transition in thin polymer films. *Advances in Colloid and Interface Science* **2001,** *94* (1-3), 167-196.

34. Lin, E. K.; Wu, W. I.; Satija, S. K., Polymer interdiffusion near an attractive solid substrate. *Macromolecules* **1997,** *30* (23), 7224-7231.

35. Shin, K.; Obukhov, S.; Chen, J. T.; Huh, J.; Hwang, Y.; Mok, S.; Dobriyal, P.; Thiyagarajan, P.; Russell, T. P., Enhanced mobility of confined polymers. *Nature Materials* **2007,** *6* (12), 961-965.

36. Soles, C. L.; Douglas, J. F.; Jones, R. L.; Wu, W. L., Unusual expansion and contraction in ultrathin glassy polycarbonate films. *Macromolecules* **2004,** *37* (8), 2901-2908.

37. Hintermeyer, J.; Herrmann, A.; Kahlau, R.; Goiceanu, C.; RoÃàssler, E. A., Molecular Weight Dependence of Glassy Dynamics in Linear Polymers Revisited. *Macromolecules* **2008,** *41* (23), 9335-9344.

38. Seemann, R.; Jacobs, K.; Landfester, K.; Herminghaus, S., Freezing of polymer thin films and surfaces: The small molecular weight puzzle. *Journal of Polymer Science Part B-Polymer Physics* **2006,** *44* (20), 2968-2979.

39. Bohme, T. R.; de Pablo, J. J., Evidence for size-dependent mechanical properties from simulations of nanoscopic polymeric structures. *Journal of Chemical Physics* **2002,** *116* (22), 9939-9951.

40. Yoshimoto, K.; Jain, T. S.; Nealey, P. F.; de Pablo, J. J., Local dynamic mechanical properties in model free-standing polymer thin films. *Journal of Chemical Physics* **2005,** *122* (14), 144712.

41. Stafford, C. M.; Vogt, B. D.; Harrison, C.; Julthongpiput, D.; Huang, R., Elastic moduli of ultrathin amorphous polymer films. *Macromolecules* **2006,** *39* (15), 5095-5099.

42. Campbell, C. G.; Vogt, B. D., Examination of the influence of cooperative segmental dynamics on the glass transition and coefficient of thermal expansion in thin films probed using poly(n-alkyl methacrylate)s. *Polymer* **2007,** *48* (24), 7169-7175.

43. Forrest, J. A.; Dalnoki-Veress, K.; Dutcher, J. R., Brillouin light scattering studies of the mechanical properties of thin freely standing polystyrene films. *Physical Review E* **1998,** *58* (5), 6109-6114.

44. Mackay, M. E.; Dao, T. T.; Tuteja, A.; Ho, D. L.; Van Horn, B.; Kim, H. C.; Hawker, C. J., Nanoscale effects leading to non-Einstein-like decrease in viscosity. *Nature Materials* **2003,** *2* (11), 762-766.

45. O'Connell, P. A.; McKenna, G. B., Rheological Measurements of the Thermoviscoelastic Response of Ultrathin Polymer Films. *Science* **2005,** *307* (5716), 1760-1763.

46. Inoue, T.; Cicerone, M. T.; Ediger, M. D., Molecular Motions and Viscoelasticity of Amorphous Polymers near Tg. *Macromolecules* **1995,** *28* (9), 3425-3433.

47. Rogers, S. S.; Madlkern, L., Glass Transitions of the Poly-(n-Alkyl Methacrylates). *Journal of Physical Chemistry* **1957,** *61* (7), 985-991.

48. Stafford, C. M.; Vogt, B. D.; Harrison, C.; Julthongpiput, D.; Huang, R., Elastic Moduli of Ultrathin Amorphous Polymer Films. *Macromolecules* **2006,** *39*, 5095-5099.

49. Van Damme, H. S.; Hogt, A. H.; Feijen, J., Surface mobility and structural transitions of poly(n-alkyl methacrylates) probed by dynamic contact angle measurements. *Journal of Colloid and Interface Science* **1986,** *114* (1), 167-172.

50. Brandrup, J.; Immergut, E. H.; Grulke, E. A., *Polymer handbook*. Wiley-Interscience: 2003.

51. Korkmaz, T.; Dogan, A.; Usanmaz, A., Dynamic mechanical analysis of provisional resin materials reinforced by metal oxides. *Bio-medical Materials and Engineering* **2005,** *15* (3), 179-188.

52. Seitz, J. T., The estimation of mechanical properties of polymers from molecular structure. *Journal of Applied Polymer Science* **1993,** *49* (8), 1331-1351.

53. Huang, R.; Stafford, C. M.; Vogt, B. D., Effect of surface properties on wrinkling of ultrathin films. *Journal of Aerospace Engineering* **2007,** *20* (1), 38-44.

54. vanZanten, J. H.; Wallace, W. E.; Wu, W. L., Effect of strongly favorable substrate interactions on the thermal properties of ultrathin polymer films. *Physical Review E* **1996,** *53* (3), R2053-R2056.

55. Wallace, W. E.; van Zanten, J. H.; Wu, W. L., Influence of an impenetrable interface on a polymer glass-transition temperature. *Physical Review E* **1995,** *52* (4), R3329.

56. Keddie, J. L.; Jones, R. A. L., Size-Dependent Depression of the Glass Transition Temperature in Polymer Films. *Europhysics Letters* **1994,** *27*, 59-64.

57. Sun, L.; Dutcher, J. R.; Giovanni, L.; Nizzoli, F.; Stevens, J. R.; Ord, J. L., Elastic and elasto-optic properties of thin films of poly (styrene) spin coated onto Si (001). *Journal of Applied Physics* **1994,** *75* (11), 7482-7488.

58. Priestley, R. D.; Ellison, C. J.; Broadbelt, L. J.; Torkelson, J. M., Structural Relaxation of Polymer Glasses at Surfaces, Interfaces, and In Between. *Science* **2005,** *309* (5733), 456-459.

59. Keddie, J. L.; Jones, R. A. L.; Cory, R. A., Interface and surface effects on the glass-transition temperature in thin polymer films. *Faraday Discussions* **1994,** *98*, 219-230.

60. Bodiguel, H.; Fretigny, C., Viscoelastic Properties of Ultrathin Polystyrene Films. *Macromolecules* **2007,** *40* (20), 7291-7298.

61. Torres, J. M. S., C.M.; Vogt, B.D., Elastic Modulus of Amorphous Polymer Thin Films: Relationship to the Glass Transition Temperature. *ACS Nano* **2009,** *3* (9), 2677.

62. Fakhraai, Z.; Forrest, J. A., Measuring the Surface Dynamics of Glassy Polymers. *Science* **2008,** *319* (5863), 600-604.

63. Stafford, C. M.; Harrison, C.; Beers, K. L.; Karim, A.; Amis, E. J.; Vanlandingham, M. R.; Kim, H. C.; Volksen, W.; Miller, R. D.; Simonyi, E. E., A buckling-based metrology for measuring the elastic moduli of polymeric thin films. *Nature Materials* **2004,** *3* (8), 545-550.

64. Sasaki, T.; Shimizu, A.; Mourey, T. H.; Thurau, C. T.; Ediger, M. D., Glass transition of small polystyrene spheres in aqueous suspensions. *Journal of Chemical Physics* **2003,** *119* (16), 8730-8735.

65. Keddie, J. L.; Jones, R. A. L.; Cory, R. A., Size-dependent depression of the glass-transition temperature in polymer-films. *Europhysics Letters* **1994,** *27* (1), 59-64.

66. Swallen, S. F.; Traynor, K.; McMahon, R. J.; Ediger, M. D.; Mates, T. E., Stable Glass Transformation to Supercooled Liquid via Surface-Initiated Growth Front. *Physical Review Letters* **2009,** *102* (6), 065503.

67. Jain, T. S.; de Pablo, J. J., Investigation of transition states in bulk and freestanding film polymer glasses. *Physical Review Letters* **2004,** *92* (15), 155505.

68. Mansfield, K. F.; Theodorou, D. N., Molecular-dynamics simulation of a glassy polymer surface. *Macromolecules* **1991,** *24* (23), 6283-6294.

69. Tseng, K. C.; Turro, N. J.; Durning, C. J., Molecular mobility in polymer thin films. *Physical Review E* **2000,** *61* (2), 1800-1811.

70. Jain, T. S.; de Pablo, J. J., Influence of confinement on the vibrational density of states and the Boson peak in a polymer glass. *Journal of Chemical Physics* **2004,** *120* (19), 9371-9375.

71. Xie, F.; Zhang, H. F.; Lee, F. K.; Du, B.; Tsui, O. K. C.; Yokoe, Y.; Tanaka, K.; Takahara, A.; Kajiyama, T.; He, T., Effect of Low Surface Energy Chain Ends on the Glass Transition Temperature of Polymer Thin Films. *Macromolecules* **2002,** *35* (5), 1491-1492.

72. Arriaga, L. R.; Monroy, F.; Langevin, D., Influence of backbone rigidity on the surface rheology of acrylic Langmuir polymer films. *Soft Matter* **2011**.

CHAPTER 3

MANIPULATIONS OF THE ELASTIC PROPERTIES OF POLYMERS AT THE NANOSCALE

3.1 Introduction

As discussed in previous chapters, at sub 100 nm length scales polymer properties begin to deviate from bulk values, including viscosity,[1] modulus,[2] compliance,[3] and relaxation dynamics[4, 5] (including surface T_g)[6]. In these studies of polymer thin films, polystyrene (PS) has been generally examined as model system. Additionally, several reports have demonstrated that surface dynamics are much faster than the bulk for PS and PMMA films, consistent with a reduced surface modulus.[7, 8] For example, Fakhraai and Forrest embedded gold nanospheres on the surface of PS thin films, annealed them at temperatures ranging from 277K to 369K and after removal of the spheres measured the surface recovery. Their results show that surface relaxation occurred at all temperatures a direct measure of enhanced surface mobility.[7] Ellison and Torkelson utilized pyrene labeled layers within PS films to examine the distribution of T_g's, which illustrates a gradient in T_g extending approximately 40 nm below the free surface at which point bulk values were reached.[6] Furthermore a similar fluorescence study on the T_g at both the free surfaces and silica interfaces of a series of poly (n-methacrylate)s revealed increases in T_g for poly (methyl methacrylate) (PMMA), decreases for poly (ethyl methacrylate) (PEMA), and invariant for poly (isobutyl methacrylate)(PiBMA).[9] This trend was

attributed to hydrogen-bonding between PMMA and the hydroxyl groups on the silica surface, in the case of PEMA the free surface reduction in T_g dominated substrate effects, while similar strengths in substrate and free-surface T_g perturbations resulted in a net cancellation in T_g for PiBMA.[9] These results indicate that the free surface of polymer films has properties that differ from the bulk. At nanometer length scales, reduced surface properties become significant and lead to a decrease in the mechanical integrity of polymeric nanostructures due to the high surface to volume ratios.[10, 11] Finite-element inversion analysis of Brillouin light scattering data as well as cantilever beam bending measurements reveal dimensional dependent elastic modulus below beam widths of 50 nm for PMMA nanostructures,[10, 11] where elastic constants in nanostructures show a 3-11% decrease at 50 nm from their corresponding bulk values.[10] Similarly, Torkelson and coworkers demonstrated that the T_g of lithographically patterned PMMA films is less than that observed for unpatterned films of identical thickness.[12] These results suggest that increasing the free surface area leads to a reduction in polymer properties. Thus, minimizing this free surface effect is necessary for generating robust polymeric nanostructures. As shown in the previous chapter, one route to decrease the free surface effect is to increase the bulk T_g of the polymeric system.[13, 14] However, high T_g polymers can be difficult to process in general due to difficulties with annealing and removal of processing history; for example, nanoimprint lithography requires processing in the melt to allow for flow of polymer into the nanostructured mold, but this temperature must

be below the degradation temperature. Therefore, reducing the free surface effect with higher T_g polymers limits processability and an alternate route is desired.

Polymer modification techniques such as electron beam, gamma ray, and ultraviolet (UV) radiation have been used extensively in industry.[15] These techniques allow for control of saturation, crosslinking, and polymer molecular weight which allows them to tune material properties.[15] It is therefore suggested that these free surfaces could be chemically modified in a manner that might improve the mechanical integrity by altering the surface properties. One common route to the modification of polymer surfaces is through use of UV radiation. Koberstein and coworkers have used UV radiation coupled with molecular oxygen to create inorganic oxide coatings on surfaces, which should be significantly more robust mechanically than the precursors.[16] Similarly, ultraviolet ozone (UVO) treatment simultaneously utilizes UV light and ozone produced *in situ* to photochemically modify the surface. In cases where oxidation and crosslinking occur such as for poly(dimethylsiloxane) (PDMS) and PS, UVO is known to improve adhesion,[17] wettability,[18] biocompatibility,[19] and toughness[18] of polymers through modification of the near surface region, ≈ 5 nm.[17, 18] However, other polymers, such as PMMA, predominantly undergo chain scission rather than crosslinking; thus UVO treatment would not appropriate for all polymers.[17, 18]

Recently, de Pablo and coworkers used simulations to identify an alternative route to eliminate the observed decrease in modulus of thin films and nanostructures: the use of an antiplasticizer.[20] These simulations also suggest that upon the confinement of a polymer/diluent system, both the initial energy barriers

for chain relaxation and T_g are unchanged, unlike the neat polymer where a reduction in bulk values are observed when confined to a thin film.[21] Simulations studying particle movement within confined polymer films suggest the addition of an antiplasticizer eliminates the propagation of free-surface effects by making the cooperative motions in the film and near surface homogeneous; thus decreasing the required cooperative motion length scale in the vicinity of the free surface for polymer relaxation.[6, 20] However, plasticizers, rather than antiplasticizers, are commonly utilized in nanoimprint lithography,[22] but Ellison *et al.* illustrated that a plasticizer, dioctyl phthalate (DOP), can effectively eliminate any finite size effects on T_g of PS.[23] The results are explained in terms of a free surface layer with reduced properties relative to the bulk due to enhanced surface dynamics. The authors argue that addition of a diluent molecule alters the dynamics in the film normally influenced by the free surface. If addition of small molecule diluents alters polymer dynamics at the free surface it is expected that the elastic modulus would be influenced as free surface effects seem to control sub 50 nm length scale modulus. However, it is presently unclear if a small molecule that acts as a plasticizer in the bulk can actually lead to apparent antiplasticization and enhancement of mechanical properties in polymer thin films and nanostructures.

In this Chapter, we examine the efficacy of two distinct processing routes, UVO treatment and addition of a plasticizer, on effectively increasing the moduli of ultrathin (< 30 nm) PS and PMMA films in comparison to their pure polymer counterparts. Elastic moduli are elucidated using the wrinkling instability of a thin polymer film on an elastic substrate discussed in the previous chapters. To

understand molecular mass effects, a high molecular mass PS and an oligomer of PS are studied using both processing routes. We demonstrate that low concentrations of a plasticizer can effectively eliminate thickness dependence of the elastic modulus in thin polymer films without significantly decreasing the modulus. A more complex situation arises with UVO treatment, where the efficacy of this method is dependent upon chemistry (PS vs. PMMA) and molecular mass (high vs. low). These experimental results can be explained in terms of near surface effects and the impact of the processing routes explored here on polymer properties in the vicinity of a free interface. Using these techniques, sub 30 nm modulus reductions are eliminated, important for next generation lithography where polymeric materials are used to generate sub 32 nm nanostructures.

3.2 Experimental

PS of varying molecular mass was purchased from Polymer Laboratories (M_n = 1.3 kg/mol, T_g = 29.9 °C; M_n = 2.3 kg/mol, T_g=64.3 °C; M_n = 492 kg/mol, T_g = 106.1 °C; M_n = 990 kg/mol, T_g = 106.3 °C). PMMA was purchased from Polymer Source (M_w = 91 kg/mol, T_g = 105 °C). Dioctyl phthalate (DOP) and toluene were purchased from Aldrich and used as received.

Silicon wafers (450 μm thick) were used as substrates for PS, cleaved into approximately 2.5 cm × 1 cm pieces and cleaned with UVO (model 42, Jelight). To assist with film transfer (interactions between silanol and methacrylates), mica sheets were used as substrates for PMMA films. Polymer films were spin-cast

from the dilute solutions in toluene onto these substrates. PDMS (Sylgard 184, Dow Corning) was prepared at a ratio of 20:1 by mass of base to curing agent, cast into 1.5 mm thick sheets, and allowed to gel at room temperature for 3 h before curing at 100 °C for 2 h. After cooling to ambient, the PDMS was cut into approximately 2.5 cm × 7.5 cm strips. The modulus of the PDMS was determined using a Texture Analyzer (TA-XT Plus) at a strain rate of 0.01 mm/s and found to be 0.7 MPa ± 0.1 MPa.

In order to exceed the critical strain required to produce surface wrinkling on all samples, the PDMS was pre-strained to 4% using a stage described previously.[24] The polymer film was then transferred to strained PDMS using differential adhesion in water. The sample was dried under vacuum at 10 °C below its bulk T_g to avoid thermal induced wrinkling. In cases where UVO treatment was used, the polymer film on the strained PDMS was exposed to UVO at a distance of approximately 10 mm from the UV source for either 30s, 60s, or 90s. The pre-strain on the PDMS was then released at a rate of 0.1 mm/s. All samples were released at ambient temperature (T = 21 °C ± 2 °C).

The thickness of the polymer film on the strained PDMS was determined using a Variable Angle Spectroscopic Ellipsometer (VASE M-2000, J.A. Woollam Co., Inc.) over a wavelength range from 250 nm to 1700 nm using three incident angles, 67°, 70°, and 73°. The data were modeled using the optical properties of the PDMS substrate and a Cauchy layer to describe the polymer film. The film thickness measured before transfer (i.e., on the silicon wafer) was found to be within 1 nm of the film thickness after transfer (i.e., on PDMS).

Additionally, the decrease in film thickness from UVO exposure is less than 1.5 nm in all cases examined.

Characterization of the wrinkled surfaces was performed using atomic force microscopy (AFM) and optical microscopy. AFM images were acquired at ambient temperature on an Agilent Technologies 5500 system in contact mode using a constant scan size of 7.5 μm × 7.5 μm at a scan rate of 1 Hz. AFM images were analyzed using 1D Fast Fourier Transform (FFT) to obtain the wavelength of the wrinkles. Optical images were acquired using a Mititoyo Ultraplan FS-110 and analyzed using 1D Fast Fourier Transform (FFT) to determine the wrinkle wavelength.

To measure the T_g of PS with 5 mass % DOP thin films on PDMS, 20:1 PDMS films were spin cast onto clean silicon wafers from a dilute toluene solution (0.5 % to 2 % by mass PDMS) and cured at 100 °C for 2 h. The PDMS layer was varied from 30 nm to 70 nm thick. PS films containing 5 mass % DOP ($h_f \approx 55$ nm) were transferred to the PDMS films from silicon wafers as described above. Ellipsometry was used to measure the thermal response of PDMS films and PDMS/PS-DOP bilayers. T_g was determined from changes in the PS-DOP film thickness measured upon cooling from 150 °C to 30 °C at 1.0 °C/min in a nitrogen purge atmosphere.

3.3 Results

As shown in Chapter 2 and reported elsewhere the modulus of PS and PMMA films confined to the nanometer length scale exhibit a dramatic decrease

when using "non-contact" metrologies such as wrinkling[25-27] and and nanobubble inflation[28]. This reduction in modulus is consistent with a reported "liquid"-like free surface layer that is dependent on both the structure and properties of the bulk polymer and the substrate.[6, 29] For polystyrene films with M_n=1.3 kg/mol and M_n=493 kg/mol the modulus as a function of film thickness has two salient features as shown in Figure 3.1. First a bulk-like modulus is observed until a critical thickness is reached. Below this critical thickness deviation from bulk values are observed. One interesting feature is that unlike the T_g of PS, the critical thickness at which deviations in the elastic modulus are observed is dependent upon molecular mass of the PS.[27] As detailed in Chapter 2, the surface layer of PS shows a molecular mass dependence, where the surface layer increases from $\delta \approx 5$ nm to $\delta \approx 52$ nm when the number-average relative molecular mass (M_n) of PS is decreased from 492 kg/mol to 1.1 kg/mol. Similar to the change in δ, the length scale below which deviations from the bulk-like modulus occurs shifts from approximately 50 nm for the high M_n PS to greater than 70 nm for the low M_n PS. If the surface of the polymer is indeed the source of the decreased modulus, one potential route to overcome the decreased mechanical robustness is to crosslink the surface of the PS in order to decrease polymer mobility and increase the surface stiffness.[30] One well established route to crosslink PS surfaces is through exposure to UVO.[17, 18] UVO crosslinking reduces the mobility of polymers by chemical reactions where the polymer chains form larger 3-dimensional networks. It is expected that this stiffening of the polymer chains would therefore increase the free surface modulus of the polymer.

The impact of exposure to UVO on the thickness dependence of the modulus for 1.3 kg/mol and 492 kg/mol PS films is shown in Figure 3.1.

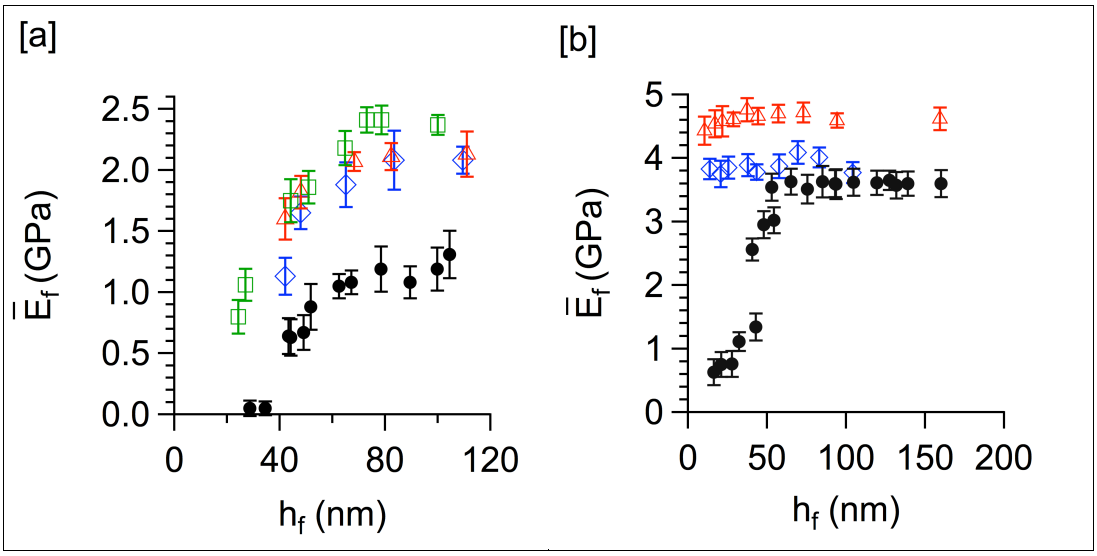

Figure 3.1 [a] Modulus as a function of film thickness for 1.3 kg/mol PS: pristine (●), after 30 s UVO exposure (◇), after 60 s UVO exposure (△), and after 90 s UVO exposure (□) [b]Modulus as a function of film thickness for 493 kg/mol PS: pristine (●), after 30 s UVO exposure (◇), and 60 s UVO exposure (△).

Interestingly for 1.3 kg/mol PS films (Figure 3.1a), a reduction from bulk values is observed even after UVO exposure at h_f <50 nm. Thus, the UVO treatment is unable to eliminate the effects of nanoconfinement on the elastic modulus of low molecular mass PS films. However compared to the unexposed low molecular mass PS, the thicker (> 50 nm) UVO exposed films show an overall increase in apparent elastic modulus from $E(t_{UVO}=0) \approx 1.06$ GPa to $E(t_{UVO}=30, 60, 90\ s) \approx 1.87$ GPa assuming a Poisson's ratio, *n*, of 0.33. This increase in bulk modulus with UVO exposure is expected as UVO has shown to

crosslink PS.[31] Note that Figure 3.1 reports the strain-plane modulus, $\overline{E} = E/\left(1-\upsilon^2\right)$. Similarly, the 492 kg/mol PS films exhibit an increase in overall modulus when exposed to UVO, but the modulus becomes independent of thickness after UVO exposure of 30 s and 60 s. The bulk elastic modulus of this unexposed PS is approximately 3.2 GPa, which increases to approximately 3.5 GPa and 4.0 GPa after 30s and 60s of UVO exposure, respectively. Additionally, a bulk-like modulus is measured for films as thin as 15 nm after this UVO exposure; this is counter to neat polymers that we have examined where a decrease in modulus relative to the bulk is observed at this length scale.[14, 32, 33] Furthermore, this increase in modulus was observed after 24 hrs of treatment, however it is expected that surface recovery would be observed at longer time scales. To explain the observed dependence on molecular mass for the efficacy of UVO treatment, an understanding of the effects of UVO on the properties of PS surfaces is required.

Fortuitously, the UVO surface treatment of PS has been widely studied and the mechanism of surface modification has been established.[17, 18, 30] UVO initially breaks molecular bonds on the surface of the polymer, allowing for the addition of oxygen atoms.[34] For short exposure times (t_{UVO} < 60 s), the concentration of chemisorbed oxygen increases linearly with time to approximately 6 atom-% after 60 s exposure.[18] Atomic oxygen then reacts with the polymer chain by an insertion reaction to form carbonyl groups or through the removal of hydrogen from the chain to yield a carbon radical; this carbon radical can lead to the formation of carboxyl groups and enables cross-linking between

polymer chains.[17, 18] As oxygen is required for these reactions, the diffusion of oxygen through the film is required; crosslinking of the surface limits the diffusion of oxygen and leads to an apparent limitation of the oxygen mediated modification to the near surface region extending approximately 5 nm into the film.[17, 18] For high molecular mass PS (492 kg/mol), the free surface layer ($h_f \approx 5$ nm) having a reduced modulus should be completely oxidized and crosslinked based on the observed diffusion-limited penetration depth of ≈ 5 nm for molecular oxygen during UVO exposure. Conversely, the UVO treatment of low molecular mass PS (1.3 kg/mol) does not eliminate the thickness dependent modulus. However, the lower molecular mass PS has a significantly larger surface layer ($\delta \approx 25$ nm) that cannot be fully oxidized and cross-linked. Crosslinking low molecular mass PS free surface is limited due to the UVO penetrating only 5 nm into the film. However some of this soft surface is converted to a less compliant oxidized, crosslinked material, thus explaining the overall observed increase in elastic modulus for a fixed thickness after UVO treatment, as illustrated in Figure 3.1. However surface rearrangement of the more rigid treated surface with the more compliant free surface layer does not allow for the thinner films to exhibit a thicker bulk-like modulus. This simple explanation based upon the finite penetration depth of the UVO treatment appears consistent with the observed data.

To further investigate the influence of UVO treatment on the mechanical properties of polymer thin films, films of PMMA were also examined. The impact of UVO exposure on the elastic modulus of PMMA is shown in Figure

3.2; the UVO treated PMMA remains statistically invariant from the unexposed PMMA at identical thickness. During exposure to UV radiation, cross-linking and chain scission occur simultaneously, but the dominance of either process is a function of the polymer structure.[35, 36] Unlike the predominance of cross-linking processes for PS, PMMA primarily undergoes chain scission of the methyl esters followed by the generation of one unsaturated bond in the polymer chain under UV irradiation.[36]

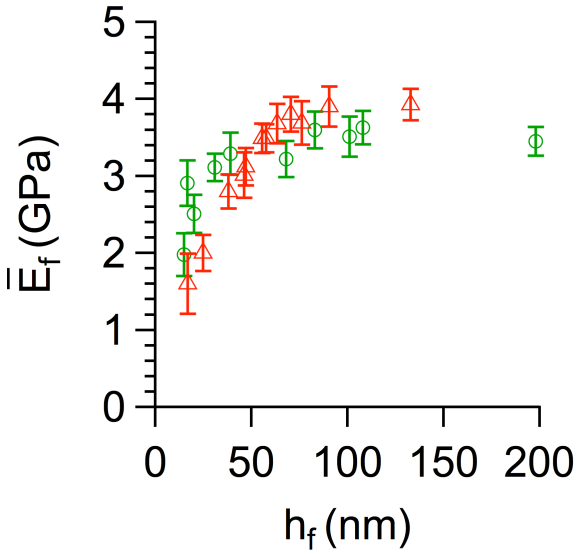

Figure 3.2 Modulus as a function of film thickness for 91 kg/mol PMMA: pristine (△) and after 30 s UVO exposure (○).

This difference in behavior has been exploited in block copolymer lithography using PS and PMMA segments to create a nanoporous template upon removal of the PMMA fragments.[37] Since the surface of the PMMA is not appreciably crosslinked by UVO exposure, there is no strengthening of the surface and hence no statistical change in the thin film moduli. However,

reduction in the molecular weight of PMMA via chain scission will ultimately lead to a decrease in the modulus. Based on the observations shown here, any decrease in average molecular mass from chain scission during a 30s UVO exposure is insufficient to adversely impact the elastic modulus in comparison to the neat unexposed PMMA. However, UVO treatment is not able to effectively eliminate decreases in the mechanical properties of ultrathin PMMA films. Thus, the data for both PMMA and the low molecular mass PS illustrate the limitations of UVO for improving the elastic modulus at the nanoscale, although UVO is effective for some specific polymer systems such as high molecular mass PS. Other polymers such as polybutadiene and polyethylene have been shown to crosslink when exposed to UV. [38, 39]

One potential alternative to UVO treatment for mechanically reinforcing polymers at the nanoscale is through the addition of an antiplasticizer.[20] Traditionally, small molecule diluents known as plasticizers are added to polymer materials to increase processability and reduce fragility/brittleness by reducing T_g. However, addition of plasticizers also leads to a decrease in the modulus, which can be detrimental for some applications. For example, phthalates are used for increasing poly (vinyl chloride)'s flexibility, while ester plasticizers are used in rubber manufacturing. Conversely, antiplasticization can occur at low diluent levels when a strong interaction is present between the small molecule and the polymer that leads to densification.[40, 41] In cases where antiplasticization occurs, the increased physical density of the material leads to an increased elastic modulus, despite a decrease in T_g from the addition of the diluent to the

polymer.[40-42] Simulations by de Pablo and coworkers indicate that antiplasticizers can also provide enhanced mechanical rigidity of polymers at the nanoscale where confinement effects are eliminated and bulk like values are possible.[20] Nealy and coworkers investigated the mechanical properties of PMMA beams with plasticizer tris(2-chloropropyl) phosphate (TCPP) via cantilever bending models and observing structure collapse. Their results show that addition of TCPP increases the elastic modulus of the PMMA nanostructures by 18% to 26%, allowing antiplasticized structures to remain stable at aspect ratios that have been shown to collapse with pure PMMA.[11]

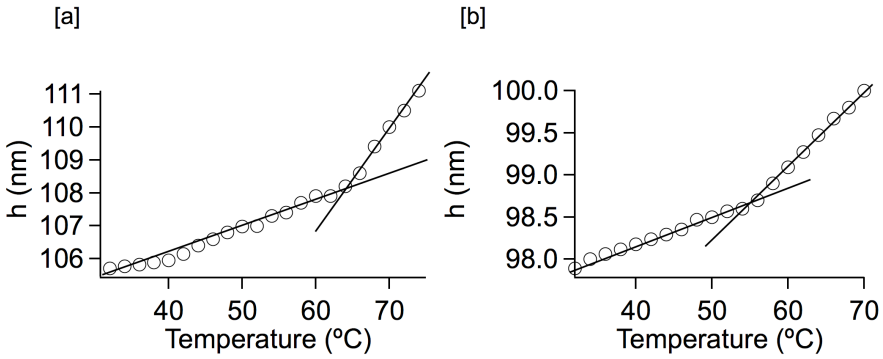

Figure 3.3 Ellipsometry data of the film thickness as a function of temperature for [a] pure 2.3 kg/mol PS with T_g = 64.3 ºC ± 1.6 ºC and [b] 5wt% DOP in 2.3 kg/mol PS with T_g =55.1ºC ± 2.1ºC.

Additionally, through molecular dynamic simulations it is found that the antiplasticizer homogenizes the polymer film in terms of cooperative rearrangement;[20] this homogenization eliminates surface effects[5] that have been attributed as the cause for a decrease in T_g[43] and bulk mechanical properties[1] of nanoconfined polymers. Experimentally, Ellison *et al.* showed that addition of approximately 9 wt % pyrene in PS eliminated any size dependencies on the film

T_g behavior;[23] this result is consistent with the aforementioned simulations where antiplasticizing diluents homogenize the film.[20] Potential π-π interactions between PS and pyrene could lead to an antiplasticization effect. However, addition of only 4 mass % DOP to PS also eliminates nanoconfinement effects on thin film T_g.[23] This results is quite curious as addition of DOP to bulk polymers leads to plasticization with a reduction in the bulk glass transition temperature and a decrease in the elastic modulus.[44, 45] In this study the addition of DOP to ≈ 100 nm thick PS films results in a decrease in both T_g and elastic modulus. Figure 3.3a shows the film thickness as a function of temperature for a 100 nm pure 2.3 kg/mol PS film. The intersection of the slope for the linear and melt behavior is used to extrapolate T_g. Without DOP, the T_g of the PS (M_n = 2.3 kg/mol) is extrapolated to be 64.3 ºC ± 1.6 ºC.

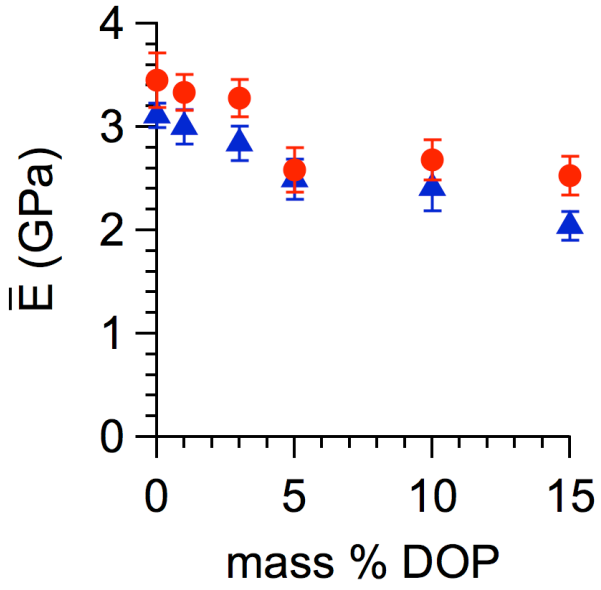

Figure 3.4 Modulus dependency on DOP mass % for both 990 kg/mol (●) and 2.3 kg/mol (▲) PS films. The error bars represent one standard deviation of the data, which is taken as the experimental uncertainty of the measurement.

However from Figure 3.3b the T_g decreases to 55.1 ºC ± 2.1 ºC with the addition of 5 mass % DOP. This depression in T_g is consistent with previous data for the T_g of DOP plasticized PS in the bulk.[46] Figure 3.4 illustrates the decrease in elastic modulus of PS films ($h_f \approx 55$ nm) from approximately 3.3 GPa at 0wt% to 2.2 GPa at 15wt%. Note that this decrease is independent of molecular weight as both the 990kg/mol PS and 2.3 kg/mol PS collapse onto a single curve. The decrease in both T_g and elastic modulus with addition of DOP in the films is indicative of plasticization of the PS. However in thin films, the thickness dependence on T_g of PS films can be eliminated by using DOP,[23] but as shown in Chapter 2 deviations in the modulus of thin poly(n-propyl methacrylate) films do not correlate with thin film T_g. Thus, it would be instructive to understand how the addition of DOP to these thin PS films impacts the elastic moduli.

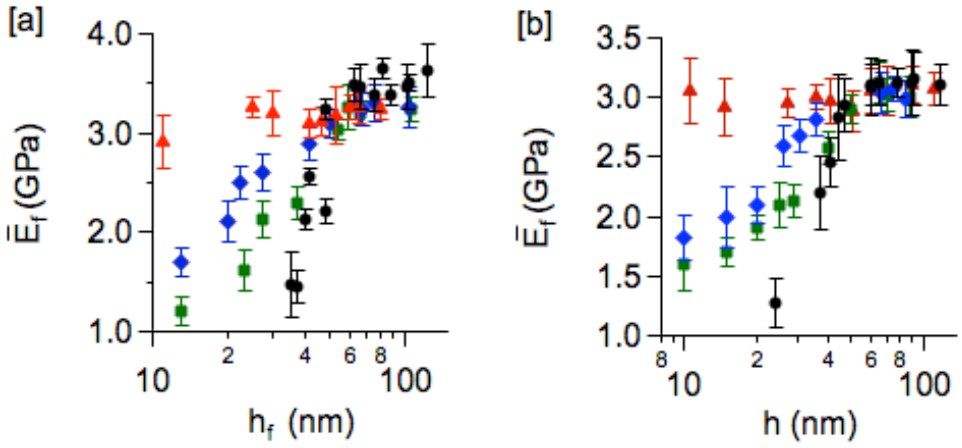

Figure 3.5 Modulus of [a] 990 kg/mol and [b] 2.3 kg/mol PS with varying DOP concentration: pure PS (●), 1 mass% (■), 3 mass% (◆), and 5 mass%(▲).

The addition of DOP to 990 kg/mol PS thin films leads to a progressive increase in the modulus for films less than approximately 50 nm thick as shown in Figure 3.5a. Although the bulk modulus is not significantly impacted by the

addition of up to 5 mass % DOP, the modulus of ultrathin (< 30 nm) films is strongly dependent upon the DOP concentration over the same range. At 5 mass % DOP, the PS film modulus is statistically independent of film thickness. This is reminiscent of the impact of DOP on the T_g of PS thin films where bulk T_g is recovered in ultrathin films if 4 mass % DOP is added,[23] although the length scale at which T_g and modulus deviations from bulk occur is not always consistent.[14]

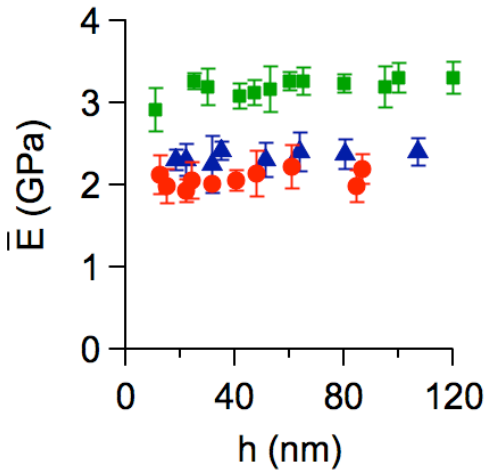

Figure 3.6 The modulus of 990 kg/mol PS with varying DOP concentration: 5 wt%(■), 10 wt%(▲), and 15 wt%(●).

The addition of non-volatile diluents appears to be a facile mechanism to improve the elastic modulus of polymers at the nanoscale. Although as previously mentioned, only diluents where polymer-diluent interactions dominate have been successful. However, the effect of UVO treatment on the mechanical behavior of both high and low molecular mass PS thin films is strikingly different, so it would be insightful to determine if similar differences exist when adding DOP to these systems. One issue that arises is the initial low T_g of the 1.3 kg/mol

PS; addition of 5 mass % DOP decreases T_g below ambient. As discussed in Chapter 2 when the T_g approaches the experimental temperature (21 ± 2°C) surface wrinkling is not stable thus precluding the formation of stable wrinkle patterns to elucidate the thin film modulus. Instead, a slightly larger molar mass is utilized for the DOP studies (2.3 kg/mol). As shown in Figure 3.5b, the addition of DOP to this lower molecular mass PS also yields improvements in the modulus of the ultrathin films. As shown, the impact of DOP on the modulus is identical between the two varying molecular masses, where the modulus is independent of film thickness for >5wt% DOP. However as the amount of plasticizer continues to increase, a significant decrease in bulk modulus, from ~3 GPa at 5wt% to 2.2 GPa at 15wt% is observed as shown in Figure 3.6. This decrease in elastic modulus at h>50 nm while increasing the sub 30 nm modulus suggest that both plasticization and antiplasticization begins to occur at DOP concentrations greater than 15 wt%. This also suggests that the mode of inhibition of nanoconfinement effects by addition of DOP is independent of the degree of mechanical heterogeneity within the film as the thickness of soft surface layer (δ) is estimated to be nearly double for the 2.3 kg/mol PS in comparison to the 990 kg/mol PS.[14] To further examine the broad applicability of adding DOP to eliminate decreases in the modulus of polymer thin films, a polymer lacking aromaticity is examined: PMMA. Figure 3.7 shows the film thickness dependence on the moduli of PMMA as a function of DOP concentration. Similar to the observed behavior for PS, addition of DOP systematically increases the modulus of ultrathin (<50 nm) films of PMMA. At 5 mass % DOP, the modulus

of the PMMA films is independent of film thickness. These results suggest that small molecules in ultrathin polymer films may be able to act as antiplasticizers, even if these diluents are plasticizers in the bulk. This is in agreement with recent experimental work by Nealy and coworkers where a maximum elastic modulus was obtained with the addition of 5wt% antiplasticizer to PMMA.[11] However Nealy and coworkers suggest a dimension-dependent elastic modulus in PMMA nanostructures, where a slight depression in bulk modulus was observed with decreasing structure size. The lower modulus in nanostructures can be attributed to a geometric difference where supported thin films are limited to one free surface and nanostructures are influenced by a series of other free surface-polymer interactions.

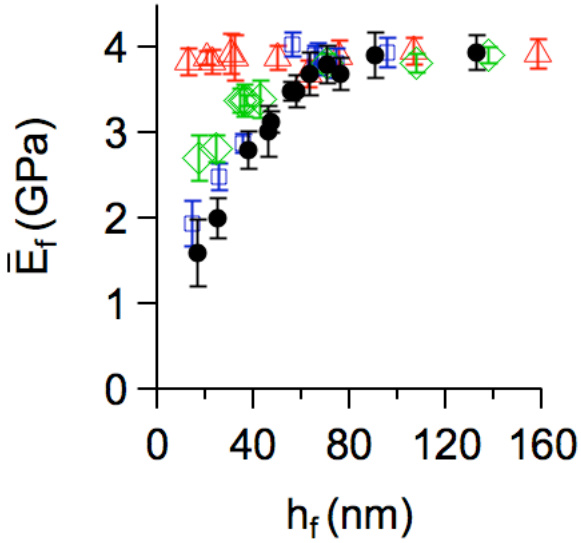

Figure 3.7 The modulus of 91 kg/mol PMMA with varying DOP concentration: 5 wt%(△), 3 wt%(◇), 1 wt%(□), and pure polymer (●).

It is unclear how the addition of a diluent to a polymer thin film can increase its modulus, but molecular dynamic simulations suggest thin films

containing a small molecule exhibit smaller-scale collective motion, which reduces the influence of the free surface layer and subsequently leads to elimination of the bulk modulus reduction that is present in the neat polymer film.[21] In order to study the collective motion of the polymers, second-order non linear optics (NLO) which monitors the rotational reorientation of extrinsic molecular probes or chromophores in polymers can be utilized. Recently NLO measurements have shown that the measured chromophore reorientation dynamics are coupled to the cooperative segmental mobility of the polymer.[47] Therefore time resolved optical techniques such as birefringence and second-order NLO allow for the detection or chromophore orientation and thus a method to measure the collective motion and cooperative rearrangement of polymer thin films. NLO would therefore be able to determine if indeed the addition of small molecules reduce collective motion within the polymer matrix.

3.4 Conclusions

The elastic moduli of neat PS and PMMA are found to decrease when the film thickness is less than 50 nm as a result of a mechanically compliant surface layer. Two strategies to limit or circumvent the reduction in modulus of polymers at the nanoscale are examined: UV-ozone promoted oxidation/crosslinking of surface and addition of liquid diluent. UVO exposure leads to oxidation and cross-linking of the near surface of PS (≈ 5 nm), which leads to in overall increase in modulus. For high molecular mass PS (492 kg/mol), the thickness of the crosslinked layer is similar to that of a soft free surface layer ($\delta \approx 5$ nm) and the modulus of these films after 30s UVO exposure is independent of film thickness.

For low molecular mass PS (1.3 kg/mol), the free surface layer ($\delta \approx 25$ nm) is larger than the depth of surface modification, thus the modulus for this low molecular mass PS is still thickness dependent after UVO exposure. Due to chain scission during the photodegradation process for PMMA, UVO exposure showed no statistical variation in the modulus from the pure nanoconfined polymer. Conversely, addition of DOP to bulk PS and PMMA leads to a reduction in the extent of decrease in moduli for ultrathin films. At 5 mass % DOP, the moduli of PS and PMMA films are independent of film thickness. This result suggests PS and PMMA are antiplasticized by up to 5wt% DOP at the nanoscale despite DOP acting as a plasticizer in the bulk for both polymers. However as previous work has shown not all plasticizers eliminate nanoconfinement effects (i.e. PS oligomers in a PS matrix).[20] Suggesting that only if interactions between the diluent and polymer matrix exist will antiplasticization occur.

3.5 References

1. Chakravartula, A.; Komvopoulos, K., Viscoelastic properties of polymer surfaces investigated by nanoscale dynamic mechanical analysis. *Applied Physics Letters* **2006,** *88* (13), 131901-3.

2. Miyake, K.; Satomi, N.; Sasaki, S., Elastic modulus of polystyrene film from near surface to bulk measured by nanoindentation using atomic force microscopy. *Applied Physics Letters* **2006,** *89* (3).

3. Tweedie, C. A.; Constantinides, G.; Lehman, K. E.; Brill, D. J.; Blackman, G. S.; Van†Vliet, K. J., Enhanced Stiffness of Amorphous Polymer Surfaces under Confinement of Localized Contact Loads. *Advanced Materials* **2007,** *19* (18), 2540-2546.

4. Mansfield, K. F.; Theodorou, D. N., Molecular-Dynamics Simulation of A Glassy Polymer Surface. *Macromolecules* **1991,** *24* (23), 6283-6294.

5. Qi, D.; Fakhraai, Z.; Forrest, J. A., Substrate and Chain Size Dependence of Near Surface Dynamics of Glassy Polymers. *Physical Review Letters* **2008,** *101* (9), 096101.

6. Ellison, C. J.; Torkelson, J. M., The distribution of glass-transition temperatures in nanoscopically confined glass formers. *Nature Materials* **2003,** *2* (10), 695-700.

7. Fakhraai, Z.; Forrest, J. A., Measuring the Surface Dynamics of Glassy Polymers. *Science* **2008,** *319* (5863), 600-604.

8. Wallace, W. E.; Van Zanten, J. H.; Wu, W., Influence of an impenetrable interface on a polymer glass-transition temperature. *Physical Review E* **1995,** *52* (4), R3329-R3332.

9. Priestley, R.; Mundra, M. K.; Barnett, N. J.; Broadbelt, L. J.; Torkelson, J. M., Effects of nanoscale confinement and interfaces on the glass transition temperatures of a series of poly(n-methacrylate) films. *Australian Journal of Chemistry* **2007,** *60* (10), 765-771.

10. Johnson, W. L.; et al., Elastic constants and dimensions of imprinted polymeric nanolines determined from Brillouin light scattering. *Nanotechnology* **2009,** *21* (7), 075703.

11. Delcambre, S. P.; Riggleman, R. A.; Pablo, J. J. d.; Nealey, P. F., Mechanical properties of antiplasticized polymer nanostructures. *Soft Matter* **2010,** *6* (11), 2475-2483.

12. Mundra, M. K.; Donthu, S. K.; Dravid, V. P.; Torkelson, J. M., Effect of spatial confinement on the glass-transition temperature of patterned polymer nanostructures. *Nano Letters* **2007,** *7* (3), 713-718.

13. Bohme, T. R.; de Pablo, J. J., Evidence for size-dependent mechanical properties from simulations of nanoscopic polymeric structures. *Journal of Chemical Physics* **2002,** *116* (22), 9939-9951.

14. Torres, J. M., Stafford, C.M., Vogt, B.D., Elastic Modulus of Amorphous Polymer Thin Films: Relationship to the Glass Transition Temperature. *ACS NANO* **2009,** *3*, 2677.

15. Fouassier, J. P.; Rabek, J. F., *Radiation Curing in Polymer Science and Technology: Fundamentals and methods*. Elsevier Applied Science: 1993.

16. Lee, K.; Pan, F.; Carroll, G. T.; Turro, N. J.; Koberstein, J. T., Photolithographic Technique for Direct Photochemical Modification and Chemical Micropatterning of Surfaces. *Langmuir* **2004,** *20* (5), 1812-1818.

17. Klein, R. J.; Fischer, D. A.; Lenhart, J. L., Systematic Oxidation of Polystyrene by Ultraviolet-Ozone, Characterized by Near-Edge X-ray Absorption Fine Structure and Contact Angle. *Langmuir* **2008,** *24* (15), 8187-8197.

18. Teare, D. O. H.; Ton-That, C.; Bradley, R. H., Surface characterization and ageing of ultraviolet-ozone-treated polymers using atomic force microscopy and x-ray photoelectron spectroscopy. *Surface and Interface Analysis* **2000,** *29* (4), 276-283.

19. Teare, D. O. H.; Emmison, N.; Ton-That, C.; Bradley, R. H., Effects of Serum on the Kinetics of CHO Attachment to Ultraviolet-Ozone Modified Polystyrene Surfaces. *Journal of Colloid and Interface Science* **2001,** *234* (1), 84-89.

20. Riggleman, R. A.; Yoshimoto, K.; Douglas, J. F.; de Pablo, J. J., Influence of Confinement on the Fragility of Antiplasticized and Pure Polymer Films. *Physical Review Letters* **2006,** *97* (4), 045502.

21. Riggleman, R. A.; Douglas, J. F.; de Pablo, J. J., Tuning polymer melt fragility with antiplasticizer additives. *The Journal of Chemical Physics* **2007,** *126* (23), 234903-10.

22. Tan, L.; Kong, Y. P.; Pang, S. W.; Yee, A. F., Imprinting of polymer at low temperature and pressure. *Journal of Vacuum Science & Technology B: Microelectronics and Nanometer Structures* **2004,** *22* (5), 2486-2492.

23. Ellison, C. J.; Ruszkowski, R. L.; Fredin, N. J.; Torkelson, J. M., Dramatic Reduction of the Effect of Nanoconfinement on the Glass Transition of

Polymer Films via Addition of Small-Molecule Diluent. *Physical Review Letters* **2004,** *92* (9), 095702.

24. Stafford, C. M.; Guo, S.; Harrison, C.; Chiang, M. Y. M., Combinatorial and high-throughput measurements of the modulus of thin polymer films. *Review of Scientific Instruments* **2005,** *76* (6).

25. Stafford, C. M.; Vogt, B. D.; Harrison, C.; Julthongpiput, D.; Huang, R., Elastic moduli of ultrathin amorphous polymer films. *Macromolecules* **2006,** *39* (15), 5095-5099.

26. Torres, J. M., Stafford, C. M., Vogt, B. D., Elastic Modulus of Amorphous Polymer Thin Films: Relationship to the Glass Transition Temperature. *ACS Nano* **2009,** *3* (9), 2677.

27. Torres, J. M., Stafford, C.M., Vogt, B.D., Impact of molecular weight on the elastic modulus of thin polystyrene films. *Submitted* **2010**.

28. O'Connell, P. A.; McKenna, G. B., Novel nanobubble inflation method for determining the viscoelastic properties of ultrathin polymer films. *Review of Scientific Instruments* **2007,** *78* (1), 013901-12.

29. Huang, R.; Stafford, C. M.; Vogt, B. D., Effect of Surface Properties on Wrinkling of Ultrathin Films. *Journal of Aerospace Engineering* **2007,** *20* (1), 38-44.

30. Callen, B. W.; Ridge, M. L.; Lahooti, S.; Neumann, A. W.; Sodhi, R. N. S., Remote plasma and ultraviolet--ozone modification of polystyrene. *Journal of Vacuum Science & Technology A: Vacuum, Surfaces, and Films* **1995,** *13* (4), 2023-2029.

31. Zhang, R.; Cherdhirankorn, T.; Graf, K.; Koynov, K.; Berger, R., Swelling of cross-linked polystyrene beads in toluene. *Microelectronic Engineering* **2007,** *85* (5-6), 1261-1264.

32. Stafford, C. M.; Vogt, B. D.; Harrison, C.; Julthongpiput, D.; Huang, R., Elastic Moduli of Ultrathin Amorphous Polymer Films. *Macromolecules* **2006,** *39*, 5095-5099.

33. Stoykovich, M. P.; Yoshimoto, K.; Nealey, P. F., Mechanical properties of polymer nanostructures: measurements based on deformation in response to capillary forces. *Applied Physics A-Materials Science & Processing* **2008,** *90* (2), 277-283.

34. Nie, H. Y.; Walzak, M. J.; Berno, B.; McIntyre, N. S., Atomic force microscopy study of polypropylene surfaces treated by UV and ozone exposure: modification of morphology and adhesion force. *Applied Surface Science* **1999,** *144-145*, 627-632.

35. Choi, J. O.; Moore, J. A.; Corelli, J. C.; Silverman, J. P.; Bakhru, H., Degradation of poly(methylmethacrylate) by deep ultraviolet, x-ray, electron beam, and proton beam irradiations. *Journal of Vacuum Science & Technology B: Microelectronics and Nanometer Structures* **1988,** *6* (6), 2286-2289.

36. Lee, E. H.; Rao, G. R.; Mansur, L. K., LET effect on cross-linking and scission mechanisms of PMMA during irradiation. *Radiation Physics and Chemistry* **1999,** *55* (3), 293-305.

37. Thurn-Albrecht, T.; Schotter, J.; Kastle, G. A.; Emley, N.; Shibauchi, T.; Krusin-Elbaum, L.; Guarini, K.; Black, C. T.; Tuominen, M. T.; Russell, T. P., Ultrahigh-Density Nanowire Arrays Grown in Self-Assembled Diblock Copolymer Templates. *Science* **2000,** *290* (5499), 2126-2129.

38. Walther, A.; Gˆldel, A.; M¸ller, A. H. E., Controlled crosslinking of polybutadiene containing block terpolymer bulk structures: A facile way towards complex and functional nanostructures. *Polymer* **2008,** *49* (15), 3217-3227.

39. Wu, C.-p.; et al., Study on preparation of UV cross-linking films of polyurethane-LiClO 4 complexes and their ionic conductivity. *Acta Physica Sinica (Overseas Edition)* **1993,** *2* (11), 841.

40. Jackson, W. J.; Caldwell, J. R., Antiplasticization. II. Characteristics of antiplasticizers. *Journal of Applied Polymer Science* **1967,** *11* (2), 211-226.

41. Jackson, W. J.; Caldwell, J. R., Antiplasticization. III. Characteristics and properties of antiplasticizable polymers. *Journal of Applied Polymer Science* **1967,** *11* (2), 227-244.

42. Zerda, A. S.; Lesser, A. J., Organophosphorous additive for fortification, processibility, and flame retardance of epoxy resins. *Journal of Applied Polymer Science* **2002,** *84* (2), 302-309.

43. Forrest, J. A.; DalnokiVeress, K.; Stevens, J. R.; Dutcher, J. R., Effect of free surfaces on the glass transition temperature of thin polymer films. *Physical Review Letters* **1996,** *77* (10), 2002-2005.

44. Cowie, J. M. G., *Polymers: Chemistry and Physics of Modern Materials*. 1998.

45. Ferry, J. D., *Viscoelastic properties of polymers*. New York, 1980; Vol. John Wiley and Sons.

46. Chiou, J. S.; Barlow, J. W.; Paul, D. R., Plasticization of glassy polymers by CO2. *Journal of Applied Polymer Science* **1985,** *30* (6), 2633-2642.

47. Hooker, J. C.; Burghardt, W. R.; Torkelson, J. M., Birefringence and second-order nonlinear optics as probes of polymer cooperative segmental mobility: Demonstration of Debye-type relaxation. *The Journal of Chemical Physics* **1999,** *111* (6), 2779-2788.

CHAPTER 4

INFLUENCE OF CHAIN STIFFNESS AND ARCHITECTURE ON THERMAL AND MECHANICAL PROPERTIES OF POLYMER THIN FILMS

4.1 Introduction

One outstanding issue in fundamental physics is characterization of the glass transition.[1-3] Over the past decades, there has been a concerted effort in examining how the glass transition temperature (T_g) changes with confinement of the glass former to nanoscale dimensions.[4-6] In particular, a single polymer, polystyrene (PS), have been examined extensively to assess how confinement to thin films its physical properties including T_g,[4, 7-9] thermal expansion,[8-10] elastic modulus,[11] chain conformation,[12] segmental motion,[13, 14] viscoelasticity,[15] creep behavior,[16] as examples. However, these studies have yielded conflicting conclusions depending upon the technique used. For example, T_g of supported ultrathin PS films has been shown to decrease when using fluorescence,[7, 17] BLS[18] or ellipsometry,[19] but micro-calorimetry[20] indicates no change in T_g irrespective of thickness. Russell and co-workers have recently suggested that the observed changes in T_g for confined thin films is a result of residual stress and not intrinsic changes in the physical properties,[21] which is similar to conclusions by Kremer and co-workers based upon long term annealing of polymer thin films.[22] Even if the thickness dependent properties of these polymer films are indeed artifacts of the film formation process, it will not always be possible to anneal out these effects in technological applications due to the time associated with the chain

relaxation. For example in microelectronics, lithographically patterning the surface of polymer thin films leads to a decrease of T_g, which is attributed to increasing the area of the free surface.[23] These discrepancies in the conclusions as well as those discussed in previous chapters provide motivation to examine the thin film behavior in greater detail. One route to improved understanding is to examine polymers other than linear PS. For example by utilizing different tacticity of poly(methyl methacrylate) (PMMA), it was shown that the specific monomer interaction with the substrate can dramatically impact the observed thickness dependent behavior.[24, 25] The homologous series of poly(n-alkyl methacrylate)s provides a facile route to examine how polymer structure impacts thin film behavior.[26] In this case, there appears to be some correlation between cooperative dynamics for the bulk and the thin film behavior.[26, 27] Similarly, Ellison and Torkelson examined how minor variations to the monomer structure of PS impacts the thin film behavior,[7] but no obvious correlation between cooperative and T_g changes are present. Additionally, the addition of diluents to the polymer appears to eliminate the influence of confinement on both T_g[28, 29] and modulus[30, 31] of polymer thin films. However in all these cases, relatively flexible polymers have been examined. When more rigid polymers have been examined such as polycarbonates, only a weak suppression in T_g was observed,[32] while the segmental dynamics appear to be suppressed upon confinement.[33] These results appear to be counter to those obtained for PS where T_g is significantly decreased and the segmental dynamics are enhanced in ultrathin films.[13, 34] Thus, a more detailed examination of monomer specific effects could provide insight into

critical parameters that control deviations in physical properties for thin film glasses.

In addition to these fundamental questions, there are a number of technologically relevant situations where functionalized polymers are utilized at the nanoscale. By varying the functionality of polymer chains, new and improved materials can be developed. For example, the melt rheological and thermodynamic properties of polyethylene can be well controlled through a combination of short-chain branching and long-chain branching to the polymer backbone.[35] To provide understanding of the impact of these parameters, a systematic variation in the polymer structure is critical in order to delineate effects. One technologically relevant route is through co-polymerization, where the ratio of each polymer block can be tuned. For example in fuel cell membranes, the ratio of sulfonated and fluorinated moieties in the polymer backbone controls the performance.[36] Similarly, the fire resistant behavior of polycarbonates can be varied through copolymerization of phosphates and arylates and further tailored by choice of polymer base, bisphenol-A or deoxybenzoin.[37, 38] These moieties provide significantly different degrees of rigidity to the polymer backbone limiting backbone rotation and thus could be able to smoothly tune the intrinsic polymer flexibility through composition.

Conjugated polymers provide another opportunity for examining rigid backbones,[39] but many of these are semi-crystalline.[40] Additionally, the pendant groups involved could significantly impact the thin film properties through interfacial interactions. One route to minimize variations in pendant groups is

through selective hydrogenation of unsaturated bonds in the polymer. Bond saturation has shown to alter the polymers thermal stability, storage and loss modulus, and optical properties.[41-44] The hydrogenation of polystyrene to poly(cyclohexylethylene) (PCHE) results in a decrease in density and T_g attributed to the cyclohexyl ring limiting the polymers ability to coil tightly.[45] Selective hydrogenation of unsaturated polymers via choice in catalyst provides a route to systematically vary the structure. Nonetheless, both discussed methods of hydrogenation and copolymerization lead to some uncertainty in the exact effects on thin film behavior due to the coupling of physical and chemical properties.

Similarly, branching of polymer chains can also influence material properties. With precise control over branching, functionality, and molecular weight enabled by synthetic advances,[46-50] branched, hyperbranched polymers and dendrimers with unique properties have been developed.[51, 52] For example, the unique architecture of these branched polymers can increase drug payload and drug release as compared to their linear counterparts.[53] Additionally, the mechanical properties of branched multigraph polyisoprene (PI) and polystyrene (PS) are improved as the number of branch points increase.[51] It is thus expected that branching will impact entanglements and/or film density directly controlling thin film T_g and modulus.

These novel architectures can also lead to changes in the nanoscale behavior. Blending linear polymers with dendrimers can inhibit dewetting of film due to dendrimer segregation to the substrate.[54] Additional thin film studies of

hyperbranched polyesters illustrated a deviation from bulk T_g in relatively thick films (~200 nm) attributed to their spatial arrangement as a result of their molecular architecture.[55] Moreover, the T_g of polymer thin films has shown that the behavior of star-shaped polymers does not directly correlate to their linear analogues.[56] Large deviations in T_g for PS thin films have typically been observed using ellipsometry or BLS;[7, 57] in contrast, hyperbranched star PS films exhibit only marginal changes in T_g for thin films.[58] A 5K, 3K, and 0K T_g suppression was found for the hyperbranched, star, and linear polystyrene respectively attributed to changes in film density of 5%, 3%, and 0%.

Although the bulk mechanical properties of branched polymers are known to change when compared to their linear counterparts,[51] their behavior in thin films is unexplored. However, the mechanical properties of linear polymer thin films have been explored via wrinkling mechanics.[59-61] In these studies, the bulk T_g of the polymer appears to control the softening of the free surface.[60] These results are consistent with some atomic force microscopy (AFM)-based indentation measurements.[62] However, other measures of the viscoelastic properties of polymer thin films have yielded conflicting results. McKenna and coworkers have reported stiffening in thin films for the rubbery films, while no change in the storage modulus of the glass near T_g is observed using nanobubble inflation rheology.[30, 63] Tsai and coworkers have used AFM to elucidate the viscoelasticity of PS thin films and simple scaling with the thin film T_g can account for film thickness dependencies.[64] This disagreement between research groups using different techniques to measure mechanical properties of thin

polymer films is not unexpected as there is still disagreement in the literature about the T_g of PS thin films despite nearly 20 years of studies.[57, 65, 66] However when using the same techniques (or ones measuring similar properties), there is generally good agreement; for example, there is generally good agreement in thin film T_g from ellipsometry, BLS and fluorescence,[67, 68] which all rely on variation in density or free volume. Thus, it might be more instructive to examine systematic series of polymers using several techniques to more clearly elucidate how confinement impacts properties, rather than focusing on a single polymer.

Therefore, in an attempt to understand the role of architecture on the properties of confined polymers, a series of PS with varying architectures will be utilized. Four different polymers of similar molecular mass are examined: trifunctional (comb), tetrafunctional (centipede), tetrafunctional (4-arm star), and linear polystyrene. In order to directly study the role of chain rigidity on the properties of confined polymers, both hydrogenation and copolymerization as described previously will be utilized in tandem. For these copolymers, a series of poly(arylate-phosphonate) produced by polycondensation of bisphenol-A (BPA) with phenylphosphonic (PPDC) and isophthaloyl chloride (IPC) are examined as a function of PPDC:IPC ratio.[38] As the PPDC content is increased, the polymer chain becomes more flexible. Similarly, poly [5-(2-phenylethylnorbornene)] (PENb) can be selectively saturated/unsaturated depending upon choice of polymerization method, addition or ring-opening metathesis polymerization (ROMP), and post-polymerization hydrogenation. Addition [5-(2-phenylethylnorbornene)] (Add PENb) yields unsaturation in the polymer

backbone, while ring-opened poly [5-(2-phenylethylnorbornene)] (hROMP PENb) produces a saturated cyclopentyl backbone. Additionally, the aromaticity of the phenyl ring can be preserved or hydrogenated to a cyclohexyl group (hROMP CENB and Add CENb).[69] These polymers provide a facile route to examine the effect of subtle changes on the mechanical and thermal properties of confined polymer glasses. Both the thermal and mechanical behavior of these polymers will be studied using ellipsometry to elucidate T_g and surface wrinkling to determine the modulus of thin films. This study will provide additional insight into the impact of backbone rigidity and polymer architecture on thin film properties.

4.2 Experimental

PS materials were synthesized through anionic polymerization.[70-72] Benzene, hexanes, styrene, butadiene, $SiCl_4$, $(CH_3)SiCl_3$, $(CH_3)_2SiCl_2$ and methanol were obtained from Aldrich and purified by using established methods. Sec-BuLi was synthesized from sec-BuCl and Li. 4-Chlorodimethylsilylstyrene (CDMSS) and 4-dichloromethylsilylstyrene (DCMSS) were each synthesized from 4-chloromethylstyrene, by transformation first into a Grignard reagent and subsequent addition to $(CH_3)_2SiCl_2$ or $(CH_3)SiCl_3$.[73-75] Polymerizations and linking reactions were conducted in all-glass, n-BuLi-washed, benzene-rinsed reactors equipped with break-seals for the addition of reagents and constrictions for the removal of intermediate aliquots and products. Linear PS was synthesized simply from polymerization of styrene from sec-BuLi. 4-arm star PS was synthesized by (1) preparing PSLi, end-capping it with a few units of butadiene to

reduce steric burdens, (2) linking these macroanions with $SiCl_4$ in slight stoichiometric want, and (3) fractionating in toluene/methanol. Comb PS was synthesized by (1) preparing PSLi and end-capping with butadiene, (2) preparing a macromonomer, in-situ, by adding this macroanion to CDMSS in a very slight stoichiometric want, and, finally, (3) polymerizing fresh styrene from sec-BuLi in the presence of this macromonomer adduct. Centipede PS was synthesized by (1) preparing PSLi and end-capping with butadiene, (2) preparing a macromonomer in-situ by adding this macroanion to DCMSS incrementally up to the 2-equivalence point, and (3) polymerizing fresh styrene from sec-BuLi in the presence of this macromonomer. Samples were characterized by using size exclusion chromatography equipped with refractive index and light scattering detection [Waters 2695 Alliance HPLC separations module, THF mobile phase at 35 °C, 3 X Polymer Labs Mixed C polystyragel separation columns, Wyatt miniDAWN triple angle laser light scattering detector, Waters 2414 refractive index detector]. Molecular characteristics are given in Table 1.

Table 4.1 Molecular characteristics of varying architecture PS samples

SAMPLE	SEC-RI		SEC-LS
	PDI	MW (kg/mol)	MW (kg/mol)
LINEAR	1.05	575	486
4-ARM STAR	1.03	–	483
(arm for star)	1.03	130	125
CENTIPEDE	1.07	–	540
(arm for centipede)	1.03	29.7	28.1
COMB	1.06	–	734
(arm for comb)	1.02	60.1	58.6

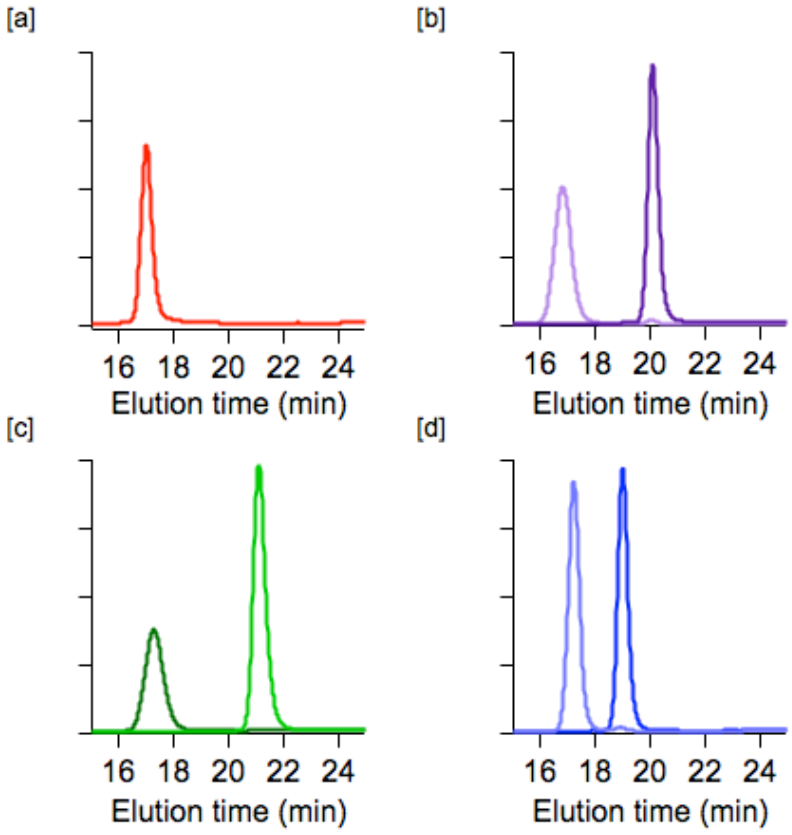

F

igure 4.1 Gel permeation chromatograph for [a] linear, [b] comb, [c] centipede and [d] star polystyrene main chain (dark) polymer arms (light).

Silicon wafers (450 μm thick) were used as substrates; the wafers were cut into approximately 3.5 cm × 3.5 cm pieces and cleaned with ultraviolet-ozone (model 42, Jelight) for 40 minutes. In order to cast PS films, varying architecture PS samples were dissolved in toluene. After complete dissolution they were spin coated onto the UVO cleaned silicon wafers for modulus and T_g measurements, respectively. The structure for each of these polymers is shown in Figure 4.2.

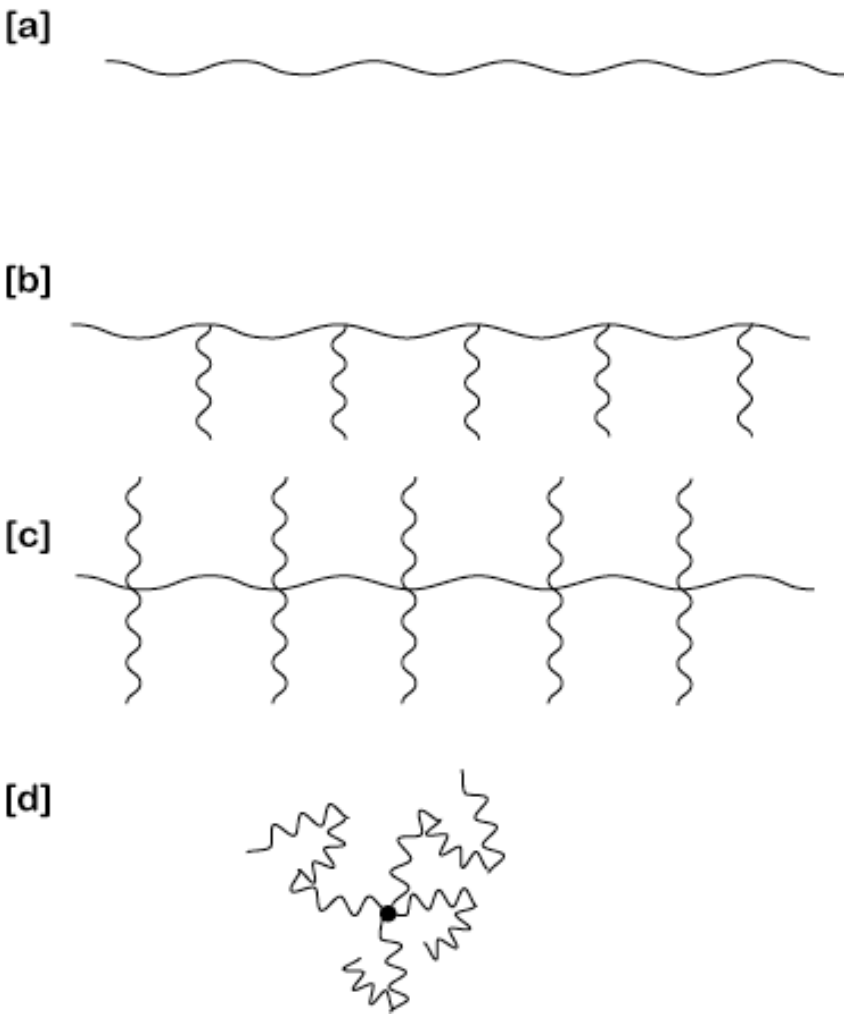

Figure 4.2 Schematic of the chain architecture for the non-linear PS samples examined: (a) comb PS, (b) centipede PS and (c) star PS.

Poly(styrene sulfonic acid) (PSS) was utilized as a release layer to enable surface wrinkling on PDMS. PSS in 2-propanol solution was spin cast onto the cleaned wafers. The film was annealed in vacuum at 130°C for 24 hrs in order to remove the remaining solvent and reduce surface roughness. After annealing, the film thickness and optical constants for the PSS layer were determined using a Variable Angle Spectroscopic Ellipsometer (VASE, J.A. Woollam Co., Inc.).

Measurements were performed from 40° to 75° in 5° increments and fit using a Cauchy model.

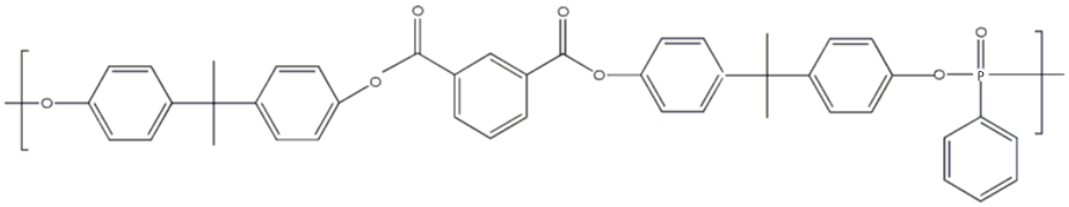

Figure 4.3 Structure of the Aryl-Phosphonate copolymer.

Aryl-phosphate copolymers were synthesized as reported previously and their structure is shown in Figure 4.3.[76] These copolymers were dissolved in anhydrous dimethylformamide and then spin coated onto the PSS coated or UVO cleaned silicon wafers for modulus and T_g measurements, respectively. The four poly [5-(2-phenylethylnorbornene)]s as reported previously[76] (hROMP PENb, hROMP CENb, Add PENb, and Add CENb) were dissolved in toluene and then spin coated to form the films. The structure for each of these polymers is shown in Figure 4.4.

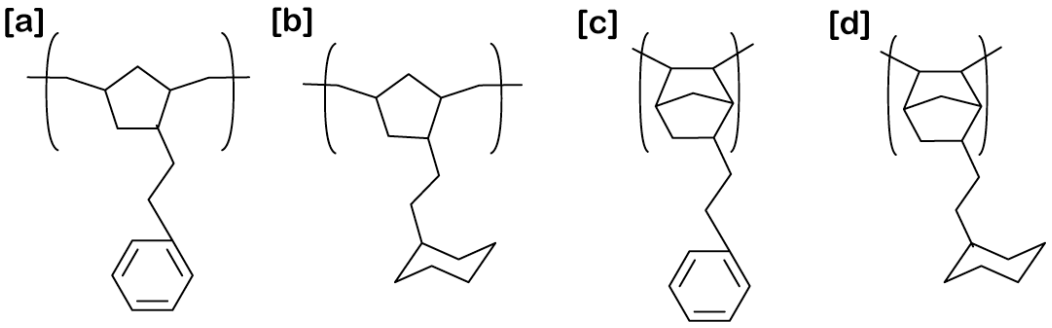

Figure 4.4 Structure of the four poly [5-(2-phenylethylnorbornene)]s [a] (hROMP PENb,[b] hROMP CENb, [c] Add PENb, and [d]Add CENb).

For all polymers variations in both solution concentration and the spin speed allowed for systematic reduction in film thickness. After spin coating the samples, the films were annealed at 200°C for 24 hrs in an inert N_2 atmosphere. The thickness of the polymer film was also determined using VASE and fit using a Cauchy model (and the previously determined optical constants and film thickness for PSS for the mechanical measurements). This measurement also allowed for a check on interdiffusion of the polymer into the PSS layer, however due to the lack of solubility of PSS in toluene or dimethylformamide no interdiffusion was observed.

To wrinkle the polymers to elucidate the elastic modulus, polydimethylsiloxane (PDMS) (Sylgard 184, Dow Corning) was utilized as the substrate and prepared at a ratio of 20:1 by mass of base to curing agent to a thickness of approximately 1.5 mm. The PDMS was allowed to degas at ambient for 3 h prior to curing at 100°C for 2 h. Slabs of PDMS measuring 2.5 × 7.5 × 1.5 mm were utilized as substrates for the wrinkling experiments. The bulk modulus of the PDMS was determined using a Texture Analyzer (TA.XT Plus, Texture Technologies). For the surface wrinkling measurements, the PDMS slab was mounted onto a custom built strain stage, pre-strained to ≈3.5% and then the polymer film of interest is transferred[77] The transfer was accomplished by placing the supported film in contact with the PDMS and immersing the system in a water bath. The polymer film transferred onto the PDMS surface, while any PSS layer dissolved in the water bath. The thickness of the transferred polymer film was measured for a second time utilizing ellipsometry in order to verify the

complete transfer of the film and removal of the PSS. The film thickness obtained after transfer was in good agreement (within 10Å) with that prior to transfer. In order to wrinkle the films, the pre-strain on the PDMS was released at a rate of 0.1 mm/s at ambient temperature (T= 21 °C ± 2 °C).

Characterization of the wrinkled surface was performed using atomic force microscopy (AFM, Agilent 5500) in intermittent contact mode using a constant scan size of 10μm by 10μm and optical microscopy (OM, Mititoyo Ultraplan FS-110) with an image resolution of 1024 pixels by 768 pixels. Both images were analyzed using a 1-D Fast Fourier Transform (FFT) in order to obtain the wavelength of the wrinkles.

The glass transition temperature (T_g) and coefficient of thermal expansion (CTE) of the polymer films directly cast onto the silicon wafer were measured using spectroscopic ellipsometry. The thermal response of the polymer was measured under a nitrogen atmosphere upon cooing from either 260 °C or 180 °C to 30 °C at 1.0 °C/min. The choice in upper bound temperature is dependent upon expected polymer T_g and in order to avoid polymer degradation. To determine the T_g of the film, the data were fit to the following empirical expression assuming a tanh profile:[6]

$$h(T) = w\left(\frac{M-G}{2}\right)\ln\left(\cosh\left(\frac{T-T_g}{w}\right)\right) + \left(T-T_g\right)\left(\frac{M+G}{2}\right) + c$$

where h is the film thickness, M and G are the linear thermal expansion coefficients of the melt and glass, w is the width of the transition, and c is the film thickness at $T = T_g$.

In order to determine the modulus of soft polymeric materials at sub 100 nm surface wrinkling is utilized. Minimization of total strain energy accounts for the resulting wrinkled surface.[78] In the linear elastic limit, the modulus of the polymeric film, $\overline{E}_f$, can be determined from the wavelength, λ, of the surface wrinkles as:[79]

$$\overline{E}_f = 3\overline{E}_s\left(\frac{\lambda}{2\pi h_f}\right)^3 \quad (2)$$

where $\overline{E}_s$, is the modulus of the PDMS substrate and h_f is the thickness of the PS film.

4.3 Results

4.3.1 Varying PS architecture

Variation in branching is known to impact the physical properties of polymers,[80-82] in particular, those related to flow or mechanics.[81, 83, 84] In this case, the selected branched polymers have a well controlled architecture via chlorosilane linking chemistry[85] and molecular mass distribution to elucidate how branching impacts the glass transition temperature (T_g) and storage modulus at ambient T of PS when confined to nanoscopic dimensions in the form of a thin film.

Figure 4.5 illustrates how T_g depends upon film thickness for the linear, comb, centipede, and star PS. For the thick films, the bulk-like T_g remains statistically invariant for all PS architectures at approximately 103 ± 2 °C as

would be expected based upon prior reports for linear PS[57] (105 °C) and a 794,00 g/mol star PS[58] (103 °C). However, there are significant differences in the thermal behavior for these different architectures for the thinner films. For example for the linear PS, a decrease in T_g is observed at approximately 30 nm with as much as a 25K reduction at 10 nm. This reduction in bulk T_g for linear PS on silicon is in agreement with previously reported work utilizing spectroscopic ellipsometry by Keddie and coworkers[86] and fluorescence with pyrene labeled linear PS by Ellison and Torkelson.[57]

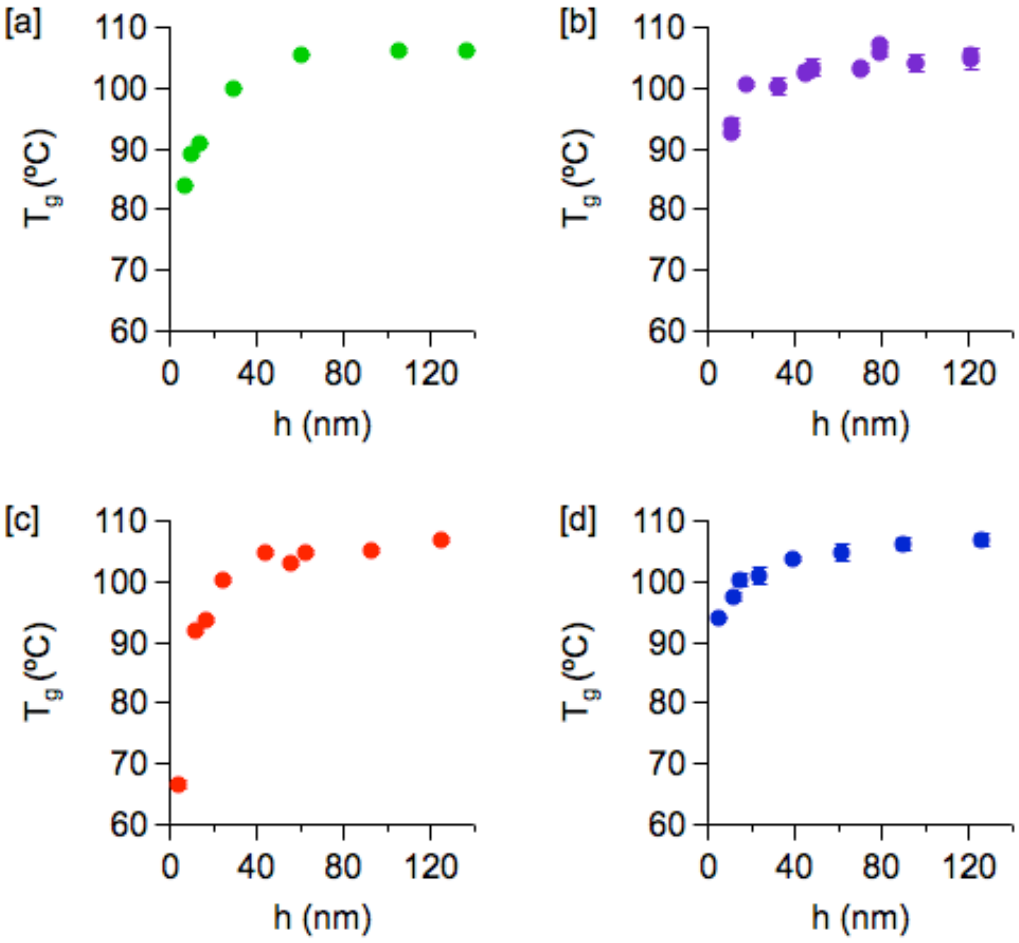

Figure 4.5 Glass transition temperature as a function of film thickness for [a] linear, [b] comb, [c] centipede and [d] star polystyrene.

Introduction of branching as a result of a trifunctional monomer results in a comb polymer that exhibits only a 10K reduction in T_g for a 10 nm thick film (Figure 4.5b). This small reduction in T_g could be attributed to increased interchain and intrachain entanglements commonly observed with increased branching,[87] as these interactions reduce segmental mobility, which appears related to T_g at the nanoscale.[14] However, altering the branching to form a centipede actually results in an increased thin film T_g depression compared to the linear PS (Figure 4.5c). For this tetrafunctional PS, a 40K depression is observed for a 10 nm thick film of the centipede PS. Interestingly, the star PS exhibits the least change in T_g of the four polymers examined with only a 8K reduction beginning at 30 nm. This result is equivalent to a 749,000 g/mol star PS where a 2K depression was observed at 10 nm;[58] this decreased sensitivity to confinement for the star polymer is attributed to reduction in density with branching.[58] This explanation is consistent for the comb and star PS examined here, but is counter to what is observed for the branched centipede PS. As the chemistry used for the synthesis is similar in each case, this divergent behavior is unexpected. However, the regularity in the branch structure of the centipede might allow for improved packing in the bulk and thus be more susceptible to conformational changes due to confinement in a thin film. As the elastic moduli of a material is generally closely tied to its physical density (in the absence of specific interaction) for the bulk, it could be instructive to examine the mechanical properties of this series of polymers to understand the origins of the different T_g behavior in thin films.

Figure 4.6 illustrates the modulus as a function of film thickness for all four PS samples. The bulk-like elastic modulus for the linear PS (Figure 4.6a) is approximately 2.57 ± 0.24 GPa, which is in contrast with previously reported modulus for a 492kg/mol PS film (3.92 ± 0.27 GPa).[60] This discrepancy in bulk modulus for linear PS could be attributed to a variation in tacticity of the PS that depends upon the synthetic protocol (prior PS examined are standards obtained from Varian), but even with this variation, the moduli lies within range of previously reported PS elastic modulus for bulk samples.[88] Despite this difference in the thick film moduli, these linear PS films exhibit an order of magnitude decrease in modulus to 0.58 ± 0.17 GPa when the film thickness is reduced to 14 nm, which agrees with the thickness dependence previously reported for the moduli of linear PS measured using wrinkling.[59, 60] Branching in the form of a comb polymer results in a slight decrease in bulk-like modulus to 1.87 ± 0.16 GPa (Figure 4.6b). This decrease in modulus relative to the linear PS is consistent with a reduced packing density as has been postulated in the prior discussion on the thin film T_g of these polymers. Although the comb PS exhibits the lowest bulk modulus, the modulus remains independent of film thickness down to 5 nm; this is similar to the limited thickness dependence of T_g for this polymer. However for the centipede PS (Figure 4.6cc), a significant increase in the bulk-like modulus is observed in comparison to the linear and comb PS examined here. It should be noted that the moduli of the thick films, 3.99 ± 0.17 GPa, is consistent with prior reports for linear PS.[59, 60] This increased modulus in comparison to the comb PS could be attributed improved packing of the more 'regular' branching of the

centipede. The improved mechanical properties of the centipede PS is consistent with a more complex series of multigraft copolymers, where tensile strength increases from comb to star to centipede for a polydiene (PI) backbone with branches of PS chains.[52] The improved mechanical properties of branched PI-PS copolymers are attributed to increased stress relaxation and tethering of the PS chains. There is a decrease in modulus as the centipede PS film becomes thinner, beginning at 40 nm. A 77% decrease in modulus is observed for a 10 nm thick film (0.75 ± 0.18 GPa). One intriguing feature for the thickness dependent moduli of this centipede PS is the narrow thickness window in which the modulus is drastically impacted. This sharp decrease in modulus is distinctly more pronounced than for the linear PS and most thin film T_g studies where a more gradual 'roll-off' behavior is observed.[65] This latter behavior is observed for the star PS (Figure 4.6d) where the modulus decreases to 0.91 ± 0.17 GPa for a 10 nm thick film. The bulk-like modulus for the star PS is 2.19 ± 0.24 GPa, which is also lower than the linear PS. Despite the similarity in bulk-like modulus to the comb PS, the modulus of the star PS is strongly dependent upon the film thickness ($h < 40$ nm).

One route to explain the differences in modulus behavior is to explore the implications of the relatively well accepted surface model, where the free surface of the polymer film has a reduced T_g and modulus in comparison to the bulk polymer.[14, 57, 67] In this case, the chain conformations at the free surface will be critical to the thin film behavior as the increased surface mobility in thin films has been attributed to enrichment of chain-end groups at the free surface.[89] The chain

ends in branched PS are surface active as evidenced by a significant reduction in surface tension when compared to their linear analogues.[90] However, the different thin film behavior between the comb and centipede PS indicates that surface conformation due to chain end segregation alone cannot account for the thickness dependent properties of polymer thin films. Alternatively, several recent reports have indicated that the thickness dependent properties of spin coated polymer glasses can be eliminated by proper long term annealing.[91, 92] Interestingly, the casting solvent can dramatically impact the viscoelastic behavior of the thinnest films;[93] this effect is attributed to the difference in chain conformation between the casting solution and the 'equilibrium' glass cooled from the melt.

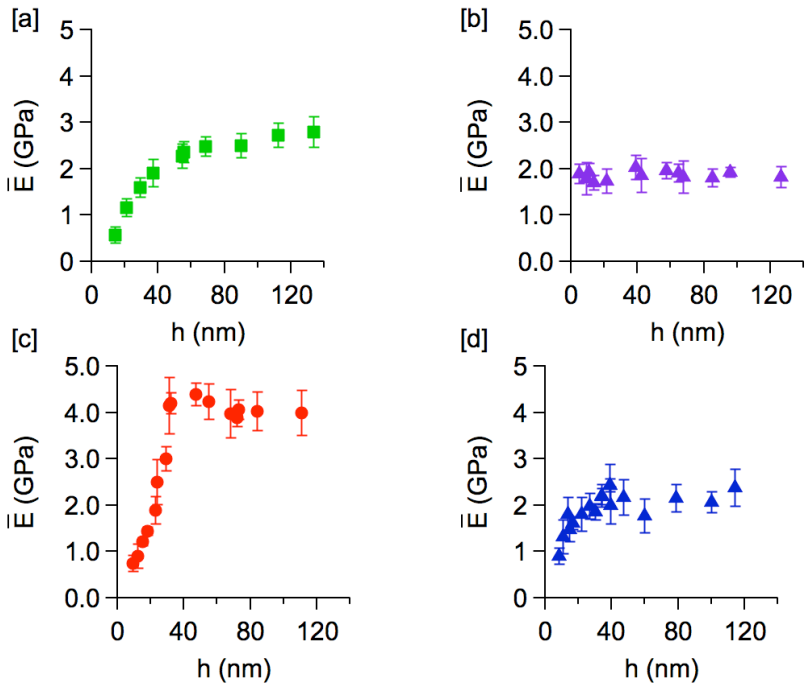

Figure 4.6 Modulus as a function of film thickness for [a] linear, [b] comb, [c] centipede and [d] star polystyrene. The error bars represent one standard deviation.

However, solution properties of branched polymers revealed an increase in stiffness in comb and centipede PS as compared to their linear counterpart due to repulsion of neighboring chains or specific phenyl ring interactions and observed by an increase in persistence length from 2 nm to 2.8 nm to 5.5 nm for the linear, centipede, and comb polystyrene respectively.[94, 95] And the slope of dependence of persistence length on molecular weight in *trans*-decalin increased from 0.46 to 0.52, and 0.6 for the comb, centipede, and linear PS.[95] It is conceivable that the lack of thickness dependencies observed for the comb PS is a result of the limited conformations available such that the chain conformation during film formation is similar to the equilibrated glass. This limited conformation should also manifest itself in a lower mass density; this would be consistent with the low modulus for the comb PS. Additional work is required to fully understand the correlations between molecular structure and thin film properties.

4.3.2 Poly [5-(2-phenylbornene)]s

Given the traditional application of these polycarbonates in fire retardant applications, the thermal behavior of the PENb and CENb polymers was examined by *in-situ* ellipsometry in order to obtain not only the T_g but also the coefficient of thermal expansion (CTE). The CTE's are determined from the slope of the temperature dependence. For AddPENb and AddCENb, two distinct CTE's can be seen from the temperature dependent thickness shown in Figure 4.7. However, due to instrument limitations only the glass CTE for the ring-opened polymers was determined.

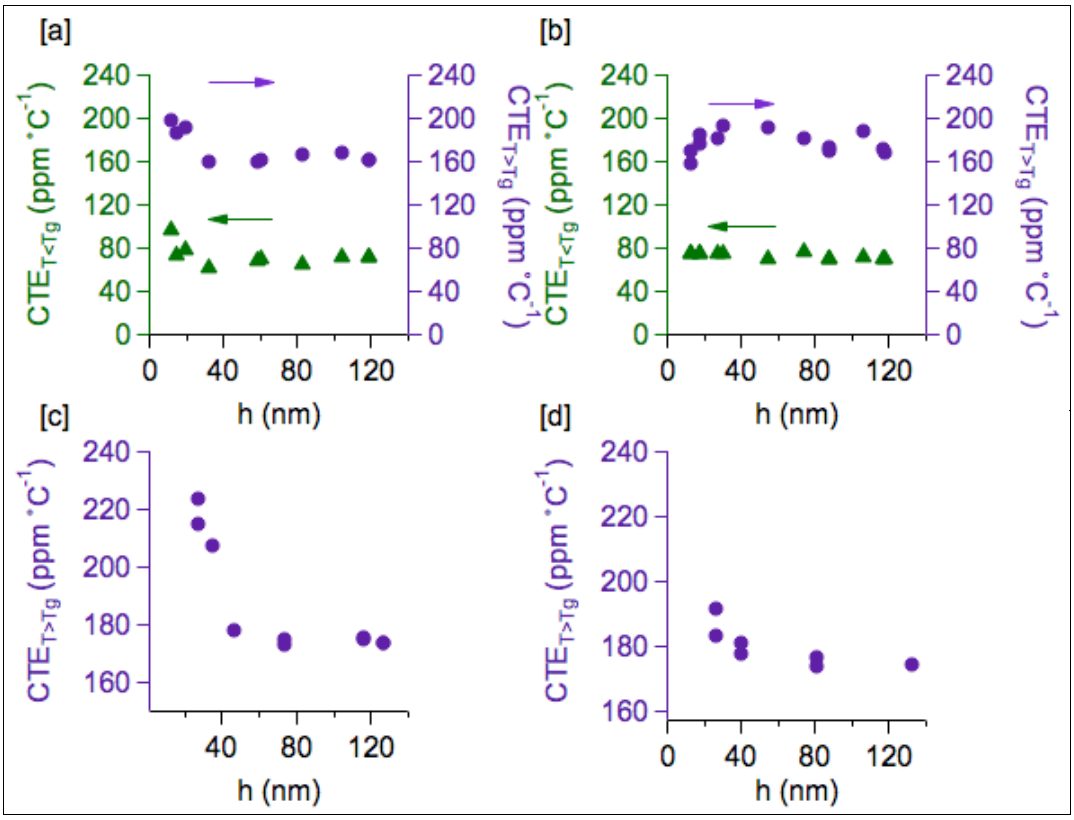

Figure 4.7 Coefficient of thermal expansion for [a]AddPENb, [b] AddCENb, [c] hROMP PENb, and [d] hROMP CENb.

The data shows a bulk glass CTE of 178ppm/°C and 175ppm/°C for the ring-opened polymers hROMP PENb and hROMP CENb. While the addition polymers exhibit bulk glass CTE's of 170ppm/°C and 160ppm/°C for AddPENB and AddCENb respectively. This slight decrease in bulk CTE is consistent with a decrease in mobility for the addition polymers due to the bridged hydrocarbon in the polymer backbone. Both ring-opened polymers exhibit an increase in CTE at sub 40 nm length scales. This increase in CTE at sub 40 nm length scales can be attributed to higher mobility as a result of a more flexible backbone. For the less flexible addition polymers the CTE for the unsaturated polymer also shows a

slight increase at sub 40 nm length scales however the addition polymer with the saturated pendant ring remains statistically invariant. This is attributed to the bulkier cyclohexyl pendant ring further reducing chain mobility. This effect can also be observed in the ring opened polymers as the increase in sub 40 nm CTE is lower for the saturated polymer than the unsaturated polymer.

However, in order to better understand and therefore explain the thermal behavior of the polynorbornene polymers, the glass transition temperature of these materials was also examined. The T_g of these films is determined from the kink in the thermal expansion. As shown in Figure 4.8, Add PENb films exhibit a T_g of 186.3 ± 3.7 ˚C that is statistically independent of film thickness; similarly, there is no thickness dependence to the T_g of Add CENb (223.1 ± 5.4˚C).

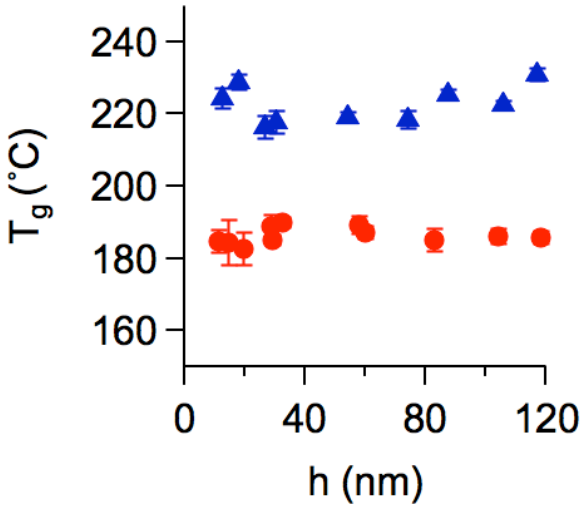

Figure 4.8 T_g as a function of film thickness for Add PENb (●) and Add CENb (▲). The error bars represent one standard deviation of the data, which is taken as the experimental uncertainty of the measurement.

This increase in T_g upon saturation of the pendent phenyl ring is consistent with previously reported data for these polymers determined via thermo-optical analysis (TOA).[69] However, there is an offset in T_g by approximately 27 ˚C between TOA and ellipsometric dilotometry; we have further examined this behavior with modulated DSC, where the T_g is found to agree with the ellipsometric measurements reported here. It is currently unclear why TOA provides such a large offset in T_g for these addition polymers. Nonetheless this increase in T_g with saturation is consistent with prior reports for polyolefins, where a systematic increase in bulk T_g with hydrogenation is observed with a 60˚C increase with complete saturation.[43] In this case, the change in T_g is attributed to a reduction in main chain cooperative motion due to the conversion of the phenyl ring into a cyclohexyl moiety, which is supported by the decrease in density with saturation.[69] Interestingly, the T_g for these materials remains statistically invariant over all thickness examined from 120 nm down to less than 10 nm. As a comparison, PS, which has a pendent phenyl ring similar to Add PENb, exhibits a large decrease in T_g at thicknesses less than 30 nm from ellipsometry measurements.[7] Hydrogenation of the phenyl (Add CENb) does not significantly impact the thin film performance. The extent of saturation of the backbone can be investigated by comparing these addition polymers (Add PENb and Add CENb) with the analogous polymers synthesized by ROMP (hROMP PENb and hROMP CENb). Unfortunately, the low T_g of these ROMP polymers prohibits the accurate identification of the glass transition by the current ellipsometry setup. However, other physical properties of these polymers can be

examined to compare their thin film behavior. Figure 4.9 shows how the room temperature modulus of each PENb-based polymer is impacted by film thickness.

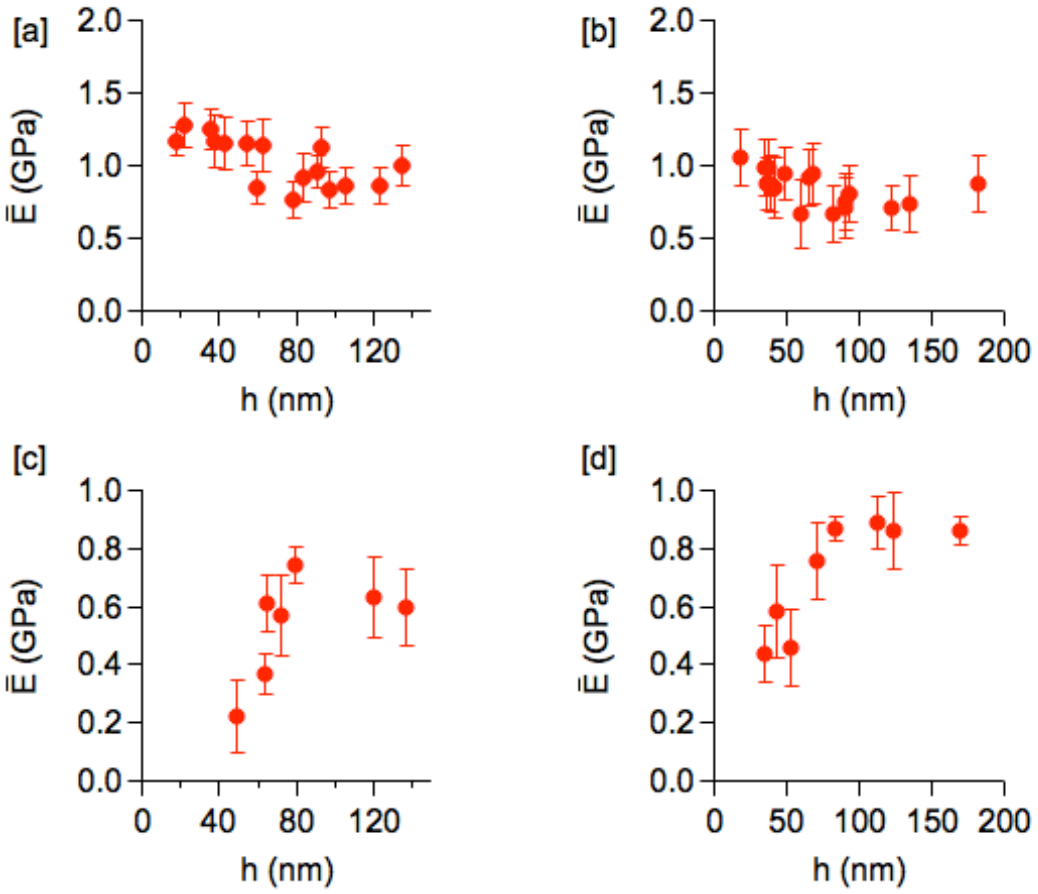

Figure 4.9 Modulus as a function of film thickness for [a] Add PENb, [b] Add CENb, [c] hROMP PENb, and [d] h ROMP CENb. The error bars represent one standard deviation of the data, which is taken as the experimental uncertainty of the measurement.

For Add PENb and Add CENb, the modulus of these materials is thickness independent, similar to the T_g behavior discussed previously. The modulus for the Add PENb polymer is approximately 1.0 ± 0.2 GPa from 140 nm down to 15 nm. The average modulus is slightly decreased to 0.88 ± 0.19 GPa with saturation of the phenyl ring into cyclohexyl (Add CENb), but this modulus is also thickness independent. In contrast to the T_g for the addition polymers, the

bulk modulus actually decreased with saturation of the phenyl ring, which is unexpected from the prospective of density and T_g. For example, the conversion of saturation of the phenyl ring in polystyrene to polycyclohexylethylene results in a decrease in density due to the bulky cyclohexyl group resulting in an decrease in T_g.[96] However, there are differences in the specific interactions present that could impact the mechanical behavior; in particular, the phenyl rings provide a route for π-π interactions that would not be present for the cyclohexyl containing polymer. Nonetheless, both T_g and modulus are statistically independent of film thickness for both addition polymers. In contrast to the addition polymers, the ring opened poly [5-(2-phenylethylnorbornene)] films exhibit a pronounced thickness dependence to the observed modulus as shown in Figure 4.9c and 4.9d. hROMP PENb with preserved phenyl ring has a modulus of 0.64 ± 0.11 GPa for films thicker than 80 nm; a 65 % decrease in modulus to 0.22 ± 0.13 GPa occurs when the thickness is decreased to 42 nm. This decrease in modulus occurs at larger thicknesses than typically observed for PS,[11] but we have found that the length scale at which deviations in modulus occurs in thin polymer films scales with the quench depth into the bulk glass.[43, 60] As the measurement temperature approaches T_g, the modulus tends to begin to decrease in thicker films. The bulk T_g for hROMP PENb and hROMP CENb is reported to be 28 ºC and 26 ºC, respectively. Based upon previous examination of flexible styrene and methacrylate polymers, a decrease in the modulus of hROMP CENb and hROMP PENb would be expected at approximately 80 nm, as is observed experimentally. Interestingly, the hROMP CENb exhibits an increase in modulus compared to the

hROMP PENb for films thicker than 80 nm (0.87 ± 0.10 GPa) and only a slight (33%) decrease in modulus to 0.58 ± 0.13 GPa at 41 nm. The modulus behavior of these hROMP polymers agrees qualitatively with previous results for flexible polymers; but to explain the behavior of the Add PENb and AddCENb thin films, a more detailed examination of other physical properties must be undertaken. We hypothesize that the stiffer polymer backbone of the addition polymers as a result of the bridge hydrocarbon in the cyclopentyl ring is responsible for the change in behavior.

4.3.3 Arylate-Phosphonate copolymers

To further examine the role of chain stiffness on thin film behavior, a series of copolymers based on bisphenol-A (BPA) with varying ratios of phenylphosphonic (PPDC) and isophthaloyl chloride (IPC) are examined. Figure 4.10 illustrates how T_g as a function of film thickness is dependent upon the aryl:phosphate ratio in the copolymer. The T_g for thick films is increased as the phosphate (PPDC) content in the copolymer is decreased. For the polymer that consists fully of BPA and PPDC, T_g is approximately 116.8 ± 1.8 ˚C from 100 nm down to 21 nm, but then rapidly decreases for films less than 20 nm thick to 107 ± 0.5˚C for a 14 nm thick film. As the IPC ratio is increased to 50:50 IPC:PPDC, the bulk-like T_g is increased to 132.5 ± 3.5˚C, but also the glass transition temperature begins to decrease at 40 nm with a decrease to 107.5 ± 1.2 ˚C at 18 nm observed. The highest T_g is observed for 80:20 IPC:PPDC copolymer with a

value of 150.7 ± 2.2 ˚C for the thickest films and only a slight decrease to 144.5 ± 0.45˚C at 12 nm.

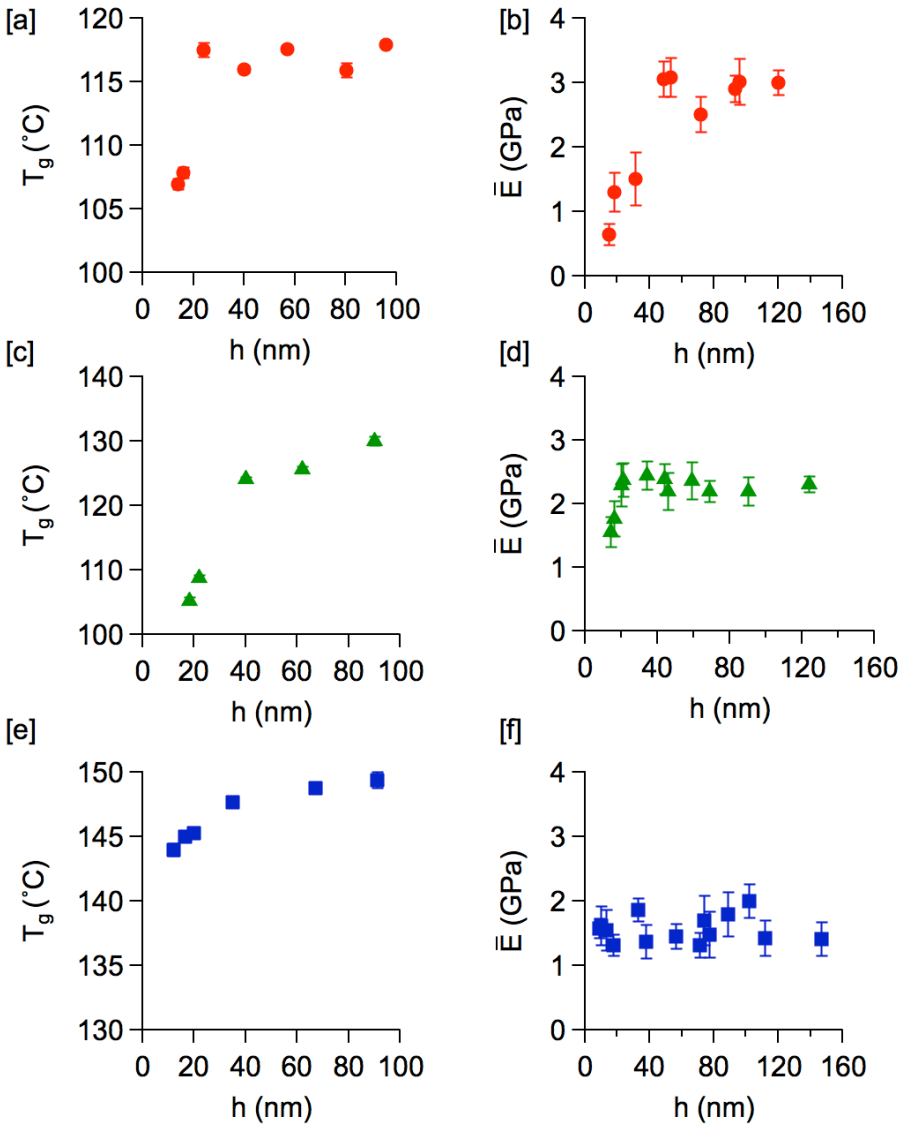

Figure 4.10 T_g as a function of film thickness and modulus as a function of film thickness for aryl-phosphate copolymers 0:100 (a,b), 50:50 (c,d), and 80:20 (e,f). The error bars represent one standard deviation of the data, which is taken as the experimental uncertainty of the measurement.

This systematic increase in T_g with increasing IPC concentration is in agreement with previously reported values where pure BPA-PPDC copolymers

exhibit a bulk T_g of only 115 ˚C, while pure BPA-IPC copolymers exhibit a bulk T_g of 183 ˚C.[43] As illustrated in Figure 4.9, T_g and modulus for the aryl-phosphate copolymers are thickness dependent for the copolymers with 100 % and 50 % PPDC concentration, but the modulus becomes thickness independent and only a slight reduction in T_g is observed when the concentration of PPDC decreases to 20 %. As shown in Figure 4.8b, the 100% PPDC polymer exhibits modulus of 2.91 ± 0.23 GPa from 100 nm down to 40 nm, but the modulus significantly decreases as the film thickness decreases below 40 nm to 0.65 ± 0.17 GPa at 10 nm (approximately 20 % of the value for the thickest films). Similarly, modulus of the 50:50 PPDC:IPC copolymer exhibits thickness dependent behavior; however, the modulus only begins to decrease from a near constant 2.32 ± 0.15 GPa, when the film thickness is less than approximately 25 nm. When the film is 10 nm thick, the modulus is reduced to 1.55 ± 0.23 GPa, a 33% decrease from the thickest films. It is interesting to note that T_g of the 50:50 PPDC:IPC copolymer also decreases in this thickness regime, but only a 19% decrease in T_g is observed. Increasing the IPC concentration in the 80:20 IPC:PPDC copolymer leads to a further decrease in the thick film modulus to 1.56 ± 0.21 GPa, however the modulus becomes thickness independent. This statistically invariant modulus is attributed to an increased stiffness of the copolymer backbone with increasing IPC concentration. The thin film mechanical behavior of tyrosine-derived polycarbonates, which are similarly stiff, has been reported to be thickness independent for films ranging from 30 to 200 nm; unfortunately, the behavior of thinner films was not reported, but these results agree well with the data presented

here.[97] These data illustrate that the thermal and mechanical properties of polymer thin films as determined by ellipsometry and surface wrinkling is strongly dependent upon the flexibility of the polymer; the deviations from bulk behavior are significantly reduced or eliminated for polymers containing stiff backbones. Interestingly, a similar behavior is obtained when a flexible polymer contains approximately 5 wt % good solvent when examining the T_g[28] and modulus[31] of polymer thin films. These similarities might not be completely unexpected as polymer chains are stretched in the presence of a good solvent and thus the chain confirmation is impacted by the residual solvent. However, this does not agree with the hypothesis that residual solvent might be responsible for the reported decrease in T_g of thin films of PS that can be eliminated by proper annealing.[92] Similarly, Thomas et al. has reported the viscoelastic properties of PS thin films to be dependent upon the casting solvent and bulk-like behavior can be recovered through annealing.[91] These experiments suggest that the highly non-equilibrium chain conformation in the vitrified film can lead to significant changes in the polymer properties. In this context, the current results might be explained based upon the chain conformations available that do not allow the film to adapt highly non-equilibrium states and thus no changes in the physical properties are observed. Additional theoretical and/or simulation work on the impact of chain stiffness on chain conformations and the glass transition near surfaces is also necessary to understand the molecular mechanisms.

4.4 Conclusion

In summary, the modulus and T_g of thin films for a series of poly (aryl phosphonate)s, poly [5-(2-phenylethylnorbornene)], and varying architecture PS films was determined using wrinkling on an elastic substrate and ellipsometry, respectively. Unlike previous wrinkling studies involving flexible polymers,[31, 98] not all polymers examined exhibit a decrease in modulus for the thin films. This behavior was found to be dependent upon the polymer flexibility. The polymers with a stiff backbone show no change in modulus as the film thickness is decreased to 10 nm; additionally, T_g is independent or only slightly dependent upon film thickness for these polymers. For the PS films with varying architecture, the bulk-like T_g and modulus was determined to be independent of polymer architecture. However, at sub 40 nm length scales the T_g and modulus suppression becomes dependent upon polymer branching resulting in either a reduction from bulk values attributed to increased interchain and intrachain entanglements or an increase in bulk values suppression attributed to improved packing as a result of regular branching.

For the PS samples, the nanometer length scale behavior could be attributed to surface effects dependent upon polymer branching. Where polymer end segregation to the free surface leads to a reduction in T_g and modulus at the surface significantly impacting the sub 40 nm length scale. This is in agreement with recent results where changes in a polymer's surface tension was achieved with changes in its architecture.[90]

4.5 References

1. Angell, C. A.; Ueno, K., Materials Science Soft Is Strong. *Nature* **2009,** *462* (7269), 45-46.

2. Kivelson, S. A.; Tarjus, G., In search of a theory of supercooled liquids. *Nature Materials* **2008,** *7* (11), 831-833.

3. McKenna, G. B., Glass dynamics - Diverging views on glass transition. *Nature Physics* **2008,** *4* (9), 673-674.

4. Forrest, J. A.; Danoki-Veress, K., The glass transition in thin polymer films. *Advances in Colloid and Interface Science* **2001,** *94* (1-3), 167-196.

5. McKenna, G. B., Size and confinement effects in glass forming liquids: Perspectives on bulk and nano-scale behaviours. *Journal de Physique Iv* **2000,** *10* (P7), 53-57.

6. McKenna, G. B., Ten (or more) years of dynamics in confinement: Perspectives for 2010. *European Physical Journal-Special Topics* **2010,** *189* (1), 285-302.

7. Ellison, C. J.; Mundra, M. K.; Torkelson, J. M., Impacts of polystyrene molecular weight and modification to the repeat unit structure on the glass transition-nanoconfinement effect and the cooperativity length scale. *Macromolecules* **2005,** *38* (5), 1767-1778.

8. Huth, H.; Minakov, A. A.; Schick, C., Differential AC-chip calorimeter for glass transition measurements in ultrathin films. *Journal of Polymer Science Part B-Polymer Physics* **2006,** *44* (20), 2996-3005.

9. Singh, L.; Ludovice, P. J.; Henderson, C. L., Influence of molecular weight and film thickness on the glass transition temperature and coefficient of thermal expansion of supported ultrathin polymer films. *Thin Solid Films* **2004,** *449* (1-2), 231-241.

10. Inoue, R.; Kanaya, T.; Miyazaki, T.; Nishida, K.; Tsukushi, I.; Shibata, K., Glass transition and thermal expansivity of polystyrene thin films. *Materials Science and Engineering A-Structural Materials Properties Microstructure and Processing* **2006,** *442* (1-2), 367-370.

11. Stafford, C. M.; Vogt, B. D.; Harrison, C.; Julthongpipet, D.; Huang, R., Elastic moduli of ultrathin amorphous polymer films. *Macromolecules* **2006,** *39*, 5095-5099.

12. Jones, R. L.; Kumar, S. K.; Ho, D. L.; Briber, R. M.; Russell, T. P., Chain conformation in ultrathin polymer films. *Nature* **1999,** *400* (6740), 146-149.

13. Akabori, K.; Tanaka, K.; Nagamura, T.; Takahara, A.; Kajiyama, T., Molecular motion in ultrathin polystyrene films: Dynamic mechanical analysis of surface and interfacial effects. *Macromolecules* **2005,** *38* (23), 9735-9741.

14. Fakhraai, Z.; Forrest, J. A., Measuring the surface dynamics of glassy polymers. *Science* **2008,** *319* (5863), 600-604.

15. Bodiguel, H.; Fretigny, C., Viscoelastic properties of ultrathin polystyrene films. *Macromolecules* **2007,** *40* (20), 7291-7298.

16. O'Connell, P. A.; Hutcheson, S. A.; McKenna, G. B., Creep behavior of ultra-thin polymer films. *Journal of Polymer Science Part B-Polymer Physics* **2008,** *46* (18), 1952-1965.

17. Ellison, C. J.; Torkelson, J. M., The distribution of glass-transition temperatures in nanoscopically confined glass formers. *Nature Materials* **2003,** *2* (10), 695-700.

18. Forrest, J. A.; DalnokiVeress, K.; Stevens, J. R.; Dutcher, J. R., Effect of free surfaces on the glass transition temperature of thin polymer films. *Physical Review Letters* **1996,** *77* (10), 2002-2005.

19. Raegen, A.; Massa, M.; Forrest, J.; noki-Veress, K., Effect of atmosphere on reductions in the glass transition of thin polystyrene films. *European Physical Journal e* **2008,** *27* (4), 375-377.

20. Schick, C., Glass transition under confinement-what can be learned from calorimetry. *European Physical Journal-Special Topics* **2010,** *189* (1), 3-36.

21. Lu, H. Y.; Chen, W.; Russell, T. P., Relaxation of Thin Films of Polystyrene Floating on Ionic Liquid Surface. *Macromolecules* **2009,** *42* (22), 9111-9117.

22. Tress, M.; Erber, M.; Mapesa, E. U.; Huth, H.; Muˆller, J.; Serghei, A.; Schick, C.; Eichhorn, K. J.; Voit, B.; Kremer, F., Glassy Dynamics and Glass Transition in Nanometric Thin Layers of Polystyrene. *Macromolecules* **2010,** *43* (23), 9937-9944.

23. Mundra, M. K.; Donthu, S. K.; Dravid, V. P.; Torkelson, J. M., Effect of spatial confinement on the glass-transition temperature of patterned polymer nanostructures. *Nano Letters* **2007,** *7* (3), 713-718.

24. Grohens, Y.; Brogly, M.; Labbe, C.; David, M. O.; Schultz, J., Glass transition of stereoregular poly(methyl methacrylate) at interfaces. *Langmuir* **1998,** *14* (11), 2929-2932.

25. Grohens, Y.; Hamon, L.; Reiter, G.; Soldera, A.; Holl, Y., Some relevant parameters affecting the glass transition of supported ultra-thin polymer films. *European Physical Journal e* **2002,** *8* (2), 217-224.

26. Priestley, R. D.; Mundra, M. K.; Barnett, N.; Broadbelt, L. J.; Torkelson, J. M., Effects of Nanoscale Confinement and Interfaces on the Glass Transition Temperatures of a Series of Poly(n-methacrylate) Films. *Australian Journal of Chemistry* **2007,** *60*, 765-771.

27. Campbell, C. G.; Vogt, B. D., Examination of the influence of cooperative segmental dynamics on the glass transition and coefficient of thermal expansion in thin films probed using poly(n-alkyl methacrylate)s. *Polymer* **2007,** *48* (24), 7169-7175.

28. Ellison, C. J.; Ruszkowski, R. L.; Fredin, N. J.; Torkelson, J. M., Dramatic reduction of the effect of nanoconfinement on the glass transition of polymer films via addition of small-molecule diluent. *Physical Review Letters* **2004,** *92* (9).

29. Kim, S.; Mundra, M. K.; Roth, C. B.; Torkelson, J. M., Suppression of the Tg Nanoconfinement Effect in Thin Poly(vinyl acetate) Films by Sorbed Water. *Macromolecules* **2010,** *43* (11), 5158-5161.

30. O'Connell, P. A.; McKenna, G. B., Rheological Measurements of the Thermoviscoelastic Response of Ultrathin Polymer Films. *Science* **2005,** *307* (5716), 1760-1763.

31. Torres, J. M.; Stafford, C. M.; Vogt, B. D., Manipulation of the Elastic Modulus of Polymers at the Nanoscale: Influence of UV-Ozone Cross-Linking and Plasticizer. *Acs Nano* **2010,** *4* (9), 5357-5365.

32. Soles, C. L.; Douglas, J. F.; Wu, W. L.; Peng, H. G.; Gidley, D. W., Comparative specular X-ray reflectivity, positron annihilation lifetime spectroscopy, and incoherent neutron scattering measurements of the dynamics in thin polycarbonate films. *Macromolecules* **2004,** *37* (8), 2890-2900.

33. Soles, C. L.; Douglas, J. F.; Wu, W. L.; Dimeo, R. M., Incoherent neutron scattering as a probe of the dynamics in molecularly thin polymer films. *Macromolecules* **2003,** *36* (2), 373-379.

34. Anastasiadis, S. H.; Karatasos, K.; Vlachos, G.; Manias, E.; Giannelis, E. P., Nanoscopic-confinement effects on local dynamics. *Physical Review Letters* **2000,** *84* (5), 915-918.

35. Kim, Y. S.; Chung, C. I.; Lai, S. Y.; Hyun, K. S., Melt rheological and thermodynamic properties of polyethylene homopolymers and poly(ethylene/+Ý-olefin) copolymers with respect to molecular composition and structure. *J.Appl.Polym.Sci.* **1996,** *59* (1), 125-137.

36. Miyatake, K.; Oyaizu, K.; Tsuchida, E.; Hay, A. S., Synthesis and Properties of Novel Sulfonated Arylene Ether/Fluorinated Alkane Copolymers. *Macromolecules* **2001,** *34* (7), 2065-2071.

37. Ellzey, K. A.; Ranganathan, T.; Zilberman, J.; Coughlin, E. B.; Farris, R. J.; Emrick, T., Deoxybenzoin-Based Polyarylates as Halogen-Free Fire-Resistant Polymers. *Macromolecules* **2006,** *39* (10), 3553-3558.

38. Ranganathan, T.; Ku, B. C.; Zilberman, J.; Beaulieu, M.; Farris, R. J.; Coughlin, E. B.; Emrick, T., Poly(arylate-phosphonate) copolymers with deoxybenzoin in the backbone: Synthesis, characterization, and thermal properties. *J.Polym.Sci.A Polym.Chem.* **2007,** *45* (20), 4573-4580.

39. Collison, C. J.; Rothberg, L. J.; Treemaneekarn, V.; Li, Y., Conformational effects on the photophysics of conjugated polymers: A two species model for MEH-PPV spectroscopy and dynamics. *Macromolecules* **2001,** *34* (7), 2346-2352.

40. Malik, S.; Nandi, A. K., Crystallization mechanism of regioregular poly(3-alkyl thiophene)s. *Journal of Polymer Science Part B-Polymer Physics* **2002,** *40* (18), 2073-2085.

41. Gehlsen, M. D.; Bates, F. S., Heterogeneous catalytic hydrogenation of polystyrene: thermodynamics of poly(vinylcyclohexane)-containing diblock copolymers. *Macromolecules* **1993,** *26* (16), 4122-4127.

42. Gehlsen, M. D.; Weimann, P. A.; Bates, F. S.; Harville, S.; Mays, J. W.; Wignall, G. D., Synthesis and characterization of poly(vinylcyclohexane) derivatives. *J.Polym.Sci.B Polym.Phys.* **1995,** *33* (10), 1527-1536.

43. Hahn, S. F.; Hillmyer, M. A., High Glass Transition Temperature Polyolefins Obtained by the Catalytic Hydrogenation of Polyindene. *Macromolecules* **2002,** *36* (1), 71-76.

44. Sae-Ma, N.; Praserthdam, P.; Panpranot, J.; Chaemchuen, S.; Dokjamp, S.; Suriye, K.; Rempel, G. L., Color improvment of C9 hydrocarbon resin by hydrogenation over 2% Pd/+Ý-alumina catalyst: Effect of degree of aromatic rings hydrogenation. *J.Appl.Polym.Sci.* **2010,** *117* (5), 2862-2869.

45. Hucul, D. A.; Hahn, S. F., Catalytic Hydrogenation of Polystyrene. *Adv.Mater.* **2000,** *12* (23), 1855-1858.

46. Gao, C.; Yan, D., Hyperbranched polymers: from synthesis to applications. *Progress in Polymer Science* **2004,** *29* (3), 183-275.

47. Hawker, C. J.; Lee, R.; Frechet, J. M. J., One-step synthesis of hyperbranched dendritic polyesters. *Journal of the American Chemical Society* **1991,** *113* (12), 4583-4588.

48. Kim, Y. H., Hyperbranchecs polymers 10 years after. *Journal of Polymer Science Part a-Polymer Chemistry* **1998,** *36* (11), 1685-1698.

49. Patten, T. E.; Matyjaszewski, K., Atom transfer radical polymerization and the synthesis of polymeric materials. *Advanced Materials* **1998,** *10* (12), 901-+.

50. Voit, B., New developments in hyperbranched polymers. *Journal of Polymer Science Part a-Polymer Chemistry* **2000,** *38* (14), 2505-2525.

51. Schlegel, R.; Staudinger, U.; Thunga, M.; Weidisch, R.; Heinrich, G.; Uhrig, D.; Mays, J. W.; Iatrou, H.; Hadjichristidis, N., Investigations on mechanical properties of PI-PS multigraft copolymers. *European Polymer Journal* **2009,** *45* (10), 2902-2912.

52. Uhrig, D.; Schlegel, R.; Weidisch, R.; Mays, J., Multigraft copolymer superelastomers: Synthesis morphology, and properties. *European Polymer Journal* **2010,** *47* (4), 560-568.

53. Perumal, O.; Khandare, J.; Kolhe, P.; Kannan, S.; Lieh-Lai, M.; Kannan, R. M., Effects of Branching Architecture and Linker on the Activity of Hyperbranched Polymer‚àíDrug Conjugates. *Bioconjugate Chemistry* **2009,** *20* (5), 842-846.

54. Mackay, M. E.; Hong, Y.; Jeong, M.; Hong, S.; Russell, T. P.; Hawker, C. J.; Vestberg, R.; Douglas, J. F., Influence of Dendrimer Additives on the Dewetting of Thin Polystyrene Films. *Langmuir* **2002,** *18* (5), 1877-1882.

55. Serghei, A.; Mikhailova, Y.; Huth, H.; Schick, C.; Eichhorn, K. J.; Voit, B.; Kremer, F., Molecular dynamics of hyperbranched polyesters in the confinement of thin films. *The European Physical Journal E: Soft Matter and Biological Physics* **2005,** *17* (2), 199-202.

56. Glynos, E.; Frieberg, B.; Oh, H.; Liu, M.; Gidley, D. W.; Green, P. F., Role of Molecular Architecture on the Vitrification of Polymer Thin Films. *Physical Review Letters* **2011,** *106* (12), 128301.

57. Ellison, C. J.; Torkelson, J. M., The distribution of glass-transition temperatures in nanoscopically confined glass formers. *Nat Mater* **2003,** *2* (10), 695-700.

58. Erber, M.; Georgi, U.; M¸ller, J.; Eichhorn, K. J.; Voit, B., Polystyrene with different topologies: Study of the glass transition temperature in confined geometry of thin films. *European Polymer Journal* **2010,** *46* (12), 2240-2246.

59. Stafford, C. M.; Vogt, B. D.; Harrison, C.; Julthongpiput, D.; Huang, R., Elastic moduli of ultrathin amorphous polymer films. *Macromolecules* **2006,** *39* (15), 5095-5099.

60. Torres, J. M.; Stafford, C. M.; Vogt, B. D., Impact of molecular mass on the elastic modulus of thin polystyrene films. *Polymer* **2010,** *51* (18), 4211-4217.

61. Torres, J. M. S., C.M.; Vogt, B.D., Elastic Modulus of Amorphous Polymer Thin Films: Relationship to the Glass Transition Temperature. *ACS Nano* **2009,** *3* (9), 2677.

62. Miyake, K.; Satomi, N.; Sasaki, S., Elastic modulus of polystyrene film from near surface to bulk measured by nanoindentation using atomic force microscopy. *Applied Physics Letters* **2006,** *89* (3), 031925-3.

63. O'Connell, P. A.; McKenna, G. B., The stiffening of ultrathin polymer films in the rubbery regime: The relative contributions of membrane stress and surface tension. *Journal of Polymer Science Part B: Polymer Physics* **2009,** *47* (24), 2441-2448.

64. Yang, Z.; Fujii, Y.; Lee, F. K.; Lam, C.-H.; Tsui, O. K. C., Glass Transition Dynamics and Surface Layer Mobility in Unentangled Polystyrene Films. *Science* **2010,** *328* (5986), 1676-1679.

65. Forrest, J. A.; Dalnoki-Veress, K., The glass transition in thin polymer films. *Advances in Colloid and Interface Science* **2001,** *94* (1-3), 167-195.

66. Forrest, J. A.; Dalnoki-Veress, K.; Dutcher, J. R., Interface and chain confinement effects on the glass transition temperature of thin polymer films. *Physical Review E* **1997,** *56* (5), 5705.

67. Forrest, J. A.; Dalnoki-Veress, K.; Stevens, J. R.; Dutcher, J. R., Effect of Free Surfaces on the Glass Transition Temperature of Thin Polymer Films. *Physical Review Letters* **1996,** *77* (19), 4108.

68. Kim, S.; Hewlett, S.; Roth, C.; Torkelson, J., Confinement effects on glass transition temperature, transition breadth, and expansivity: Comparison of ellipsometry and fluorescence measurements on polystyrene films. *The European Physical Journal E: Soft Matter and Biological Physics* **2009,** *30* (1), 83-92.

69. Bishop, J. P.; Register, R. A., Poly(phenylethylnorbornene)s and their Hydrogenated Derivatives. *Macromol.Rapid Commun.* **2008,** *29* (9), 713-718.

70. Hadjichristidis, N.; Iatrou, H.; Pispas, S.; Pitsikalis, M., Anionic polymerization: High vacuum techniques. *Journal of Polymer Science Part A: Polymer Chemistry* **2000,** *38* (18), 3211-3234.

71. Morton, M.; Fetters, L. J., Anionic Polymerization of Vinyl Monomers. *Rubber Chemistry and Technology* **1975,** *48* (3), 359-409.

72. Uhrig, D.; Mays, J. W., Experimental techniques in high-vacuum anionic polymerization. *Journal of Polymer Science Part A: Polymer Chemistry* **2005,** *43* (24), 6179-6222.

73. Chalari, I.; Hadjichristidis, N., Synthesis of well-defined second-generation dendritic polymers of isoprene (I) and styrene (S): (S2I)3, (SI′I)3, (I″I′I)3, and (I′2I)4. *Journal of Polymer Science Part A: Polymer Chemistry* **2002,** *40* (10), 1519-1526.

74. Driva, P.; Iatrou, H.; Lohse, D. J.; Hadjichristidis, N., Anionic homo- and copolymerization of double-tailed macromonomers: A route to novel macromolecular architectures. *Journal of Polymer Science Part A: Polymer Chemistry* **2005,** *43* (18), 4070-4078.

75. Koutalas, G.; Iatrou, H.; Lohse, D. J.; Hadjichristidis, N., Well-Defined Comb, Star‚àíComb, and Comb-on-Comb Polybutadienes by Anionic Polymerization and the Macromonomer Strategy. *Macromolecules* **2005,** *38* (12), 4996-5001.

76. Roth, C. B.; Dutcher, J. R., Glass transition temperature of freely-standing films of atactic poly(methyl methacrylate). *European Physical Journal e* **2003,** *12*, S103-S107.

77. Stafford, C. M.; Harrison, C.; Beers, K. L.; Karim, A.; Amis, E. J.; Vanlandingham, M. R.; Kim, H. C.; Volksen, W.; Miller, R. D.; Simonyi, E. E., A buckling-based metrology for measuring the elastic moduli of polymeric thin films. *Nature Materials* **2004,** *3* (8), 545-550.

78. Huang, Z.; Hong, W.; Suo, Z., Evolution of wrinkles in hard films on soft substrates. *Physical Review E* **2004,** *70* (3), 030601.

79. Stafford, C. M.; Guo, S.; Harrison, C.; Chiang, M. Y. M., Combinatorial and high-throughput measurements of the modulus of thin polymer films. *Review of Scientific Instruments* **2005,** *76* (6), 062207.

80. Jikei, M.; Kakimoto, M., Hyperbranched polymers: a promising new class of materials. *Progress in Polymer Science* **2001,** *26* (8), 1233-1285.

81. Merino, S.; Brauge, L.; Caminade, A. M.; Majoral, J. P.; Taton, D.; Gnanou, Y., Synthesis and characterization of linear, hyperbranched, and dendrimer-like polymers constituted of the same repeating unit. *Chemistry-a European Journal* **2001,** *7* (14), 3095-3105.

82. Teertstra, S. J.; Gauthier, M., Dendrigraft polymers: macromolecular engineering on a mesoscopic scale. *Progress in Polymer Science* **2004,** *29* (4), 277-327.

83. Milner, S. T.; McLeish, T. C. B., Arm-length dependence of stress relaxation in star polymer melts. *Macromolecules* **1998,** *31* (21), 7479-7482.

84. Pearson, D. S.; Helfand, E., Viscoelastic properties of star-shaped polymers. *Macromolecules* **1984,** *17* (4), 888-895.

85. Hadjichristidis, N.; Pispa, S.; Latrou, H.; Pitsilkalis, M., Linking Chemistry and Anionic Polymerization. *Current Organic Chemistry* **2002,** *6*, 155-176.

86. Keddie, J. L.; et al., Size-Dependent Depression of the Glass Transition Temperature in Polymer Films. *EPL (Europhysics Letters)* **1994,** *27* (1), 59.

87. Berry, G.; Fox, T. G., The viscosity of polymers and their concentrated solutions. In *Fortschritte der Hochpolymeren-Forschung*, Springer Berlin / Heidelberg: 1968; Vol. 5, pp 261-357.

88. Harper, C. A., *Handbook of plastics, elastomers, and composites*. McGraw-Hill: 2002.

89. Brown, H. R.; Russell, T. P., Entanglements at polymer surfaces and interfaces. *Macromolecules* **1996,** *29* (2), 798-800.

90. Qian, Z.; Minnikanti, V. S.; Sauer, B. B.; Dee, G. T.; Archer, L. A., Surface Tension of Symmetric Star Polymer Melts. *Macromolecules* **2008,** *41* (13), 5007-5013.

91. Thomas, K. R.; Chenneviere, A.; Reiter, G.; Steiner, U., Nonequilibrium behavior of thin polymer films. *Physical Review E* **2011,** *83* (2), 021804.

92. Tress, M.; Erber, M.; Mapesa, E. U.; Huth, H.; MuÃàller, J.; Serghei, A.; Schick, C.; Eichhorn, K.-J.; Voit, B.; Kremer, F., Glassy Dynamics and Glass Transition in Nanometric Thin Layers of Polystyrene. *Macromolecules* **2010,** *43* (23), 9937-9944.

93. Thomas, K. R.; Chenneviere, A.; Reiter, G.; uuml; nter; Steiner, U., Nonequilibrium behavior of thin polymer films. *Physical Review E* **2011,** *83* (2), 021804.

94. Nakamura, Y.; Wan, Y.; Mays, J. W.; Iatrou, H.; Hadjichristidis, N., Radius of Gyration of Polystyrene Combs and Centipedes in Solution. *Macromolecules* **2000,** *33* (22), 8323-8328.

95. Terao, K.; Farmer, B. S.; Nakamura, Y.; Iatrou, H.; Hong, K.; Mays, J. W., Radius of Gyration of Polystyrene Combs and Centipedes in a œë Solvent. *Macromolecules* **2005,** *38* (4), 1447-1450.

96. Nakatani, H.; Nitta, K.-h.; Soga, K., Effect of hydrogenation on dynamic mechanical relaxation 1. Atactic polystyrene. *Polymer* **1998,** *39* (18), 4273-4278.

97. Aamer, K. A.; Stafford, C. M.; Richter, L. J.; Kohn, J.; Becker, M. L., Thin Film Elastic Modulus of Degradable Tyrosine-Derived Polycarbonate Biomaterials and Their Blends. *Macromolecules* **2009,** *42* (4), 1212-1218.

98. Torres, J. M.; Stafford, C. M.; Vogt, B. D., Elastic Modulus of Amorphous Polymer Thin Films: Relationship to the Glass Transition Temperature. *Acs Nano* **2009,** *3* (9), 2677-2685.

CHAPTER 5

THICKNESS DEPENDENCE MODULUS OF VACUUM DEPOSITED ORGANIC MOLECULAR GLASSES FOR ORGANIC ELECTRONIC APPLICATIONS

5.1 Introduction

Organic based electronics, in particular organic light emitting devices (OLEDs), have recently been incorporated into commercial flat panel displays,[1, 2] but there is significant interest in extending these materials into cost effective *flexible* devices.[3-5] The potential fully organic electronic devices could be ultralow-cost, lightweight and compatible with the flexible substrates and employing well-established printing techniques in a roll-to-roll process.[2, 6] Furthermore, low temperature processing allows for next generation flexible electronics on plastic substrates. These flexible electronics enable the development of conformal, lightweight, rugged devices with implications in fields such as photovoltaics,[6] displays[7], medical devices[8], and detectors[9]. The electric and optic properties of organic materials could be strongly affected by their molecular packing due to changes in orbital overlap, which could be easily influenced with the different mechanical stresses that the organic thin films undergo as a result of thermal contraction during operation or bending during handling.[11] Thus, how organic materials respond to strain during bending could be critical to the performance of flexible electronic devices.[12] The mechanics of flexible electronics utilizing inorganic active components has been examined

more rigorously due to their propensity for cracking, therefore a significant decrease in performance has been observed at strains much less than the strain at failure.[13] The success of flexible devices depends on mechanical robustness of the active materials under operational induced strain. Rogers and coworkers have developed engineered stretchable interconnects based upon wrinkling of rigid inorganic active materials to enable flexible photodetectors[14] and sensors.[8,15] Despite these successes, there are issues with this process as it is necessary to transfer the active circuitry from a rigid substrate where fabrication occurs to the flexible substrate. Direct fabrication of electronics on flexible plastic substrates has been demonstrated using inorganic active materials,[16] but these devices have limited flexibility where bending can led to catastrophic device failure.[13] Polymers are significantly more compliant than these inorganic materials, but their electronic properties are generally inferior.[17] Organic small molecules can generally provide improved electronic performance when compared to polymeric materials, but very little is known about their mechanical properties. To begin to address this issue in rapidly emerging organic electronics, the mechanical properties of organic electronic materials need to be understood at the corresponding scale and morphology or molecular packing associated with the actual devices.

Although the properties of organic small molecules at the nanometer length scale have not been determined. The nanometer length scale glass transition temperature (T_g) behavior of glass forming liquids confined to nanopores, 2-100 nm in diameter, has been examined. First reports by Jackson

and McKenna show a 10K decrease in T_g for ortho-terphenyl (o-TP) as the pore size was decreased from 73 nm down to 4 nm.[18] This is attributed to a size effect, where either an increase in entropy or free volume due to reduced packing efficiency explains such a decrease in T_g. Further work by Park and McKenna shows that the confinement of o-TP results in two T_g's, one below and one above the bulk T_g.[19] The glass transition temperature less than the bulk value is associated with a size effect, previously reported by the same group, and the T_g greater than the bulk value is considered a surface effect.[18, 19] This surface effect is believed to be a result of an interacting layer at the pore surface and hence the higher T_g. Continued work on the two transitions revealed T_g's that either increased or decreased dependent on the strength of the interaction between the wall of the pore and the confined liquid.[20-22] Where strong surface interactions found an increase in surface T_g and weak interactions found a decrease in surface T_g, however both found a core T_g less than bulk T_g.[20, 21] On the other hand, Alba-Siminonesco and co-workers, reported only one T_g for both benzene and toluene confined to silicate nanopores with a non-monotonically varying T_g.[23] They reported a slight decrease in T_g followed by an increase in the T_g with decreasing pore size of both toluene and benzene confined to silicate nanopores.[23] The 37K increase in T_g when confined to a 2.4 nm pore diameter is attributed to the interactions between the confined molecules and the pore walls, while the decrease in T_g at larger pore sizes is attributed to an intrinsic size effect. Not only is the T_g of small molecules impacted by confinement but also the melting temperature,[24] crystallization,[25] and density[24]. For example, Jackson et al. have

reported the inability of cylcohexane and decaline to crystallize in pores with diameters less than 4 nm.[24] Although complex observations have been found with regards to the thermal properties of confined organic glasses, it is well stated that at the nanometer length scale materials exhibit properties that differ from their bulk counterparts.

The abundance of research into the thermal properties of confined organic glasses has been enhanced due to the availability of non-invasive thermodynamic and dynamic measuring techniques that allow for the determination of T_g from the non-linear behavior of the materials properties or shifts in input frequency. However, there are numerous challenges involved in measuring the mechanical properties of organic electronic materials. First, many active materials are glasses vapor deposited as thin films; thus, bulk measurements would likely not accurately capture the mechanical properties of the material in functioning devices. Furthermore, the expense of many OLED materials precludes the use of bulk tensile testing even if the bulk and thin film properties are identical. Nanoindentation (NI)[26] and Brillouin light scattering (BLS)[27] are commonly used to assess the elastic properties of films; however, for highly complaint materials like most organics and polymers, the mechanical properties of the substrate can be convoluted with those of the film of interest.[28] Application of atomic force microscopy (AFM) to control indentation depth has enabled the near surface modulus of glassy films to be determined. A reduced elastic modulus in the top (5 to 7) nm of polystyrene (PS) has been elucidated using this technique.[29] Conversely, van Vliet and coworkers showed a significant increase in surface

stiffness within 200 nm of the PS surface using nanoindentation.[30] Further, nanoindentation measurements of >100 nm thick films of a common OLED material, tris(8-hydroxyquinolinato)aluminum (Alq_3), have demonstrated a strong dependence of the elastic properties on the supporting substrate.[31, 32] On hard silicon substrates, the Alq_3 modulus is extrapolated to be on the order of 100 GPa; while on plastic substrates, the modulus of the same material is only on the order of 1 GPa.[31, 32] One potential route to overcome these difficulties in determining the elastic modulus of soft materials in thin films is through surface wrinkling instability, which occurs upon compression of a system consisting of a stiff film on a soft substrate.[33] This technique has been applied to determining the elastic moduli of ultrathin (down to 5 nm) polymer films[34, 35] and organic electronic materials.[36] The latter study demonstrated that the mechanical properties of several active organic electronic materials could be determined using surface wrinkling for thicknesses (30 nm to 200 nm) comparable to those utilized in functional devices.[36]

The layers in many organic electronic devices, in particular OLEDs, are in the sub-50 nm range.[37] This length scale also corresponds with dimensions where the thermophysical behavior of glass forming materials has been shown to deviate from bulk properties.[25, 34, 38-41] Recently, we have investigated the mechanical properties of several confined polymer thin film systems.[34, 35, 42] For all glassy polymers examined, there is a decrease in the elastic modulus of ultrathin (< 30 nm) films in comparison to the bulk modulus. The length scale at which deviations in the elastic moduli occur are found to scale with the bulk T_g of the

polymer[35, 43] in agreement with molecular simulations[43]. However, very little is known regarding the mechanical properties of organic molecular glasses at the nanoscale. Recently, Kearns *et al.* utilized BLS to determine the modulus of vapor deposited indomethacin films;[44] however, the films were required to be 10 μm to 15 μm thick.[44] Kang and coworkers have utilized surface wrinkling to determine the elastic modulus of thin pentacene films that are prepared by vapor deposition.[36] However because these films are polycrystalline they have a reported elastic modulus of approximately 15 GPa. The quality of the wrinkles formed from the pentacene films is poor and apparent delamination occurs at modest strain (10 %), thus it is unclear if surface wrinkling is appropriate for determining the elastic properties of small molecule organic electronic materials.

In this chapter, the mechanical properties of sub-100 nm, vapor deposited tris(8-hydroxyquinolinato)aluminum (Alq_3), triarylamines: 4'-N,N'-dicarbazole-biphenyl (CBP), N,N-diphenyl-N,N-bis(3-methylphenyl)-1,1-biphenyl-4,4-diamine (TPD), and N,N'-Di-[(1-Naphthyl)-(N,N'-diphenyl]-1,1'-biphenyl)-4-4'-diamine (NPD) films are determined using surface wrinkling. These materials are widely used as an electron transporting layer, electron injecting-layer, hole transporting layer, and host material for various dyes in OLEDs due to their luminescent properties, high carrier mobility, and high thermal and electrochemical stability.[45, 46] In an attempt to mitigate substrate influences, the modulus ranging from 10 nm to 100 nm in thickness is determined using surface wrinkling. Not only does this provide the mechanical properties these materials that will enable a deeper understanding as to how bending/stretching will impact

performance of OLEDs, these measurements provide the first experimental data demonstrating a thickness-dependent moduli for an organic molecular glass.

5.2 Experimental

Alq_3, NPD, CBP, and TPD were purchased (from Sigma Aldrich) and purified by thermal evaporation. The structure for each of these molecules is shown in Figure 5.1.

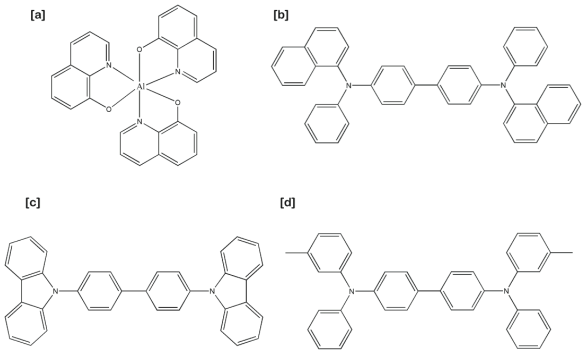

Figure 5.1 Schematic of [a] Alq_3 [b] NPD [c] CBP and [d] TPD

For an elastic substrate for wrinkling, polydimethylsiloxane (PDMS) (Sylgard 184, Dow Corning) was cast at either 10:1 or 20:1 base:cure agent onto float glass and allowed to degass and gel at ambient for 3 h. The PDMS was then cured at 100°C or 120°C for 2 h. Variation in the formulation ratio or cure temperature impacts the mechanical properties of the PDMS, but does not change the calculated moduli for the films. 75 mm × 25 mm × 1.5 mm slabs of PDMS are then pre-strained.[47]

Alq_3, NPD, CBP, and TPD were deposited directly on the strained substrate using resistively heated tantalum at pressures below 10^{-7} Torr in a vacuum thermal deposition system (Trovato Mfg.). A shadow mask restricted

deposition to a 16 mm diameter circular pattern. Deposition rate was controlled between 1 and 1.5 Å/s with the use of crystal growth monitors. The film growth rate calibrations necessary to report absolute thin film thicknesses ranging from 8 nm to 100 nm were accomplished through agreement between three sources of measurement. First, direct measurements of the film(s) on PDMS were collected after small molecule deposition using Variable Angle Spectroscopic Ellipsometer (VASE, J.A. Woollam Co., Inc.). Identical depositions for thicknesses representing the full range of experimental data were also performed with silicon substrates loaded in place of the PDMS and their thickness was measured by VASE and profilometry (P-6, KLA-Tencor). Profile scans were collected across shadow masked edges as well as ledges exposed by post deposition removal of Kapton® tape to enable sampling at the center of the film. All methods agreed to confirm predictable deposition rates.

Initially, the stability of Alq_3 films on PDMS was monitored using VASE and fit to a three layer model consisting of a PDMS substrate, an intermixed layer, and a Cauchy layer representing Alq_3 (for wavelengths between 650 nm and 1700 nm). The intermixed layer was used to model the diffusion of Alq_3 into PDMS through weighting of the PDMS and Alq_3 optical constants.[41] Significant changes in the Alq_3 film thickness suggest that diffusion of Alq_3 into PDMS can obfuscate mechanical analyses.

To prevent diffusion of Alq_3 into the PDMS substrate, polystyrene (PS, M_n = 9.4 kg/mol, Polymer Laboratories) or addition polynorbornene (Add PENb)[48] films were utilized as barrier coatings to inhibit the diffusion of the small

molecules into PDMS. These polymers were spin cast onto cleaned silicon wafers, annealed under nitrogen at $T=T_g + 20$ ºC and transferred to the pre-strained PDMS. Alq_3, NPD, CBP, and TPD were vacuum deposited (Trovato Mfg.) onto the pre-strained polymer-PDMS. Surface wrinkling was induced by releasing the pre-strain at approximately 0.1 mm/s under ambient conditions (T = 21 °C ± 2 °C).

The thickness of the PS or Add PENb was determined using a VASE over a wavelength range from 250 nm to 1700 nm measured at three incident angles (65°, 70°, and 75°) both on the silicon wafer and once transferred onto the PDMS utilizing proper material files and Cauchy layers. The thickness of the molecular glass thin films was also determined VASE utilizing a two-layer model (polymer/PDMS). The thickness of these barrier films ranged from 24-26 nm. The modulus of PDMS was determined using a Texture Analyzer (TA.XT Plus, Texture Technologies).

The wavelength of the wrinkled surface was determined using atomic force microscopy (AFM, Park XE-150) in intermittent contact mode using a constant scan size of 10 μm by 10 μm, and optical microscopy (OM, Mititoyo Ultraplan FS-110) with an image resolution of 1024 pixels × 768 pixels. AFM images were analyzed using a 1D Fast Fourier Transform (FFT) in XEI software in order to obtain the wavelength of the wrinkles. Similarly, the wrinkling wavelength from the OM images was determined using a 1D FFT of the micrographs using custom written Matlab code.

5.3 Results

5.3.1 Stability of Alq_3 films on PDMS

One of the first indications that Alq_3 films directly deposited onto PDMS are not stable is a change in the color of the as-deposited film over the course of several hours. To quantify the changes in the films, the ellipsometric angles, Ψ and Δ, for the film are obtained at 55° as a function of time. As shown in Figure 5.1 when Alq_3 is deposited directly onto PDMS, there is a significant reduction in the film thickness as the film ages at ambient conditions.

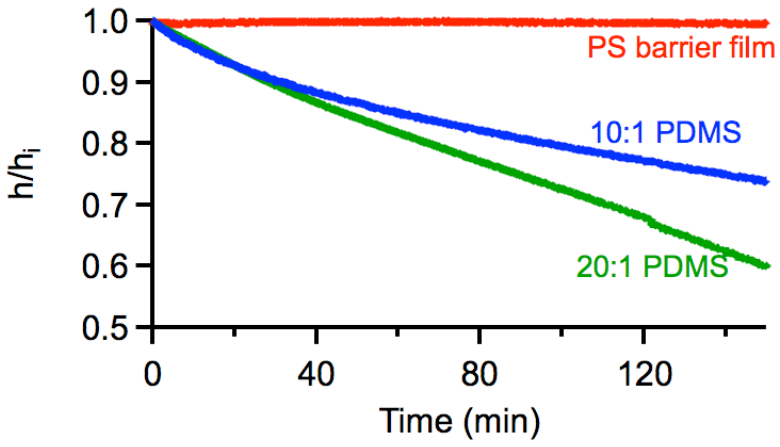

Figure 5.2 Apparent Alq_3 normalized film thickness (h/h_i) as a function of time on 10:1 ≈2 MPa PDMS, 20:1 ≈0.7MPa PMDS, and 20:1 ≈0.7MPa PDMS with a 20 nm PS barrier film. The decrease in thickness for the Alq_3 film for both bare PDMS substrates is attributed to diffusion of Alq_3 into the PDMS layer.

Although Alq_3 is known to be marginally unstable in air,[49] the change in thickness is too great to be attributed to degradation. PDMS formulated with 20:1 base to curing agent forms a network with a modulus of ≈0.7MPa. This loose network enables Alq_3 to diffuse into the PDMS substrate. After 150 min, the thickness of the Alq_3 layer decreased by 40%. By increasing the base to curing

agent ratio to 10:1, the crosslink density of the PDMS increases leading to a modulus of ≈2MPa. Comparatively, Alq_3 deposited onto 10:1 PDMS exhibited a decrease in film thickness of 23% after 150 min, as shown in Figure 5.1.

As of result of increased packing density and hence higher bulk elastic modulus, attempts to wrinkle these films yield ill-defined structures as shown in Figure 5.3. This result is reminiscent of the poorly formed wrinkles using pentacene vapor deposited onto PDMS reported by Tahk *et al*.[36] The low glass transition temperature of PDMS (T_g = -125°C)[50] and large free volume of PDMS appears to enable diffusion of Alq_3 and potentially other small molecules into the PDMS network;[51] this may lead to a poorly defined system for wrinkling analysis. Thus, direct vapor deposition of small molecules on PDMS is likely problematic for determining their elastic moduli using wrinkling.

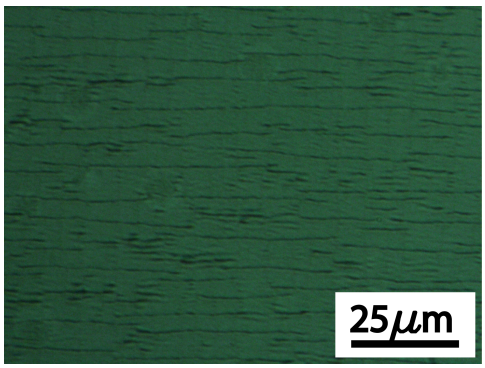

Figure 5.3 Wrinkled films of Alq_3 directly deposited onto the PDMS substrate.

However it is possible prevent diffusion of Alq_3 into the PDMS substrate by addition of a barrier film; in this case, a nominal 20 nm polystyrene (PS) film as shown in Figure 5.1 appears to prevent diffusion of the Alq_3 into the PDMS

substrate. The thickness of Alq_3 film remains invariant due to the limited free volume in PS and the slow glassy chain dynamics. By insuring sharp interfaces with the use of a barrier, the Alq_3 – polymer composite film on PDMS yields well defined wrinkles as illustrated in Figure 5.4.

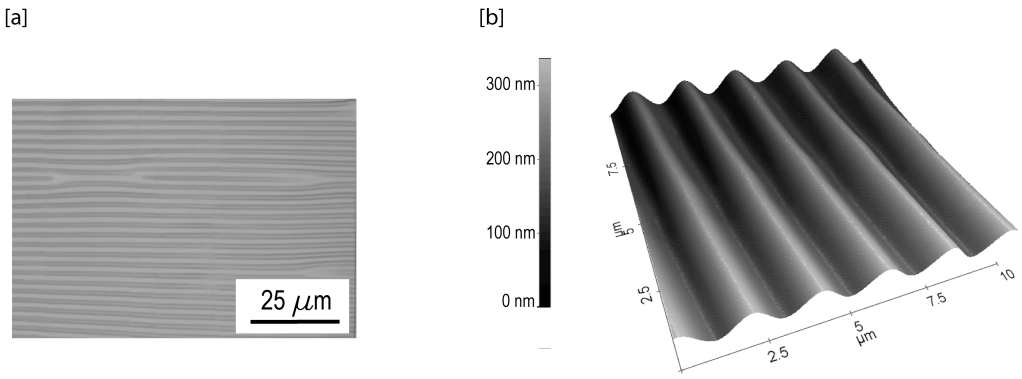

Figure 5.4 [a] Optical image of a 36 nm Alq_3 film where the wavelength is 1.17 μm ± 0.18 μm [b] AFM image of an 8 nm Alq_3 film with a 1.76 μm ± 0.22 μm wavelength.

An Alq_3 film (h_{Alq3} = 36 nm) on a PS film (h_{PS} = 22 nm) wrinkles with a uniform wavelength of 3.5 μm ± 0.13 μm (Figure 5.4a). Figure 5.4b shows an AFM micrograph of an 8 nm Alq_3 film on 22 nm PS film with wavelength of 2.1 μm ± 0.15 μm. These well-defined wrinkles are similar to those observed for most glassy polymers, but the added PS layer must be included in the analysis of the wrinkling to determine the elastic modulus of Alq_3.

5.3.2 Elastic modulus

The elastic modulus of the vacuum deposited materials ($\overline{E}_i$) was determined using well-established two-plate buckling mechanics.[52, 53] Due the inclusion of the barrier layer leads to a modification of the typical analysis for an

elastic rigid film on a soft substrate, such that an effective modulus ($\overline{E}_{eff}$) for the barrier and vacuum deposited material is determined first as:

$$\overline{E}_{eff} = 3\overline{E}_s\left(\frac{\lambda}{2\pi d_t}\right)^3$$

Where d_t is the total film thickness (barrier + vacuum deposited materials), λ is the measured wrinkle wavelength, and $\overline{E}_s$ is the plane strain modulus of the PDMS. To determine the elastic properties of the film of interest, bending mechanics can be applied to describe the composite structure of the film + barrier as:

$$\overline{E}_i = \frac{\frac{E_{eff}}{4} - E_1\left[\left(\phi_2 - \frac{\kappa}{2}\right)^3 + \left(\frac{\kappa}{2}\right)^3\right]}{\left(1 - \frac{\kappa}{2}\right)^3 - \left(\phi_2 - \frac{\kappa}{2}\right)^3}$$

where the deviation from the neutral axis, κ, of bending is given by $\kappa = \frac{1 + \phi_2{}^2\left(\frac{\overline{E}_1}{\overline{E}_i} - 1\right)}{1 + \phi_2\left(\frac{\overline{E}_1}{\overline{E}_i} - 1\right)}$, ϕ_2 is the ratio of the thickness of the barrier film to the triarylamine and $\overline{E}_1$ is the modulus of the barrier film: 3.6 ± 0.24 GPa for PS[42] and 1.0 ± 0.2 GPa for the Add PEN. This approach has been applied previously to describe the modulus of polyeletrolyte layer-by-layer films.[52] Changing the barrier film from PS to Add PEN does not statistically impact the $\overline{E}_i$ calculated for a given material.

Utilizing two-plate mechanics, the Young's modulus of the 36 nm thick Alq_3 film (Figure 5.4a) is 1.17 ± 0.18 GPa. This is significantly less than the

estimated 100 GPa modulus for Alq_3 determined using 100 nm thick films on silicon wafers with nanoindentation.[31] This modulus from nanoindentation is extremely large for an organic molecule and is similar to that of the hard support ($E_{silicon}$ = 130 GPa). However, the modulus of most organic glass formers formed by supercooling the liquid is between 1 and 2 GPa; this is in agreement with the modulus of Alq_3 determined by wrinkling. Even for vapor deposited glasses, Kearns *et al.* have recently shown that the elastic modulus of indomethacin and trisnaphthylbenzene is between 4 GPa and 5 GPa using BLS.[44] It should be noted that the Young's modulus of these vapor deposited organic glasses is dependent on deposition conditions. Nonetheless, the elastic modulus of the Alq_3 film reported here appears to be reasonable based upon comparison to other organic molecular glasses. On the other hand, the wrinkled 8 nm thick Alq_3 film shown in Figure 5.4b is calculated to have a Young's modulus of 1.76 GPa ± 0.22 GPa. This suggests that the modulus of Alq_3 increases if it is confined to nanoscale dimensions. Figure 5.5a illustrates how the plane strain modulus of Alq_3 depends on film thickness. For films thicker than 20 nm, the modulus is independent of film thickness at approximately 1.2 GPa. This is similar to the modulus of pentacene, which has been shown to be independent of film thickness down to 25 nm.[36] However as the film thickness of Alq_3 is reduced from 20 nm to 10 nm, the plane-strain modulus increases significantly. For example, decreasing the thickness from 20 nm to 10 nm results in an increase in the plane-strain modulus from 1.21 GPa ± 0.31 GPa to 2.35 ± 0.41 GPa. Thus, there is nearly an 80 % increase in the elastic properties of Alq_3 when confined to 10 nm. This large

increase in elastic modulus is counter to most reports for glassy polymers where 10 nm films can exhibit a modulus that is only 10 % of the bulk.[34] However, enhancements in the yield strength and ductility of metallic glasses upon confinement to the nanoscale have been reported for a number of different systems.[54] Thus, enhancements in mechanical properties for Alq_3 upon confinement to the nanoscale are not completely unexpected. However, changes in the modulus for Alq_3 occur when the film is less than 20 nm thick, whereas enhancements in the yield stress of metallic glasses typically are observed at sizes greater than 100 nm.[54, 55]

Figure 5.5b illustrates the thickness dependent moduli of NPD. The modulus of NPD is independent of thickness for films greater than 20 nm thick (1.65 ± 0.23 GPa). For a 10.3 nm thick film, the modulus of NPD is also increased by approximately 50 % to 2.39 ± 0.33GPa. This behavior is similar to that for Alq_3 as shown in Figure 5.5a.

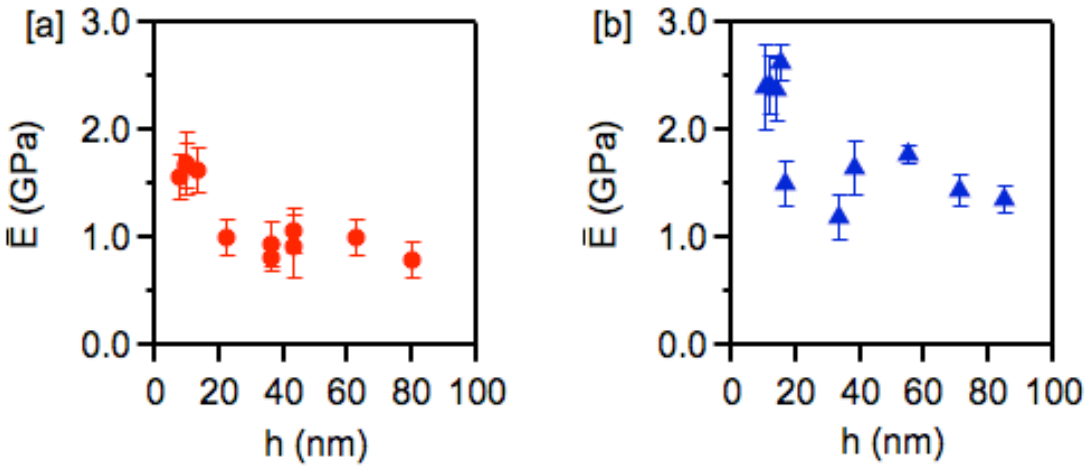

Figure 5.5 Modulus as a function of film thickness for [a] NPD and [b] Alq_3 determined using the two-plate composite calculations. The error bars represent

one standard deviation of the data, which is taken as the experimental uncertainty of the measurement.

Figure 5.6a illustrates the thickness dependencies in the moduli of CBP. The bulk-like modulus of CBP is 1.9 ± 0.4 GPa and remains constant down to film thicknesses of approximately 20 nm. One unusual feature in these data is the large variation in moduli for these thicker films; the probable origins of this behavior will be addressed later. Nonetheless, further decreasing the thickness of the CBP leads to a decrease in the film modulus. For example, a 9.6 nm thick film of CBP exhibits factor of four reduction in modulus to 0.51 ± 0.20 GPa. This behavior is more characteristic of thin polymer films where an order of magnitude decrease is observed for 10 nm PS films[34] than Alq_3 and NPD previously examined where a factor of two increase in modulus is found. Thus, the thin film mechanical behavior of glassy films is molecularly dependent, but it is not clear what factors control this behavior.

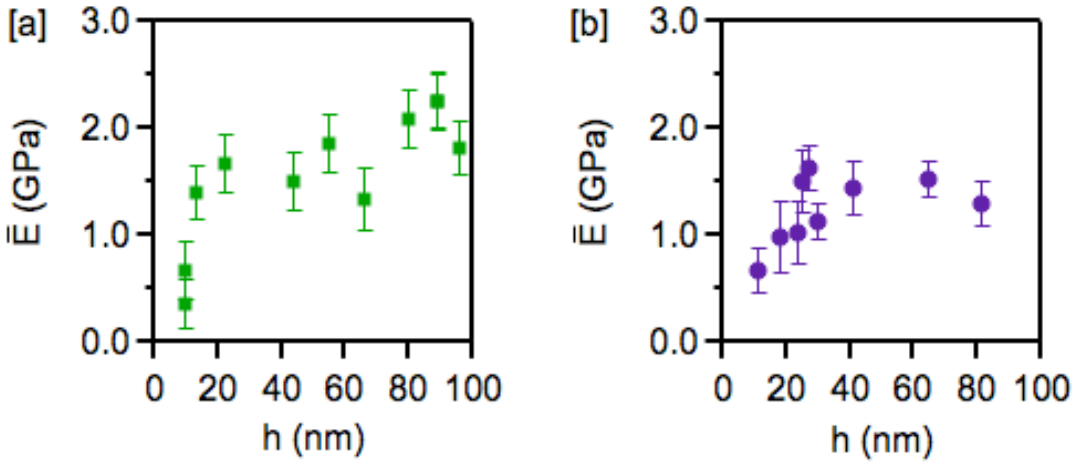

Figure 5.6 Modulus as a function of film thickness for [a] CBP and [b] TPD determined using the two-plate composite calculations. The error bars represent one standard deviation of the data, which is taken as the experimental uncertainty of the measurement.

In an attempt to understand these factors, the structure of the CBP is modified by changing two of the phenyl moieties to naphthalene groups to make TPD. In this case, the bulk T_g of the molecule only increases slightly from 60 °C to 62 °C by changing from CBP to TPD. Figure 5.6b shows the moduli as a function of film thickness for TPD. Unlike the CBP, the variation in the thickness independent modulus is within the error of each individual measurement (approximately 1.42 ± 0.18 GPa). By decreasing the thickness to 10.3 nm, the modulus of TPD is reduced by a factor of two to 0.66 ± 0.22 GPa. As the behavior for polymer thin films is similar to that observed for CBP and TPD, it is instructive to examine why a reduction in moduli are observed for polymers; this has typically been attributed to a reduced modulus at the polymer-air interface[56] that has been directly measured via indentation.[29] Thus, a similar effect could be present in these materials.

For polymer thin films, the proximetry of the bulk T_g to the measurement temperature is a critical factor in determining the length scale at which deviations from the bulk modulus are observed.[41] The thin film behavior of polymers has been shown to not only depend upon the free surface,[57] but also the substrate interface.[58] Contratry to polymers, these small molecules are vacuum deposited and therefore packing of the molecules is dependent upon deposition conditions. Recent work by Ediger and coworkers has illustrated that vacuum deposition conditions for two model systems, Indomethacin (IMD, T_g ~ 42 °C) and Trisnaphthylbenzene (TNB, T_g ~ 75 °C), can result in variations in packing density for these small molecules.[59-61] The proximety of the substrate temperature

to bulk T_g has been found to be critical for the density, aging and thermal properties of the glass. For IMD and TNB, an optimal deposition temperature of 40°C below bulk T_g ($0.85T_g$ with T_g in Kelvin) for stability of the glass has been identify using Neutron Reflectivity to measure interdiffusion of deuterated and protonated layers.[61] Deposition temperatures close to T_g yields a monolayer of increased mobility that allows for configurational sampling of the molecule as it arrives at the substrate. This configurational sampling increases the molecules packing density.[59] Utilizing these enhanced dynamics the molecules can assemble in an efficient layer-by-layer fashion. The modulus of these more stable films (15μm IMD and TNB film) deposited at $0.85T_g$ is increased by 19% and 14%, respectively, in comparison to the ordinary glass created by colling the liquid.[62]

The room temperature deposition of CBP and TPD with T_g's of 60°C and 62°C is $0.89T_g$ and $0.88T_g$, which is slightly greater than the optimum conditions of $0.85T_g$. Thus, one would expect significant rearrangement of the surface to enable improved packing. The origin for the decrease in moduli for these molecules for sub-20 nm films is likely this enhanced mobility surface. An increase in molecular mobility should lead to a decrease in the capacity of the material to store stress and hence a decrease in modulus. This enhanced mobility surface in the molecular glass is similar to what has been reported for PS surfaces[63] where a decrease in moduli for ultrathin films[56] has been reported. To explain the thin film moduli behavior of Alq_3 ($T_g \sim 175$°C) and NPD ($T_g \sim 95$°C), we can utilize a similar argument. At deposition temperatures significantly below

T_g (<0.85T_g), molecules hit the surface with less rearrangement and the structure is instanteously frozen during deposition. This lack of rearrangement creates glasses with high molar volumes or low packing densities, and high enthalpies. The surface should not be mobile as the deposition conditions correspond to 0.66T_g and 0.78T_g. Additionally, the deposition surface can impact the structure of the film for vacuum deposited molecules. For example, hole injection barrier for NPD and pentacene reveals a magnitude difference in carrier mobility between the materials deposited on Au or electronic polymer layers, which is attributed to the impact of the substrate on the packing on the molecules.[64] Moreover, an increase in mobility of the first monolayer of pentacene has been attributed to a unique packing of the first monolayer of pentacene.[65] Thus, the initial monolayer of Alq_3 and NPD may be more densely packed due to interactions with the substrate. As the film grows, the lack of surface mobility of the molecules lead to a decrease in packing efficiency. This proposed behavior is consistent with the thickness dependent moduli reported for Alq_3 and NPD. These results indicate that the bulk T_g of the molecule is a critical factor in assessing the thickness dependent behavior. For molecules with T_g near ambient T, there is a significant decrease in modulus in the thinnest films due to a mobile surface layer; conversely for molecules with T_g significantly greater than ambient T, the thinnest films exhibit a larger modulus than thick films due to poor molecular packing during film growth.

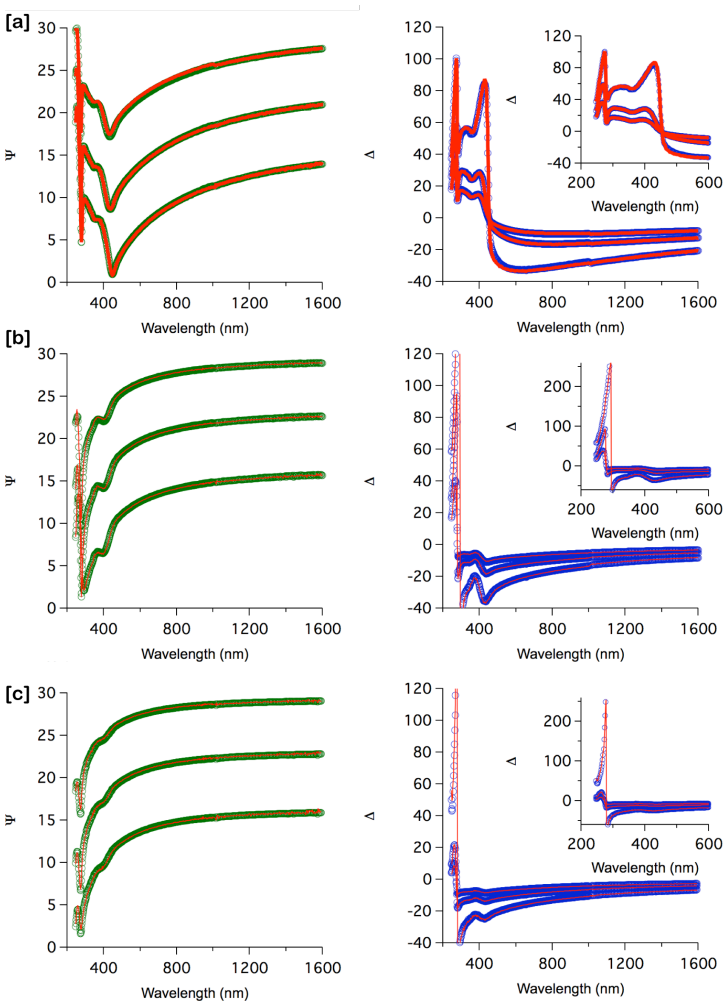

Figure 5.7 Ellipsometric fits for Alq_3 deposited on the PS/PDMS substrate [a] 80 nm Alq_3 [b] 20 nm Alq_3 and [c] 12 nm Alq_3.

Furthermore, it is known that the change in morphology from thin film to bulk is accompanied by a corresponding change in the optical properties of the film. Thus, thickness dependent structure of the vacuum deposited films should be marked by changes in the optical constant of the film as well. After vapor deposition of the Alq_3, the thickness and optical constants for the Alq_3 in the transparent region (600-1600 nm) are determined by fitting D and Y using a

Cauchy dispersion model. The ellipsometric angles, Ψ and Δ, as well as their fits are shown in Figure 5.7 below for a wide range of Alq_3 film thickness.

To assess these changes, the absorption coefficient, *k*, is also determined for each film. The film thickness is extracted from the original fit shown in Figure 5.7 and remains fixed. The optical constants are then fit utilizing multiple Lorenzian oscillators following the procedure of Djurisic and coworkers.[66] The absorption coefficient as a function of film thickness is ploted in Figure 5.8.

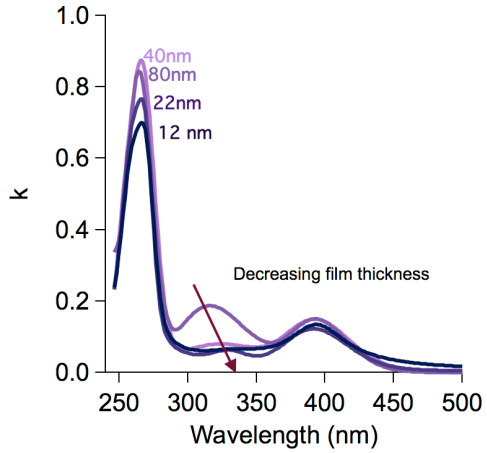

Figure 5.8 Optical constant of Alq_3 films with thicknesses of 80 nm, 44 nm, 22 nm, and 12 nm. Peaks at 260 nm and 385 nm are present for all Alq_3 films with decreasing intensity as the film thickness is reduced. The intermediate adsorption band (310-340 nm) associated with aggregates of Alq_3 shifts to larger wavelength as the film thickness decreases with no peak observed for the 12 nm thick film.

Figure 5.8 illustrates how the extinction coefficient varies with thickness for Alq_3 films ranging from 80 nm to 12 nm. For all films, there are two absorption peaks at 260 nm and 385 nm which correspond to those observed for a dilute Alq_3 solution.[67] This suggests that these adsorption bands are associated with the isolated Alq_3 molecule. For the thicker films, another absorption band in

the range of 310-340 nm is observed that is indicative of the formation of Alq_3 aggregates. This peak shifts to higher wavelength as the thickness of the film is reduced, which suggests a change in the molecular packing. However, it is not well understood how different molecular packing influences the absorption energy and intensity. To quantify differences in the aggregates as a function of film thickness will require improved morphological characterization techniques and a more diverse group of materials to enable correlation of shifts in adsorption bands with aggregate size/shape.

It should also be noted that the optical constants for Alq_3 deposited on silicon wafers were also measured in order to determine if there is a difference in morphology that manifests itself in the optical properties. The fits of Alq_3 on Si and PS/PDMS are shown in Figure 5.9. Figure 5.9 shows that the optical constants determined from spectroscopic ellipsometry are similar for Alq_3 irrespective of substrate. It should also be noted that a decrease in the single molecule adsorption peaks (~10-15 %) was also observed for very thin Alq_3 films deposited directly on a silicon wafer using analogous deposition rates, where there is no possibility for interdiffusion. These results suggest that the changes in the fit adsorption spectra are not from interdiffusion.

It should be noted that the wrinkling metrology utilized here appears capable of mitigating substrate effects to determining the modulus of small organic glasses at the nanometer length scale. These results therefore indicate the bulk T_g of the molecule impacts the thickness dependent modulus due to packing differentials preliminarily observed via optical constant variations.

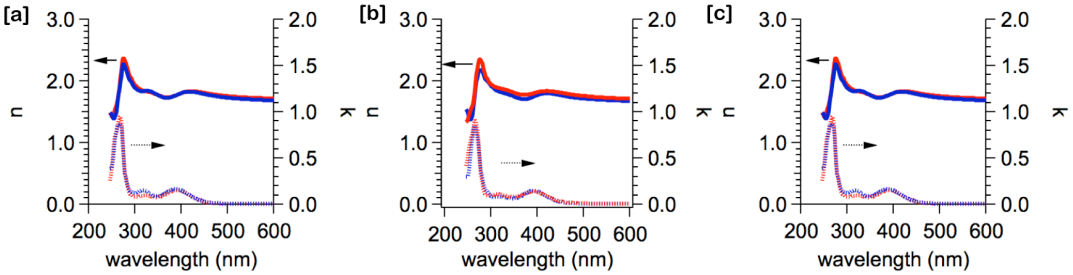

Figure 5.9 Refractive index and extinction coefficient of Alq_3 films deposited on Si (red, circles) and PS/PDMS (blue, lines) with thicknesses of [a] 50 nm, [b] 20 nm, and [c] 12 nm.

5.4 Conclusion

The elastic modulus of a series of triarylamines, NPD, CBP, and TPD, films was determined utilizing a two plate wrinkling instability as a function of film thickness. The moduli of sub 20 nm thick films is dependent on the bulk T_g of the deposited molecule. For materials with a deposited at $T > 0.85T_g$ a systematic decrease from bulk modulus for sub 20 nm films is observed. This behavior is similar to that observed in polymeric thin films, which has been attributed to free surface effects. For these vacuum deposited small molecules increased mobility of the surface monolayer is consistent with recent studies on ultrastable organic glasses. Materials with higher bulk T_g (deposited at $T < 0.85T_g$) exhibit an increase in sub-20 nm moduli that is attributed to increased packing frustration due to initial surface directed packing and lower surface mobility of the material during film growth.

5.5 References

1. *CHEMICAL & ENGINEERING NEWS* **2007,** *85* (41), 21-21.

2. Forrest, S. R., The path to ubiquitous and low-cost organic electronic appliances on plastic. *Nature* **2004,** *428* (6986), 911-918.

3. Burrows, P. E. G., G.; Bulovic, V.; Shen, Z.; Forrest, S.R.; Thompson, M.E.;, Achieving full-color organic light-emitting devices for lightweight, flat-panel displays. *IEEE TRANSACTIONS ON ELECTRON DEVICES* **1997,** *44* (8), 1188-1203.

4. Kelley, T. W.; Baude, P. F.; Gerlach, C.; Ender, D. E.; Muyres, D.; Haase, M. A.; Vogel, D. E.; Theiss, S. D., Recent Progress in Organic Electronics: Materials, Devices, and Processes. *Chemistry of Materials* **2004,** *16* (23), 4413-4422.

5. McGehee, M. D., Goh, C., Organic Semiconductors for Low-Cost Solar Cells. *Frontiers of Engineering: Reports on Leading-Edge Engineering 2005 Symposium* **2006**, 119-130.

6. Coakley, K. M.; McGehee, M. D., Conjugated polymer photovoltaic cells. *Chemistry of Materials* **2004,** *16* (23), 4533-4542.

7. Rogers, J. A.; Bao, Z.; Baldwin, K.; Dodabalapur, A.; Crone, B.; Raju, V. R.; Kuck, V.; Katz, H.; Amundson, K.; Ewing, J.; Drzaic, P., Paper-like electronic displays: Large-area rubber-stamped plastic sheets of electronics and microencapsulated electrophoretic inks. *Proceedings of the National Academy of Sciences* **2001,** *98* (9), 4835-4840.

8. Kim, D.-H.; Viventi, J.; Amsden, J. J.; Xiao, J.; Vigeland, L.; Kim, Y.-S.; Blanco, J. A.; Panilaitis, B.; Frechette, E. S.; Contreras, D.; Kaplan, D. L.; Omenetto, F. G.; Huang, Y.; Hwang, K.-C.; Zakin, M. R.; Litt, B.; Rogers, J. A., Dissolvable films of silk fibroin for ultrathin conformal bio-integrated electronics. *Nat Mater* **2010,** *9* (6), 511-517.

9. Ko, H. C.; Stoykovich, M. P.; Song, J.; Malyarchuk, V.; Choi, W. M.; Yu, C.-J.; Geddes Iii, J. B.; Xiao, J.; Wang, S.; Huang, Y.; Rogers, J. A., A hemispherical electronic eye camera based on compressible silicon optoelectronics. *Nature* **2008,** *454* (7205), 748-753.

10. Lee, M. L.; Fitzgerald, E. A.; Bulsara, M. T.; Currie, M. T.; Lochtefeld, A., Strained Si, SiGe, and Ge channels for high-mobility metal-oxide-semiconductor field-effect transistors. *Journal of Applied Physics* **2005,** *97* (1), 011101-28.

11. Anthony, J. E.; Eaton, D. L.; Parkin, S. R., A Road Map to Stable, Soluble, Easily Crystallized Pentacene Derivatives. *Organic Letters* **2001,** *4* (1), 15-18.

12. Kline, R. J.; DeLongchamp, D. M.; Fischer, D. A.; Lin, E. K.; Heeney, M.; McCulloch, I.; Toney, M. F., Significant dependence of morphology

and charge carrier mobility on substrate surface chemistry in high performance polythiophene semiconductor films. *Applied Physics Letters* **2007,** *90* (6), 062117-3.

13. Gleskova, H.; Cheng, I. C.; Wagner, S.; Sturm, J. C.; Suo, Z., Mechanics of thin-film transistors and solar cells on flexible substrates. *Solar Energy* **2006,** *80* (6), 687-693.

14. Sun, Y.; Choi, W. M.; Jiang, H.; Huang, Y. Y.; Rogers, J. A., Controlled buckling of semiconductor nanoribbons for stretchable electronics. *Nat Nano* **2006,** *1* (3), 201-207.

15. Wang, Y.; Yang, R.; Shi, Z.; Zhang, L.; Shi, D.; Wang, E.; Zhang, G., Super Elastic Graphene Ripples for Flexible Strain Sensors. *ACS Nano* **2011**, null-null.

16. Wagner, S.; Fonash, S. J.; Jackson, T. N.; Thomas, T. N.; Strum, J. C., *Flexible display enabling technology*. Society of Photo-Optical Instrumentation Engineers: Bellingham, WA, INTERNATIONAL, 2001; Vol. 4362, p X, 332 p.

17. Sirringhaus, H.; Kawase, T.; Friend, R. H.; Shimoda, T.; Inbasekaran, M.; Wu, W.; Woo, E. P., High-Resolution Inkjet Printing of All-Polymer Transistor Circuits. *Science* **2000,** *290* (5499), 2123-2126.

18. Jackson, C. L.; McKenna, G. B., The glass transition of organic liquids confined to small pores. *Journal of Non-Crystalline Solids* **1991,** *131-133* (Part 1), 221-224.

19. Park, J.-Y.; McKenna, G. B., Size and confinement effects on the glass transition behavior of polystyrene/o-terphenyl polymer solutions. *Physical Review B* **2000,** *61* (10), 6667.

20. Pissis, P.; Kyritsis, A.; Daoukaki, D.; Barut, G.; Pelster, R.; Nimtz, G., Dielectric studies of glass transition in confined propylene glycol. *Journal of Physics: Condensed Matter* **1998,** (28), 6205.

21. Scheidler, P.; Kob, W.; Binder, K., Cooperative motion and growing length scales in supercooled confined liquids. *EPL (Europhysics Letters)* **2002,** (5), 701.

22. Schuller, J.; Richert, R.; Fischer, E. W., Dielectric relaxation of liquids at the surface of a porous glass. *Physical Review B* **1995,** *52* (21), 15232.

23. Alba-Simionesco, C.; Dosseh, G.; Dumont, E.; Frick, B.; Geil, B.; Morineau, D.; Teboul, V.; Xia, Y., Confinement of molecular liquids: Consequences on thermodynamic, static and dynamical properties of benzene and toluene. *Eur. Phys. J. E* **2003,** *12* (1), 19-28.

24. Jackson, C. L.; McKenna, G. B., The melting behavior of organic materials confined in porous solids. *The Journal of Chemical Physics* **1990,** *93* (12), 9002-9011.

25. Jackson, C. L.; McKenna, G. B., The glass-transition of organic liquids confined to small pores. *Journal of Non-Crystalline Solids* **1991,** *131*, 221-224.

26. Pharr, G. M., Oliver, W. C., Measurement of Thin-Film Mechanical-Properties Using Nanoindentation. *MRS Bulletin* **1992,** *17* (7), 28-33.

27. Ferrari, A. C.; Robertson, J.; Beghi, M. G.; Bottani, C. E.; Ferulano, R.; Pastorelli, R., Elastic constants of tetrahedral amorphous carbon films by surface Brillouin scattering. *Applied Physics Letters* **1999,** *75* (13), 1893-1895.

28. VanLandingham, M. R.; Villarrubia, J. S.; Guthrie, W. F.; Meyers, G. F., Nanoindentation of polymers: An overview. *Macromolecular Symposia* **2001,** *167*, 15-43.

29. Miyake, K.; Satomi, N.; Sasaki, S., Elastic modulus of polystyrene film from near surface to bulk measured by nanoindentation using atomic force microscopy. *Applied Physics Letters* **2006,** *89* (3), 031925-3.

30. Tweedie, C. A.; Constantinides, G.; Lehman, K. E.; Brill, D. J.; Blackman, G. S.; VanVliet, K. J., Enhanced Stiffness of Amorphous Polymer Surfaces under Confinement of Localized Contact Loads. *Advanced Materials* **2007,** *19* (18), 2540-2546.

31. Chiang, C.-J.; Bull, S.; Winscom, C.; Monkman, A., A nano-indentation study of the reduced elastic modulus of Alq3 and NPB thin-film used in OLED devices. *Organic Electronics* **2010,** *11* (3), 450-455.

32. Chiang, C.-J.; Winscom, C.; Bull, S.; Monkman, A., Mechanical modeling of flexible OLED devices. *Organic Electronics* **2009,** *10* (7), 1268-1274.

33. Stafford, C. M.; Harrison, C.; Beers, K. L.; Karim, A.; Amis, E. J.; Vanlandingham, M. R.; Kim, H. C.; Volksen, W.; Miller, R. D.; Simonyi, E. E., A buckling-based metrology for measuring the elastic moduli of polymeric thin films. *Nature Materials* **2004,** *3* (8), 545-550.

34. Stafford, C. M.; Vogt, B. D.; Harrison, C.; Julthongpiput, D.; Huang, R., Elastic moduli of ultrathin amorphous polymer films. *Macromolecules* **2006,** *39* (15), 5095-5099.

35. Torres, J. M., Stafford, C. M., Vogt, B. D., Elastic Modulus of Amorphous Polymer Thin Films: Relationship to the Glass Transition Temperature. *ACS Nano* **2009,** *3* (9), 2677.

36. Tahk, D.; Lee, H. H.; Khang, D.-Y., Elastic Moduli of Organic Electronic Materials by the Buckling Method. *Macromolecules* **2009,** *42* (18), 7079-7083.

37. Qi, Q.; Wu, X.; Hua, Y.; Hou, Q.; Dong, M.; Mao, Z.; Yin, B.; Yin, S., Enhancement of performance for blue organic light emitting devices based on double emission layers. *Organic Electronics* **2010,** *11* (3), 503-507.

38. de Gennes, P. G., Glass transitions in thin polymer films. *European Physical Journal E* **2000,** *2* (3), 201-203.

39. Forrest, J. A.; Dalnoki-Veress, K., The glass transition in thin polymer films. *Advances in Colloid and Interface Science* **2001,** *94* (1-3), 167-196.

40. Forrest, J. A.; Mattsson, J., Reductions of the glass transition temperature in thin polymer films: Probing the length scale of cooperative dynamics. *Physical Review E* **2000,** *61* (1), R53-R56.

41. Torres, J. M. S., C.M.; Vogt, B.D., Elastic Modulus of Amorphous Polymer Thin Films: Relationship to the Glass Transition Temperature. *ACS Nano* **2009,** *3* (9), 2677.

42. Torres, J. M., Stafford, C.M., Vogt, B.D., Impact of molecular mass on the elastic modulus of ultrathin polystyrene films. *Submitted* **2010**.

43. Yoshimoto, K.; Jain, T. S.; Nealey, P. F.; de Pablo, J. J., Local dynamic mechanical properties in model free-standing polymer thin films. *Journal of Chemical Physics* **2005,** *122* (14), 144712.

44. Kearns, K. L.; Still, T.; Fytas, G.; Ediger, M. D., High-Modulus Organic Glasses Prepared by Physical Vapor Deposition. *Advanced Materials 22* (1), 39-42.

45. Lian, J.-r.; Yuan, Y.-b.; Cao, L.-f.; Zhang, J.; Pang, H.-q.; Zhou, Y.-f.; Zhou, X., Improved efficiency in OLEDs with a thin Alq3 interlayer. *Journal of Luminescence* **2010,** *122-123*, 660-662.

46. Tang, C. W.; VanSlyke, S. A., Organic electroluminescent diodes. *Applied Physics Letters* **1987,** *51* (12), 913.

47. Stafford, C. M.; Guo, S.; Harrison, C.; Chiang, M. Y. M., Combinatorial and high-throughput measurements of the modulus of thin polymer films. *Review of Scientific Instruments* **2005,** *76* (6).

48. Bishop, J. P.; Register, R. A., Poly(phenylethylnorbornene)s and their Hydrogenated Derivatives. *Macromolecular Rapid Communications* **2008,** *29* (9), 713-718.

49. Vivo, P.; Jukola, J.; Ojala, M.; Chukharev, V.; Lemmetyinen, H., Influence of Alq3/Au cathode on stability and efficiency of a layered organic solar cell in air. *Solar Energy Materials and Solar Cells* **2008,** *92* (11), 1416-1420.

50. Lotters, J. C.; Olthuis, W.; Veltink, P. H.; Bergveld, P., The mechanical properties of the rubber elastic polymer polydimethylsiloxane for sensor applications. *Journal of Micromechanics and Microengineering* **1997,** (3), 145.

51. Gobel, R.; Krska, R.; Kellner, R.; Seitz, R. W.; Tomellini, S. A., Investigation of Different Polymers as Coating Materials for IR/ATR Spectroscopic Trace Analysis of Chlorinated Hydrocarbons in Water. *Applied Spectroscopy* **1994,** *48*, 678-683.

52. Nolte, A. J.; Cohen, R. E.; Rubner, M. F., A two-plate buckling technique for thin film modulus measurements: Applications to polyelectrolyte multilayers. *Macromolecules* **2006,** *39* (14), 4841-4847.

53. Stafford, C. M.; Guo, S.; Harrison, C.; Chiang, M. Y. M., Combinatorial and high-throughput measurements of the modulus of thin polymer films. *Review of Scientific Instruments* **2005,** *76* (6), 062207-5.

54. Jang, D. C.; Greer, J. R., Transition from a strong-yet-brittle to a stronger-and-ductile state by size reduction of metallic glasses. *Nature Materials* **2010,** *9* (3), 215-219.

55. Volkert, C. A.; Donohue, A.; Spaepen, F., Effect of sample size on deformation in amorphous metals. *Journal of Applied Physics* **2008,** *103* (8).

56. Torres, J. M., Stafford, C.M., Vogt, B.D., Impact of molecular mass on the elastic modulus of thin polystyrene films. *Polymer* **2010,** *51* (18), 4211.

57. Mundra, M. K.; Donthu, S. K.; Dravid, V. P.; Torkelson, J. M., Effect of Spatial Confinement on the Glass-Transition Temperature of Patterned Polymer Nanostructures. *Nano Letters* **2007,** *7* (3), 713-718.

58. Tsui, O. K. C.; Russell, T. P.; Hawker, C. J., Effect of Interfacial Interactions on the Glass Transition of Polymer Thin Films. *Macromolecules* **2001,** *34* (16), 5535-5539.

59. Dawson, K. J.; Kearns, K. L.; Yu, L.; Steffen, W.; Ediger, M. D., Physical vapor deposition as a route to hidden amorphous states. *Proceedings of*

the National Academy of Sciences of the United States of America **2009,** *106* (36), 15165-15170.

60. Kearns, K. L.; Still, T.; Fytas, G.; Ediger, M. D., High-Modulus Organic Glasses Prepared by Physical Vapor Deposition. *Advanced Materials* **2009,** *22* (1), 39-42.

61. Swallen, S. F.; Kearns, K. L.; Mapes, M. K.; Kim, Y. S.; McMahon, R. J.; Ediger, M. D.; Wu, T.; Yu, L.; Satija, S., Organic glasses with exceptional thermodynamic and kinetic stability. *Science* **2007,** *315* (5810), 353-356.

62. Kearns, K. L.; Still, T.; Fytas, G.; Ediger, M. D., High-Modulus Organic Glasses Prepared by Physical Vapor Deposition. *Advanced Materials* **2009,** *22* (1), 39 - 42.

63. Fakhraai, Z.; Forrest, J. A., Measuring the Surface Dynamics of Glassy Polymers. *Science* **2008,** *319* (5863), 600-604.

64. Koch, N.; Elschner, A.; Schwartz, J.; Kahn, A., Organic molecular films on gold versus conducting polymer: Influence of injection barrier height and morphology on current--voltage characteristics. *Applied Physics Letters* **2003,** *82* (14), 2281-2283.

65. Mayer, A. C.; Ruiz, R.; Headrick, R. L.; Kazimirov, A.; Malliaras, G. G., Early stages of pentacene film growth on silicon oxide. *Organic Electronics* **2004,** *5* (5), 257-263.

66. Djurisic, A. B.; Kwong, C. Y.; Guo, W. L.; Lau, T. W.; Li, E. H.; Liu, Z. T.; Kwok, H. S.; Lam, L. S. M.; Chan, W. K., Spectroscopic ellipsometry of the optical functions of tris (8-hydroxyquinoline) aluminum (Alq3). *Thin Solid Films* **2002,** *416* (1-2), 233-241.

67. Aziz, A.; Narasimhan, K. L., Optical Absorption in AlQ. *Synthetic Metals* **2000,** *114* (2), 133-137.

CHAPTER 6

PHOTOINITIATED WRINKLES FROM LIQUID COATINGS

6.1 Introduction

Surface wrinkling was first experimentally observed as a result of thermal contraction after electron beam deposition of a 50 nm gold film onto polydimethylsiloxane (PDMS).[1] In order to minimize the compressive stress induced by thermal contraction the gold/PDMS system deformed developing surface wrinkles. This instability has since been exploited as a technique that can generate complex surfaces through physical self-assembly driven by relaxation of a mechanical,[2, 3] thermal,[1] or osmotic[4, 5] compressive force. The potential to develop complex patterns with long-range order has been of interest for a variety of systems. For example, Whitesides and coworkers were able to control and orient the wrinkling morphology of the metallic films on PDMS by patterning relief structures on the PDMS.[1] Similarly, Chua and coworkers patterned a PDMS substrate prior to plasma exposure and reported complex patterns via buckling of the silica-like layer.[6] Furthermore, Whitesides and coworkers also observed the reversibility of buckling, or the appearance and disappearance of wrinkles, through repeated heating and cooling cycles.[1] Recently, two-dimensional microstructures with multiple polymer components have been reported by selectively depositing polymers into pre-wrinkled substrates.[7] By taking advantage of embossing techniques the multicomponent patterns were also transferred onto silicon wafers.[7] Similarly utilizing polyelectrolyte multilayers researchers have been able to induce patterned wrinkling by patterning the substrates with relief structures followed with embossing.[8]

Various surface wrinkling morphologies have also been obtained by controlling the applied overstress to a system. For example, work by Breid and coworkers studied the impact of overstress on the surface morphology of crosslinked PDMS.[4] A systematic increase in overstress induced by a combination of UV exposure and solvent vapor pressure revealed morphologies including dimples, bumps, and herringbones.[4] The evolution of a wide range of surface microstructures such as peanut shapes, lamellar, and wormlike, have also been reported by swelling of a hydrogel with a well controlled gradient in crosslink density developed via variations in UV exposure.[9] Surface wrinkling patterns in response to osmotic stresses including spokes and targets have also been developed by swelling of a crosslinked polystyrene film and morphology controlled via ultraviolet (UV) exposure times.[10] Yang and coworkers have reported a variety of surface patterns by simply adjusting the relative mechanical strain applied in the different planar directions.[11] By either simultaneously or sequentially applying a compressive force in both planar directions of an oxidized PDMS surface transitions from one-dimensional ripples to two-dimensional herringbone surfaces were obtained.[11] Researchers have demonstrated the ability to obtain complex wrinkle patterns by utilizing nanobubble inflation to control the applied compressive stress applied on a PDMS film combined with soft lithography to generated ordered wrinkles.[12]

Recently, these ordered surface microstructures have been studied as templates for nanoparticle assembly with implications in optical and electronic devices[13] and as stamps for micro contact printing.[14] For example, by varying UV

exposure times in an oxidized PDMS system researchers have been able to develop hierarchical wrinkling patterns.[15] These nestled wrinkles have been exploited as particle sieves resulting in monodispersed linear arrangement of particles.[15] Researchers have combined wrinkling with layer-by-layer self-assembly as a lithography free method to pattern three-dimensional colloidal assemblies with precise control over width and number of sphere layers by varying wavelength and amplitudes of the polymer film.[16] Microcontact printing of polyelectrolytes and proteins has been demonstrated utilizing wrinkled PDMS with 400 nm wavelengths and 40 nm amplitudes generated via plasma exposure.[14] The potential to develop well controlled complex surface microstructures via surface wrinkling continues to be of particular interest due to the reduced cost and ease of fabrication in comparison to common lithographic techniques.

Here we describe a simple process to generate a variety of surface morphologies including surface wrinkling, folding, and dimples at the micrometer length scale on a unpatterned surface with no need of a compliant PDMS like substrate. First a solution of furfuryl alcohol and photo acid generator (PAG) is drop cast onto a substrate. The system is then exposed to UV where surface segregation of PAG increases the polymerization rate at the free surface. This mismatch in polymerization rates generates a pseudo-bilayer system with a stiff layer at the free surface. As the bulk of the solution continues to polymerize and shrink, a net compressive force is applied to the system inducing a surface instability. Adjusting the concentration of PAG as well as the substrate temperature can act to control the surface microstructure. The regime of the

substrate instability and tunability of the characteristic properties of the morphology are examined as a function of processing conditions. Therefore we demonstrate that the characteristic wavelength of the surface wrinkling regime can also be controlled. Furthermore, pyrolysis of polyfurfuryl alcohol, a carbon precursor, has the potential to generate carbon films with controlled morphologies. This carbon film would exhibit enhanced chemical and physical properties such as high hardness and resistance to acid, alkalies, and solvents allowing the substrate to be used in a variety of different envinronments. Furthermore, if utilized as nanostructures in microelectronics the crosslinked and carbonized surface morphology will not be impacted by processing or operating conditions unlike patterned polymer films.

6.2 Experimental

Silicon wafers (450 μm thick) were cut into 1cm × 1 cm pieces and cleaned with ultraviolet-ozone (model 42, Jelight) for 40 min and used as substrates. The substrates were placed on a hot plate for 20 min prior to further use in order to equilibrate the substrate temperature. The temperature of the hot plate was varied from 65°C, 80°C, 120°C, and 150°C in order to study the effect of temperature on the polymerization of the PAG/FA and the resulting morphology. Solutions containing 0.025 wt%, 0.05 wt%, 0.1 wt%, 0.15 wt%, and 0.2 wt% of the photo acid generator, triphenylsulfonium triflate, in polyfurfuryl alcohol were prepared. 30μL of each solution were drop cast onto the silicon wafer substrates and placed on a hot plate.

Patterning of the wrinkling morphology was obtained by utilizing metal masks with linear, circular, and curvilinear patterns. The silicon substrate was heated to 150°C prior to drop casting the 0.1 wt% PAG furfuryl alcohol solution. The desired mask was placed ~1 mm above the drop cast solution followed by 254 nm UV radiation for 20 min until the surface morphology developed. Lastly the film was annealed at 120°C in order to complete the polymerization and crosslinking reactions. Carbonization of the films was performed under nitrogen in a furnace at 400°C with a 1°C/min ramp rate. The sample was maintained at 400°C for 3 hrs.

6.3 Results

6.3.1 Drop cast films

Furfuryl alcohol undergoes an acid catalyzed polycondensation reaction.[17, 18] First, the PAG in this case triphenylsulfonium triflate ($[C_6H_5)_3S^+][CF_3SO_3^-]$) absorbs UV light decomposing into triflic acid (CF_3SO_3H) as shown below.[19]

$$[C_6H_5)_3S^+][CF_3SO_3^-] + h\upsilon \rightarrow [C_6H_5)_2S^+][CF_3SO_3^-] + C_6H_5^-$$

$$[C_6H_5)_3S^+][CF_3SO_3^-] + C_6H_5^- \rightarrow (C_6H_5C_6H_4)(C_6H_5)S + CF_3SO_3H$$

This triflic acid becomes the catalyst required to initiate furfuryl alcohol polymerization. Triflic acid is a hygroscopic molecule with a pKa ~15 this is considered a super acid.[20]

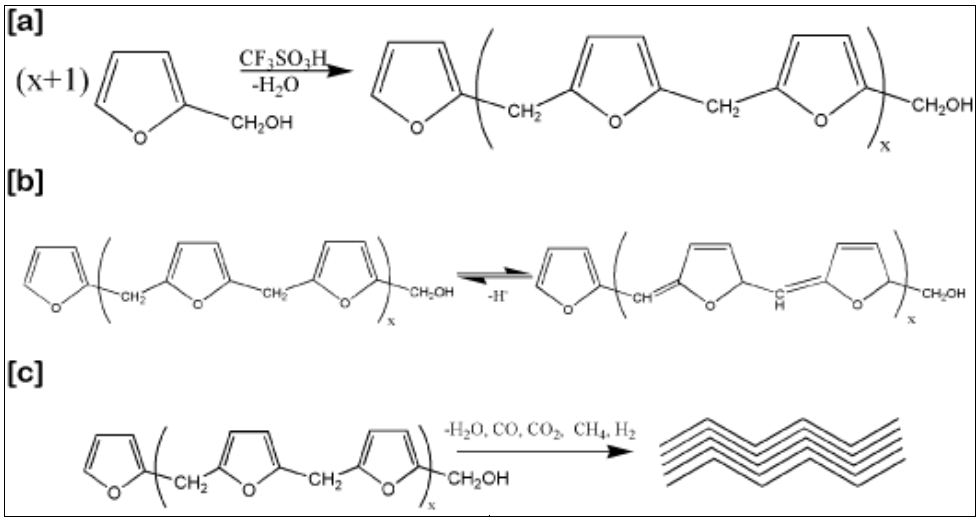

Figure 6.1 Furfuryl alcohol polymerization schematic [a] Initial growth via methylene linkages and elimination of water [b] continued crosslinking and [c] development of amorphous carbon during pyrolysis.

Next, a condensation reaction leads to methylene linkages between two furan rings and elimination of water. These linear oligomers continue their step growth followed by further crosslinking resulting in nontransparent polyfurfuryl alcohol films as illustrated in Figure 6.1b.[18] Continued treatment under an inert atmosphere at temperatures greater than 400°C then generate amorphous carbon (Figure 6.1c).[21]

However, it is well known that photo acid generators in polymer matrixes can segregate to the free surface due to a combination of both entropic and enthalpic effects.[22, 23] For example, by comparing the electron and fluorescent yield of a photoresist system a significant increase in the surface reaction rate as compared to the bulk rate has been observed and attributed to segregation of the photo acid generator to the air interface.[23] At the surface the mole fraction of PAG was 20-70 times greater than in the bulk.[23] Similarly, roughness measurements of PAG polymer films show increased surface roughness with

increasing PAG concentration and curing temperature, not only suggesting surface segregation of the PAG but a temperature dependent segregation.[22] Furthermore, the triflic acid is hygroscopic and therefore expected to rapidly segregate to the free surface. This surface segregation of the photo acid generator combined with ultraviolet (UV) exposure increases the rate of polymerization at the polymer-free surface compared to the bulk. As the system continues to polymerize, the film continues to shrink and a compressive force is developed due to the geometrically constrained film. Once the compressive force is greater than the critical stress required for wrinkling or creasing, the film undergoes deformation. This deformation is then characterized by optical micrographs as shown below in Figure 6.2.

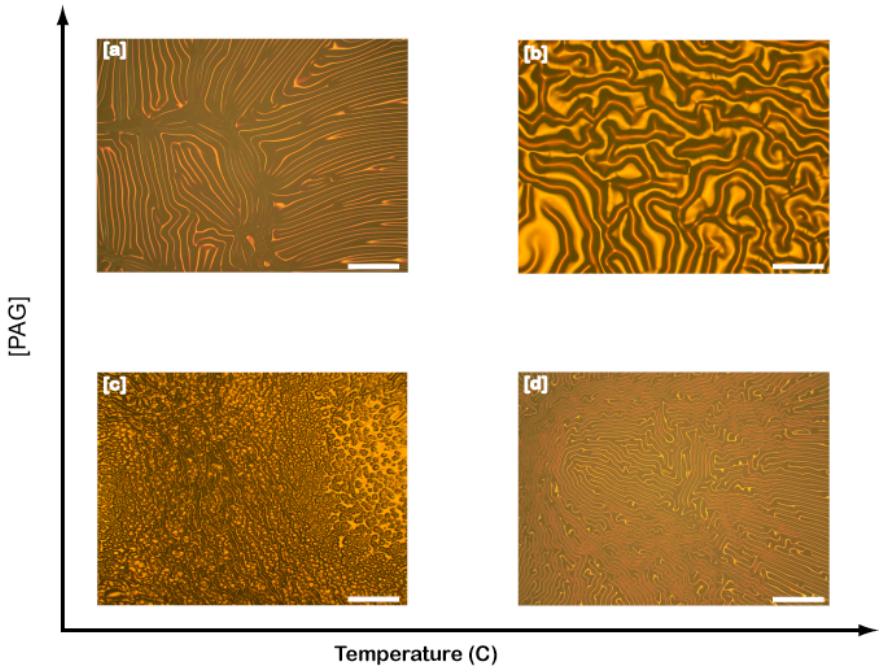

Figure 6.2 Buckling regime of polyfurfuryl alcohol films as a function of PAG concentration and substrate temperature. [a] 0.25 wt% and 65°C, [b] [a] 0.25 wt% and 120°C [c] 0.01 wt% and 65°C, and [d] 0.15 wt% and 120°C. The scale bars are 1000μm.

Figure 6.2, shows the different buckling regimes observed as a function of PAG concentration and substrate temperature. At low PAG concentrations, 0.01 wt%, and low substrate temperatures ≈65°C, a dimple regime is observed. Dimples have been previously reported at a low overstress for UV treated PDMS.[4] Dimple patterns are single points with local maxima and minima. However, as the PAG concentration is increased to 0.25 wt%, a wrinkling morphology is observed with characteristic wrinkle wavelength of 107.26 ± 5.55μm. On the other hand, at high temperatures ≈120°C this high PAG concentration film exhibits significant creasing. Creasing occurs as large strain induces a buckling instability that leads to the film collapsing or folding. While at these high temperatures and lower PAG concentration, 0.15 wt%, smaller wavelength wrinkles, 86.23± 3.12 μm, are observed. This suggests that the morphology of the film is dependent upon the overall compressive stress applied to the system in agreement with previous work on the morphologies of wrinkled hydrogels and oxidized PDMS surfaces.[4, 9] A system under low compressive stress or at low PAG concentrations and temperatures exhibits dimples. An increase in compressive stress can be induced by increasing the rate of PAG segregation to the free surface via substrate temperature or by increasing PAG concentration. Increased PAG at the free surface leads to an increase in the ratio of the polymerization at the free surface to the bulk. By increasing the stress with either an increase in PAG concentration or substrate temperature the critical stress for wrinkling is surpassed and wrinkles are observed. Further increasing the compressive stress by both increasing the PAG concentration and substrate

temperature leads to creasing of the film. This is in agreement with recently published work on the morphologies of crosslinked PDMS, where by systematically increasing the overstress researchers obtained dimples, wrinkles, and creases on the surface.[4] Furthermore, the critical strain for creasing has been suggested to be ~0.35%,[24] significantly greater than the critical stress for wrinkling, ~0.01%,[25] suggesting increased compressive stress is obtained by simultaneously increasing substrate temperature and PAG concentration.

In order to better characterize the surface morphologies as a function of PAG concentration and substrate temperature, previously described wrinkling mechanics can be considered. In previous chapters, the equilibrium wavelength (λ) of a stiff film on a compliant substrate is controlled by the film thickness (h) and the ratio of the modulus of the film (E_f) to the modulus of the substrate (E_s) as shown in Equation 1.[2]

$$\lambda = 2\pi h\left(\frac{E_f}{3E_s}\right)^{1/3} \quad (1)$$

Therefore it is possible to understand the surface morphology of the polyfurfuryl alcohol film as a function of PAG at the surface which impacts the film thickness and the rate of polymerization which controls the ratio E_f / E_s.

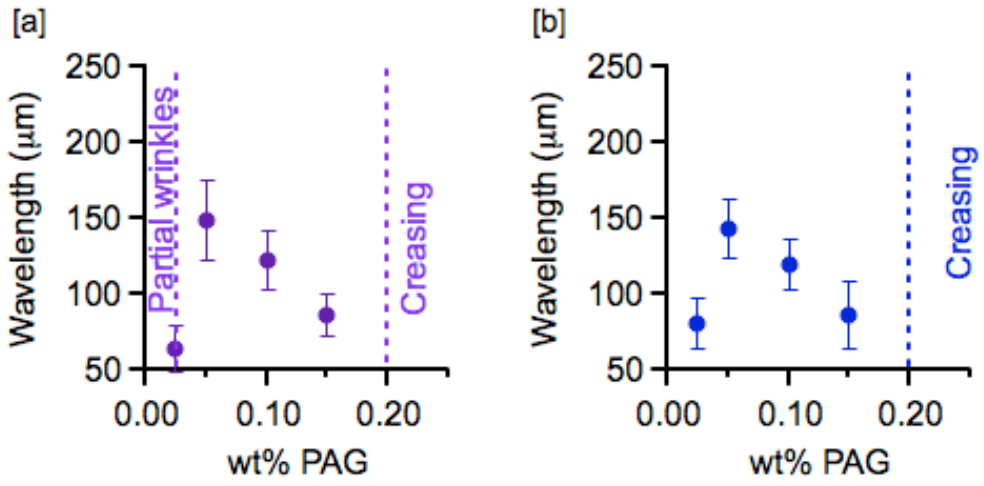

Figure 6.3 Wavelength as a function of PAG concentration for substrates at [a] 80°C and [b] 150°C. The error bars represent one standard deviation of the measurement, which is taken as the experimental uncertainty.

Figure 6.3, shows the wavelength as a function of PAG concentration for films cast onto substrates at 80°C and 150°C. Interestingly the characteristic wavelength as a function of PAG concentration follows similar behavior for both temperatures studied, 80°C and 150°C. This can be attributed to the fact that the wrinkle wavelength is determined by the intrinsic properties of the film and suggests that the critical parameter is PAG concentration. However, as shown in Figure 6.3 at low temperatures and minimal PAG concentration no wrinkling is observed. It is expected that at low temperature the viscosity of the furfuryl alcohol limits diffusion of PAG to the surface and becomes the rate limiting step in the polymerization process and therefore the critical stress required for buckling is not reached.[18] At higher temperatures, 150°C, (Figure 6.3b) the viscosity of the furfuryl acohol film is reduced and diffusion of PAG to the surface leads to an increase in polymerization rate at the surface generating the

compressive force required for wrinkling.[18] As shown in Figure 6.3, increasing the PAG concentration from 0.025 wt% to 0.05 wt% doubles the wrinkling wavelength from 71.97 ± 11.35 μm to 145.94 ± 3.64 μm. This is similar with previous work on polyhydroxylethylmethacrylate (PHEMA), where increasing crosslinker concentration increases the modulus of the PHEMA film. [26] It is expected that increased PAG at the surface will increase the rate of polymerization and therefore crosslinking at the surface. However, as the PAG concentration increases to 0.1 wt% and 0.15 wt% the wavelength decreases to 120.85 ± 3.63μm and 86.13 ± 3.90 μm respectively. This is could be attributed to the fact that as PAG gets to the surface and the polymerization reaction begins to crosslink leading to an increase in film viscosity. This increase in film viscosity limits diffusion of the remaining PAG. Due to this diffusion limitations the ratio of the modulus of the free surface layer to the substrate modulus decreases as more PAG remains in the bulk and therefore systematically decreasing the characteristic wavelength. These results suggest that the optimal crosslink density, highest E_f / E_s ratio, and therefore larger wavelength is found at 0.05 wt%.

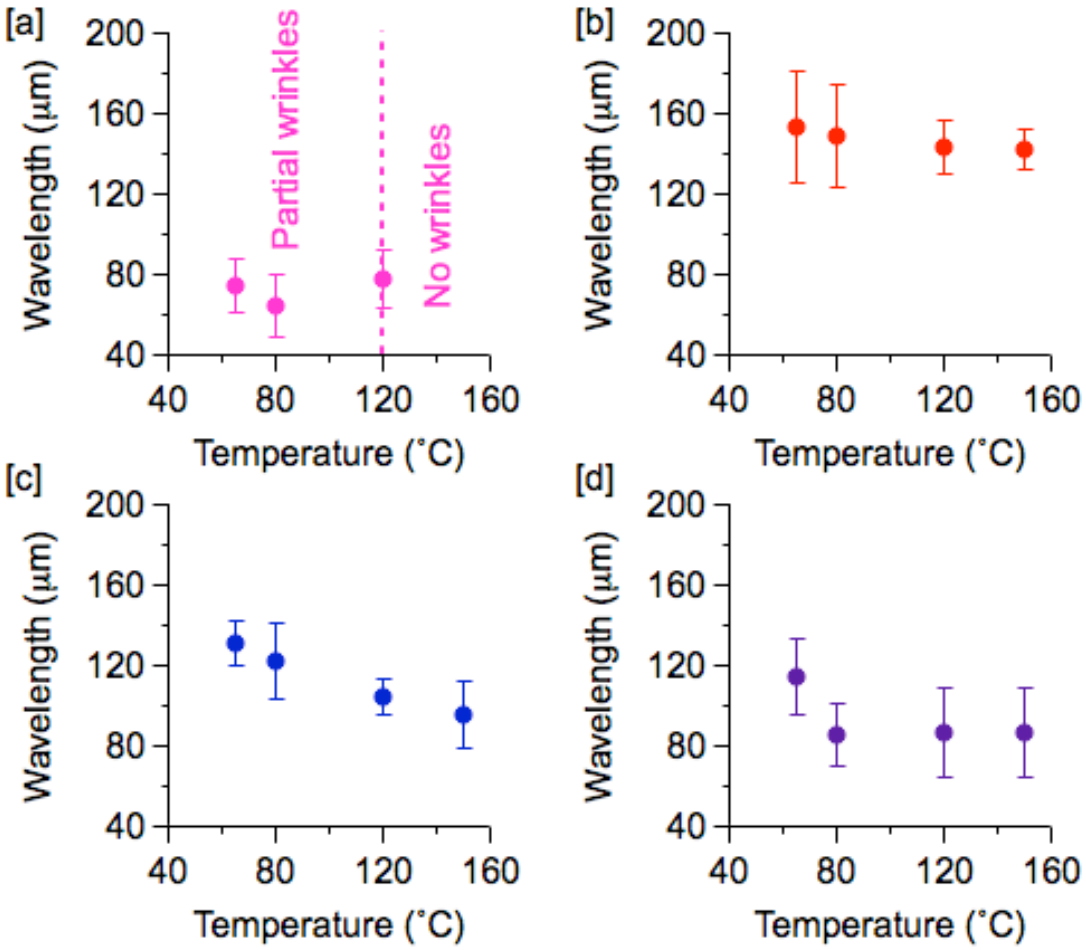

Figure 6.4 Wavelength as a function of substrate temperature with PAG concentration of [a] 0.025 wt% [b] 0.05 wt%, [c] 0.1 wt% and [d] 0.15 wt%. The error bars represent one standard deviation of the data, which is taken as the experimental uncertainty of the measurement.

The wavelength of the surface morphology as a function of substrate temperature for all PAG concentrations studied is shown in Figure 6.4. As shown in Figure 6.4a, at low PAG concentrations partial or no wrinkles are observed over the temperature range studied. This could be attributed to a lack of PAG required to generate a stiff surface layer and therefore the critical stress required for out of plane deformation is not reached. Furthermore, at the higher PAG concentrations studied a slight decrease in average wavelength with increasing

substrate temperature is observed. This decrease in wavelength with an increase in temperature is more pronounced at intermediate concentrations as shown in Figure 6.4c and Figure 6.5. This slight decrease in wavelength with increasing substrate temperature could be attributed to an increase in polymerization rate limiting the amount of PAG segregating to the free surface and therefore the film thickness, which is directly proportional to the wavelength as shown in Equation 1.

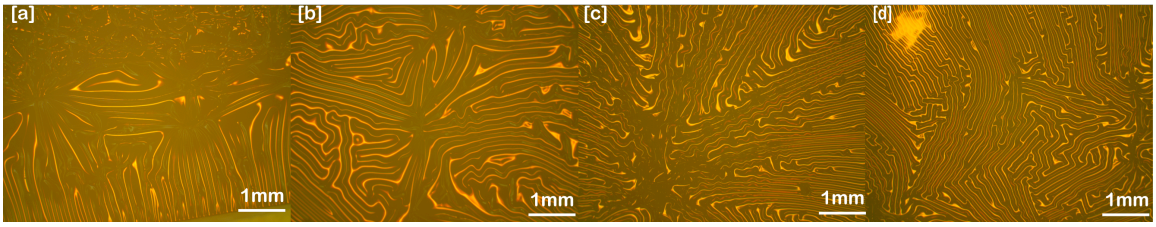

Figure 6.5 Optical micrographs for 0.1 wt% PAG in FA polymerized at [a] 65°C [b] 80°C [c] 120°C and [d] 150°C.

6.3.2 Patterning

One common feature of all the samples in the previous section is disordered surface wrinkles in the center of the film. However near the edges, an ordering of wrinkles is observed. This ordering of wrinkles near the edge is in agreement with previous work where lateral stress relaxation in stretchable gold conductors leads to the development of parallel waves.[27] Therefore, long-range order of the wrinkled film is obtained by exploiting edge effects via templates. In this process the desired template was placed over the drop cast film followed by UV radiation. The irradiated regions undergo photopolymerization resulting in an ordered wrinkled pattern commensurate with the chosen mask.

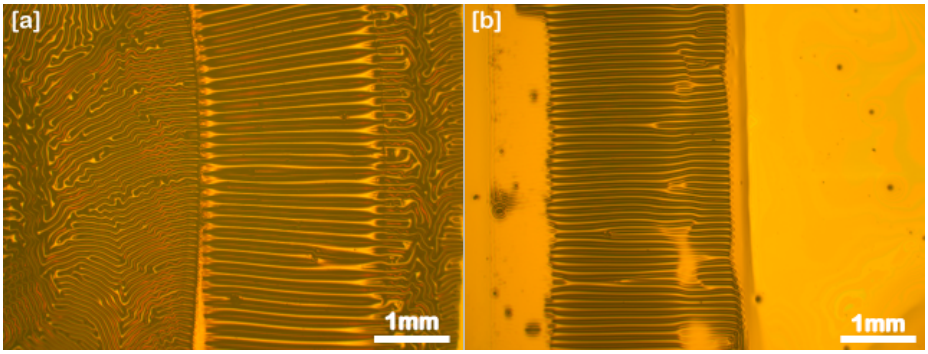

Figure 6.6 Optical micrographs for [a] partial at 120°C and [b] complete polymerization at 150°C with selective UV exposure.

Figure 6.6 illustrates patterning of polyfurfuryl alcohol substrates with 2.5 mm wide linear patterns. In the case where both a combination of selective UV exposure and overall film exposure were utilized, the film patterned by the mask exhibits aligned wrinkles while the unpatterned areas show disordered wrinkles (Figure 6.6a). However if selective UV exposure was allowed until the film was completely crosslinked no wrinkles were observed in the unexposed region and ordered wrinkles were observed as patterned by the mask (Figure 6.6b). It is also important to note that the wavelength for Figure 6.6a is 91.1 μm while Figure 6.6b is only 57.5 μm, this is in agreement with section 6.3.1 where an increase in substrate temperature reduced the wrinkle wavelength due to an increase in the rate of polymerization.

As shown in Figure 6.7, curvilinear wrinkles were also generated, where the wrinkles pinned at the edges of the exposed region developed in a matching curvilinear pattern. These curvilinear wrinkles suggest the possibility of generating a series of complex poly furfuryl alcohol patterns commensurate with the chosen mask.

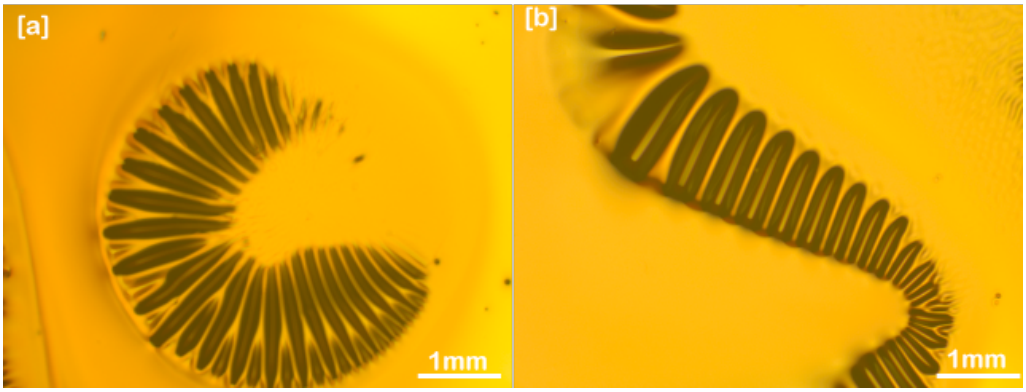

Figure 6.7 Curvilinear patterns generated with 0.1 wt% at 150 °C.

Not only were a linear mask utilized but 3.5 mm diameter circular patterns were also studied as shown in Figure 6.8. As shown in Figure 6.8 by systematically increasing the PAG concentration generation of shell-like to flower-like patterns. In the shell-like patterns wrinkling was observed throughout the UV exposed area. However, with decreasing PAG concentration flower-like patterns emerged were wrinkles are observed at the exterior edges and dimples at the interior of the film. It is important to note that it was not possible to generate ordered patterns at higher PAG concentrations or lower temperatures. Utilizing circular patterns at these extremes resulted in creasing and random wrinkling within the UV exposed region.

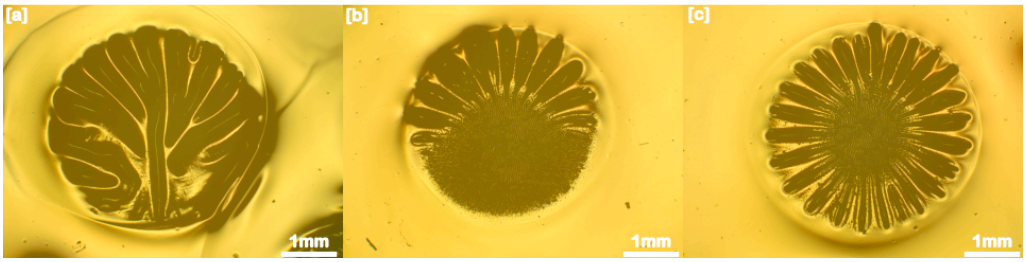

Figure 6.8 Optical micrographs for circular patterned films with varying PAG concentration [a] 0.15 wt% [b] 0.1 wt% and [c] 0.05 wt% with a substrate temperature of at 150 °C.

6.4 Conclusions

In summary, polyfurfuryl alcohol wrinkles were generated by UV exposure of a drop cast PAG and furfuryl alcohol solution. A combination of surface segregation of PAG and continued polymerization generated the required compressive force to generate surface wrinkles. To control the wavelength of the surface wrinkles the substrate temperature and the PAG concentration were tuned. Furthermore it was possible to generate ordered surface wrinkles by utilizing a mask which allowed for selective UV exposure of the drop cast material. Linear, shell-like, flower-like, and curvilinear patterns were successfully generated.

6.5 References

1. Bowden, N.; Brittain, S.; Evans, A. G.; Hutchinson, J. W.; Whitesides, G. M., Spontaneous formation of ordered structures in thin films of metals supported on an elastomeric polymer. *Nature* **1998,** *393* (6681), 146-149.

2. Stafford, C. M.; Guo, S.; Harrison, C.; Chiang, M. Y. M., Combinatorial and high-throughput measurements of the modulus of thin polymer films. *Review of Scientific Instruments* **2005,** *76* (6).

3. Yang, S.; Khare, K.; Lin, P.-C., Harnessing Surface Wrinkle Patterns in Soft Matter. *Advanced Functional Materials* **2010,** *20* (16), 2550-2564.

4. Breid, D.; Crosby, A. J., Effect of stress state on wrinkle morphology. *Soft Matter* **2011,** *7* (9), 4490-4496.

5. Chan, E. P.; Smith, E. J.; Hayward, R. C.; Crosby, A. J., Surface Wrinkles for Smart Adhesion. *Advanced Materials* **2008,** *20* (4), 711-716.

6. Chua, D. B. H.; Ng, H. T.; Li, S. F. Y., Spontaneous formation of complex and ordered structures on oxygen-plasma-treated elastomeric polydimethylsiloxane. *Applied Physics Letters* **2000,** *76* (6), 721-723.

7. Hyun, D. C.; Moon, G. D.; Park, C. J.; Kim, B. S.; Xia, Y.; Jeong, U., Buckling-Assisted Patterning of Multiple Polymers. *Advanced Materials* **2010,** *22* (24), 2642-2646.

8. Lu, C.; Mohwald, H.; Fery, A., Large-Scale Regioselective Formation of Well-Defined Stable Wrinkles of Multilayered Films via Embossing. *Chemistry of Materials* **2008,** *20* (22), 7052-7059.

9. Guvendiren, M.; Yang, S.; Burdick, J. A., Swelling-Induced Surface Patterns in Hydrogels with Gradient Crosslinking Density. *Advanced Functional Materials* **2009,** *19* (19), 3038-3045.

10. Chung, J. Y.; Nolte, A. J.; Stafford, C. M., Diffusion-Controlled, Self-Organized Growth of Symmetric Wrinkling Patterns. *Advanced Materials* **2009,** *21* (13), 1358-1362.

11. Lin, P.-C.; Yang, S., Spontaneous formation of one-dimensional ripples in transit to highly ordered two-dimensional herringbone structures through sequential and unequal biaxial mechanical stretching. *Applied Physics Letters* **2007,** *90* (24), 241903-3.

12. Zhang, P.; Yang, D.; Li, Z.; Ma, H., Controlled wrinkle formation via bubble inflation strain engineering. *Soft Matter* **2010,** *6* (18), 4580-4584.

13. Schweikart, A.; Fortini, A.; Wittemann, A.; Schmidt, M.; Fery, A., Nanoparticle assembly by confinement in wrinkles: experiment and simulations. *Soft Matter* **2010,** *6* (23), 5860-5863.

14. Pretzl, M.; Schweikart, A.; Hanske, C.; Chiche, A.; Zettl, U.; Horn, A.; Boàker, A.; Fery, A., A Lithography-Free Pathway for Chemical Microstructuring of Macromolecules from Aqueous Solution Based on Wrinkling. *Langmuir* **2008,** *24* (22), 12748-12753.

15. Efimenko, K.; Rackaitis, M.; Manias, E.; Vaziri, A.; Mahadevan, L.; Genzer, J., Nested self-similar wrinkling patterns in skins. *Nat Mater* **2005,** *4* (4), 293-297.

16. Lu, C.; Mohwald, H.; Fery, A., A lithography-free method for directed colloidal crystal assembly based on wrinkling. *Soft Matter* **2007,** *3* (12), 1530-1536.

17. Choura, M.; Belgacem, N. M.; Gandini, A., Acid-Catalyzed Polycondensation of Furfuryl Alcohol: Mechanisms of Chromophore Formation and Cross-Linking. *Macromolecules* **1996,** *29* (11), 3839-3850.

18. Guigo, N.; Mija, A.; Vincent, L.; Sbirrazzuoli, N., Chemorheological analysis and model-free kinetics of acid catalysed furfuryl alcohol polymerization. *Physical Chemistry Chemical Physics* **2007,** *9* (39), 5359-5366.

19. Potje-Kamloth, K.; Polk, B. J.; Josowicz, M.; Janata, J. ô., Doping of Polyaniline in the Solid State with Photogenerated Triflic Acid. *Chemistry of Materials* **2002,** *14* (6), 2782-2787.

20. Luckenbach, R., *Beilstein handbook of organic chemistry: fifth supplementary series, covering the literature from 1960 through 1979*. Springer: 1990.

21. Li, G.; Lu, Z.; Huang, B.; Wang, Z.; Huang, H.; Xue, R.; Chen, L., Raman scattering investigation of carbons obtained by heat treatment of a polyfurfuryl alcohol. *Solid State Ionics* **1996,** *89* (3-4), 327-331.

22. Fedynyshyn, T. H.; Sinta, R. F.; Astolfi, D. K.; Goodman, R. B.; Cabral, A.; Roberts, J.; Meagley, R., Resist deconstruction as a probe for innate material roughness. *Journal of Microlithography, Microfabrication, and Microsystems* **2006,** *5* (4), 043010-12.

23. Lenhart, J. L.; Jones, R. L.; Lin, E. K.; Soles, C. L.; Wu, W.-l.; Fischer, D. A.; Sambasivan, S.; Goldfarb, D. L.; Angelopoulos, M. In *Probing surface and bulk chemistry in resist films using near edge x-ray absorption fine structure*, Papers from the 46th International Conference on Electron, Ion, and Photon Beam Technology and Nanofabrication, Anaheim, California (USA), AVS: Anaheim, California (USA), 2002; pp 2920-2926.

24. Hong, W.; Zhao, X.; Suo, Z., Formation of creases on the surfaces of elastomers and gels. *Applied Physics Letters* **2009,** *95* (11), 111901-3.

25. Huang, Z. Y.; Hong, W.; Suo, Z., Nonlinear analyses of wrinkles in a film bonded to a compliant substrate. *Journal of the Mechanics and Physics of Solids* **2005,** *53* (9), 2101-2118.

26. Wilder, E. A.; Guo, S.; Lin-Gibson, S.; Fasolka, M. J.; Stafford, C. M., Measuring the Modulus of Soft Polymer Networks via a Buckling-Based Metrology. *Macromolecules* **2006,** *39* (12), 4138-4143.

27. Lacour, S. P.; Wagner, S.; Huang, Z.; Suo, Z., Stretchable gold conductors on elastomeric substrates. *Applied Physics Letters* **2003,** *82* (15), 2404-2406.

CHAPTER 7

FUTURE WORK

An initial study on the modulus of amorphous organic glasses has been performed in this work. Other factors including processing conditions, film growth, aging effects, and understanding the behavior of nanocomposite films still remain an unstudied part of this research work and a challenge in the development of next generation technologies.

For the successful implementation of polymeric thin films in end use applications, the effects of aging need to be addressed. Aging or structural relaxation is the drift of properties of a glassy polymer towards equilibrium. During aging, a loss of free volume is observed where thin films undergo densification, which significantly alters mechanical, thermal, optical and transport properties of polymers. Aging in the bulk has been observed via changes in properties as function of storage time, both macrostructural properties such as specific volume, enthalpy, mechanical, and dielectric response and microstructural such as free volume and mobility (Hutchinson, 1995). While in thin films, a reduction in the rate of permeability has been observed with aging, the aging rate was also found to increase at higher temperatures and for thinner films (Huang *et al*, 2005). A change in aging rate has also been observed in ultrathin polystyrene (PS) films attributed to the reduced T_g of the confined film (Priestley, Broadbelt *et al.*, 2005). More in depth fluorescence studies show a distribution in structural relaxation rates of poly (methyl methacrylate) (PMMA) due to free surface and substrate effects which were found to extend over 100 nm

into the film (Priestley, Ellison *et al.*, 2005). This distance is significantly greater than the layer of increased mobility, ~4 nm, previously reported (Stafford, Vogt *et al.*, 2006). As shown in Chapters 2 and 3, a layer of enhanced mobility of 4-20 nm at the free surface impacts the overall modulus significantly at sub 100 nm. Therefore it is expected that the enhanced relaxation at the interfaces resulting in polymer densification will significantly alter the modulus at the nanometer length scale. If indeed enhanced relaxation and therefore densification of the interfaces is observed, an increase in sub 40 nm to bulk-like modulus is expected as the free surface effect is eliminated. It is possible to study the effect of aging on the modulus of ultra thin films by isothermally aging the spin cast polymer films. Prior to isothermally aging the polymer the thermal history of the polymer is eliminated by careful annealing at temperatures above their bulk T_g. The modulus of the aged films as a function of time can easily be determined via surface wrinkling and characterization.

Next, the addition nanoparticles into polymeric thin films would continue to elucidate interface and confinement effects on the modulus of ultrathin nanocomposite films. The addition of nanoparticles inhibits polymer mobility and increases interface effects due to their high surface areas. Studies by Torkelson and coworkers have reported modification of confinement effects via T_g enhancements relative to the bulk for PMMA-silica nanopoarticle films due to attractive interactions between the polymers and nanoparticles (Rittigstein *et al.*, 2006). The focus here is the addition of C_{60} nanoparticles due to their significance for both the organic electronics and photovoltaics applications (Hiroyoshi *et al.*,

2006; Akihiko *et a.l*, 2007). Efforts to understand the behavior of C_{60} in aromatic solvents has shown that these fullerenes form nanometer length scale aggregates (Rudalevige, Francis *et al.*, 1998). Using static and dynamic light scattering Ying and coworkers have shown significant aggregation of C_{60} nanoparticles in benzene (Ying, Marecek *et al.*, 1994). Via static and dynamic Rayleigh scattering aggregation of C_{60} in solvent has been reported in single-solvent toluene solutions as well as binary solvent mixtures, where binary solvent mixtures exhibit enhanced aggregation kinetics (Rudalevige, Francis *et al.*, 1998). This nanoparticle aggregation has been observed in solution as well as polymer thin films. For example, the addition of C_{60} fullerenes has eliminated the dewetting tendency of ultrathin unentangled PS thin films by modifying the polymer-substrate interaction (Barnes, Karim *et al.*, 2000). Neutron reflectivity measurements of these PS-C_{60} show a diffuse layer of C_{60} particles at the polymer-substrate interface of spin cast films once the nanoparticle loading reaches 1wt% (Barnes, Karim *et al.*, 2000). The nanoparticle cluster dimensions are on the order of 10 nm for a 3wt% C_{60} in PS while at 4wt% 1-2 μm clusters are observed (Han, Lee *et al.*, 2009). Similarly, neutron reflectivity measurements for spinodal clustering studies revealed annealed low molecular weight films (<10 kg/mol) maintained a stable diffuse C_{60} layer at the polymer-substrate interface while similar high molecular weight films (>270 kg/mol) films exhibit clustering at the same interface (Wong e Cabral, 2010). Studies on the T_g of C_{60}-PS films have shown a systematic increase in the T_g of the C_{60}-PS film as the C_{60} concentration increases from 1wt% to 4wt%, while at higher loadings the film

exhibits bulk T_g (Balberg, Naidis *et al.*, 2001). Recent inelastic incoherent neutron scattering studies have reported reduced mobility of PMMA-C_{60} films, suggesting strong interactions between the PMMA and the C_{60} particles (Kropka, Putz *et al.*, 2007). While similar studies on PS-C_{60} films show enhanced polymer dynamics with the addition of C_{60} similar to the addition of small molecule diluents or plasticization (Sanz, Ruppel *et al.*, 2008). Although there is a lack of literature on the modulus of ultrathin films with respect to C_{60} loading, the properties of PS and other nanoparticles in bulk have been studied. In order to uniformly disperse the nanoparticles into the polymer matrix surface modifications of the particles with compatible ligands have been studied (Ahmed, Jones, *et al.,* 1990). Studying a system of PS ligand modified cadnium selenide nanoparticles in PS, Lee and coworkers have shown an exponential decrease in the bulk modulus as nanoparticle loading increased from 0 to 12wt% while a minimal impact on T_g was reported (Lee, Su *et al.*, 2007). By decoupling the ligand and nanoparticle effect, Lee and coworkers concluded the effect of nanoparticles on modulus is determined by the enthalpic and entropic interaction between particle and polymer matrix. Where low enthalpic interactions between the polymer and nanoparticles leads to reductions in polymer density near the nanoparticle and hence reductions in T_g and modulus. While Ji and coworkers also determined the size of the nanoparticle in a attractive polymer-nanoparticle system influences the bulk modulus, where due to an increase in interfacial regions small particles lead to an increase in bulk modulus (Ji, Jing *et al.*, 2002). It is expected that due to the higher modulus of C_{60}, a higher overall bulk modulus would be observed. While

at the sub 40 nm length scales the polymer chain-C_{60} interactions will become dominant and influence the overall modulus. Where an increase in C_{60} aggregation decreases the available C_{60}-PS interface and will enable us to understand the influence of these interactions in detail.

It is proposed to therefore study the impact of C_{60} and C_{60} aggregation on the modulus of ultrathin films. Determining the aggregation of C_{60} in solution can be carried out using dynamic light scattering by monitoring the change in scattering intensity of the solution with time. While the aggregation of C_{60} clusters at the polymer-free surface and polymer-substrate interface can be studied using atomic force microscopy (AFM). AFM images of spin cast films will be monitored for polymer-free surface aggregation and once transferred onto the PDMS the polymer-silicon substrate interface can be studied. Since previous observations suggest that polymer-particle interactions of PS and PMMA lead to significantly different dynamics (Lee, Su *et al.*, 2007), a study on both PS and PMMA with similar molecular weight would lead to a better understanding of nanoparticle-polymer interactions. In order to determine the effect of annealing on these systems, thermal wrinkling above PS T_g in vacuum can also be examined as previous work has shown annealing segregates the nanoparticles to the polymer-substrate interface (Barnes, Karim *et al.*, 2000). Furthermore, the addition of meso fillers and its impact on the modulus of ultrathin films could also be of interest as these particles are larger than the polymer chains. As well as the addition of particles to polymer blends or block copolymers where the nanoparticle fillers would preferentially wet one of the components and

significantly alter material properties (Balazs, Emrick *et al.*, 2006). The effect of not only spherical but rod like, plate like, and nanosheet particles such as nanotubes and clays can also be explored. It is expected that since nanoparticles preferentially wet one component in either the polymer blends or block copolymers, two distinct moduli and T_g will be observed. Where an increase in modulus could be possible in the wetted phase due to the higher modulus of the nanoparticle and an unchanged modulus for the plain phase.

With the development of flexible organic technologies the electronic and mechanical properties of organic electronic materials are of interest. A recent report shows that the moduli of conjugated polymers can be well correlated with their electronic properties like mobility (O'Connor, Chan *et al.*). Furthermore, they have found that annealing of polymeric semiconductor films results in a two-fold increase in modulus and a four-fold increase in hole mobility. These results are consistent with the expectations that the improved crystallinity during annealing would lead to a more densely packed and higher density film; both electrical and mechanical properties of materials are strongly correlated with physical density (Al-Douri, Abid *et al.*, 2001). Work performed in Chapter 5 suggested a modulus dependent on deposition conditions. More specifically in agreement with work by Ediger and coworkers where an increase in film density and resulting modulus was observed for indomethacin and trisnaphthylbenzene films deposited at temperatures greater than 85% of the materials bulk glass transition temperature (T_g) (Kearns, Swallen *et al.*, 2007).

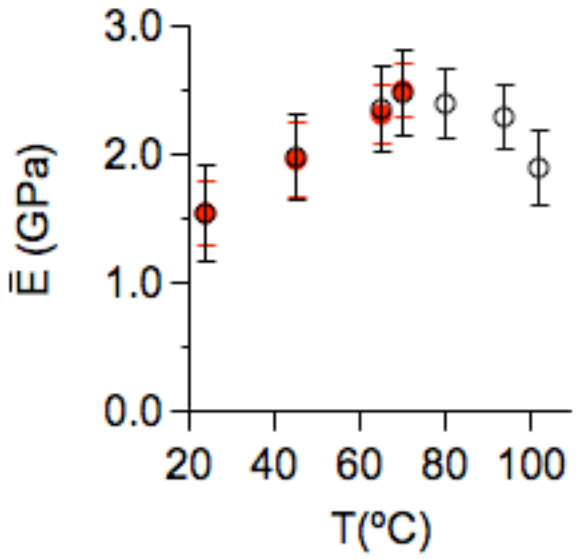

Figure 7.1 Modulus as a function of substrate temperature for NPD. Measurements on a polystyrene barrier film (closed, red) and on an addition polynorbornene barrier film (open, black). The error bars represent one standard deviation of the data, which is taken as the experimental uncertainty of the measurement.

Therefore an initial study on the modulus of N,N'-Di-[(1-Naphthyl)-(N,N'-diphenyl]-1,1'-biphenyl)-4-4'-diamine (NPD) with substrate temperatures ranging from 24°C to 100°C was recently examined. The modulus as a function of film thickness is shown in Figure 7.1 above. As reported in Chapter 5, the bulk modulus for NPD vacuum deposited at room temperature (24 ± 1ºC) exhibits a bulk modulus of 1.54± 0.24 GPa. As the substrate temperature is slowly increased the bulk modulus increases to 1.96± 0.29 GPa, 2.31± 0.23 GPa, and, 2.50 ± 0.20 GPa at 45ºC, 65ºC, and 70ºC respectively. As the substrate temperature increases to 80ºC and 94ºC the bulk modulus remains at 2.40 ± 0.27 GPa and 2.30 ± 0.20 GPa however at temperatures above T_g the modulus decreases to 1.89 ± 0.28 GPa at 102ºC. Here the highest modulus obtained was at approximately 0.91 and 0.93T_g, in agreement with Edgier's work where the

increased packing efficiency is expected at T>0.85Tg. Atomic force microscopy was utilized to characterize the surface of the NPD films at all temperatures and atomic scale resolution was obtained for all samples suggesting minimal crystallization. However, in order to properly characterize the crystallization of the NPD films, differential scanning calorimetry (DSC) measurements can be performed. DSC measurements can be utilized to extract the thermodynamic and kinetic stability of the deposited films, that is both a fictive temperature and an onset temperature can be calculated. The onset temperature represents the kinetic stability of the film, as it marks the temperature at which heat absorbed by the sample induces mobility. While the fictive temperature represents the thermodynamic stability of the film as it represents the intersection of the liquid enthalpy and the vacuum deposited enthalpy. DSC also allows for the determination of percent crystalline by comparison of the heat absorbed at the materials melting temperature while carefully remaining below the materials crystallization temperature as to not induce crystallization. Crystallization of the NPD films can also be monitored via Raman spectroscopy. NPD films have shown slight shifts and width changes in the Raman spectra with crystallization (Sugiyama, Furukawa *et al.*, 2005). For example, at 532 nm NPD exhibits in three characteristic bands at 1609cm^{-1} (ring stretch), 1288 cm^{-1} (C-C stretch), and 1198 cm^{-1} (C-H bond) a red shift in wavenumber and a decrease in bandwidth has been reported with polycrystallization (Sugiyama, Furukawa *et al.*, 2005). Crystallization of NPD could be expected as it has previously been reported

during device operation and high temperature treatments (Sugiyama, Furukawa *et al.*, 2005; Kim, Kim *et al.*, 2006).

Furthermore, if as suggested in Chapter 5 deposition of NPD at $T>85\%T_g$ leads to an increase in packing density and therefore an increase in modulus, the overall density of the film would be of interest. Quartz Crystal Microbalance (QCM) allows for a quantitative technique to determine the density of the film. QCM determines the water uptake of the NPD film which is expected to decrease as the film density increases. The amount of water uptake as a function of NPD film conditions can be obtained by measuring the changes in resonant frequency of the crystal and the Sauerbrey equation as shown below (Sauerbrey, 1959).

$$\Delta f = -C_f \Delta m$$

Where, Δf is the observed frequency change in Hz, C_f is the sensitivity factor in $Hz/ng/cm^2$, and Δm is the change in mass per unit area in ng/cm^2.

QCM can therefore potentially discern density changes while revealing pertinent information for future device stability as moisture uptake is detrimental to organic electronics. Finally, the performance of a single carrier hole-only OLED device with an anode/NPD/cathode structure where different NPD deposition conditions are utilized can be characterized. It is then possible to extract carrier mobility of the various NPD films utilizing the space charge limited current region of the current-voltage curve. A more detailed understanding of the impact of high temperature NPD deposition can also be obtained by characterizing fully developed OLED devices. This series of

experiments would allow for the development of any potential correlations between bulk modulus, carrier mobility, density, and device stability.

Furthermore, although correlations between polymeric semiconductors and elastic modulus have been reported, no information on carrier mobility of the wrinkled surface has been reported. Understanding the electronic properties of wrinkled materials is of interest in flexible organic electronics as flexible electronics are subjected to high strains during operation. Recent work has shown that compressive strain on pentacene thin-film transistors results in increased mobility due to decreased energy barrier between grain boundaries with compression of the system (Chen, Chen *et al.*, 2011). Research has shown a significant increase in the conductivity of organic semiconducting polymers with increased pressure explained in terms of reduction in energy barriers due to compressible intermolecular distances or an increase in the π-π overlap (Pohl, Rembaum *et al.*, 1962). The conductivity of organic molecules is attributed to their conjugated structure and delocalized π electrons. It is therefore expected that the pressure applied in the valleys of a wrinkled film will impact carrier mobility, which will be a function of compressive strain due to variations in π-π overlap. A study on the mobility of these wrinkling films as a function of pressure (wrinkling wavelength) could therefore be of interest for the development of flexible electronics.

Lastly, a large amount of work is still to be studied with the recent development of poly furfuryl alcohol wrinkles in Chapter 6. Under inert

conditions polyfurfuryl alcohol begins to carbonize at 450°C (Li, Lu *et al.*, 1996). Therefore the potential to develop carbon substrates with controlled morphologies could be achieved by simple pyrolysis of current polyfurfuryl alcohol films. However, in order to mitigate stress within the film, a heat treatment process would need to be developed with proper annealing, pyrolysis recipes, and if needed an intermediate elastic layer such as polydimethylsiloxane (PDMS) film.

The ability to carbonize poly furfuryl alcohol films allows for the use of these substrates in a wide range of systems from micro-mechanical devices to sensors and biologically related fields. Both work on biological systems and as substrates for the development of sensors is achievable. For example, past research has shown that cells tend to elongate and align in the presence of patterned grooves (Singhvi, Stephanopoulos *et al.*, 1994; Teixeira, Abrams *et al.*, 2003). Jiang and coworkers have shown that chemically modified wrinkled PDMS surfaces are also successful in inducing contact guidance of bovine capillary endothelial cells (Jiang, Takayama *et al.*, 2002). Likewise, Wilkinson and coworkers have shown increased alignment and elongation of cells when exposed to carbon surfaces with micrometer etched grooves (Wilkinson, Riehle *et al.*, 2002). Therefore, these wrinkled carbon surfaces could become a tool or model in understanding cell-substrate interactions important for the development of medical implants and cell cultures. Future work could include a study on cell elongation and behavior on these substrates with systematically varying wrinkling wavelength, amplitude, and topography controlled via photo acid generator concentration and substrate temperature.

Due to the inert nature of carbon materials these wrinkled surfaces could also be coated with metals via electrochemistry or sputtering. Previous research has successfully shown uniform deposition of Au replicating a master pattern via electrochemical deposition (Lee, Alexe *et al.*, 2005). These coated surfaces with controlled surface topology could then have applications in sensors. Furthermore, surface energy can also be controlled, surface wettability is traditionally controlled via surface chemistry and surface roughness (Encinas, 2010). However, recent work on wrinkling has shown a relationship between surface energy and wrinkle wavelength and amplitude (Chung, Youngblood *et al.*, 2007; Bukowsky, Torres *et al.*, 2010). Controlling the hydrophobicity of amorphous carbon or coated surfaces has an important role for adsorption, adhesion, coatings, and catalysis. This two step wrinkling process is an attractive cost saving way to develop patterned amorphous carbon substrates with controlled surface energy.

BIBLIOGRAPHY

Ahmed, S. e F. R. Jones. A review of particulate reinforcement theories for polymer composites. Journal of Materials Science, v.25, n.12, p.4933-4942. 1990.

Akihiko, F. e Et Al. Organic Electronic Devices Based on Polymeric Material and Tunable Photonic Crystal. Japanese Journal of Applied Physics, v.46, n.no. 9a, p.5655. 2007.

Al-Douri, Y., H. Abid*, et al.* Correlation between the bulk modulus and the charge density in semiconductors. Physica B: Condensed Matter, v.305, n.2, p.186-190. 2001.

Balazs, A. C., T. Emrick*, et al.* Nanoparticle Polymer Composites: Where Two Small Worlds Meet. Science, v.314, n.5802, November 17, 2006, p.1107-1110. 2006.

Balberg, I., R. Naidis*, et al.* Bipolar phototransport in pi-conjugated polymer/C-60 composites. Applied Physics Letters, v.79, n.2, Jul, p.197-199. 2001.

Barnes, K. A., A. Karim, *et al.* Suppression of dewetting in nanoparticle-filled polymer films. Macromolecules, v.33, n.11, May, p.4177-4185. 2000.

Bukowsky, C., J. M. Torres, *et al.* Slip-stick wetting and large contact angle hysteresis on wrinkled surfaces. Journal of Colloid and Interface Science, v.354, n.2, p.825-831. 2010.

Chen, F.-C., T.-D. Chen, *et al.* Influence of mechanical strain on the electrical properties of flexible organic thin-film transistors. Semiconductor Science and Technology, v.26, n.3, p.034005. 2011.

Chung, J. Y., J. P. Youngblood, *et al.* Anisotropic wetting on tunable micro-wrinkled surfaces. Soft Matter, v.3, n.9, p.1163-1169. 2007.

Encinas, N. P., M.; Abenjoar, J., Martinez, M.A. Control of Wettability of Polymers by Surface Roughness Modification. Journal of Adhesion Science and Technology, v.24, p.1869-1883. 2010.

Han, J. T., G. W. Lee, *et al.* Direct observation of interfacial C-60 cluster formation in polystyrene-C-60 nanocomposite films. Nanotechnology, v.20, n.10, Mar. 2009.

Hiroyoshi, M. e Et Al. Surface and interface morphology observation and photovoltaic properties of C 60 /conducting polymer interpenetrating heterojunction devices. Journal of Physics D: Applied Physics, v.39, n.8, p.1521. 2006.

Huang, Y. e D. R. Paul. Effect of Temperature on Physical Aging of Thin Glassy Polymer Films. Macromolecules, v.38, n.24, p.10148-10154. 2005.

Hutchinson, J. M. Physical aging of polymers. Progress in Polymer Science, v.20, n.4, p.703-760. 1995.

Ji, X. L., J. K. Jing, *et al.* Tensile modulus of polymer nanocomposites. Polymer Engineering & Science, v.42, n.5, p.983-993. 2002.

Jiang, X. Y., S. Takayama, *et al.* Controlling mammalian cell spreading and cytoskeletal arrangement with conveniently fabricated continuous wavy features on poly(dimethylsiloxane). Langmuir, v.18, n.8, Apr, p.3273-3280. 2002.

Kearns, K. L., S. F. Swallen, *et al.* Influence of substrate temperature on the stability of glasses prepared by vapor deposition. Journal of Chemical Physics, v.127, n.15, Oct. 2007.

Kim, S. Y., K. Y. Kim*, et al.* Dark spot formation mechanism in organic light emitting diodes. Applied Physics Letters, v.89, n.13, p.132108-3. 2006.

Kropka, J. M., K. W. Putz*, et al.* Origin of dynamical properties in PMMA-C-60 nanocomposites. Macromolecules, v.40, n.15, Jul, p.5424-5432. 2007.

Lee, J.-Y., K. E. Su*, et al.* Impact of Surface-Modified Nanoparticles on Glass Transition Temperature and Elastic Modulus of Polymer Thin Films. Macromolecules, v.40, n.22, p.7755-7757. 2007.

Lee, W., M. Alexe*, et al.* Metal Membranes with Hierarchically Organized Nanotube Arrays. Chemistry of Materials, v.17, n.13, p.3325-3327. 2005.

Li, G., Z. Lu*, et al.* Raman scattering investigation of carbons obtained by heat treatment of a polyfurfuryl alcohol. Solid State Ionics, v.89, n.3-4, p.327-331. 1996.

O'connor, B., E. P. Chan*, et al.* Correlations between Mechanical and Electrical Properties of Polythiophenes. ACS Nano, v.4, n.12, p.7538-7544.

Pohl, H. A., A. Rembaum*, et al.* Effects of High Pressure on Some Organic Semiconducting Polymers. Journal of the American Chemical Society, v.84, n.14, p.2699-2704. 1962.

Priestley, R. D., L. J. Broadbelt*, et al.* Physical Aging of Ultrathin Polymer Films above and below the Bulk Glass Transition Temperature:, Effects of Attractive vs Neutral Polymer, Substrate Interactions Measured by Fluorescence. Macromolecules, v.38, n.3, p.654-657. 2005.

Priestley, R. D., C. J. Ellison*, et al.* Structural Relaxation of Polymer Glasses at Surfaces, Interfaces, and In Between. Science, v.309, n.5733, July 15, 2005, p.456-459. 2005.

Rittigstein, P. e J. M. Torkelson. Polymer-nanoparticle interfacial interactions in polymer nanocomposites: Confinement effects on glass transition temperature and suppression of physical aging. Journal of Polymer Science Part B-Polymer Physics, v.44, n.20, Oct, p.2935-2943. 2006.

Rudalevige, T., A. H. Francis*, et al.* Spectroscopic studies of fullerene aggregates. Journal of Physical Chemistry A, v.102, n.48, Nov, p.9797-9802. 1998.

Sanz, A., M. Ruppel*, et al.* Plasticization effect of C-60 on the fast dynamics of polystyrene and related polymers: an incoherent neutron scattering study. Journal of Physics-Condensed Matter, v.20, n.10, Mar. 2008.

Sauerbrey, G. Verwendung von Schwingquarzen zur Wägung dünner Schichten und zur Mikrowägung. Zeitschrift für Physik A Hadrons and Nuclei, v.155, n.2, p.206-222. 1959.

Singhvi, R., G. Stephanopoulos*, et al.* Effects of substratum morphology on cell physiology-Review. Biotechnology and Bioengineering, v.43, n.8, Apr, p.764-771. 1994.

Stafford, C. M., B. D. Vogt*, et al.* Elastic moduli of ultrathin amorphous polymer films. Macromolecules, v.39, n.15, Jul, p.5095-5099. 2006.

Sugiyama, T., Y. Furukawa*, et al.* Crystalline/amorphous Raman markers of hole-transport material NPD in organic light-emitting diodes. Chemical Physics Letters, v.405, n.4-6, p.330-333. 2005.

Teixeira, A. I., G. A. Abrams*, et al.* Epithelial contact guidance on well-defined micro- and nanostructured substrates. J Cell Sci, v.116, n.10, May 15, 2003, p.1881-1892. 2003.

Wilkinson, C. D. W., M. Riehle*, et al.* The use of materials patterned on a nano- and micro-metric scale in cellular engineering. Materials Science & Engineering C-Biomimetic and Supramolecular Systems, v.19, n.1-2, Jan, p.263-269. 2002.

Wong, H. C. e J. T. Cabral. Spinodal Clustering in Thin Films of Nanoparticle-Polymer Mixtures. Physical Review Letters, v.105, n.3, Jul. 2010.

Ying, Q. C., J. Marecek*, et al.* Solution behavior of buckminsterfullerene (C-60) in benzene. Journal of Chemical Physics, v.101, n.4, Aug, p.2665-2672. 1994.

CHAPTER 8

REFERENCES

1. *CHEMICAL & ENGINEERING NEWS* **2007,** *85* (41), 21-21.

2. Aamer, K. A.; Stafford, C. M.; Richter, L. J.; Kohn, J.; Becker, M. L., Thin Film Elastic Modulus of Degradable Tyrosine-Derived Polycarbonate Biomaterials and Their Blends. *Macromolecules* **2009,** *42* (4), 1212-1218.

3. Ahmed, S.; Jones, F. R., A review of particulate reinforcement theories for polymer composites. *Journal of Materials Science* **1990,** *25* (12), 4933-4942.

4. Akabori, K.; Tanaka, K.; Nagamura, T.; Takahara, A.; Kajiyama, T., Molecular motion in ultrathin polystyrene films: Dynamic mechanical analysis of surface and interfacial effects. *Macromolecules* **2005,** *38* (23), 9735-9741.

5. Akihiko, F.; et al., Organic Electronic Devices Based on Polymeric Material and Tunable Photonic Crystal. *Japanese Journal of Applied Physics* **2007,** *46* (no. 9a), 5655.

6. Al-Douri, Y.; Abid, H.; Aourag, H., Correlation between the bulk modulus and the charge density in semiconductors. *Physica B: Condensed Matter* **2001,** *305* (2), 186-190.

7. Alba-Simionesco, C.; Dosseh, G.; Dumont, E.; Frick, B.; Geil, B.; Morineau, D.; Teboul, V.; Xia, Y., Confinement of molecular liquids: Consequences on thermodynamic, static and dynamical properties of benzene and toluene. *Eur. Phys. J. E* **2003,** *12* (1), 19-28.

8. Alcoutlabi, M.; McKenna, G. B., Effects of confinement on material behaviour at the nanometre size scale. *Journal of Physics-Condensed Matter* **2005,** *17* (15), R461-R524.

9. Alig, I.; Lellinger, D.; Sulimma, J.; Tadjbakhsch, S., Ultrasonic shear wave reflection method for measurements of the viscoelastic properties of polymer films. *Review of Scientific Instruments* **1997,** *68* (3), 1536-1542.

10. Anastasiadis, S. H.; Karatasos, K.; Vlachos, G.; Manias, E.; Giannelis, E. P., Nanoscopic-confinement effects on local dynamics. *Physical Review Letters* **2000,** *84* (5), 915-918.

11. Angell, C. A.; Ueno, K., Materials Science Soft Is Strong. *Nature* **2009,** *462* (7269), 45-46.

12. Anthony, J. E.; Eaton, D. L.; Parkin, S. R., A Road Map to Stable, Soluble, Easily Crystallized Pentacene Derivatives. *Organic Letters* **2001,** *4* (1), 15-18.

13. Arndt, M.; Stannarius, R.; Groothues, H.; Hempel, E.; Kremer, F., Length scale of cooperativity in the dynamic glass transition. *Physical Review Letters* **1997,** *79* (11), 2077-2080.

14. Arriaga, L. R.; Monroy, F.; Langevin, D., Influence of backbone rigidity on the surface rheology of acrylic Langmuir polymer films. *Soft Matter* **2011**.

15. Aziz, A.; Narasimhan, K. L., Optical Absorption in AlQ. *Synthetic Metals* **2000,** *114* (2), 133-137.

16. Balazs, A. C.; Emrick, T.; Russell, T. P., Nanoparticle Polymer Composites: Where Two Small Worlds Meet. *Science* **2006,** *314* (5802), 1107-1110.

17. Balberg, I.; Naidis, R.; Lee, M. K.; Shinar, J.; Fonseca, L. F., Bipolar phototransport in pi-conjugated polymer/C-60 composites. *Applied Physics Letters* **2001,** *79* (2), 197-199.

18. Balmforth, N. J.; Craster, R. V.; Slim, A. C., On the buckling of elastic plates. *Q J Mechanics Appl Math* **2008,** *61* (2), 267-289.

19. Barnes, K. A.; Karim, A.; Douglas, J. F.; Nakatani, A. I.; Gruell, H.; Amis, E. J., Suppression of dewetting in nanoparticle-filled polymer films. *Macromolecules* **2000,** *33* (11), 4177-4185.

20. Beaucage, G.; Composto, R.; Stein, R. S., Ellipsometric study of the glass-transition and thermal-expansion coefficients of thin polymer-films. *Journal of Polymer Science Part B-Polymer Physics* **1993,** *31* (3), 319-326.

21. Benor, A.; Takizawa, S.-y.; PÈrez-BolÌvar, C.; Anzenbacher Jr, P., Efficiency improvement of fluorescent OLEDs by tuning the working function of PEDOT:PSS using UV-ozone exposure. *Organic Electronics* **2010,** *11* (5), 938-945.

22. Berry, G.; Fox, T. G., The viscosity of polymers and their concentrated solutions. In *Fortschritte der Hochpolymeren-Forschung*, Springer Berlin / Heidelberg: 1968; Vol. 5, pp 261-357.

23. Biot, M. A., Bending of an infinite beam on an elastic foundation. *Journal of Applied Mechanics* **1937,** *203* (A1).

24. Bishop, J. P.; Register, R. A., Poly(phenylethylnorbornene)s and their Hydrogenated Derivatives. *Macromol.Rapid Commun.* **2008,** *29* (9), 713-718.

25. Bodiguel, H.; Fretigny, C., Reduced Viscosity in Thin Polymer Films. *Physical Review Letters* **2006,** *97* (26), 266105.

26. Bodiguel, H.; Fretigny, C., Viscoelastic Properties of Ultrathin Polystyrene Films. *Macromolecules* **2007,** *40* (20), 7291-7298.

27. Bohme, T. R.; de Pablo, J. J., Evidence for size-dependent mechanical properties from simulations of nanoscopic polymeric structures. *Journal of Chemical Physics* **2002,** *116* (22), 9939-9951.

28. Boland, T.; Ratner, B. D., Direct measurement of hydrogen bonding in DNA nucleotide bases by atomic force microscopy. *Proceedings of the National Academy of Sciences of the United States of America* **1995,** *92* (12), 5297-5301.

29. Boudaoud, A.; Chaieb, S., Mechanical phase diagram of shrinking cylindrical gels. *Physical Review E* **2003,** *68* (2).

30. Bowden, N.; Brittain, S.; Evans, A. G.; Hutchinson, J. W.; Whitesides, G. M., Spontaneous formation of ordered structures in thin films of metals supported on an elastomeric polymer. *Nature* **1998,** *393* (6681), 146-149.

31. Bowden, N.; Huck, W. T. S.; Paul, K. E.; Whitesides, G. M., The controlled formation of ordered, sinusoidal structures by plasma oxidation of an elastomeric polymer. *Applied Physics Letters* **1999,** *75* (17), 2557-2559.

32. Bowen, W. R.; Lovitt, R. W.; Wright, C. J., Atomic Force Microscopy Study of the Adhesion of Saccharomyces cerevisiae. *Journal of Colloid and Interface Science* **2001,** *237* (1), 54-61.

33. Brandrup, J.; Immergut, E. H.; Grulke, E. A., *Polymer handbook*. Wiley-Interscience: 2003.

34. Breid, D.; Crosby, A. J., Effect of stress state on wrinkle morphology. *Soft Matter* **2011,** *7* (9), 4490-4496.

35. Briscoe, B. J.; Sebastian, K. S.; Sinha, S. K., Application of the compliance method to microhardness measurements of organic polymers. *Philosophical Magazine a-Physics of Condensed Matter Structure Defects and Mechanical Properties* **1996,** *74* (5), 1159-1169.

36. Brown, H. R.; Russell, T. P., Entanglements at polymer surfaces and interfaces. *Macromolecules* **1996,** *29* (2), 798-800.

37. Bukowsky, C.; Torres, J. M.; Vogt, B. D., Slip-stick wetting and large contact angle hysteresis on wrinkled surfaces. *Journal of Colloid and Interface Science* **2010,** *354* (2), 825-831.

38. Burnham, N. A.; Colton, R. J., Measuring the nanomechanical properties and surface forces of materials using an atomic force microscope. *Journal of Vacuum Science & Technology a-Vacuum Surfaces and Films* **1989,** *7* (4), 2906-2913.

39. Burnham, N. A.; Colton, R. J., Measuring the nanomechanical properties and surface forces of materials using an atomic force miscroscope. *Journal of Vacuum Science & Technology a-Vacuum Surfaces and Films* **1989,** *7* (4), 2906-2913.

40. Burrows, P. E. G., G.; Bulovic, V.; Shen, Z.; Forrest, S.R.; Thompson, M.E.;, Achieving full-color organic light-emitting devices for lightweight, flat-panel displays. *IEEE TRANSACTIONS ON ELECTRON DEVICES* **1997,** *44* (8), 1188-1203.

41. Callen, B. W.; Ridge, M. L.; Lahooti, S.; Neumann, A. W.; Sodhi, R. N. S., Remote plasma and ultraviolet--ozone modification of polystyrene. *Journal of*

Vacuum Science & Technology A: Vacuum, Surfaces, and Films **1995,** *13* (4), 2023-2029.

42. Cammarata, R. C.; Sieradzki, K., Effects of surface stress on the elastic moduli of thin films and superlattices. *Physical Review Letters* **1989,** *62* (17), 2005.

43. Campbell, C. G.; Vogt, B. D., Examination of the influence of cooperative segmental dynamics on the glass transition and coefficient of thermal expansion in thin films probed using poly(n-alkyl methacrylate)s. *Polymer* **2007,** *48* (24), 7169-7175.

44. Cappella, B.; Kaliappan, S. K.; Sturm, H., Using AFM force-distance curves to study the glass-to-rubber transition of amorphous polymers and their elastic-plastic properties as a function of temperature. *Macromolecules* **2005,** *38* (5), 1874-1881.

45. Chakravartula, A.; Komvopoulos, K., Viscoelastic properties of polymer surfaces investigated by nanoscale dynamic mechanical analysis. *Applied Physics Letters* **2006,** *88* (13), 131901-3.

46. Chalari, I.; Hadjichristidis, N., Synthesis of well-defined second-generation dendritic polymers of isoprene (I) and styrene (S): (S2I)3, (SI′I)3, (I″I′I)3, and (I′2I)4. *Journal of Polymer Science Part A: Polymer Chemistry* **2002,** *40* (10), 1519-1526.

47. Chan, E. P.; Crosby, A. J., Spontaneous formation of stable aligned wrinkling patterns. *Soft Matter* **2006,** *2* (4), 324-328.

48. Chan, E. P.; Kundu, S.; Lin, Q.; Stafford, C. M., Quantifying the Stress Relaxation Modulus of Polymer Thin Films via Thermal Wrinkling. *ACS Applied Materials & Interfaces* **2010,** *3* (2), 331-338.

49. Chan, E. P.; Smith, E. J.; Hayward, R. C.; Crosby, A. J., Surface wrinkles for smart adhesion. *Advanced Materials* **2008,** *20* (4), 711-+.

50. Chen, F.-C.; Chen, T.-D.; Zeng, B.-R.; Chung, Y.-W., Influence of mechanical strain on the electrical properties of flexible organic thin-film transistors. *Semiconductor Science and Technology* **2011,** *26* (3), 034005.

51. Chiang, C.-J.; Bull, S.; Winscom, C.; Monkman, A., A nano-indentation study of the reduced elastic modulus of Alq3 and NPB thin-film used in OLED devices. *Organic Electronics* **2010,** *11* (3), 450-455.

52. Chiang, C.-J.; Winscom, C.; Bull, S.; Monkman, A., Mechanical modeling of flexible OLED devices. *Organic Electronics* **2009,** *10* (7), 1268-1274.

53. Chiou, J. S.; Barlow, J. W.; Paul, D. R., Plasticization of glassy polymers by CO2. *Journal of Applied Polymer Science* **1985,** *30* (6), 2633-2642.

54. Choi, J. O.; Moore, J. A.; Corelli, J. C.; Silverman, J. P.; Bakhru, H., Degradation of poly(methylmethacrylate) by deep ultraviolet, x-ray, electron beam, and proton beam irradiations. *Journal of Vacuum Science & Technology B: Microelectronics and Nanometer Structures* **1988,** *6* (6), 2286-2289.

55. Chou, S. Y.; Krauss, P. R.; Renstrom, P. J., Imprint Lithography with 25-Nanometer Resolution. *Science* **1996,** *272* (5258), 85-87.

56. Chou, S. Y.; Krauss, P. R.; Zhang, W.; Guo, L.; Zhuang, L. In *Sub-10 nm imprint lithography and applications*, Papers from the 41st international conference on electron, ion, and photon beam technology and nanofabrication, Dana Point, California (USA), AVS: Dana Point, California (USA), 1997; pp 2897-2904.

57. Choura, M.; Belgacem, N. M.; Gandini, A., Acid-Catalyzed Polycondensation of Furfuryl Alcohol: Mechanisms of Chromophore Formation and Cross-Linking. *Macromolecules* **1996,** *29* (11), 3839-3850.

58. Chua, D. B. H.; Ng, H. T.; Li, S. F. Y., Spontaneous formation of complex and ordered structures on oxygen-plasma-treated elastomeric polydimethylsiloxane. *Applied Physics Letters* **2000,** *76* (6), 721-723.

59. Chung, J. Y.; Nolte, A. J.; Stafford, C. M., Diffusion-Controlled, Self-Organized Growth of Symmetric Wrinkling Patterns. *Advanced Materials* **2009,** *21* (13), 1358-1362.

60. Chung, J. Y.; Youngblood, J. P.; Stafford, C. M., Anisotropic wetting on tunable micro-wrinkled surfaces. *Soft Matter* **2007,** *3* (9), 1163-1169.

61. Clough, A.; Peng, D.; Yang, Z.; Tsui, O. K. C., Glass Transition Temperature of Polymer Films That Slip. *Macromolecules* **2011,** *44* (6), 1649-1653.

62. Coakley, K. M.; McGehee, M. D., Conjugated polymer photovoltaic cells. *Chemistry of Materials* **2004,** *16* (23), 4533-4542.

63. Collison, C. J.; Rothberg, L. J.; Treemaneekarn, V.; Li, Y., Conformational effects on the photophysics of conjugated polymers: A two species model for MEH-PPV spectroscopy and dynamics. *Macromolecules* **2001,** *34* (7), 2346-2352.

64. Conroy, M., Advances in thick and thin film analysis using interferometry. *Wear* **2009,** *266* (5-6), 502-506.

65. Corcoran, S. G.; Colton, R. J.; Lilleodden, E. T.; Gerberich, W. W., Anomalous plastic deformation at surfaces: Nanoindentation of gold single crystals. *Physical Review B* **1997,** *55* (24), 16057-16060.

66. Cowie, J. M. G., *Polymers: Chemistry and Physics of Modern Materials*. 1998.

67. Dalnoki-Veress, K.; Forrest, J. A.; Murray, C.; Gigault, C.; Dutcher, J. R., Molecular weight dependence of reductions in the glass transition temperature of thin, freely standing polymer films. *Physical Review E* **2001,** *63* (3).

68. Dawson, K. J.; Kearns, K. L.; Yu, L.; Steffen, W.; Ediger, M. D., Physical vapor deposition as a route to hidden amorphous states. *Proceedings of the National Academy of Sciences of the United States of America* **2009,** *106* (36), 15165-15170.

69. De Gennes, P. G., Glass transitions in thin polymer films. *European Physical Journal E* **2000,** *2* (3), 201-203.

70. Delcambre, S. P.; Riggleman, R. A.; Pablo, J. J. d.; Nealey, P. F., Mechanical properties of antiplasticized polymer nanostructures. *Soft Matter* **2010,** *6* (11), 2475-2483.

71. DeMaggio, G. B.; Frieze, W. E.; Gidley, D. W.; Zhu, M.; Hristov, H. A.; Yee, A. F., Interface and surface effects on the glass transition in thin polystyrene films. *Physical Review Letters* **1997,** *78* (8), 1524-1527.

72. Despotopoulou, M. M.; Frank, C. W.; Miller, R. D.; Rabolt, J. F., Kinetics of Chain Organization in Ultrathin Poly(di-n-hexylsilane) Films,Ä†. *Macromolecules* **1996,** *29* (18), 5797-5804.

73. Dimitriadis, E. K.; Horkay, F.; Maresca, J.; Kachar, B.; Chadwick, R. S., Determination of elastic moduli of thin layers of soft material using the atomic force microscope. *Biophysical Journal* **2002,** *82* (5), 2798-2810.

74. Ding, Y.; Ro, H.; Douglas, J. F.; Jones, R. L.; Karim, A.; Soles, C. L., Polymer viscoelasticity and residual stress effects on nanoimprint lithography. *Advanced Materials* **2007,** *19*, 1377-1382.

75. Djurisic, A. B.; Kwong, C. Y.; Guo, W. L.; Lau, T. W.; Li, E. H.; Liu, Z. T.; Kwok, H. S.; Lam, L. S. M.; Chan, W. K., Spectroscopic ellipsometry of the optical functions of tris (8-hydroxyquinoline) aluminum (Alq3). *Thin Solid Films* **2002,** *416* (1-2), 233-241.

76. Driva, P.; Iatrou, H.; Lohse, D. J.; Hadjichristidis, N., Anionic homo- and copolymerization of double-tailed macromonomers: A route to novel macromolecular architectures. *Journal of Polymer Science Part A: Polymer Chemistry* **2005,** *43* (18), 4070-4078.

77. Dutcher, J. R.; Forrest, J. A.; Dalnoki-Veress, K., Interface and chain confinement effects on the glass transition temperature of thin polymer films. *Abstracts of Papers of the American Chemical Society* **1998,** *215*, 276-COLL.

78. Efimenko, K.; Finlay, J.; Callow, M. E.; Callow, J. A.; Genzer, J., Development and Testing of Hierarchically Wrinkled Coatings for Marine Antifouling. *ACS Applied Materials & Interfaces* **2009,** *1* (5), 1031-1040.

79. Efimenko, K.; Rackaitis, M.; Manias, E.; Vaziri, A.; Mahadevan, L.; Genzer, J., Nested self-similar wrinkling patterns in skins. *Nature Materials* **2005,** *4* (4), 293-297.

80. Efimenko, K.; Wallace, W. E.; Genzer, J., Surface Modification of Sylgard-184 Poly(dimethyl siloxane) Networks by Ultraviolet and

Ultraviolet/Ozone Treatment. *Journal of Colloid and Interface Science* **2002,** *254* (2), 306-315.

81. Ellison, C. J.; Kim, S. D.; Hall, D. B.; Torkelson, J. M., Confinement and processing effects on glass transition temperature and physical aging in ultrathin polymer films: Novel fluorescence measurements. *European Physical Journal E* **2002,** *8* (2), 155-166.

82. Ellison, C. J.; Mundra, M. K.; Torkelson, J. M., Impacts of polystyrene molecular weight and modification to the repeat unit structure on the glass transition-nanoconfinement effect and the cooperativity length scale. *Macromolecules* **2005,** *38* (5), 1767-1778.

83. Ellison, C. J.; Ruszkowski, R. L.; Fredin, N. J.; Torkelson, J. M., Dramatic Reduction of the Effect of Nanoconfinement on the Glass Transition of Polymer Films via Addition of Small-Molecule Diluent. *Physical Review Letters* **2004,** *92* (9), 095702.

84. Ellison, C. J.; Torkelson, J. M., Sensing the glass transition in thin and ultrathin polymer films via fluorescence probes and labels. *Journal of Polymer Science Part B-Polymer Physics* **2002,** *40* (24), 2745-2758.

85. Ellison, C. J.; Torkelson, J. M., The distribution of glass-transition temperatures in nanoscopically confined glass formers. *Nature Materials* **2003,** *2* (10), 695-700.

86. Ellzey, K. A.; Ranganathan, T.; Zilberman, J.; Coughlin, E. B.; Farris, R. J.; Emrick, T., Deoxybenzoin-Based Polyarylates as Halogen-Free Fire-Resistant Polymers. *Macromolecules* **2006,** *39* (10), 3553-3558.

87. Encinas, N. P., M.; Abenjoar, J., Martinez, M.A., Control of Wettability of Polymers by Surface Roughness Modification. *Journal of Adhesion Science and Technology* **2010,** *24*, 1869-1883.

88. Erber, M.; Georgi, U.; M¸ller, J.; Eichhorn, K. J.; Voit, B., Polystyrene with different topologies: Study of the glass transition temperature in confined geometry of thin films. *European Polymer Journal* **2010,** *46* (12), 2240-2246.

89. Erber, M.; Tress, M.; Mapesa, E. U.; Serghei, A.; Eichhorn, K.-J.; Voit, B.; Kremer, F., Glassy Dynamics and Glass Transition in Thin Polymer Layers of

PMMA Deposited on Different Substrates. *Macromolecules* **2010,** *43* (18), 7729-7733.

90. Every, A. G., Measurement of the near-surface elastic properties of solids and thin supported films. *Measurement Science & Technology* **2002,** *13* (5), R21-R39.

91. Fakhraai, Z.; Forrest, J. A., Measuring the Surface Dynamics of Glassy Polymers. *Science* **2008,** *319* (5863), 600-604.

92. Fedynyshyn, T. H.; Sinta, R. F.; Astolfi, D. K.; Goodman, R. B.; Cabral, A.; Roberts, J.; Meagley, R., Resist deconstruction as a probe for innate material roughness. *Journal of Microlithography, Microfabrication, and Microsystems* **2006,** *5* (4), 043010-12.

93. Ferrari, A. C.; Robertson, J.; Beghi, M. G.; Bottani, C. E.; Ferulano, R.; Pastorelli, R., Elastic constants of tetrahedral amorphous carbon films by surface Brillouin scattering. *Applied Physics Letters* **1999,** *75* (13), 1893-1895.

94. Ferry, J. D., *Viscoelastic properties of polymers*. John Wiley and Sons: New York, 1980.

95. Fischer, H., Thermal probe surface treatment of a bulk polymer: Does a surface layer with a lower glass transition than the bulk exist? *Macromolecules* **2002,** *35* (9), 3592-3595.

96. Flory, P. J.; Rehner, J. J., Statistical Mechanics of Cross-Linked Polymer Networks II. Swelling. *The Journal of Chemical Physics* **1943,** *11* (11), 521-526.

97. Forrest, J. A.; Dalnoki-Veress, K., The glass transition in thin polymer films. *Advances in Colloid and Interface Science* **2001,** *94* (1-3), 167-196.

98. Forrest, J. A.; Dalnoki-Veress, K.; Dutcher, J. R., Brillouin light scattering studies of the mechanical properties of thin freely standing polystyrene films. *Physical Review E* **1998,** *58* (5), 6109-6114.

99. Forrest, J. A.; DalnokiVeress, K.; Dutcher, J. R., Interface and chain confinement effects on the glass transition temperature of thin polymer films. *Physical Review E* **1997,** *56* (5), 5705-5716.

100. Forrest, J. A.; DalnokiVeress, K.; Stevens, J. R.; Dutcher, J. R., Effect of free surfaces on the glass transition temperature of thin polymer films. *Physical Review Letters* **1996,** *77* (10), 2002-2005.

101. Forrest, J. A.; Danoki-Veress, K., The glass transition in thin polymer films. *Advances in Colloid and Interface Science* **2001,** *94* (1-3), 167-196.

102. Forrest, J. A.; Mattsson, J., Reductions of the glass transition temperature in thin polymer films: Probing the length scale of cooperative dynamics. *Physical Review E* **2000,** *61* (1), R53-R56.

103. Forrest, S. R., The path to ubiquitous and low-cost organic electronic appliances on plastic. *Nature* **2004,** *428* (6986), 911-918.

104. Fouassier, J. P.; Rabek, J. F., *Radiation Curing in Polymer Science and Technology: Fundamentals and methods*. Elsevier Applied Science: 1993.

105. Frank, B.; Gast, A. P.; Russell, T. P.; Brown, H. R.; Hawker, C. J., Polymer mobility in thin films. *Macromolecules* **1996,** *29* (20), 6531-6534.

106. Fryer, D. S.; Nealey, P. F.; de Pablo, J. J., Thermal probe measurements of the glass transition temperature for ultrathin polymer films as a function of thickness. *Macromolecules* **2000,** *33* (17), 6439-6447.

107. Fryer, D. S.; Peters, R. D.; Kim, E. J.; Tomaszewski, J. E.; de Pablo, J. J.; Nealey, P. F.; White, C. C.; Wu, W.-l., Dependence of the Glass Transition Temperature of Polymer Films on Interfacial Energy and Thickness. *Macromolecules* **2001,** *34* (16), 5627-5634.

108. Fukao, K., Dynamics in thin polymer films by dielectric spectroscopy. *European Physical Journal E* **2003,** *12* (1), 119-125.

109. Fukao, K.; Miyamoto, Y., Glass transition temperature and dynamics of alpha process in thin polymer films. *EPL (Europhysics Letters)* **1999,** *46* (5), 649.

110. Fukao, K.; Miyamoto, Y., Glass transitions and dynamics in thin polymer films: Dielectric relaxation of thin films of polystyrene. *Physical Review E* **2000,** *61* (2), 1743-1754.

111. Gao, C.; Yan, D., Hyperbranched polymers: from synthesis to applications. *Progress in Polymer Science* **2004,** *29* (3), 183-275.

112. Ge, S.; Pu, Y.; Zhang, W.; Rafailovich, M.; Sokolov, J.; Buenviaje, C.; Buckmaster, R.; Overney, R. M., Shear modulation force microscopy study of near surface glass transition temperatures. *Physical Review Letters* **2000,** *85* (11), 2340-2343.

113. Gehlsen, M. D.; Bates, F. S., Heterogeneous catalytic hydrogenation of polystyrene: thermodynamics of poly(vinylcyclohexane)-containing diblock copolymers. *Macromolecules* **1993,** *26* (16), 4122-4127.

114. Gehlsen, M. D.; Weimann, P. A.; Bates, F. S.; Harville, S.; Mays, J. W.; Wignall, G. D., Synthesis and characterization of poly(vinylcyclohexane) derivatives. *J.Polym.Sci.B Polym.Phys.* **1995,** *33* (10), 1527-1536.

115. Genzer, J.; Groenewold, J., Soft matter with hard skin: From skin wrinkles to templating and material characterization. *Soft Matter* **2006,** *2* (4), 310-323.

116. Gleskova, H.; Cheng, I. C.; Wagner, S.; Sturm, J. C.; Suo, Z., Mechanics of thin-film transistors and solar cells on flexible substrates. *Solar Energy* **2006,** *80* (6), 687-693.

117. Glynos, E.; Frieberg, B.; Oh, H.; Liu, M.; Gidley, D. W.; Green, P. F., Role of Molecular Architecture on the Vitrification of Polymer Thin Films. *Physical Review Letters* **2011,** *106* (12), 128301.

118. Gobel, R.; Krska, R.; Kellner, R.; Seitz, R. W.; Tomellini, S. A., Investigation of Different Polymers as Coating Materials for IR/ATR Spectroscopic Trace Analysis of Chlorinated Hydrocarbons in Water. *Applied Spectroscopy* **1994,** *48*, 678-683.

119. Goken, M.; Kempf, M.; Nix, W. D., Hardness and modulus of the lamellar microstructure in PST-TiAl studied by nanoindentations and AFM. *Acta Materialia* **2001,** *49* (5), 903-911.

120. Gomopoulos, N.; Cheng, W.; Efremov, M.; Nealey, P. F.; Fytas, G., Out-of-Plane Longitudinal Elastic Modulus of Supported Polymer Thin Films. *Macromolecules* **2009,** *42* (18), 7164-7167.

121. Graz, I. M.; Cotton, D. P. J.; Lacour, S. P., Extended cyclic uniaxial loading of stretchable gold thin-films on elastomeric substrates. *Applied Physics Letters* **2009,** *94* (7), 071902-3.

122. Grohens, Y., Hamon, L., Carriere, P., Holl, Y., Schultz, J., Tacticity and surface chemistry effects on the glass transition temperature of thin supported PMMA films. *Materials Research Society Symposium* **2001,** (629), FF171-77.

123. Grohens, Y.; Brogly, M.; Labbe, C.; David, M. O.; Schultz, J., Glass transition of stereoregular poly(methyl methacrylate) at interfaces. *Langmuir* **1998,** *14* (11), 2929-2932.

124. Grohens, Y.; Hamon, L.; Reiter, G.; Soldera, A.; Holl, Y., Some relevant parameters affecting the glass transition of supported ultra-thin polymer films. *European Physical Journal E* **2002,** *8* (2), 217-224.

125. Guigo, N.; Mija, A.; Vincent, L.; Sbirrazzuoli, N., Chemorheological analysis and model-free kinetics of acid catalysed furfuryl alcohol polymerization. *Physical Chemistry Chemical Physics* **2007,** *9* (39), 5359-5366.

126. Guvendiren, M.; Yang, S.; Burdick, J. A., Swelling-Induced Surface Patterns in Hydrogels with Gradient Crosslinking Density. *Advanced Functional Materials* **2009,** *19* (19), 3038-3045.

127. Hadjichristidis, N.; Iatrou, H.; Pispas, S.; Pitsikalis, M., Anionic polymerization: High vacuum techniques. *Journal of Polymer Science Part A: Polymer Chemistry* **2000,** *38* (18), 3211-3234.

128. Hadjichristidis, N.; Pispa, S.; Latrou, H.; Pitsilkalis, M., Linking Chemistry and Anionic Polymerization. *Current Organic Chemistry* **2002,** *6*, 155-176.

129. Hahn, S. F.; Hillmyer, M. A., High Glass Transition Temperature Polyolefins Obtained by the Catalytic Hydrogenation of Polyindene. *Macromolecules* **2002,** *36* (1), 71-76.

130. Hall, D. B.; Torkelson, J. M., Small Molecule Probe Diffusion in Thin and Ultrathin Supported Polymer Films. *Macromolecules* **1998,** *31* (25), 8817-8825.

131. Hamdorf, M.; Johannsmann, D., Surface-rheological measurements on glass forming polymers based on the surface tension driven decay of imprinted corrugation gratings. *Journal of Chemical Physics* **2000,** *112* (9).

132. Han, J. T.; Lee, G. W.; Kim, S.; Lee, H. J.; Douglas, J. F.; Karim, A., Direct observation of interfacial C-60 cluster formation in polystyrene-C-60 nanocomposite films. *Nanotechnology* **2009,** *20* (10).

133. Harper, C. A., *Handbook of plastics, elastomers, and composites*. McGraw-Hill: 2002.

134. Harrison, C.; Stafford, C. M.; Zhang, W. H.; Karim, A., Sinusoidal phase grating created by a tunably buckled surface. *Applied Physics Letters* **2004,** *85* (18), 4016-4018.

135. Hartschuh, R.; Ding, Y.; Roh, J. H.; Kisliuk, A.; Sokolov, A. P.; Soles, C. L.; Jones, R. L.; Hu, T. J.; Wu, W. L.; Mahorowala, A. P., Brillouin scattering studies of polymeric nanostructures. *Journal of Polymer Science Part B-Polymer Physics* **2004,** *42* (6), 1106-1113.

136. Hawker, C. J.; Lee, R.; Frechet, J. M. J., One-step synthesis of hyperbranched dendritic polyesters. *Journal of the American Chemical Society* **1991,** *113* (12), 4583-4588.

137. Hayward, R. C.; Chmelka, B. F.; Kramer, E. J., Template cross-linking effects on morphologies of swellable block copolymer and mesostructured silica thin films. *Macromolecules* **2005,** *38* (18), 7768-7783.

138. Hendricks, T. R.; Lee, I., Wrinkle-Free Nanomechanical Film: Control and Prevention of Polymer Film Buckling. *Nano Letters* **2006,** *7* (2), 372-379.

139. Herzinger, C. M.; Johs, B.; McGahan, W. A.; Woollam, J. A.; Paulson, W., Ellipsometric determination of optical constants for silicon and thermally grown silicon dioxide via a multi-sample, multi-wavelength, multi-angle investigation. *Journal of Applied Physics* **1998,** *83* (6), 3323-3336.

140. Hintermeyer, J.; Herrmann, A.; Kahlau, R.; Goiceanu, C.; RoÃàssler, E. A., Molecular Weight Dependence of Glassy Dynamics in Linear Polymers Revisited. *Macromolecules* **2008,** *41* (23), 9335-9344.

141. Hiroyoshi, M.; et al., Surface and interface morphology observation and photovoltaic properties of C 60 /conducting polymer interpenetrating heterojunction devices. *Journal of Physics D: Applied Physics* **2006,** *39* (8), 1521.

142. Hong, W.; Liu, Z.; Suo, Z., Inhomogeneous swelling of a gel in equilibrium with a solvent and mechanical load. *International Journal of Solids and Structures* **2009,** *46* (17), 3282-3289.

143. Hong, W.; Zhao, X.; Suo, Z., Formation of creases on the surfaces of elastomers and gels. *Applied Physics Letters* **2009,** *95* (11), 111901-3.

144. Hooker, J. C.; Burghardt, W. R.; Torkelson, J. M., Birefringence and second-order nonlinear optics as probes of polymer cooperative segmental mobility: Demonstration of Debye-type relaxation. *The Journal of Chemical Physics* **1999,** *111* (6), 2779-2788.

145. Huang, R., Kinetic wrinkling of an elastic film on a viscoelastic substrate. *Journal of the Mechanics and Physics of Solids* **2005,** *53* (1), 63-89.

146. Huang, R.; Stafford, C. M.; Vogt, B. D., Effect of surface properties on wrinkling of ultrathin films. *Journal of Aerospace Engineering* **2007,** *20* (1), 38-44.

147. Huang, Y.; Paul, D. R., Effect of Temperature on Physical Aging of Thin Glassy Polymer Films. *Macromolecules* **2005,** *38* (24), 10148-10154.

148. Huang, Y.; Paul, D. R., Effect of Film Thickness on the Gas-Permeation Characteristics of Glassy Polymer Membranes. *Industrial & Engineering Chemistry Research* **2007,** *46* (8), 2342-2347.

149. Huang, Z. Y.; Hong, W.; Suo, Z., Evolution of wrinkles in hard films on soft substrates. *Physical Review E* **2004,** *70* (3).

150. Huang, Z. Y.; Hong, W.; Suo, Z., Nonlinear analyses of wrinkles in a film bonded to a compliant substrate. *Journal of the Mechanics and Physics of Solids* **2005,** *53* (9), 2101-2118.

151. Huck, W. T. S., Artificial skins: Hierarchical wrinkling. *Nat Mater* **2005,** *4* (4), 271-272.

152. Hucul, D. A.; Hahn, S. F., Catalytic Hydrogenation of Polystyrene. *Adv.Mater.* **2000,** *12* (23), 1855-1858.

153. Hutchinson, J. M., Physical aging of polymers. *Progress in Polymer Science* **1995,** *20* (4), 703-760.

154. Huth, H.; Minakov, A. A.; Schick, C., Differential AC-chip calorimeter for glass transition measurements in ultrathin films. *Journal of Polymer Science Part B-Polymer Physics* **2006,** *44* (20), 2996-3005.

155. Huth, H.; Minakov, A. A.; Serghei, A.; Kremer, F.; Schick, C., Differential AC-chip calorimeter for glass transition measurements in ultra thin polymeric films. *European Physical Journal-Special Topics* **2007,** *141*, 153-160.

156. Hyun, D. C.; Moon, G. D.; Park, C. J.; Kim, B. S.; Xia, Y.; Jeong, U., Buckling-Assisted Patterning of Multiple Polymers. *Advanced Materials* **2010,** *22* (24), 2642-2646.

157. Inoue, R.; Kanaya, T.; Miyazaki, T.; Nishida, K.; Tsukushi, I.; Shibata, K., Glass transition and thermal expansivity of polystyrene thin films. *Materials Science and Engineering A-Structural Materials Properties Microstructure and Processing* **2006,** *442* (1-2), 367-370.

158. Inoue, T.; Cicerone, M. T.; Ediger, M. D., Molecular Motions and Viscoelasticity of Amorphous Polymers near Tg. *Macromolecules* **1995,** *28* (9), 3425-3433.

159. Jackson, C. L.; McKenna, G. B., The melting behavior of organic materials confined in porous solids. *The Journal of Chemical Physics* **1990,** *93* (12), 9002-9011.

160. Jackson, C. L.; McKenna, G. B., The glass transition of organic liquids confined to small pores. *Journal of Non-Crystalline Solids* **1991,** *131-133* (Part 1), 221-224.

161. Jackson, W. J.; Caldwell, J. R., Antiplasticization. II. Characteristics of antiplasticizers. *Journal of Applied Polymer Science* **1967,** *11* (2), 211-226.

162. Jackson, W. J.; Caldwell, J. R., Antiplasticization. III. Characteristics and properties of antiplasticizable polymers. *Journal of Applied Polymer Science* **1967,** *11* (2), 227-244.

163. Jain, T. S.; de Pablo, J. J., Investigation of transition states in bulk and freestanding film polymer glasses. *Physical Review Letters* **2004,** *92* (15), 155505.

164. Jain, T. S.; de Pablo, J. J., Influence of confinement on the vibrational density of states and the Boson peak in a polymer glass. *Journal of Chemical Physics* **2004,** *120* (19), 9371-9375.

165. Jang, D. C.; Greer, J. R., Transition from a strong-yet-brittle to a stronger-and-ductile state by size reduction of metallic glasses. *Nature Materials* **2010,** *9* (3), 215-219.

166. Jean, Y. C.; Zhang, R. W.; Cao, H.; Yuan, J. P.; Huang, C. M.; Nielsen, B.; AsokaKumar, P., Glass transition of polystyrene near the surface studied by slow-positron-annihilation spectroscopy. *Physical Review B* **1997,** *56* (14), R8459-R8462.

167. Jellison, G. E., *Data analysis for spectroscopic ellipsometry*. Elsevier: Lausanne, SUISSE, 1993.

168. Jeong, H. E.; Kwak, M. K.; Suh, K. Y., Stretchable, Adhesion-Tunable Dry Adhesive by Surface Wrinkling. *Langmuir* **2010,** *26* (4), 2223-2226.

169. Ji, X. L.; Jing, J. K.; Jiang, W.; Jiang, B. Z., Tensile modulus of polymer nanocomposites. *Polymer Engineering & Science* **2002,** *42* (5), 983-993.

170. Jiang, X. Y.; Takayama, S.; Qian, X. P.; Ostuni, E.; Wu, H. K.; Bowden, N.; LeDuc, P.; Ingber, D. E.; Whitesides, G. M., Controlling mammalian cell spreading and cytoskeletal arrangement with conveniently fabricated continuous wavy features on poly(dimethylsiloxane). *Langmuir* **2002,** *18* (8), 3273-3280.

171. Jikei, M.; Kakimoto, M., Hyperbranched polymers: a promising new class of materials. *Progress in Polymer Science* **2001,** *26* (8), 1233-1285.

172. Johnson, W. L.; et al., Elastic constants and dimensions of imprinted polymeric nanolines determined from Brillouin light scattering. *Nanotechnology* **2009,** *21* (7), 075703.

173. Jones, J., Lacour, S.P., Suo, Z., Wagner, S., A method for making elastic metal interconnects. *Materials Research Society Symposium* **2003,** *736* (H6), 1-6.

174. Jones, R. A. L., The dynamics of thin polymer films. *Current Opinion in Colloid & Interface Science* **1999,** *4* (2), 153-158.

175. Jones, R. L.; Kumar, S. K.; Ho, D. L.; Briber, R. M.; Russell, T. P., Chain conformation in ultrathin polymer films. *Nature* **1999,** *400* (6740), 146-149.

176. Joyce, S. A.; Houston, J. E., A new force sensor incorporating force-feedback control for interfacial force microscopy. *Review of Scientific Instruments* **1991,** *62* (3), 710-715.

177. Kajiyama, T.; Tanaka, K.; Satomi, N.; Takahara, A., Surface Relaxation Process of Monodisperse Polystyrene Film Based on Lateral Force Microscopic Measurements. *Macromolecules* **1998,** *31* (15), 5150-5151.

178. Kanaya, T.; Miyazaki, T.; Watanabe, H.; Nishida, K.; Yamana, H.; Tasaki, S.; Bucknall, D. B., Annealing effects on thickness of polystyrene thin films as studied by neutron reflectivity. *Polymer* **2003,** *44* (14), 3769-3773.

179. Kang, H.-S.; Park, K.-N.; Cho, Y.-R.; Park, D.-W.; Choe, Y., Enhanced performance of organic electroluminescence diodes with a 2-TNATA:C60 hole injection layer. *Journal of Industrial and Engineering Chemistry* **2009,** *15* (5), 752-757.

180. Kawana, S.; Jones, R. A. L., Character of the glass transition in thin supported polymer films. *Physical Review E* **2001,** *63* (2).

181. Kawana, S.; Jones, R. A. L., Effect of physical ageing in thin glassy polymer films. *European Physical Journal E* **2003,** *10* (3), 223-230.

182. Kearns, K. L.; Still, T.; Fytas, G.; Ediger, M. D., High-Modulus Organic Glasses Prepared by Physical Vapor Deposition. *Advanced Materials* **2009,** *22* (1), 39-42.

183. Kearns, K. L.; Swallen, S. F.; Ediger, M. D.; Wu, T.; Yu, L., Influence of substrate temperature on the stability of glasses prepared by vapor deposition. *Journal of Chemical Physics* **2007,** *127* (15).

184. Keddie, J. L.; Jones, R. A. L., Glass-transition behavior in ultra-thin polystyrene films. *Israel Journal of Chemistry* **1995,** *35* (1), 21-26.

185. Keddie, J. L.; Jones, R. A. L.; Cory, R. A., Size-dependent depression of the glass-transition temperature in polymer-films. *Europhysics Letters* **1994,** *27* (1), 59-64.

186. Keddie, J. L.; Jones, R. A. L.; Cory, R. A., Interface and surface effects on the glass-transition temperature in thin polymer films. *Faraday Discussions* **1994,** *98*, 219-230.

187. Kelley, T. W.; Baude, P. F.; Gerlach, C.; Ender, D. E.; Muyres, D.; Haase, M. A.; Vogel, D. E.; Theiss, S. D., Recent Progress in Organic Electronics: Materials, Devices, and Processes. *Chemistry of Materials* **2004,** *16* (23), 4413-4422.

188. Kim, D.; Kim, S.; Kong, H. J.; Lee, Y., Measurement of the thickness profile of a transparent thin film deposited upon a pattern structure with an acousto-optic tunablefilter. *Opt. Lett.* **2002,** *27* (21), 1893-1895.

189. Kim, D.-H.; Viventi, J.; Amsden, J. J.; Xiao, J.; Vigeland, L.; Kim, Y.-S.; Blanco, J. A.; Panilaitis, B.; Frechette, E. S.; Contreras, D.; Kaplan, D. L.; Omenetto, F. G.; Huang, Y.; Hwang, K.-C.; Zakin, M. R.; Litt, B.; Rogers, J. A., Dissolvable films of silk fibroin for ultrathin conformal bio-integrated electronics. *Nat Mater* **2010,** *9* (6), 511-517.

190. Kim, J. H.; Jang, J.; Zin, W. C., Estimation of the thickness dependence of the glass transition temperature in various thin polymer films. *Langmuir* **2000,** *16* (9), 4064-4067.

191. Kim, S.; Hewlett, S.; Roth, C.; Torkelson, J., Confinement effects on glass transition temperature, transition breadth, and expansivity: Comparison of ellipsometry and fluorescence measurements on polystyrene films. *The European Physical Journal E: Soft Matter and Biological Physics* **2009,** *30* (1), 83-92.

192. Kim, S.; Mundra, M. K.; Roth, C. B.; Torkelson, J. M., Suppression of the Tg Nanoconfinement Effect in Thin Poly(vinyl acetate) Films by Sorbed Water. *Macromolecules* **2010,** *43* (11), 5158-5161.

193. Kim, S. Y.; Kim, K. Y.; Tak, Y.-H.; Lee, J.-L., Dark spot formation mechanism in organic light emitting diodes. *Applied Physics Letters* **2006,** *89* (13), 132108-3.

194. Kim, Y. H., Hyperbranchecs polymers 10 years after. *Journal of Polymer Science Part a-Polymer Chemistry* **1998,** *36* (11), 1685-1698.

195. Kim, Y. S.; Chung, C. I.; Lai, S. Y.; Hyun, K. S., Melt rheological and thermodynamic properties of polyethylene homopolymers and poly(ethylene/+Ý-olefin) copolymers with respect to molecular composition and structure. *J.Appl.Polym.Sci.* **1996,** *59* (1), 125-137.

196. Kivelson, S. A.; Tarjus, G., In search of a theory of supercooled liquids. *Nature Materials* **2008,** *7* (11), 831-833.

197. Klein, R. J.; Fischer, D. A.; Lenhart, J. L., Systematic oxidation of polystyrene by ultraviolet-ozone, characterized by near-edge X-ray absorption fine structure and contact angle. *Langmuir* **2008,** *24* (15), 8187-8197.

198. Kline, R. J.; DeLongchamp, D. M.; Fischer, D. A.; Lin, E. K.; Heeney, M.; McCulloch, I.; Toney, M. F., Significant dependence of morphology and charge carrier mobility on substrate surface chemistry in high performance polythiophene semiconductor films. *Applied Physics Letters* **2007,** *90* (6), 062117-3.

199. Ko, H. C.; Stoykovich, M. P.; Song, J.; Malyarchuk, V.; Choi, W. M.; Yu, C.-J.; Geddes Iii, J. B.; Xiao, J.; Wang, S.; Huang, Y.; Rogers, J. A., A hemispherical electronic eye camera based on compressible silicon optoelectronics. *Nature* **2008,** *454* (7205), 748-753.

200. Koch, N.; Elschner, A.; Schwartz, J.; Kahn, A., Organic molecular films on gold versus conducting polymer: Influence of injection barrier height and morphology on current--voltage characteristics. *Applied Physics Letters* **2003,** *82* (14), 2281-2283.

201. Korkmaz, T.; Dogan, A.; Usanmaz, A., Dynamic mechanical analysis of provisional resin materials reinforced by metal oxides. *Bio-medical Materials and Engineering* **2005,** *15* (3), 179-188.

202. Koutalas, G.; Iatrou, H.; Lohse, D. J.; Hadjichristidis, N., Well-Defined Comb, Star, Comb, and Comb-on-Comb Polybutadienes by Anionic Polymerization and the Macromonomer Strategy. *Macromolecules* **2005,** *38* (12), 4996-5001.

203. Kropka, J. M.; Putz, K. W.; Pryamitsyn, V.; Ganesan, V.; Green, P. F., Origin of dynamical properties in PMMA-C-60 nanocomposites. *Macromolecules* **2007,** *40* (15), 5424-5432.

204. Kwon, S. J.; Park, J. H.; Park, J. G., Wrinkling of a sol-gel-derived thin film. *Physical Review E* **2005,** *71* (1).

205. Lacour, S. P., Huang, Z., Suo, Z., Wagner, S., Deformable interconnects for conformal integrated circuits. *Materials Research Society Symposium* **2002,** *736* (D4.8), 1-6.

206. Lacour, S. P.; Wagner, S.; Huang, Z. Y.; Suo, Z., Stretchable gold conductors on elastomeric substrates. *Applied Physics Letters* **2003,** *82* (15), 2404-2406.

207. Lee, E. H.; Rao, G. R.; Mansur, L. K., LET effect on cross-linking and scission mechanisms of PMMA during irradiation. *Radiation Physics and Chemistry* **1999,** *55* (3), 293-305.

208. Lee, J.-Y.; Su, K. E.; Chan, E. P.; Zhang, Q.; Emrick, T.; Crosby, A. J., Impact of Surface-Modified Nanoparticles on Glass Transition Temperature and Elastic Modulus of Polymer Thin Films. *Macromolecules* **2007,** *40* (22), 7755-7757.

209. Lee, K.; Pan, F.; Carroll, G. T.; Turro, N. J.; Koberstein, J. T., Photolithographic Technique for Direct Photochemical Modification and Chemical Micropatterning of Surfaces. *Langmuir* **2004,** *20* (5), 1812-1818.

210. Lee, W.; Alexe, M.; Nielsch, K.; G√∂sele, U., Metal Membranes with Hierarchically Organized Nanotube Arrays. *Chemistry of Materials* **2005,** *17* (13), 3325-3327.

211. Lei, J.; Fan, J.; Yu, C. Z.; Zhang, L. Y.; Jiang, S. Y.; Tu, B.; Zhao, D. Y., Immobilization of enzymes in mesoporous materials: controlling the entrance to nanospace. *Microporous and Mesoporous Materials* **2004,** *73* (3), 121-128.

212. Lenhart, J. L.; Jones, R. L.; Lin, E. K.; Soles, C. L.; Wu, W.-l.; Fischer, D. A.; Sambasivan, S.; Goldfarb, D. L.; Angelopoulos, M. In *Probing surface and bulk chemistry in resist films using near edge x-ray absorption fine structure*, Papers from the 46th International Conference on Electron, Ion, and Photon Beam Technology and Nanofabrication, Anaheim, California (USA), AVS: Anaheim, California (USA), 2002; pp 2920-2926.

213. Li, G.; Lu, Z.; Huang, B.; Wang, Z.; Huang, H.; Xue, R.; Chen, L., Raman scattering investigation of carbons obtained by heat treatment of a polyfurfuryl alcohol. *Solid State Ionics* **1996,** *89* (3-4), 327-331.

214. Li, L.; Ng, K.-M.; Chan, C.-M.; Feng, J.-Y.; Zeng, X.-M.; Weng, L.-T., Surface Studies of the Rearrangement of End Groups of a Polymer by ToF, SIMS and AFM. *Macromolecules* **2000,** *33* (15), 5588-5592.

215. Lian, J. R.; Yuan, Y.-b.; Cao, L.-f.; Zhang, J.; Pang, H.-q.; Zhou, Y.-f.; Zhou, X., Improved efficiency in OLEDs with a thin Alq3 interlayer. *Journal of Luminescence* **2010,** *122-123*, 660-662.

216. Lin, E. K.; Kolb, R.; Satija, S. K.; Wu, W. L., Reduced polymer mobility near the polymer solid interface as measured by neutron reflectivity. *Macromolecules* **1999,** *32* (11), 3753-3757.

217. Lin, E. K.; Wu, W. I.; Satija, S. K., Polymer interdiffusion near an attractive solid substrate. *Macromolecules* **1997,** *30* (23), 7224-7231.

218. Lin, P.-C.; Vajpayee, S.; Jagota, A.; Hui, C.-Y.; Yang, S., Mechanically tunable dry adhesive from wrinkled elastomers. *Soft Matter* **2008,** *4* (9), 1830-1835.

219. Lin, P. C.; Yang, S., Spontaneous formation of one-dimensional ripples in transit to highly ordered two-dimensional herringbone structures through sequential and unequal biaxial mechanical stretching. *Applied Physics Letters* **2007,** *90* (24).

220. Liu, Y.; Russell, T. P.; Samant, M. G.; Stohr, J.; Brown, H. R.; Cossy-Favre, A.; Diaz, J., Surface Relaxations in Polymers. *Macromolecules* **1997,** *30* (25), 7768-7771.

221. Lotters, J. C.; Olthuis, W.; Veltink, P. H.; Bergveld, P., The mechanical properties of the rubber elastic polymer polydimethylsiloxane for sensor applications. *Journal of Micromechanics and Microengineering* **1997,** (3), 145.

222. Lu, C.; MoÃàhwald, H.; Fery, A., Large-Scale Regioselective Formation of Well-Defined Stable Wrinkles of Multilayered Films via Embossing. *Chemistry of Materials* **2008,** *20* (22), 7052-7059.

223. Lu, C.; Mohwald, H.; Fery, A., A lithography-free method for directed colloidal crystal assembly based on wrinkling. *Soft Matter* **2007,** *3* (12), 1530-1536.

224. Lu, H. Y.; Chen, W.; Russell, T. P., Relaxation of Thin Films of Polystyrene Floating on Ionic Liquid Surface. *Macromolecules* **2009,** *42* (22), 9111-9117.

225. Luckenbach, R., *Beilstein handbook of organic chemistry: fifth supplementary series, covering the literature from 1960 through 1979*. Springer: 1990.

226. Mackay, M. E.; Dao, T. T.; Tuteja, A.; Ho, D. L.; Van Horn, B.; Kim, H.; Hawker, C. J., Nanoscale effects leading to non-Einstein-like decrease in viscosity. *Nature Materials* **2003,** *2* (11), 762-766.

227. Mackay, M. E.; Dao, T. T.; Tuteja, A.; Ho, D. L.; Van Horn, B.; Kim, H. C.; Hawker, C. J., Nanoscale effects leading to non-Einstein-like decrease in viscosity. *Nature Materials* **2003,** *2* (11), 762-766.

228. Mackay, M. E.; Hong, Y.; Jeong, M.; Hong, S.; Russell, T. P.; Hawker, C. J.; Vestberg, R.; Douglas, J. F., Influence of Dendrimer Additives on the Dewetting of Thin Polystyrene Films. *Langmuir* **2002,** *18* (5), 1877-1882.

229. Malik, S.; Nandi, A. K., Crystallization mechanism of regioregular poly(3-alkyl thiophene)s. *Journal of Polymer Science Part B-Polymer Physics* **2002,** *40* (18), 2073-2085.

230. Mansfield, K. F.; Theodorou, D. N., Molecular-dynamics simulation of a glassy polymer surface. *Macromolecules* **1991,** *24* (23), 6283-6294.

231. Mansfield, M.; Needs, R. J., Surface energy and stress of lead (111) and (110) surfaces. *Physical Review B* **1991,** *43* (11), 8829.

232. Marlo, M.; Milman, V., Density-functional study of bulk and surface properties of titanium nitride using different exchange-correlation functionals. *Physical Review B* **2000,** *62* (4), 2899.

233. Matsuo, E. S.; Tanaka, T., Patterns in shrinking gels. *Nature* **1992,** *358* (6386), 482-485.

234. Mattsson, J.; Forrest, J. A.; Borjesson, L., Quantifying glass transition behavior in ultrathin free-standing polymer films. *Physical Review E* **2000,** *62* (4), 5187-5200.

235. Mayer, A. C.; Ruiz, R.; Headrick, R. L.; Kazimirov, A.; Malliaras, G. G., Early stages of pentacene film growth on silicon oxide. *Organic Electronics* **2004,** *5* (5), 257-263.

236. McGehee, M. D., Goh, C., Organic Semiconductors for Low-Cost Solar Cells. *Frontiers of Engineering: Reports on Leading-Edge Engineering 2005 Symposium* **2006**, 119-130.

237. McKenna, G. B., Size and confinement effects in glass forming liquids: Perspectives on bulk and nano-scale behaviours. *Journal de Physique Iv* **2000,** *10* (P7), 53-57.

238. McKenna, G. B., Glass dynamics - Diverging views on glass transition. *Nature Physics* **2008,** *4* (9), 673-674.

239. McKenna, G. B., Ten (or more) years of dynamics in confinement: Perspectives for 2010. *European Physical Journal-Special Topics* **2010,** *189* (1), 285-302.

240. Mei, H. X.; Huang, R.; Chung, J. Y.; Stafford, C. M.; Yu, H. H., Buckling modes of elastic thin films on elastic substrates. *Applied Physics Letters* **2007,** *90* (15).

241. Merino, S.; Brauge, L.; Caminade, A. M.; Majoral, J. P.; Taton, D.; Gnanou, Y., Synthesis and characterization of linear, hyperbranched, and dendrimer-like polymers constituted of the same repeating unit. *Chemistry-a European Journal* **2001,** *7* (14), 3095-3105.

242. Milner, S. T.; McLeish, T. C. B., Arm-length dependence of stress relaxation in star polymer melts. *Macromolecules* **1998,** *31* (21), 7479-7482.

243. Miyake, K.; Satomi, N.; Sasaki, S., Elastic modulus of polystyrene film from near surface to bulk measured by nanoindentation using atomic force microscopy. *Applied Physics Letters* **2006,** *89* (3).

244. Miyatake, K.; Oyaizu, K.; Tsuchida, E.; Hay, A. S., Synthesis and Properties of Novel Sulfonated Arylene Ether/Fluorinated Alkane Copolymers. *Macromolecules* **2001,** *34* (7), 2065-2071.

245. Mora, T.; Boudaoud, A., Buckling of swelling gels. *European Physical Journal E* **2006,** *20* (2), 119-124.

246. Morton, M.; Fetters, L. J., Anionic Polymerization of Vinyl Monomers. *Rubber Chemistry and Technology* **1975,** *48* (3), 359-409.

247. Mukherjee, M.; Singh, A.; Daillant, J.; Menelle, A.; Cousin, F., Effect of Solvent, Polymer Interaction in Swelling Dynamics of Ultrathin Polyacrylamide Films:, A Neutron and X-ray Reflectivity Study. *Macromolecules* **2007,** *40* (4), 1073-1080.

248. Mundra, M. K.; Donthu, S. K.; Dravid, V. P.; Torkelson, J. M., Effect of spatial confinement on the glass-transition temperature of patterned polymer nanostructures. *Nano Letters* **2007,** *7* (3), 713-718.

249. Myoung-Woon, M.; Sang Hoon, L.; Jeong-Yun, S.; Kyu Hwan, O.; Ashkan, V.; John, W. H., Controlled formation of nanoscale wrinkling patterns on polymers using focused ion beam. **2007,** *57* (8), 747-750.

250. Nakamura, Y.; Wan, Y.; Mays, J. W.; Iatrou, H.; Hadjichristidis, N., Radius of Gyration of Polystyrene Combs and Centipedes in Solution. *Macromolecules* **2000,** *33* (22), 8323-8328.

251. Nakatani, H.; Nitta, K.-h.; Soga, K., Effect of hydrogenation on dynamic mechanical relaxation 1. Atactic polystyrene. *Polymer* **1998,** *39* (18), 4273-4278.

252. Ngai, K. L.; Plazek, D. J., Identification of different modes of molecular-motion in polymers that cause themorheological complexity. *Rubber Chemistry and Technology* **1995,** *68* (3), 376-434.

253. Nie, H. Y.; Walzak, M. J.; Berno, B.; McIntyre, N. S., Atomic force microscopy study of polypropylene surfaces treated by UV and ozone exposure: modification of morphology and adhesion force. *Applied Surface Science* **1999,** *144-145*, 627-632.

254. Nolte, A. J.; Cohen, R. E.; Rubner, M. F., A two-plate buckling technique for thin film modulus measurements: Applications to polyelectrolyte multilayers. *Macromolecules* **2006,** *39* (14), 4841-4847.

255. Nolte, A. J.; Takane, N.; Hindman, E.; Gaynor, W.; Rubner, M. F.; Cohen, R. E., Thin Film Thickness Gradients and Spatial Patterning via Salt Etching of Polyelectrolyte Multilayers. *Macromolecules* **2007,** *40* (15), 5479-5486.

256. Nolte, A. J.; Treat, N. D.; Cohen, R. E.; Rubner, M. F., Effect of Relative Humidity on the Young's Modulus of Polyelectrolyte Multilayer Films and Related Nonionic Polymers. *Macromolecules* **2008,** *41* (15), 5793-5798.

257. O'Connell, P.; McKenna, G., Dramatic stiffening of ultrathin polymer films in the rubbery regime. *The European Physical Journal E: Soft Matter and Biological Physics* **2006,** *20* (2), 143-150.

258. O'Connell, P. A.; Hutcheson, S. A.; McKenna, G. B., Creep behavior of ultra-thin polymer films. *Journal of Polymer Science Part B-Polymer Physics* **2008,** *46* (18), 1952-1965.

259. O'Connell, P. A.; McKenna, G. B., Rheological Measurements of the Thermoviscoelastic Response of Ultrathin Polymer Films. *Science* **2005,** *307* (5716), 1760-1763.

260. O'Connell, P. A.; McKenna, G. B., Novel nanobubble inflation method for determining the viscoelastic properties of ultrathin polymer films. *Review of Scientific Instruments* **2007,** *78* (1), 013901-12.

261. O'Connell, P. A.; McKenna, G. B., The stiffening of ultrathin polymer films in the rubbery regime: The relative contributions of membrane stress and surface tension. *Journal of Polymer Science Part B: Polymer Physics* **2009,** *47* (24), 2441-2448.

262. O'Connor, B.; Chan, E. P.; Chan, C.; Conrad, B. R.; Richter, L. J.; Kline, R. J.; Heeney, M.; McCulloch, I.; Soles, C. L.; DeLongchamp, D. M., Correlations between Mechanical and Electrical Properties of Polythiophenes. *ACS Nano* **2010,** *4* (12), 7538-7544.

263. Ohno, H.; Kobayashi, N.; Takeoka, S.; Ishizaka, H.; Tsuchida, E., Larger cations can move faster in solid polymer electrolytes. *Solid State Ionics* **1990,** *40-41* (Part 2), 655-658.

264. Oliver, W. C.; Pharr, G. M., An improved technique for determining hardnress and elastic-modulus using load and dispalcement sensing indentation experiments. *Journal of Materials Research* **1992,** *7* (6), 1564-1583.

265. Orts, W. J.; Vanzanten, J. H.; Wu, W. L.; Satija, S. K., Observation of temperature-dependent thicknesses in ultrathin polystyrene films on silicon. *Physical Review Letters* **1993,** *71* (6), 867-870.

266. Ozin, G. A.; Yang, S. M., The race for the photonic chip: Colloidal crystal assembly in silicon wafers. *Advanced Functional Materials* **2001,** *11* (2), 95-104.

267. Park, J.-Y.; McKenna, G. B., Size and confinement effects on the glass transition behavior of polystyrene/o-terphenyl polymer solutions. *Physical Review B* **2000,** *61* (10), 6667.

268. Park, M.; Harrison, C.; Chaikin, P. M.; Register, R. A.; Adamson, D. H., Block copolymer lithography: Periodic arrays of similar to 10(11) holes in 1 square centimeter. *Science* **1997,** *276* (5317), 1401-1404.

269. Patten, T. E.; Matyjaszewski, K., Atom transfer radical polymerization and the synthesis of polymeric materials. *Advanced Materials* **1998,** *10* (12), 901-+.

270. Pearson, D. S.; Helfand, E., Viscoelastic properties of star-shaped polymers. *Macromolecules* **1984,** *17* (4), 888-895.

271. Perumal, O.; Khandare, J.; Kolhe, P.; Kannan, S.; Lieh-Lai, M.; Kannan, R. M., Effects of Branching Architecture and Linker on the Activity of Hyperbranched Polymer,àíDrug Conjugates. *Bioconjugate Chemistry* **2009,** *20* (5), 842-846.

272. Pfromm, P. H.; Koros, W. J., Accelerated physical ageing of thin glassy polymer films: evidence from gas transport measurements. *Polymer* **1995,** *36* (12), 2379-2387.

273. Pharr, G. M., Oliver, W. C., Measurement of Thin-Film Mechanical-Properties Using Nanoindentation. *MRS Bulletin* **1992,** *17* (7), 28-33.

274. Pissis, P.; Kyritsis, A.; Daoukaki, D.; Barut, G.; Pelster, R.; Nimtz, G., Dielectric studies of glass transition in confined propylene glycol. *Journal of Physics: Condensed Matter* **1998,** (28), 6205.

275. Pohl, H. A.; Rembaum, A.; Henry, A., Effects of High Pressure on Some Organic Semiconducting Polymers. *Journal of the American Chemical Society* **1962,** *84* (14), 2699-2704.

276. Potje-Kamloth, K.; Polk, B. J.; Josowicz, M.; Janata, J. ô., Doping of Polyaniline in the Solid State with Photogenerated Triflic Acid. *Chemistry of Materials* **2002,** *14* (6), 2782-2787.

277. Pretzl, M.; Schweikart, A.; Hanske, C.; Chiche, A.; Zettl, U.; Horn, A.; Boàker, A.; Fery, A., A Lithography-Free Pathway for Chemical Microstructuring of Macromolecules from Aqueous Solution Based on Wrinkling. *Langmuir* **2008,** *24* (22), 12748-12753.

278. Priestley, R.; Mundra, M. K.; Barnett, N. J.; Broadbelt, L. J.; Torkelson, J. M., Effects of nanoscale confinement and interfaces on the glass transition temperatures of a series of poly(n-methacrylate) films. *Australian Journal of Chemistry* **2007,** *60* (10), 765-771.

279. Priestley, R. D., Physical aging of confined glasses. *Soft Matter* **2009,** *5* (5), 919-926.

280. Priestley, R. D.; Broadbelt, L. J.; Torkelson, J. M., Physical Aging of Ultrathin Polymer Films above and below the Bulk Glass Transition Temperature:

Effects of Attractive vs Neutral Polymer,àíSubstrate Interactions Measured by Fluorescence. *Macromolecules* **2005,** *38* (3), 654-657.

281. Priestley, R. D.; Broadbelt, L. J.; Torkelson, J. M., Physical Aging of Ultrathin Polymer Films above and below the Bulk Glass Transition Temperature:, Effects of Attractive vs Neutral Polymer, Substrate Interactions Measured by Fluorescence. *Macromolecules* **2005,** *38* (3), 654-657.

282. Priestley, R. D.; Ellison, C. J.; Broadbelt, L. J.; Torkelson, J. M., Structural Relaxation of Polymer Glasses at Surfaces, Interfaces, and In Between. *Science* **2005,** *309* (5733), 456-459.

283. Priestley, R. D.; Mundra, M. K.; Barnett, N.; Broadbelt, L. J.; Torkelson, J. M., Effects of Nanoscale Confinement and Interfaces on the Glass Transition Temperatures of a Series of Poly(n-methacrylate) Films. *Australian Journal of Chemistry* **2007,** *60*, 765-771.

284. Prucker, O.; Christian, S.; Bock, H.; Ruhe, J.; Frank, C. W.; Knoll, W., On the glass transition in ultrathin polymer films of different molecular architecture. *Macromolecular Chemistry and Physics* **1998,** *199* (7), 1435-1444.

285. Qi, D.; Fakhraai, Z.; Forrest, J. A., Substrate and Chain Size Dependence of Near Surface Dynamics of Glassy Polymers. *Physical Review Letters* **2008,** *101* (9), 096101.

286. Qi, Q.; Wu, X.; Hua, Y.; Hou, Q.; Dong, M.; Mao, Z.; Yin, B.; Yin, S., Enhancement of performance for blue organic light emitting devices based on double emission layers. *Organic Electronics* **2010,** *11* (3), 503-507.

287. Qian, Z.; Minnikanti, V. S.; Sauer, B. B.; Dee, G. T.; Archer, L. A., Surface Tension of Symmetric Star Polymer Melts. *Macromolecules* **2008,** *41* (13), 5007-5013.

288. Raegen, A.; Massa, M.; Forrest, J.; noki-Veress, K., Effect of atmosphere on reductions in the glass transition of thin polystyrene films. *European Physical Journal e* **2008,** *27* (4), 375-377.

289. Ramanathan, M.; Darling, S. B.; Sumant, A. V.; Auciello, O. In *Nanopatterning of ultrananocrystalline diamond thin films via block copolymer lithography*, AVS: 2010; pp 979-983.

290. Ranganathan, T.; Ku, B. C.; Zilberman, J.; Beaulieu, M.; Farris, R. J.; Coughlin, E. B.; Emrick, T., Poly(arylate-phosphonate) copolymers with deoxybenzoin in the backbone: Synthesis, characterization, and thermal properties. *J.Polym.Sci.A Polym.Chem.* **2007,** *45* (20), 4573-4580.

291. Reiter, G., Mobility of polymers in films thinner than their unperturbed size. *Europhysics Letters* **1993,** *23* (8), 579-584.

292. Riggleman, R. A.; Douglas, J. F.; de Pablo, J. J., Tuning polymer melt fragility with antiplasticizer additives. *The Journal of Chemical Physics* **2007,** *126* (23), 234903-10.

293. Riggleman, R. A.; Yoshimoto, K.; Douglas, J. F.; de Pablo, J. J., Influence of Confinement on the Fragility of Antiplasticized and Pure Polymer Films. *Physical Review Letters* **2006,** *97* (4), 045502.

294. Rittigstein, P.; Torkelson, J. M., Polymer-nanoparticle interfacial interactions in polymer nanocomposites: Confinement effects on glass transition temperature and suppression of physical aging. *Journal of Polymer Science Part B-Polymer Physics* **2006,** *44* (20), 2935-2943.

295. Rogers, J. A.; Bao, Z., Printed plastic electronics and paperlike displays. *Journal of Polymer Science Part A: Polymer Chemistry* **2002,** *40* (20), 3327-3334.

296. Rogers, J. A.; Bao, Z.; Baldwin, K.; Dodabalapur, A.; Crone, B.; Raju, V. R.; Kuck, V.; Katz, H.; Amundson, K.; Ewing, J.; Drzaic, P., Paper-like electronic displays: Large-area rubber-stamped plastic sheets of electronics and microencapsulated electrophoretic inks. *Proceedings of the National Academy of Sciences* **2001,** *98* (9), 4835-4840.

297. Rogers, S. S.; Madlkern, L., Glass Transitions of the Poly-(n-Alkyl Methacrylates). *Journal of Physical Chemistry* **1957,** *61* (7), 985-991.

298. Rogers, S. S.; Mandelkern, L., Glass formation in polymers 1. The glass transitions of the Poly-(-Alkyl Methacrylates). *Journal of Physical Chemistry* **1957,** *61* (7), 985-990.

299. Rotella, C.; Napolitano, S.; De Cremer, L.; Koeckelberghs, G.; Wubbenhorst, M., Distribution of Segmental Mobility in Ultrathin Polymer Films. *Macromolecules* **2010,** *43* (20), 8686-8691.

300. Roth, C. B.; Dutcher, J. R., Glass transition temperature of freely-standing films of atactic poly(methyl methacrylate). *European Physical Journal E* **2003,** *12*, S103-S107.

301. Roth, C. B.; Dutcher, J. R., Glass transition and chain mobility in thin polymer films. *Journal of Electroanalytical Chemistry* **2005,** *584* (1), 13-22.

302. Rowland, H. D.; King, W. P.; Pethica, J. B.; Cross, G. L. W., Molecular Confinement Accelerates Deformation of Entangled Polymers During Squeeze Flow. *Science* **2008,** *322* (5902), 720-722.

303. Rudalevige, T.; Francis, A. H.; Zand, R., Spectroscopic studies of fullerene aggregates. *Journal of Physical Chemistry A* **1998,** *102* (48), 9797-9802.

304. Sae-Ma, N.; Praserthdam, P.; Panpranot, J.; Chaemchuen, S.; Dokjamp, S.; Suriye, K.; Rempel, G. L., Color improvment of C9 hydrocarbon resin by hydrogenation over 2% Pd/+Ý-alumina catalyst: Effect of degree of aromatic rings hydrogenation. *J.Appl.Polym.Sci.* **2010,** *117* (5), 2862-2869.

305. Sanz, A.; Ruppel, M.; Douglas, J. F.; Cabral, J. T., Plasticization effect of C-60 on the fast dynamics of polystyrene and related polymers: an incoherent neutron scattering study. *Journal of Physics-Condensed Matter* **2008,** *20* (10).

306. Sasaki, T.; Shimizu, A.; Mourey, T. H.; Thurau, C. T.; Ediger, M. D., Glass transition of small polystyrene spheres in aqueous suspensions. *Journal of Chemical Physics* **2003,** *119* (16), 8730-8735.

307. Sauerbrey, G., Verwendung von Schwingquarzen zur Wägung dünner Schichten und zur Mikrowägung. *Zeitschrift für Physik A Hadrons and Nuclei* **1959,** *155* (2), 206-222.

308. Scheidler, P.; Kob, W.; Binder, K., Cooperative motion and growing length scales in supercooled confined liquids. *EPL (Europhysics Letters)* **2002,** (5), 701.

309. Schick, C., Glass transition under confinement-what can be learned from calorimetry. *European Physical Journal-Special Topics* **2010,** *189* (1), 3-36.

310. Schlegel, R.; Staudinger, U.; Thunga, M.; Weidisch, R.; Heinrich, G.; Uhrig, D.; Mays, J. W.; Iatrou, H.; Hadjichristidis, N., Investigations on mechanical properties of PI-PS multigraft copolymers. *European Polymer Journal* **2009,** *45* (10), 2902-2912.

311. Schuller, J.; Richert, R.; Fischer, E. W., Dielectric relaxation of liquids at the surface of a porous glass. *Physical Review B* **1995,** *52* (21), 15232.

312. Schwab, A. D.; Agra, D. M. G.; Kim, J. H.; Kumar, S.; Dhinojwala, A., Surface dynamics in rubbed polymer thin films probed with optical birefringence measurements. *Macromolecules* **2000,** *33* (13), 4903-4909.

313. Schweikart, A.; Fortini, A.; Wittemann, A.; Schmidt, M.; Fery, A., Nanoparticle assembly by confinement in wrinkles: experiment and simulations. *Soft Matter* **2010,** *6* (23), 5860-5863.

314. Seemann, R.; Jacobs, K.; Landfester, K.; Herminghaus, S., Freezing of polymer thin films and surfaces: The small molecular weight puzzle. *Journal of Polymer Science Part B-Polymer Physics* **2006,** *44* (20), 2968-2979.

315. Seitz, J. T., The estimation of mechanical properties of polymers from molecular structure. *Journal of Applied Polymer Science* **1993,** *49* (8), 1331-1351.

316. Serghei, A.; Huth, H.; Schick, C.; Kremer, F., Glassy Dynamics in Thin Polymer Layers Having a Free Upper Interface. *Macromolecules* **2008,** *41* (10), 3636-3639.

317. Serghei, A.; Mikhailova, Y.; Huth, H.; Schick, C.; Eichhorn, K. J.; Voit, B.; Kremer, F., Molecular dynamics of hyperbranched polyesters in the confinement of thin films. *The European Physical Journal E: Soft Matter and Biological Physics* **2005,** *17* (2), 199-202.

318. Shin, K.; Obukhov, S.; Chen, J. T.; Huh, J.; Hwang, Y.; Mok, S.; Dobriyal, P.; Thiyagarajan, P.; Russell, T. P., Enhanced mobility of confined polymers. *Nature Materials* **2007,** *6* (12), 961-965.

319. Singh, L.; Ludovice, P. J.; Henderson, C. L., Influence of molecular weight and film thickness on the glass transition temperature and coefficient of thermal expansion of supported ultrathin polymer films. *Thin Solid Films* **2004,** *449* (1-2), 231-241.

320. Singhvi, R.; Stephanopoulos, G.; Wang, D. I. C., Effects of substratum morphology on cell physiology-Review. *Biotechnology and Bioengineering* **1994,** *43* (8), 764-771.

321. Sirringhaus, H.; Kawase, T.; Friend, R. H.; Shimoda, T.; Inbasekaran, M.; Wu, W.; Woo, E. P., High-Resolution Inkjet Printing of All-Polymer Transistor Circuits. *Science* **2000,** *290* (5499), 2123-2126.

322. Solak, H. H.; David, C.; Gobrecht, J.; Golovkina, V.; Cerrina, F.; Kim, S. O.; Nealey, P. F., Sub-50nm Period Patterns with EUV Interference Litrhography. *Microelectronic Engineering* **2003,** *67*, 56-62.

323. Soles, C. L.; Douglas, J. F.; Jones, R. L.; Wu, W. L., Unusual expansion and contraction in ultrathin glassy polycarbonate films. *Macromolecules* **2004,** *37* (8), 2901-2908.

324. Soles, C. L.; Douglas, J. F.; Wu, W. L.; Dimeo, R. M., Incoherent neutron scattering as a probe of the dynamics in molecularly thin polymer films. *Macromolecules* **2003,** *36* (2), 373-379.

325. Soles, C. L.; Douglas, J. F.; Wu, W. L.; Peng, H. G.; Gidley, D. W., Comparative specular X-ray reflectivity, positron annihilation lifetime spectroscopy, and incoherent neutron scattering measurements of the dynamics in thin polycarbonate films. *Macromolecules* **2004,** *37* (8), 2890-2900.

326. Southern, E.; Thomas, A. G., Effect of constraints on equilibrium swelling of rubber vulcanizates. *Journal of Polymer Science Part a-General Papers* **1965,** *3* (2PA), 641-&.

327. Stafford, C. M.; Guo, S.; Harrison, C.; Chiang, M. Y. M., Combinatorial and high-throughput measurements of the modulus of thin polymer films. *Review of Scientific Instruments* **2005,** *76* (6).

328. Stafford, C. M.; Harrison, C.; Beers, K. L.; Karim, A.; Amis, E. J.; Vanlandingham, M. R.; Kim, H. C.; Volksen, W.; Miller, R. D.; Simonyi, E. E., A

buckling-based metrology for measuring the elastic moduli of polymeric thin films. *Nature Materials* **2004,** *3* (8), 545-550.

329. Stafford, C. M.; Vogt, B. D.; Harrison, C.; Julthongpiput, D.; Huang, R., Elastic moduli of ultrathin amorphous polymer films. *Macromolecules* **2006,** *39* (15), 5095-5099.

330. Stoykovich, M. P.; Nealey, P. F., Block copolymers and conventional lithography. *Materials Today* **2006,** *9* (9), 20-29.

331. Stoykovich, M. P.; Yoshimoto, K.; Nealey, P. F., Mechanical properties of polymer nanostructures: measurements based on deformation in response to capillary forces. *Applied Physics A-Materials Science & Processing* **2008,** *90* (2), 277-283.

332. Sugiyama, T.; Furukawa, Y.; Fujimura, H., Crystalline/amorphous Raman markers of hole-transport material NPD in organic light-emitting diodes. *Chemical Physics Letters* **2005,** *405* (4-6), 330-333.

333. Sun, L.; Dutcher, J. R.; Giovanni, L.; Nizzoli, F.; Stevens, J. R.; Ord, J. L., Elastic and elasto-optic properties of thin films of poly (styrene) spin coated onto Si (001). *Journal of Applied Physics* **1994,** *75* (11), 7482-7488.

334. Sun, Y.; Choi, W. M.; Jiang, H.; Huang, Y. Y.; Rogers, J. A., Controlled buckling of semiconductor nanoribbons for stretchable electronics. *Nat Nano* **2006,** *1* (3), 201-207.

335. Swallen, S. F.; Kearns, K. L.; Mapes, M. K.; Kim, Y. S.; McMahon, R. J.; Ediger, M. D.; Wu, T.; Yu, L.; Satija, S., Organic glasses with exceptional thermodynamic and kinetic stability. *Science* **2007,** *315* (5810), 353-356.

336. Swallen, S. F.; Traynor, K.; McMahon, R. J.; Ediger, M. D.; Mates, T. E., Stable Glass Transformation to Supercooled Liquid via Surface-Initiated Growth Front. *Physical Review Letters* **2009,** *102* (6), 065503.

337. Tahk, D.; Lee, H. H.; Khang, D.-Y., Elastic Moduli of Organic Electronic Materials by the Buckling Method. *Macromolecules* **2009,** *42* (18), 7079-7083.

338. Tan, L.; Kong, Y. P.; Pang, S. W.; Yee, A. F., Imprinting of polymer at low temperature and pressure. *Journal of Vacuum Science & Technology B: Microelectronics and Nanometer Structures* **2004,** *22* (5), 2486-2492.

339. Tanaka, H.; Tomita, H.; Takasu, A.; Hayashi, T.; Nishi, T., Morphological and kinetic evolution of surface patterns in gels during the swelling process-evidence of dynamic pattern ordering. *Physical Review Letters* **1992,** *68* (18), 2794-2797.

340. Tanaka, K.; Takahara, A.; Kajiyama, T., Film Thickness Dependence of the Surface Structure of Immiscible Polystyrene/Poly(methyl methacrylate) Blends. *Macromolecules* **1996,** *29* (9), 3232-3239.

341. Tanaka, K.; Yoon, J.-S.; Takahara, A.; Kajiyama, T., Ultrathinning-Induced Surface Phase Separation of Polystyrene/Poly(vinyl methyl ether) Blend Film. *Macromolecules* **1995,** *28* (4), 934-938.

342. Tanaka, T.; Morigami, M.; Atoda, N., Mechanism of resists pattern collapse during development process. *Japanese Journal of Applied Physics Part 1-Regular Papers Short Notes & Review Papers* **1993,** *32* (12B), 6059-6064.

343. Tang, C. W.; VanSlyke, S. A., Organic electroluminescent diodes. *Applied Physics Letters* **1987,** *51* (12), 913.

344. Tate, R. S.; Fryer, D. S.; Pasqualini, S.; Montague, M. F.; de Pablo, J. J.; Nealey, P. F., Extraordinary elevation of the glass transition temperature of thin polymer films grafted to silicon oxide substrates. *Journal of Chemical Physics* **2001,** *115* (21), 9982-9990.

345. Teare, D. O. H.; Emmison, N.; Ton-That, C.; Bradley, R. H., Effects of Serum on the Kinetics of CHO Attachment to Ultraviolet-Ozone Modified Polystyrene Surfaces. *Journal of Colloid and Interface Science* **2001,** *234* (1), 84-89.

346. Teare, D. O. H.; Ton-That, C.; Bradley, R. H., Surface characterization and ageing of ultraviolet-ozone-treated polymers using atomic force microscopy and x-ray photoelectron spectroscopy. *Surface and Interface Analysis* **2000,** *29* (4), 276-283.

347. Teertstra, S. J.; Gauthier, M., Dendrigraft polymers: macromolecular engineering on a mesoscopic scale. *Progress in Polymer Science* **2004,** *29* (4), 277-327.

348. Teixeira, A. I.; Abrams, G. A.; Bertics, P. J.; Murphy, C. J.; Nealey, P. F., Epithelial contact guidance on well-defined micro- and nanostructured substrates. *J Cell Sci* **2003,** *116* (10), 1881-1892.

349. Terao, K.; Farmer, B. S.; Nakamura, Y.; Iatrou, H.; Hong, K.; Mays, J. W., Radius of Gyration of Polystyrene Combs and Centipedes in a œë Solvent. *Macromolecules* **2005,** *38* (4), 1447-1450.

350. Thomas, K. R.; Chenneviere, A.; Reiter, G.; uuml; nter; Steiner, U., Nonequilibrium behavior of thin polymer films. *Physical Review E* **2011,** *83* (2), 021804.

351. Thurn-Albrecht, T.; Schotter, J.; Kastle, G. A.; Emley, N.; Shibauchi, T.; Krusin-Elbaum, L.; Guarini, K.; Black, C. T.; Tuominen, M. T.; Russell, T. P., Ultrahigh-Density Nanowire Arrays Grown in Self-Assembled Diblock Copolymer Templates. *Science* **2000,** *290* (5499), 2126-2129.

352. Torres, J. A.; Nealey, P. F.; de Pablo, J. J., Molecular simulation of ultrathin polymeric films near the glass transition. *Physical Review Letters* **2000,** *85* (15), 3221-3224.

353. Torres, J. M., Stafford, C.M., Vogt, B.D., Elastic Modulus of Amorphous Polymer Thin Films: Relationship to the Glass Transition Temperature. *ACS NANO* **2009,** *3*, 2677.

354. Torres, J. M.; Stafford, C. M.; Vogt, B. D., Manipulation of the Elastic Modulus of Polymers at the Nanoscale: Influence of UV-Ozone Cross-Linking and Plasticizer. *ACS Nano* **2010,** *4* (9), 5357-5365.

355. Torres, J. M.; Stafford, C. M.; Vogt, B. D., Impact of molecular mass on the elastic modulus of thin polystyrene films. *Polymer* **2010,** *51* (18), 4211-4217.

356. Tress, M.; Erber, M.; Mapesa, E. U.; Huth, H.; MuÃàller, J.; Serghei, A.; Schick, C.; Eichhorn, K.-J.; Voit, B.; Kremer, F., Glassy Dynamics and Glass Transition in Nanometric Thin Layers of Polystyrene. *Macromolecules* **2010,** *43* (23), 9937-9944.

357. Trujillo, V.; Kim, J.; Hayward, R. C., Creasing instability of surface-attached hydrogels. *Soft Matter* **2008,** *4* (3), 564-569.

358. Tseng, K. C.; Turro, N. J.; Durning, C. J., Tracer diffusion in thin polystyrene films. *Polymer* **2000,** *41* (12), 4751-4755.

359. Tseng, K. C.; Turro, N. J.; Durning, C. J., Molecular mobility in polymer thin films. *Physical Review E* **2000,** *61* (2), 1800-1811.

360. Tsui, O. K. C.; Russell, T. P.; Hawker, C. J., Effect of interfacial interactions on the glass transition of polymer thin films. *Macromolecules* **2001,** *34* (16), 5535-5539.

361. Tweedie, C. A.; Constantinides, G.; Lehman, K. E.; Brill, D. J.; Blackman, G. S.; Van Vliet, K. J., Enhanced Stiffness of Amorphous Polymer Surfaces under Confinement of Localized Contact Loads. *Advanced Materials* **2007,** *19* (18), 2540-2546.

362. Uhrig, D.; Mays, J. W., Experimental techniques in high-vacuum anionic polymerization. *Journal of Polymer Science Part A: Polymer Chemistry* **2005,** *43* (24), 6179-6222.

363. Uhrig, D.; Schlegel, R.; Weidisch, R.; Mays, J., Multigraft copolymer superelastomers: Synthesis morphology, and properties. *European Polymer Journal* **2010,** *47* (4), 560-568.

364. Van Damme, H. S.; Hogt, A. H.; Feijen, J., Surface mobility and structural transitions of poly(n-alkyl methacrylates) probed by dynamic contact angle measurements. *Journal of Colloid and Interface Science* **1986,** *114* (1), 167-172.

365. VanLandingham, M. R.; Villarrubia, J. S.; Guthrie, W. F.; Meyers, G. F., Nanoindentation of polymers: An overview. *Macromolecular Symposia* **2001,** *167*, 15-43.

366. VanZanten, J. H.; Wallace, W. E.; Wu, W. L., Effect of strongly favorable substrate interactions on the thermal properties of ultrathin polymer films. *Physical Review E* **1996,** *53* (3), R2053-R2056.

367. Vivo, P.; Jukola, J.; Ojala, M.; Chukharev, V.; Lemmetyinen, H., Influence of Alq3/Au cathode on stability and efficiency of a layered organic solar cell in air. *Solar Energy Materials and Solar Cells* **2008,** *92* (11), 1416-1420.

368. Voit, B., New developments in hyperbranched polymers. *Journal of Polymer Science Part a-Polymer Chemistry* **2000,** *38* (14), 2505-2525.

369. Volkert, C. A.; Donohue, A.; Spaepen, F., Effect of sample size on deformation in amorphous metals. *Journal of Applied Physics* **2008,** *103* (8).

370. Volynskii, A. L.; Bazhenov, S.; Lebedeva, O. V.; Bakeev, N. F., Mechanical buckling instability of thin coatings deposited on soft polymer substrates. *Journal of Materials Science* **2000,** *35* (3), 547-554.

371. Wagner, S.; Fonash, S. J.; Jackson, T. N.; Thomas, T. N.; Strum, J. C., *Flexible display enabling technology*. Society of Photo-Optical Instrumentation Engineers: Bellingham, WA, INTERNATIONAL, 2001; Vol. 4362, p X, 332 p.

372. Wagner, S.; Lacour, S. P.; Jones, J.; Hsu, P. H. I.; Sturm, J. C.; Li, T.; Suo, Z. G., Electronic skin: architecture and components. *Physica E-Low-Dimensional Systems & Nanostructures* **2004,** *25* (2-3), 326-334.

373. Wallace, W. E.; Vanzanten, J. H.; Wu, W. L., Influence of an impenetrable interface on a polymer glass-transition temperature. *Physical Review E* **1995,** *52* (4), R3329-R3332.

374. Walther, A.; Gˆldel, A.; M¸ller, A. H. E., Controlled crosslinking of polybutadiene containing block terpolymer bulk structures: A facile way towards complex and functional nanostructures. *Polymer* **2008,** *49* (15), 3217-3227.

375. Wang, S.; Xiao, J.; Song, J.; Ko, H. C.; Hwang, K.-C.; Huang, Y.; Rogers, J. A., Mechanics of curvilinear electronics. *Soft Matter* **2010,** *6* (22), 5757-5763.

376. Wang, Y.; Yang, R.; Shi, Z.; Zhang, L.; Shi, D.; Wang, E.; Zhang, G., Super Elastic Graphene Ripples for Flexible Strain Sensors. *ACS Nano* **2011**, null-null.

377. Wilder, E. A.; Guo, S.; Lin-Gibson, S.; Fasolka, M. J.; Stafford, C. M., Measuring the Modulus of Soft Polymer Networks via a Buckling-Based Metrology. *Macromolecules* **2006,** *39* (12), 4138-4143.

378. Wilkinson, C. D. W.; Riehle, M.; Wood, M.; Gallagher, J.; Curtis, A. S. G., The use of materials patterned on a nano- and micro-metric scale in cellular engineering. *Materials Science & Engineering C-Biomimetic and Supramolecular Systems* **2002,** *19* (1-2), 263-269.

379. Williams, M. L.; Landel, R. F.; Ferry, J. D., Mechanical properties of substances of high molecular weight .19. The temperature dependence of relaxation mechanisms in amorphous polymers and other glass-forming liquids. *Journal of the American Chemical Society* **1955,** *77* (14), 3701-3707.

380. Winey, K. I.; Vaia, R. A., Polymer nanocomposites. *MRS Bulletin* **2007,** *32*, 314-322.

381. Wong, H. C.; Cabral, J. T., Spinodal Clustering in Thin Films of Nanoparticle-Polymer Mixtures. *Physical Review Letters* **2010,** *105* (3).

382. Wong, W. S.; Sallea, A., *Flexible electronics: materials and applications*. Springer: New York, 2009.

383. Wu, C.-p.; et al., Study on preparation of UV cross-linking films of polyurethane-LiClO 4 complexes and their ionic conductivity. *Acta Physica Sinica (Overseas Edition)* **1993,** *2* (11), 841.

384. Xie, F.; Zhang, H. F.; Lee, F. K.; Du, B.; Tsui, O. K. C.; Yokoe, Y.; Tanaka, K.; Takahara, A.; Kajiyama, T.; He, T., Effect of Low Surface Energy Chain Ends on the Glass Transition Temperature of Polymer Thin Films. *Macromolecules* **2002,** *35* (5), 1491-1492.

385. Xie, L.; Demaggio, G. B.; Frieze, W. E.; Devries, J.; Gidley, D. W.; Hristov, H. A.; Yee, A. F., Positronium formation as a probe of polymer surfaces and thin-films. *Physical Review Letters* **1995,** *74* (24), 4947-4950.

386. Yang, S.; Khare, K.; Lin, P.-C., Harnessing Surface Wrinkle Patterns in Soft Matter. *Advanced Functional Materials* **2010,** *20* (16), 2550-2564.

387. Yang, Z.; Fujii, Y.; Lee, F. K.; Lam, C.-H.; Tsui, O. K. C., Glass Transition Dynamics and Surface Layer Mobility in Unentangled Polystyrene Films. *Science* **2010,** *328* (5986), 1676-1679.

388. Ying, Q. C.; Marecek, J.; Chu, B., Solution behavior of buckminsterfullerene (C-60) in benzene. *Journal of Chemical Physics* **1994,** *101* (4), 2665-2672.

389. Yoshimoto, K.; Jain, T. S.; Nealey, P. F.; de Pablo, J. J., Local dynamic mechanical properties in model free-standing polymer thin films. *Journal of Chemical Physics* **2005,** *122* (14), 144712.

390. Zerda, A. S.; Lesser, A. J., Organophosphorous additive for fortification, processibility, and flame retardance of epoxy resins. *Journal of Applied Polymer Science* **2002,** *84* (2), 302-309.

391. Zhang, J.; Liu, G.; Jonas, J., Effects of confinement on the glass-transition temperature of molecular liquids. *Journal of Physical Chemistry* **1992,** *96* (8), 3478-3480.

392. Zhang, P.; Yang, D.; Li, Z.; Ma, H., Controlled wrinkle formation via bubble inflation strain engineering. *Soft Matter* **2010,** *6* (18), 4580-4584.

393. Zhang, R.; Cherdhirankorn, T.; Graf, K.; Koynov, K.; Berger, R., Swelling of cross-linked polystyrene beads in toluene. *Microelectronic Engineering* **2007,** *85* (5-6), 1261-1264.

394. Zheng, X.; Rafailovich, M. H.; Sokolov, J.; Strzhemechny, Y.; Schwarz, S. A.; Sauer, B. B.; Rubinstein, M., Long-range effects on polymer diffusion induced by a bounding interface. *Physical Review Letters* **1997,** *79* (2), 241-244.

395. Zheng, X.; Sauer, B. B.; Vanalsten, J. G.; Schwarz, S. A.; Rafailovich, M. H.; Sokolov, J.; Rubinstein, M., Reptation dynamics of polymer melt near an attractive solid surface. *Physical Review Letters* **1995,** *74* (3), 407-410.